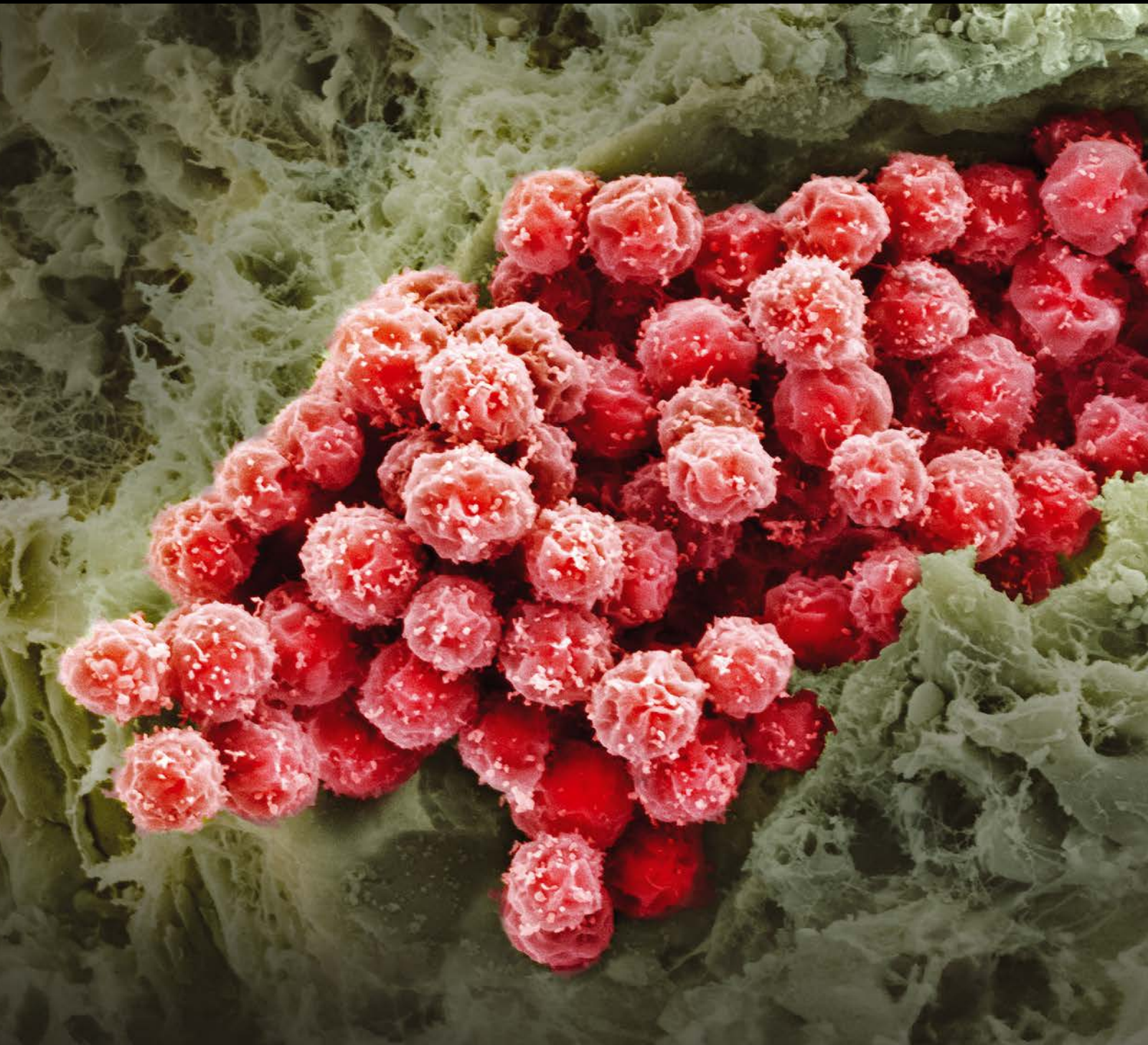


# Manufacturing Cells for Clinical Use

Guest Editors: Mark L. Weiss, Mahendra S. Rao, Robert Deans,  
and Peter Czermak





---

# **Manufacturing Cells for Clinical Use**

Stem Cells International

---

## **Manufacturing Cells for Clinical Use**

Guest Editors: Mark L. Weiss, Mahendra S. Rao, Robert Deans,  
and Peter Czermak



Copyright © 2016 Hindawi Publishing Corporation. All rights reserved.

This is a special issue published in “Stem Cells International.” All articles are open access articles distributed under the Creative Commons Attribution License, which permits unrestricted use, distribution, and reproduction in any medium, provided the original work is properly cited.



## Editorial Board

James Adjaye, Germany  
Nadire N. Ali, UK  
Dominique Bonnet, UK  
Marco Bregni, Italy  
Silvia Brunelli, Italy  
Bruce A. Bunnell, USA  
Kevin D. Bunting, USA  
Benedetta Bussolati, Italy  
Yilin Cao, China  
Yuqingeugene Chen, USA  
Kyunghee Choi, USA  
Gerald A. Colvin, USA  
Christian Dani, France  
Varda Deutsch, Israel  
Leonard M. Eisenberg, USA  
Marina Emborg, USA  
Franca Fagioli, Italy  
Tong-Chuan He, USA  
Boon Chin Heng, Switzerland  
Toru Hosoda, Japan  
Xiao J. Huang, China  
Thomas Ichim, USA  
Joseph Itskovitz-Eldor, Israel  
Pavla Jendelova, Czech Republic  
Arne Jensen, Germany

Atsuhiko Kawamoto, Japan  
Armand Keating, Canada  
Mark D. Kirk, USA  
Valerie Kouskoff, UK  
Joanne Kurtzberg, USA  
Andrzej Lange, Poland  
Laura Lasagni, Italy  
Renke Li, Canada  
Tao-Sheng Li, Japan  
Susan Liao, Singapore  
Ching-Shwun Lin, USA  
Shinn-Zong Lin, Taiwan  
Matthias Lutolf, Switzerland  
Gary E. Lyons, USA  
Yupo Ma, USA  
Athanasios Mantalaris, UK  
Eva Mezey, USA  
Claudia Montero-Menei, France  
Karim Nayernia, UK  
Sue O'Shea, USA  
Bruno Péault, USA  
Stefan Przyborski, UK  
Peter J. Quesenberry, USA  
Pranela Rameshwar, USA  
Bernard A.J Roelen, Netherlands

Peter Rubin, USA  
Hannele T. Ruohola-Baker, USA  
Donald S. Sakaguchi, USA  
Ghasem Hosseini Salekdeh, Iran  
Heinrich Sauer, Germany  
Coralie Sengenès, France  
Ashok K. Shetty, USA  
Shimon Slavin, Israel  
Joost Sluijter, Netherlands  
Igor Slukvin, USA  
Shay Soker, USA  
Giorgio Stassi, Italy  
Ann Steele, USA  
Alexander Storch, Germany  
Corrado Tarella, Italy  
Yang D. Teng, USA  
Antoine Toubert, France  
Hung-Fat Tse, Hong Kong  
Marc Turner, UK  
Chia-Lin Wei, Singapore  
Dominik Wolf, Austria  
Qingzhong Xiao, UK  
Zhaohui Ye, USA  
Wen-Jie Zhang, China

# Contents

---

## **Manufacturing Cells for Clinical Use**

Mark L. Weiss, Mahendra S. Rao, Robert Deans, and Peter Czermak  
Volume 2016, Article ID 1750697, 5 pages

## **Regenerative Therapy of Type 1 Diabetes Mellitus: From Pancreatic Islet Transplantation to Mesenchymal Stem Cells**

Nadine E. Rekitke, Meidjie Ang, Divya Rawat, Rahul Khatri, and Thomas Linn  
Volume 2016, Article ID 3764681, 22 pages

## **Attachment, Growth, and Detachment of Human Mesenchymal Stem Cells in a Chemically Defined Medium**

Denise Salzig, Jasmin Leber, Katharina Merkewitz, Michaela C. Lange, Natascha Köster, and Peter Czermak  
Volume 2016, Article ID 5246584, 10 pages

## **Theoretical and Practical Issues That Are Relevant When Scaling Up hMSC Microcarrier Production Processes**

Valentin Jossen, Cedric Schirmer, Dolman Mostafa Sindi, Regine Eibl, Matthias Kraume, Ralf Pörtner, and Dieter Eibl  
Volume 2016, Article ID 4760414, 15 pages

## **Standardizing Umbilical Cord Mesenchymal Stromal Cells for Translation to Clinical Use: Selection of GMP-Compliant Medium and a Simplified Isolation Method**

J. Robert Smith, Kyle Pfeifer, Florian Petry, Natalie Powell, Jennifer Delzeit, and Mark L. Weiss  
Volume 2016, Article ID 6810980, 14 pages

## **Evaluation of Tissue Homogenization to Support the Generation of GMP-Compliant Mesenchymal Stromal Cells from the Umbilical Cord**

Ryan J. Emnett, Aparna Kaul, Aleksandar Babic, Vicki Geiler, Donna Regan, Gilad Gross, and Salem Akel  
Volume 2016, Article ID 3274054, 9 pages

## **Stem Cell Therapy for Treatment of Stress Urinary Incontinence: The Current Status and Challenges**

Shukui Zhou, Kaile Zhang, Anthony Atala, Oula Khoury, Sean V. Murphy, Weixin Zhao, and Qiang Fu  
Volume 2016, Article ID 7060975, 7 pages

## **Stem Cell Mobilization with G-CSF versus Cyclophosphamide plus G-CSF in Mexican Children**

José Eugenio Vázquez Meraz, José Arellano-Galindo, Armando Martínez Avalos, Emma Mendoza-García, and Elva Jiménez-Hernández  
Volume 2016, Article ID 4078215, 4 pages

## Editorial

# Manufacturing Cells for Clinical Use

**Mark L. Weiss,<sup>1</sup> Mahendra S. Rao,<sup>2</sup> Robert Deans,<sup>3</sup> and Peter Czermak<sup>4,5</sup>**

<sup>1</sup>*Department of Anatomy and Physiology, Midwest Institute for Comparative Stem Cell Biology, Kansas State University, Manhattan, KS 66506, USA*

<sup>2</sup>*The New York Stem Cell Foundation, New York, NY 10023, USA*

<sup>3</sup>*Rubius Therapeutics, Cambridge, MA 02139, USA*

<sup>4</sup>*Institute of Bioprocess Engineering and Pharmaceutical Technology, University of Applied Sciences Mittelhessen, 35390 Giessen, Germany*

<sup>5</sup>*Faculty of Biology and Chemistry, Justus Liebig University Giessen, 35390 Giessen, Germany*

Correspondence should be addressed to Mark L. Weiss; [mlweiss@k-state.edu](mailto:mlweiss@k-state.edu)

Received 31 March 2016; Accepted 3 April 2016

Copyright © 2016 Mark L. Weiss et al. This is an open access article distributed under the Creative Commons Attribution License, which permits unrestricted use, distribution, and reproduction in any medium, provided the original work is properly cited.

## 1. Introduction

The growth in the number of registered clinical trials indicates that there is a need for cells for many types of cell therapy. Figure 1, which is reprinted from the excellent blog maintained by Alexi Bersenev, shows that the cell type used in most clinical trials worldwide is the mesenchymal stromal cell (MSC). The MSC type requires *in vitro* expansion to reach a clinical dose and thus there is a desire to optimize and standardize processes and procedures for MSC manufacture specifically for clinical use.

When considering MSC, there are “issues” associated with manufacturing which warrant special consideration. Some of these issues are associated with the identification of the MSC source used for therapeutic cells because MSCs can be isolated from different tissues. For example, they can be isolated from fat, bone marrow, or fetal tissues such as placenta or umbilical cord. For autologous use, MSCs from fat have received attention. MSCs can be isolated from donors of different age or sex. Finally, the health status of the donor may affect MSC function. These factors may affect MSC isolation, expansion capability, function, and/or survival after transplantation. Thus, MSCs from one tissue may be superior to MSCs from another for a particular clinical application. However, if one cannot expand the MSCs to a therapeutic dose, it moots the point.

Much attention has focused upon manufacturing or expanding MSCs for clinical use. There is a lack of standardization with MSC characterization, as recently reviewed [1, 2].

Some researchers suggested that “standardized” MSCs be derived, expanded, and provided to the research community as a means of addressing the differences in MSC characterization found between laboratories [2, 3]. Other researchers suggested that standardization of the characterization methods and tools is needed [1]. When one considers that MSC manufacturing and passaging contribute to the differences mentioned above, for example, MSCs isolated from different passages [4, 5] or from donors of different tissues, ages, or health status reflecting the inherent biological variability, MSCs might defy standardization [2, 6–8]. As a first step, it might be easiest to establish standardized characterization tools and protocols or perhaps to use a certification procedure to make the characterization of MSCs between laboratories more uniform.

In this issue, eight articles address different aspects of manufacturing cells for cell therapy. These articles can be broken down into two groups. The first group deals with scale-up and manufacturing of MSCs and consists of five papers (those of J. R. Smith et al., F. Petry et al., D. Salzig et al., R. J. Emmett et al., and V. Jossen et al.). The second group deals with application and optimizing of cell therapy and consists of three papers (those of N. E. Reikittke et al., S. Zhou et al., and J. E. V. Meraz et al.).

## 2. Manufacturing MSCs for Clinical Use

J. R. Smith et al. focused efforts to standardize and optimize the isolation of MSCs from the umbilical cord. They

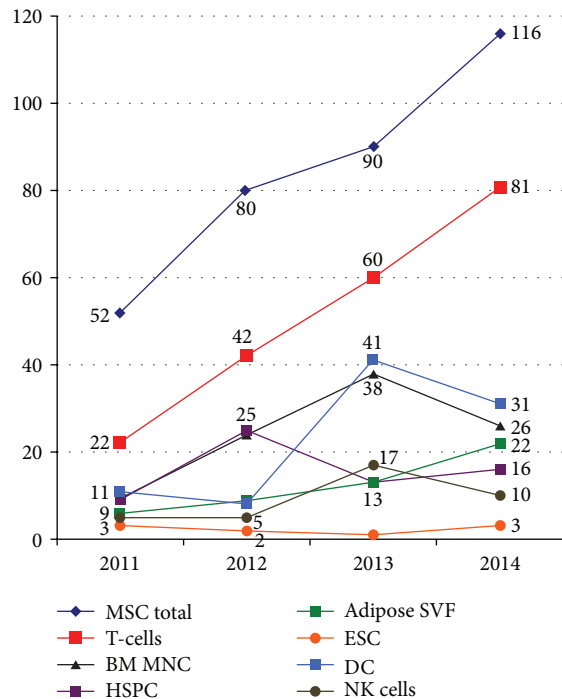


FIGURE 1: Number of stem cell therapy trials by cell type worldwide (reprinted from [9]).

developed a process to extract cells using Miltenyi C-tubes coupled with enzymatic digestion with minimal dissection that resulted in 10x more MSCs than their previously described method, while also reducing contamination risk. They expanded the MSCs in xenogeneic-material-free conditions using 10% pooled human platelet lysate to supplement the growth medium. MSCs produced using their new method met the minimal definition of MSCs set by ISCT's MSC working group. They also had one unexpected finding: a higher yield of MSCs from cords derived from natural births compared to Caesarian-section births. They did not identify the mechanism responsible. Taken together, their findings provided a more streamline extraction method and an optimized expansion protocol suitable for translation to clinical manufacturing. The main limitation for clinical translation is the use of enzymatic digestion.

The contribution by F. Petry et al. involves the growth of MSCs in three dimensions (3D) with scale-up to clinical manufacturing in a stirred tank bioreactor. They started the scale-up by identifying microcarriers that would be suitable to the umbilical cord MSCs in small-scale spinner flasks. Interestingly, the umbilical cord MSCs preferred a plastic microcarrier, as opposed to the treated glass microcarrier that telomerase immortalized bone marrow MSCs prefer [10–12]. It appears that MSCs from different tissue sources have different attachment requirements. Or perhaps the differences are due to the use of pooled human platelet lysate as a medium additive in F. Petry et al.'s paper compared to fetal bovine serum used to expand the bone marrow-derived MSCs. After identifying the best microcarrier, F. Petry et al. tested seeding protocols and feeding strategies in spinner flasks. The paper

culminated in scale-up to 2.5 L in a Millipore Mobius single use stirred tank bioreactor. This paper identified scaling factors and set the stage for more highly refined optimization and an SOP for MSC expansion. The MSCs produced in 3D met the minimal definition of MSCs and were not obviously different from the MSCs expanded in 2D in their companion paper (J. R. Smith et al.).

The paper by D. Salzig et al. involved the optimization of MSC expansion in chemically defined medium (CDM) for GMP manufacturing. The use of a chemically defined medium might eliminate the need for batch-to-batch comparison and validation of medium which employs biologics. D. Salzig et al. compared the growth of both an immortalized MSC line and primary MSCs from bone marrow or adipose tissues in CDM following various surface treatments of the substrate to enhance attachment. They found a difference in the surface attachment requirements between the MSC types. For example, bone marrow-derived MSCs did not attach rapidly in CDM, compared to immortalized MSCs or adipose-derived MSCs that attached in 2–5 hrs. Immortalized MSCs attached readily to specialized tissue culture plastic in CDM and grew as well as or better than MSCs seeded onto standard tissue culture plastics in serum containing medium. In contrast, surface coating with collagen type IV or fibronectin, but not laminin, was important for bone marrow-derived MSC's attachment and growth. Interestingly, for the bone marrow MSCs, D. Salzig et al. were unable to achieve MSC expansion equal to serum containing medium. Next, they evaluated the detachment efficiency of four different enzymes (trypsin, accutase, prolyl-specific peptidase (PsP), and collagenase) on bone marrow-derived MSCs and immortalized MSCs. Again, they found differences between MSCs source and the type of medium on the detachment efficiency. For immortalized MSCs, CDM reduced the efficiency to detach, compared to serum containing medium, and collagenase was inferior to trypsin, accutase, and PsP. In contrast, all four enzymes performed equally well for detaching bone marrow-derived MSCs grown in serum containing medium, with little or no effect of surface treatment. These results indicate that derivation of SOPs for MSC expansion and harvest might need to be customized for each type of medium used and MSCs tissue source. The data in this paper argues against the notion that standardized conditions for MSCs can be generalized across tissue source.

R. J. Emmett et al. developed a GMP-compliant method to isolate mesenchymal stromal cells (MSCs) from the umbilical cord. Since many of the currently described methods use enzymatic digestion to extract cells from the cord and since that step introduces xenogeneic reagents, R. J. Emmett et al. were determined to extract MSCs following mechanical disruption of the cord using a tissue homogenizer and they compared the yield to that obtained following collagenase digestion. Next, they expanded MSCs in medium supplemented with 10% pooled human platelet lysate or 20% fetal bovine serum. They found that mechanical disruption produced an identical yield as collagenase extraction at the initial isolation step. However, following expansion, fewer cells were produced after mechanical dissociation compared to enzymatic extraction. Mechanical extraction may have

introduced higher levels of cellular stress and this could have produced the observed slower expansion at both early passage (P1–P3) and later passage (P7–P9). Mechanical dissociation impaired colony-forming efficiency of MSCs compared to MSCs enzymatically extracted when MSCs were expanded in pooled human platelet lysate, also suggesting that MSCs isolated by mechanical disruption were stressed. R. J. Emmett et al. calculated that they could theoretically reach their manufacturing goals of 30 billion MSCs within approximately one month of culture for either method. Their method is easily scaled up, requires minimal manipulation of the cord tissues prior to extraction within a closed system, and produces MSCs that meet the ISCT definition for surface marker expression and trilineage differentiation. While additional characterization work would be needed to validate that MSCs expanded following mechanical extraction are bioequivalent to MSCs expanded following enzymatic isolation methods, the simplicity of this method is encouraging and easily standardized between laboratories.

V. Jossen et al. examined the expansion of human adipose-derived MSCs on microcarriers for manufacturing scale-up in both stirred tank bioreactor and a bag (wave-mixer type) bioreactor. Their intent was to investigate the relationship between impeller speed and shear stress and to minimize the aggregation of microcarriers which is thought to result in limitations of mass transfer and heterogeneous distribution of cells on the carriers. Further, aggregation of carriers may interfere with the use of computational methods to model scale-up results. Here, V. Jossen et al. used adipose-derived MSCs from a single donor. These MSCs were expanded in Lonza specialty medium supplemented with 5% fetal bovine serum using polystyrene microcarriers. The authors found the largest expansion factor at impeller speeds that were slower than the suspension speed ( $N_{s1}$ ), at a speed they term  $N_{siu}$ . It should be noted that  $N_{s1}$  (sometimes called  $N_{sj}$ ) is used in the industry as an accepted impeller speed since this is the minimal speed to suspend the carriers in the fluid column, thereby maximize mass transfer, and minimize the possibility of heterogeneous distribution of cells on the carriers. The authors show enhanced growth rate and therefore expansion factor at a slightly slower impeller speed ( $N_{siu}$ ) and suggest that the lower shear stress on the cells may explain the differences. One confounding factor to their experiment was that aggregates of MSCs and microcarriers occurred by the end of the culture period. Thus, there are still issues to be resolved. V. Jossen et al. performed experiments expanding MSCs in a bag type of bioreactor to evaluate the differences between  $N_{s1}$  and  $N_{siu}$  between the two types of bioreactors. They evaluated the maximum power and the shear stress in the wave type bioreactor, which provides a rhythmic periodic stress as opposed to the constant stresses provided in stirred tank bioreactors. Finally, they performed a proof-of-concept expansion of MSCs to compare yields between stirred tank and wave type bioreactors. While propagation of MSCs was possible in both bioreactors, the yield in the wave type bioreactor was three times lower than the stirred tank system. In addition, the wave type bioreactor produced larger aggregates, up to 6 mm in size. Their results confirm earlier reports that  $N_{siu}$  produces superior propagation of

MSCs in stirred tank bioreactors and that stirred tank bioreactors are superior for MSC expansion compared to wave type bioreactors. These data confirm that shear stress and aggregate formation negatively affect MSC expansion. When this paper is taken in the context of others within this special edition, one wonders whether these data can be extended to other media conditions, such as a chemically defined medium as discussed in R. J. Emmett et al.'s paper, or whether these data can be extended to other MSC sources (as in D. Salzig et al.'s paper). Using mathematical modeling to optimize MSC manufacturing is a new topic that will be refined as additional results identify the key variables.

**2.1. Application and Optimizing of Stem Cell Therapy.** When treating many forms of hematological cancers or solid tumors, hematopoietic stem cell transplants reconstitute hematopoiesis after myeloablative therapy to reduce tumor burden. Mobilized peripheral blood progenitor cells collected by aphaeresis have become a common means to treat myeloablative therapy in such patients, replacing even bone marrow transplant due to the rapid recovery following transplantation. J. E. V. Meraz et al. compared three different stem cell mobilization methods in children with malignant cancers to evaluate which was best for hematopoietic stem cell mobilization. The three methods were cyclophosphamide (CFA) and hematopoietic growth factor G-CSF with aphaeresis beginning when white blood count (WBC) exceeded  $1 \times 10^9$ /liter (group A), CFA with G-CSF with aphaeresis beginning when WBC exceeded  $10 \times 10^9$ /liter (group B), or G-CSF alone for 4 days followed by aphaeresis beginning on the fifth day (group C). In each case, aphaeresis continued until the target dose of CD34+ cells and MNCs reached  $2 \times 10^8$ /kg and  $4 \times 10^8$ /kg, respectively. Adverse events, recorded as hospitalization instances due to neutropenia, were recorded in the CFA-treated groups (groups A and B), but not in the G-CSF only group (group C). While group B appears to be superior to group A for mobilization (total MNC and CD34+ cell number), there were no differences between groups B and C. J. E. V. Meraz et al. concluded that CFA and G-CSF mobilization when WBCx exceeds  $10 \times 10^9$ /kg had similar efficacy to mobilization with G-CSF alone, but G-CSF alone had fewer adverse events. Since their research did not follow through with transplantation outcomes, it is unclear whether the hematopoietic transplant of mobilized blood from G-CSF alone (group C) would reconstitute the patients more rapidly than those patients receiving the combined CFA and G-CSF. J. E. V. Meraz et al.'s results suggest that the G-CSF protocol is currently the best preparation for hematopoietic stem cell transplantation in children.

N. E. Rekitke et al. provided a review of the state of the art of regenerative medicine therapy for type 1 diabetes mellitus. Their review focuses on pancreatic islet transplantation and on undifferentiated MSC transplantation and transdifferentiated MSCs to endoderm or pancreatic progenitor cells. Pancreatic islet transplants have been evaluated in clinic studies in the USA and abroad. N. E. Rekitke et al.'s review covers the major progress in islet transplantation trials through three iterations: improvements in cadaveric islet



processing to reduce damage and refinements of immune suppression in the recipient represent the important stages of progress. According to N. E. Reikittke et al.'s review, following the latest procedures, the majority of diabetic patients who receive islet transplantation can expect to become insulin-independent for up to five years. N. E. Reikittke et al. discussed unsolved issues of human islet transplants including the blood-mediated inflammation that impairs islet function and survival and the need to develop improved islet isolation protocols which enhance islet function and survival and reduce demand for cadaveric material to meet demand. In addition to reviewing translation research on islet transplantation, N. E. Reikittke et al. discussed the use of MSCs for type I diabetes therapy. This review indicates that progress in islet isolation and immune suppression of the recipient is responsible for the great progress in pancreatic islet transplantation. If the improved immune suppression regimes developed for pancreatic islet cell transplantation also can enable other allogeneic cell transplantation, this work may have a tremendous impact on the patients needing tissue transplantation.

Closing out this special issue on manufacturing cells for cell therapy, S. Zhou et al. provided a state-of-the-art review on the use of stem cell therapy to treat stress urinary incontinence (SUI). SUI may affect more than 200 million people worldwide and disproportionately affects women at a ratio of 3:1. Pregnancy and having a child by vaginal birth are risk factors for SUI due to functional loss of levator ani muscles. Similarly, men who have radical prostatectomy are at increased risk for SUI. The most common and effective treatments of SUI are bulking agent injections to augment levator ani function. These bulking agents are associated with a variety of adverse events suggesting that an alternative approach, such as the use of stem cells, may assist with regeneration or repair of levator ani and be effective for treating SUI. S. Zhou et al. reviewed the preclinical literature which supports the use of various autologous stem cell sources, including muscle-derived stem cells, adipose-derived MSCs, and bone marrow-derived MSCs, for treating SUI. This work is still in the preclinical stage, mostly, and a few safety studies were discussed. While injection of stem cells as bulking agents for levator ani muscle is one direction for SUI treatment, S. Zhou et al. discuss the tissue engineering approach, too, which involves the use of scaffolds seeded with autologous stem cells. Work to date includes preclinical testing in the rat SUI model as an alternative to surgical tape. Limitation of both approaches included the need to improve cell survival after transplantation. This limitation was identified by the review by N. E. Reikittke et al. also in this issue, which indicated that the rapid progression and increased therapeutic impact after islet transplantation in type I diabetes were coupled with improving the quality of transplanted cells and improved immune suppression. Since stem cells transplanted to treat SUI were of autologous origin, it is likely that larger improvements will be obtained by improving the cell preparation and transplantation to reduce cell stress and improve survival after transplantation. While one might expect that immune suppression would not be required in the autologous transplantation setting, it is likely

that transient immune suppression is also likely to improve outcomes in this situation, too.

### 3. Conclusions

Cellular manufacturing for clinical applications is moving forward rapidly due to pressing need created by the hundreds of ongoing clinical trials and due to the research results providing the fundamental knowledge about barriers and how to overcome them. In this special issue, topics ranged from isolation and manufacturing of MSCs to critical reviews of the application of cell therapy for treating type I diabetes using islet transplantation or treatment of stress induced urinary incontinence. From reviewing the issues, a key take-home message is that it is not enough to produce cells in sufficient numbers. Equally important is to produce cells that survive and function following transplantation. In summary, the manufacture of clinical doses of robust functional cells is one key piece to cell therapy; the other key is the preparative regime given to the patient to enable engraftment and function of cells. Looking back in history, we find this to be a recurrent theme from hematopoietic stem cell transplantation. Understanding how to manufacture cells for clinical purpose is fundamental to improving outcomes and provides a starting point to evaluate patient preparative regimens.

Mark L. Weiss  
Mahendra S. Rao  
Robert Deans  
Peter Czermak

### References

- [1] M. Mendicino, A. M. Bailey, K. Wonnacott, R. K. Puri, and S. R. Bauer, "MSC-based product characterization for clinical trials: an FDA perspective," *Cell Stem Cell*, vol. 14, no. 2, pp. 141–145, 2014.
- [2] S. Viswanathan, A. Keating, R. Deans et al., "Soliciting strategies for developing cell-based reference materials to advance mesenchymal stromal cell research and clinical translation," *Stem Cells and Development*, vol. 23, no. 11, pp. 1157–1167, 2014.
- [3] R. Deans, "Towards the creation of a standard MSC line as a calibration tool," *Cytotherapy*, vol. 17, no. 9, pp. 1167–1168, 2015.
- [4] I. H. Bellayr, J. G. Catalano, S. Lababidi et al., "Gene markers of cellular aging in human multipotent stromal cells in culture," *Stem Cell Research and Therapy*, vol. 5, article 59, 2014.
- [5] S. T. Mindaye, J. Lo Surdo, S. R. Bauer, and M. A. Alterman, "The proteomic dataset for bone marrow derived human mesenchymal stromal cells: effect of in vitro passaging," *Data in Brief*, vol. 5, pp. 864–870, 2015.
- [6] M. J. Hoogduijn, M. J. Crop, A. M. A. Peeters et al., "Human heart, spleen, and perirenal fat-derived mesenchymal stem cells have immunomodulatory capacities," *Stem Cells and Development*, vol. 16, no. 4, pp. 597–604, 2007.
- [7] M. J. Hoogduijn, M. G. H. Betjes, and C. C. Baan, "Mesenchymal stromal cells for organ transplantation: different sources and unique characteristics?" *Current Opinion in Organ Transplantation*, vol. 19, no. 1, pp. 41–46, 2014.

- [8] M. T. Koobatian, M.-S. Liang, D. D. Swartz, and S. T. Andreadis, "Differential effects of culture senescence and mechanical stimulation on the proliferation and leiomyogenic differentiation of MSC from different sources: implications for engineering vascular grafts," *Tissue Engineering Part A*, vol. 21, no. 7-8, pp. 1364–1375, 2015.
- [9] A. Bersenev, "Trends in cell therapy clinical trials 2011–2014," *Cell Trials Blog*, 2015.
- [10] C. L. Elseberg, J. Leber, D. Salzig et al., "Microcarrier-based expansion process for hMSCs with high vitality and undifferentiated characteristics," *International Journal of Artificial Organs*, vol. 35, no. 2, pp. 93–107, 2012.
- [11] C. L. Elseberg, D. Salzig, and P. Czermak, "Bioreactor expansion of human mesenchymal stem cells according to GMP requirements," *Methods in Molecular Biology*, vol. 1283, pp. 199–218, 2015.
- [12] D. Salzig, A. Schmiermund, P. P. Grace, C. Elseberg, C. Weber, and P. Czermak, "Enzymatic detachment of therapeutic mesenchymal stromal cells grown on glass carriers in a bioreactor," *Open Biomedical Engineering Journal*, vol. 7, no. 1, pp. 147–158, 2013.

## Review Article

# Regenerative Therapy of Type 1 Diabetes Mellitus: From Pancreatic Islet Transplantation to Mesenchymal Stem Cells

**Nadine E. Rekittke, Meidjie Ang, Divya Rawat, Rahul Khatri, and Thomas Linn**

*Clinical Research Unit, Zentrum für Innere Medizin, Fachbereich Medizin, Justus Liebig Universität Giessen, 35392 Giessen, Germany*

Correspondence should be addressed to Thomas Linn; [thomas.linn@innere.med.uni-giessen.de](mailto:thomas.linn@innere.med.uni-giessen.de)

Received 1 October 2015; Accepted 14 December 2015

Academic Editor: Robert Deans

Copyright © 2016 Nadine E. Rekittke et al. This is an open access article distributed under the Creative Commons Attribution License, which permits unrestricted use, distribution, and reproduction in any medium, provided the original work is properly cited.

Type 1 diabetes is an autoimmune disease resulting in the permanent destruction of pancreatic islets. Islet transplantation to portal vein provides an approach to compensate for loss of insulin producing cells. Clinical trials demonstrated that even partial islet graft function reduces severe hypoglycemic events in patients. However, therapeutic impact is restrained due to shortage of pancreas organ donors and instant inflammation occurring in the hepatic environment of the graft. We summarize on what is known about regenerative therapy in type 1 diabetes focusing on pancreatic islet transplantation and new avenues of cell substitution. Metabolic pathways and energy production of transplanted cells are required to be balanced and protection from inflammation in their intravascular bed is desired. Mesenchymal stem cells (MSCs) have anti-inflammatory features, and so they are interesting as a therapy for type 1 diabetes. Recently, they were reported to reduce hyperglycemia in diabetic rodents, and they were even discussed as being turned into endodermal or pancreatic progenitor cells. MSCs are recognized to meet the demand of an individual therapy not raising the concerns of embryonic or induced pluripotent stem cells for therapy.

## 1. Clinical Results of Pancreatic Islet Transplantation

Since the introduction of the ground-breaking Edmonton protocol in 1999 [1], pancreatic islet transplantation has become more common treatment for individuals with type 1 diabetes mellitus (T1DM) suffering from recurrent severe hypoglycemia or glycemic lability. Islet transplantation has been associated with limited success during the earlier years, but the clinical results have improved greatly after the Edmonton report [2]. The following section summarizes clinical findings of islet transplantation with focus on metabolic outcomes and diabetic complications in T1DM patients.

*1.1. Metabolic Outcomes: Glycemic Control and Hypoglycemia.* Adult patients included in the islet transplantation process usually have T1DM for more than 5 years, have no preserved

endogenous insulin production with negative stimulated C-peptide levels ( $<0.3$  ng/mL), and are prone to severe hypoglycemic episodes or exhibit glycemic instability despite adequate insulin therapy [3]. Hypoglycemia unawareness results often from intensified insulin treatment and is considered the major eligibility criterion for islet transplantation in T1DM patients [4].

In the original Edmonton protocol, seven T1DM patients who received a sufficient islet mass from 2 to 3 donor pancreases became insulin independent with normalized glycosylated hemoglobin ( $HbA_{1c}$ ) levels following a median follow-up of one year. All patients were under corticosteroid-free immunosuppressive regimen consisting of sirolimus, low dose tacrolimus, and daclizumab [1]. After this initial report, follow-up studies in 12 and 17 transplanted patients continued to show positive results including significant decreases in fasting and postprandial glucose levels, normalized  $HbA_{1c}$

levels, and improved fasting and postmeal C-peptide secretion as well as increased acute insulin responses to arginine and intravenous glucose tolerance test [5, 6]. A subsequent international trial at nine centers confirmed the reproducibility of the Edmonton results in 21 of 36 patients (58%) who attained posttransplant insulin independence [7]. Other centers that initialized islet transplantation program and adapted the protocol demonstrated comparable outcomes [8, 9]. However, most islet transplant patients returned to insulin injections after a five-year follow-up in Edmonton center. Only ~10% of 65 patients maintained insulin independence, although ~80% remained C-peptide positive. The HbA<sub>1c</sub> level was nevertheless well controlled in those with partial graft function but increased in those without functioning graft (C-peptide negative). By contrast, hypoglycemic events which were quantified by hypoglycemic scores (HYPO scores) [10] remained significantly improved during the 4-year posttransplant [11], suggesting that even a partial graft function can prevent hypoglycemia and stabilize glycemic control.

Several studies have attempted to refine the Edmonton protocol for achieving and maintaining sustained long-term insulin independence, enhancing islet engraftment, and particularly reducing requirement for multiple islet donors. In 2005, Hering et al. demonstrated restoration of insulin independence following transplantation of islet derived from only a single donor in all eight patients who underwent new immunosuppressive treatment including T-cell depleting antibody (TCDAb) antithymocyte globulin, tumor necrosis factor- $\alpha$  inhibitor (TNF- $\alpha$ -i) etanercept, and mycophenolate mofetil [12]. A few years later, the same group published a slightly modified protocol using a different maintenance immunosuppression (cyclosporine and everolimus) while retaining the induction therapy (antithymocyte globulin and etanercept) and demonstrated a prolonged insulin independence for a mean of 3.4 years following transplant in four recipients [13]. A more recent study by the same authors reported promising five-year insulin independence rates in patients (50%) receiving induction drugs either with anti-CD3 monoclonal antibody or with the combination of TCDAb and TNF- $\alpha$ -i, regardless of maintenance immunosuppression [14]. Similarly, other studies have also applied various immunosuppressive regimens [15–18] and used human islet culture for maximizing islet yield at isolation, ensuring its quality of preparation, and decreasing immunogenicity of allograft tissue [15, 16]. The University of Illinois at Chicago demonstrated recently 60% insulin independence rates in a five-year follow-up trial using immunosuppressive agents etanercept and exenatide without TCDAb. Exenatide, a glucagon-like peptide-1 analog, has the potential to maintain islet survival [18]. Together, all attempts aimed to improve immunologic factors such as alloimmune rejection, autoimmune recurrence, and immunosuppressive drug toxicity as well as nonimmunologic factors including exhaustion of marginal  $\beta$ -cell mass [14, 18], all of which have been proposed to cause waning of insulin independence over time. Interestingly, HbA<sub>1c</sub> was retained within an optimal range (<7.2%) for a 5-year follow-up period in 10 islet recipients irrespective of achieving insulin independence [19].

The most comprehensive results of islet transplantation activity in the last decade were provided by the Collaborative Islet Transplant Registry (CITR). The CITR has collected islet transplant data since 1999 from multiple centers including USA, Canada, Europe, and Australia. At a 3-year interval posttransplant analysis of 677 islet-alone or islet-after-kidney recipients, insulin independence was reported to increase significantly from 27% during the period 1999–2002 to 37% and 44%, respectively, for the years 2003–2006 and 2007–2010. Fasting C-peptide levels decreased less steeply over time, indicating a durability improvement of graft function in the later years. The percentage of patients with HbA<sub>1c</sub> levels less than 6.5% or a drop by 2% increased accordingly. Additionally, severe hypoglycemic events, defined if patients require outside assistance, were almost abolished (>90% of patients) during the 5-year follow-up of each interval. Overall, metabolic outcomes in patients receiving islet transplantation in 2007–2010 were improved compared with those in 1999–2006 [20]. A number of advancements in transplantation procedure contribute to improved results, including donor selection, islet isolation, islet culture, and peritransplant management, as well as modification in immunosuppression therapy [14, 20, 21].

Intrahepatic islet transplantation has been consistently shown to reduce [11, 16, 22] or even give full protection from hypoglycemia or severe hypoglycemic episodes [1, 5–9, 12–15, 17, 19] and restore hypoglycemia counterregulation in T1DM patients [23–25]. Severe hypoglycemic events can be prevented in islet recipients while C-peptide remained positive but may recur in those with failed grafts [16, 22] albeit less frequent than those prior to transplantation [26]. Hypoglycemia counterregulatory hormones including glucagon, epinephrine, norepinephrine, cortisol, and growth hormone are usually blunted in T1DM patients but were demonstrated to be restored in islet transplanted recipients [23–25]. Normal suppression of endogenous insulin secretion, improved counterregulatory hormone responses [23–25], and increased endogenous glucose production, as well as decreased systemic and muscle glucose uptake [23] all contribute to improving severe hypoglycemia in islet transplanted T1DM patients. Moreover, islet transplantation can ameliorate insulin sensitivity at both liver and peripheral sites as assessed using hyperinsulinemic-euglycemic clamps in 12 T1DM patients [27]. Fear of hypoglycemia, which was quantified using hypoglycemia fear survey, was reduced substantially in T1DM patients following a single islet infusion and was further improved with subsequent infusions [28], confirming the benefit of islet transplantation to abrogate hypoglycemia.

**1.2. Secondary Diabetic Complications.** Long-term near-normalization of blood glucose levels has been reported to significantly delay the progression of microvascular complications including retinopathy, nephropathy, and neuropathy in T1DM [29–31]. Numerous studies have demonstrated stabilized glycemic control following islet transplantation in T1DM patients [1, 5–7, 9, 11–19, 22]. Thus, it appears that islet transplantation may reduce the risk of developing secondary T1DM complications. However, contradictory results exist

Shrinking motivation to donate organs  
 Allocation of high-quality pancreas in an aging population  
 Attack on intraportally transplanted islets by innate immune system components (Instant Blood mediated Inflammation Reaction IBMIR)  
 Need to repeated transplantations within a few years due to little regenerating capacity  
 No complete freedom from insulin shots  
 Life-long immunosuppression

Box 1: Detriments of cadaveric human islet transplantation.

concerning renal function; some of those studies found elevated creatinine levels, reduced glomerular filtration rate (GFR), and increased albuminuria in islet recipient subjects [5–7, 11, 13, 15–17], while others did not confirm deteriorated kidney function [1, 12, 18]. Moreover, one study demonstrated improvement of kidney graft survival rates, restoration of  $\text{Na}^+/\text{K}^+$ -ATPase activity, reduction of natriuresis, and stable urinary albumin excretion in T1DM patients with islet-kidney transplants [32]. Further improvements such as stable creatinine levels and reduced renal resistance index were observed in 24 islet-kidney recipients compared to those with kidney transplant only [33]. By contrast, three other studies showed renal impairment in both islet-kidney and islet-transplant-alone patients, particularly in those with preexisting defect [34–36]. Possible explanations for these observations could be drug-related side effects of sirolimus and tacrolimus [11, 17, 35, 36] or different baseline kidney function prior to islet transplantation [36]. Notably, no evidence of worsening renal function [37, 38] but a slower decline in GFR was found in T1DM patients following islet transplantation compared to control subjects receiving medical treatment [39], indicating less progression of diabetic nephropathy after islet transplantation.

With regard to the effects of islet transplantation on retina function, most studies generally observed a stabilization of retinopathy. In a 2-year follow-up of eight islet recipients, one patient experienced improvement from mild retinopathy to disappearance of the disease at one year and the other seven patients retained pretransplant retinopathy status throughout the follow-up period [40]. In another study, a significant increase of arterial and venous retinal blood flow velocities was found after one year in 10 islet-transplant-alone patients [41]. Further studies consistently demonstrated reduced progression of retinopathy in T1DM patients receiving islet infusion compared to those treated with intensive medical therapy [38, 39, 42].

Islet transplantation may slow the development and progression of diabetic neuropathy. Both sensory and motor nerve conduction velocities (NCV) remained stable in a 2-year posttransplant follow-up of eight patients [40]. Similarly, no significant differences of NCV were observed in islet transplanted subjects compared to control patients receiving medical therapy after a follow-up of one [38] and six years [39], without any changes from baseline in both groups [38, 39]. A significant improvement in NCV was noticed in 18

patients who received islet-after-kidney transplantation for a 4-year period (versus baseline), albeit not different compared to nine control subjects without islet transplantation [43]. Interestingly, a recent study demonstrated an overall amelioration of sensory parameters in 21 T1DM patients over a 5-year posttransplantation period [44], indicating a potential benefit of islet transplantation for the prevention of neuropathy.

Islet transplantation may have positive effects to slow down macrovascular complications. Several studies have demonstrated improvements in vascular function in islet-kidney recipients, including stabilized intima media thickness, decreased signs of endothelial injuring at skin biopsy, increased endothelial-dependent dilation, restored nitric oxide production, and improved atherothrombotic risk factors with elevated levels of natural anticoagulant protein [45, 46]. An overall improvement in cardiovascular parameters was subsequently reported in T1DM patients with end-stage renal disease who received kidney and functioning islet transplants compared to those without islet transplantation or functioning graft [47]. Finally, a 15-month follow-up showed near-normalization of hemostatic and cerebral abnormalities in 12 islet recipient subjects [48].

Thus islet transplantation is principally effective in clinical studies and in different health care systems. However, there are concerns that imply finding alternative technologies as substitute for cadaveric pancreas (Box 1).

## 2. Unsolved Issues of Human Islet Transplantation

**2.1. Blood Mediated Inflammation at Intravascular Injection.** Multiple transplants are required to achieve significant reduction of insulin shots because a thrombotic reaction occurs immediately when isolated islets are exposed to ABO-compatible blood [58]. The reaction is termed Instant Blood Mediated Inflammatory Reaction (IBMIR) and platelets are suggested to take an active part in it. IBMIR further comprises complement getting started and thrombus formed. Blood clots entrapping islets are believed to cause impairment of insulin production of the transplanted islets due to shutting them off from oxygen and to attracting immunocytes [59]. Platelets aggregated in blood clots are recognized to be involved in IBMIR, cellular matrix organization, and cell proliferation and angiogenesis [60].



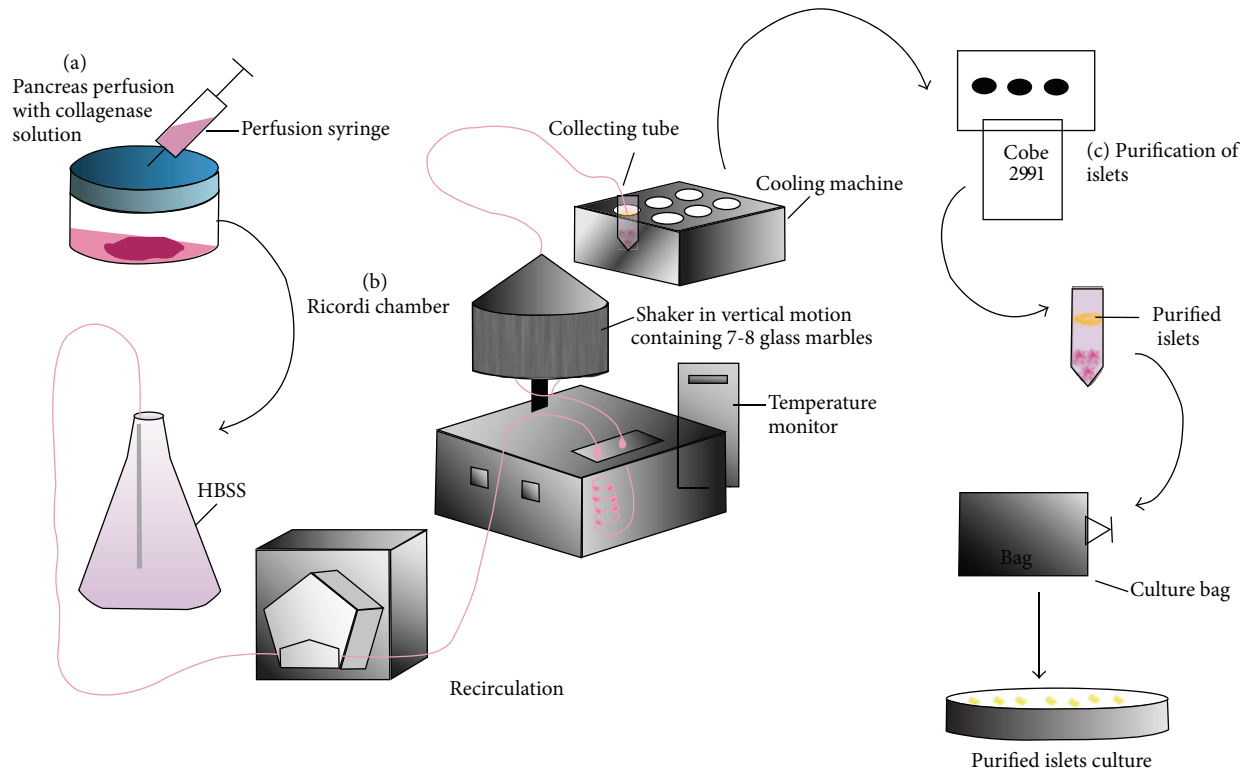


FIGURE 1: Schematic representation on mass islet isolation from human or pig. (a) Pancreas perfusion with collagenase NB 8. (b) Pancreatic digestion. (c) Purification of islets.

*In vivo*, platelets get activated if any damage occurs in a blood vessel. They play an essential role in responding to injury that involves the process of haemostasis, thrombus formation, and vascular and connective tissue healing [70]. Platelets come in contact with damaged or disrupted endothelium of the vessel wall and change their shape as they adhere to the damaged site. Collagen is part of the basal membrane of endothelial cells exposed to platelets at sites of vascular injury. Glycoproteins GPVI and GPIIb/IIIa are collagen receptors on platelet surface. Adherence to collagen IV in particular is followed by release of granules containing ADP and TXA which amplify platelet aggregation [71, 72]. Pancreatic islets isolated with collagenase and injected into the portal vein are assumed to include a sufficient quantity of collagen residues to elicit platelet adhesion. GPVI glycoprotein is a strong mediator of platelet-collagen interaction which is associated with FcR gamma chain coreceptor in human and mouse platelets [73, 74]. Furthermore, secretion of inflammatory cytokines IL-1beta, TNF-alpha, IFN-gamma and secondary agonist, and platelet activating factor (PAF) as well as NO production by immune cells and hepatocytes was observed after islet transplantation [75]. These factors reinforce collagen-induced platelet activation and inflammation resulting in positive feedback and causing instability of the graft [76, 77]. It was observed that CD11b and GR1 positive cells were created in the transplantation, promoting inflammatory cytokines production, and cause early graft loss [78].

**2.2. Organ Quality and Standardized Mass Isolation of Islets.** The primary object of isolating human pancreatic islets is for treatment of type 1 diabetic patients by intraportal injection to restore beta-cells functions. Our group has isolated mass numbers of human and pig islets for research purposes (Figure 1). Attention to key factors like enzymatic digestion of pancreatic tissue containing islets, pH of solutions used in isolation, purification of islets, and temperature during isolation is essential for successful islet isolation and culture to maintain viability for mass production [79, 80]. In principle, the resected pancreas is perfused with collagenase solution consisting of collagenase NB 8 (SERVA Electrophoresis, cat. number I7456) and neutral protease via the pancreatic ducts. After filling with collagenase solution pancreas is transferred to Ricordi Chamber (digestion chamber) [79, 81, 82] on top of the 7 to 8 glass marbles under continuous perfusion with HBSS (Biochrom). The aim is to dissolve connective tissue at room temperature and thus to release the islets from exocrine. The chamber is connected with a tubing system to recirculate fresh solution and maintain dissection temperature between 32 and 37°C. Ricordi Chamber is set in vertical motion; shaking is initiated automatically and manually followed by two centrifugation steps at 80 ×g. Digestion progress is monitored by taking samples repeatedly to identify number and size of isolated islets. Furthermore, islets are purified by centrifugation with a Cobe 2991 using a continuous HBSS-Ficoll gradient. Purified islets fractions are finally cultured either in CMRL 1066 or in RPMI 1640, with supplement

including antibiotic and serum at 37°C [83, 84]. Prolonged cultivation will enhance survival and functional quality of transplanted islets by reducing IBMIR [85, 86].

In the long run, sources of pancreatic beta-cells should be investigated which are more flexible and circumvent all of the disadvantages delineated in Box 1. Recently, pluripotent embryonic stem cells have been extensively studied, but there are major ethical issues. Moreover, teratoma formation prevented clinical studies up to now. One of the more promising options is the use of multipotent adult stem cells because they can be retrieved from the same individual, they are less prone to malignant transformation compared to embryonic stem cells (ESC), and clinical trials in diabetes treatment have successfully been initiated [87, 88].

### 3. Mesenchymal Stem Cells

Mesenchymal stem cells (MSCs) are nonhematopoietic, multipotent, self-renewing cells. First they were isolated and described from bone marrow in 1968 and described as adherent, spindle-shaped, and with the ability to differentiate into bone and cartilage [89]. They were described as stromal cells [90, 91] and later also as mesenchymal stem cells [92]. Since then it was discovered that mesenchymal stem cells can originate from a wide range of different tissues such as skeletal muscle [93], skin and foreskin [94, 95], adipose tissue (AD-MSC or AT-MSC or ASCs) [96], pancreas (P-MSCs) [97], dental pulp (DPSCs) [98], salivary gland [99], endometrium [100], placenta (PL-MSCs) [101], amniotic membrane and fluid (AM-MSCs) [102–105], umbilical cord matrix/umbilical cord blood (UC-MSCs/UCB-MSCs) [106, 107], and Wharton's jelly (WT-MSCs) [108].

First it was thought that MSCs could only differentiate into somatic cells of the same germ layer, but they have shown a much higher level of plasticity and are able to differentiate *in vitro* across germinal boundaries. To date, MSCs have been shown to differentiate *in vitro* into adipocytes, chondrocytes, osteoblasts, myoblasts, tenocytes, cardiomyocytes, marrow stromal cells, hepatocytes, endothelial cells, hematopoietic cells, neuronal cells, renal cells, and pancreatic cells [49, 96, 109–120].

According to the International Society for Cellular Therapy (ISCT), the standard criteria for all human MSC are threefold: plastic adherence under standard culture conditions; a positive phenotype ( $\geq 95\%$ ) for CD105, CD73, and CD90; and a negative phenotype ( $\leq 2\%$ ) for CD45, CD34, CD14, or CD11b; CD79alpha or CD19; HLA-DR; they must be able to differentiate to adipocytes, chondroblasts, and osteoblasts under standard *in vitro* culture conditions, demonstrated by *in vitro* staining. As MSCs have to be isolated from surrounding tissue and infiltrating cell types, like immune cells, blood cells, and endothelial cells, negative phenotype antigens were selected to exclude these other cell types. To determine the state of stimulation of MSCs, the surface marker HLA-DR is chosen. Unstimulated, HLA-DR is not expressed but, after stimulation, for example, with IFN- $\gamma$ , HLA-DR is expressed on the cell surface [121, 122].

### 4. Bone Marrow Mesenchymal Stem Cells (BM-MSCs) and Adipose Tissue Derived Mesenchymal Stem Cells (AT-MSCs, ASCs, and AD-MSCs)

BM-MSCs and AD-MSCs are very similar in their expression pattern of surface markers; both express the marker which identifies them as MSC according to the ISCT guidelines as described before. Accordingly, both cell types are positive for CD105, CD73, and CD90 [121]. Several research groups published new markers for MSC and propose that these should be added to the list of suitable markers to describe them, like STRO-1 [123, 124], STRO-3 [125], CD56, CD271, mesenchymal stem cell antigen-1 (MSCA-1) [126, 127], and CD166 (ALCAM) [109]. Additionally, BM-MSCs and AD-MSCs both show expression of CD177 (stem cell factor receptor) [128], CD29 (beta-1 integrin), CD44 (hyaluronate receptor), CD49e (alpha-5 integrin, important for cell adhesion to fibronectin), CD146 [109], CD9, CD10, CD13, and CD59 [129].

Although the patterns of surface markers expressed from AD-MSCs and BM-MSCs are very similar, there are some differences: BM-MSCs are positive for CD106 (VCAM-1), which lacks in AD-MSCs, and they are negative for CD49d (VLA-4), which is strongly expressed in AD-MSCs [130, 131]. Interestingly, CD106 is the receptor for the related agonist CD49d and these molecules are involved in hematopoietic stem and progenitor cell homing to and mobilization from the bone marrow [132, 133]. Both express CD54 (ICAM-1), but AD-MSCs are in higher levels compared to BM-MSCs [130]. AD-MSCs can be retrieved in a much higher number and under surgical easier conditions with lesser pain for the patient or donor than BM-MSCs [134] and they tend to be genetically more stable in long-term culture [135, 136]. AD-MSCs and BM-MSCs express Nestin and the pancreatic transcription factors ISL-1 and Pax6, which indicates that the use of these for endodermal differentiation may be advantageous, compared to other MSCs [49–51, 69].

### 5. Immunomodulatory/Immunosuppressive Effects of MSCs

**5.1. MSCs as “Helper” Cells in Transplantation.** Transfusion of MSCs in streptozotocin-induced diabetes in mice reduces hyperglycemia and enhances beta-cell function and survival. However, it is not clear whether this is caused by the MSCs themselves or through the release of trophic factors [137, 138].

Cotransplantation of MSCs with pancreatic islets in mice leads to improved islet function and survival. Borg et al. observed improved glucose homeostasis and reduced islet apoptosis after cotransplantation of islets with MSC at three different locations: kidney capsule, liver, and eye. According to the authors, MSCs did not increase beta-cell proliferation and MSC differentiation into pancreatic beta-cells could not be detected [139].

MSCs from various tissues show immunomodulatory and/or immunosuppressive properties. Transplanted or cotransplanted MSCs decrease proliferation and activation

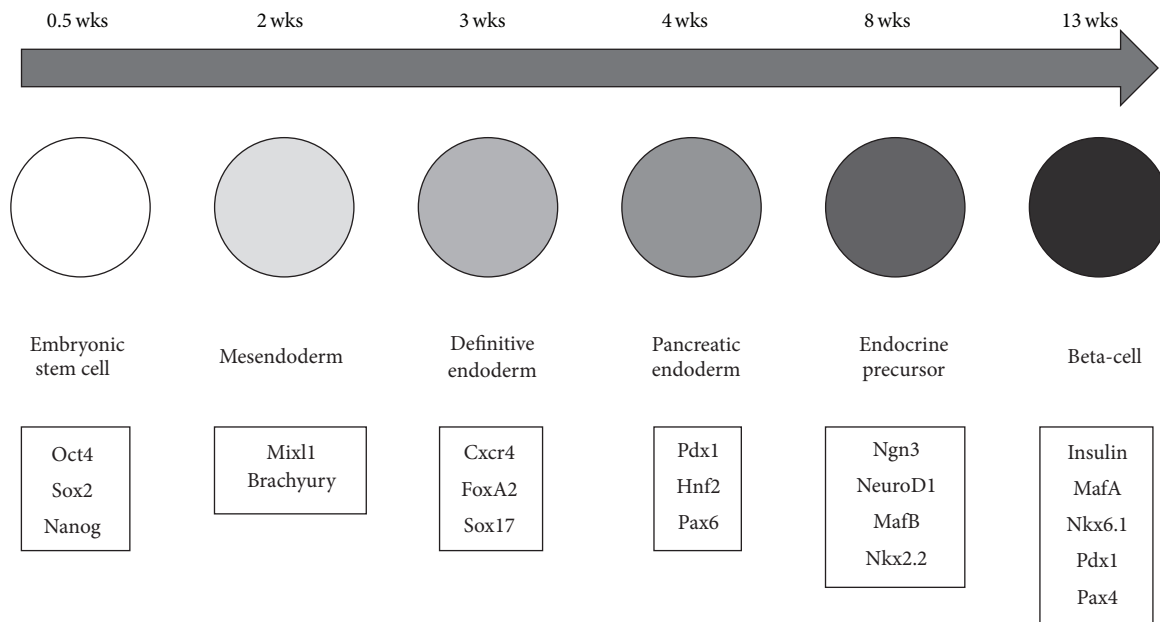


FIGURE 2: Beta-cell development-scheme in human embryo.

of T-cells, dendritic cells, and NK cells in the recipient. They decrease the secretion of inflammatory cytokines, like IFN-gamma, TNF-alpha, GM-CSF, and MCP-1. Additionally, they act as immunomodulator and help in the establishment of a graft vascular network by secreting angiogenic paracrine factors as VEGF, IL-6, IL-8, HGF, PDGF, and TGF beta and the secretion of matrix metalloproteinases. Furthermore, TGF beta, HGF, and IL-6 have antiapoptotic effects and increase the expression of protective genes against hypoxia [140–143].

## 6. Endocrine Pancreas Cell Lineage

Pancreatic development is a highly regulated and complex process, which is guided by multiple signaling pathways and transcription factor cascades (Figure 2). First epiblast cells ingress in the primitive streak to form the mesendoderm, characterized by the transcription factors *Mixl1* and *Brachyury*, and then the definitive endoderm [144, 145]. Definitive endoderm cells expressing transcription factors such as *Cxcr4*, *FoxA2*, and *Sox17* form the gastrointestinal organs, such as liver, lungs, thymus, respiratory and digestive tract, and pancreas [146–148]. They are, however, not committed towards a specific cell or tissue lineage in the initial differentiation. Thus, an important specification step occurs when the definitive endoderm cells form the posterior gut endoderm, which develops subsequently into the intestines [147, 149]. At the foregut-midgut junction, the expression factor *Pdx1* is expressed. *Pdx1*-positive cells were shown to contribute to the formation of exocrine and endocrine compartments of the pancreas [150, 151]. Posterior and anterior foregut endoderm develop into the ventral and dorsal pancreatic buds. In this phase, the interaction with the mesoderm-driven neighboring tissues, cardiac mesenchyme at the ventral bud and notochord at the dorsal bud, regulates

pancreas organogenesis and the subsequent specification steps [152]. Involved morphogens are activin A and fibroblast growth factor (FGF) from the notochord and fibroblast growth factor and bone morphogenic proteins from the cardiac mesoderm [148, 151, 153, 154].

After this, the pancreatic buds are formed from multipotent progenitors that contribute to all pancreatic cell types. These epithelial buds invade the surrounding mesenchyme by successive waves of branching morphogenesis called the primary and secondary transition. The period of active pancreatic progenitor proliferation, followed by expansion of the epithelial network, is identified as primary transition. The first endocrine cells are detected at this stage [155, 156]. In the secondary transition, the morphogenetic transformation of pancreatic epithelium occurs. The specification of the multipotent progenitors towards the differentiated lineages occurs in this period. Particularly, the endocrine cell specification and differentiation occur via the inhibition of Notch signaling, which leads to the expression of *Ngn3* [157, 158]. This triggers the expression of a multitude of expression factors, including *Nkx2.2*, *NeuroD*, *Nkx6.1*, *Pax4*, *Pax6*, and *Isl1*, controlling endocrine cell differentiation [151, 159]. Afterwards those endocrine cells begin pancreatic islet morphogenesis through aggregation into small cell clusters [160]. The final maturation of the Langerhans islets takes place after birth [161].

Two crucial postnatal maturation events need to occur for fully functional beta-cells: (1) glucose sensing is enhanced and the amount of insulin-containing dense core secretory granules increases. (2) Beta-cell mass appropriate to the individual body weight is established. Several genes encoding important factors are involved in this process of postnatal beta-cell maturation: insulin and preproinsulin; glucose transporter (*Glut2*) and glucokinase (*GK*); *Pdx1*, *MafA*, and *NeuroD* (important transcription factors for development

TABLE 1: Factors involved in beta-cell differentiation.

Compound	Role in beta-cell differentiation
High glucose	Increases beta-cell replication
Activin A	Promotes beta-cell regeneration and increases cell mass
N2 and B27 supplements	Act as serum supplements in serum-free medium
FGF2	Is important in early stage differentiation
EGF	Accelerates beta-cell proliferation and supports final stages of insulin expression
Beta-cellulin	Promotes beta-cell regeneration and increases cell mass
HGF	Induces beta-cell formation, especially in combination with activin A
RA	Induces endocrine and ductal differentiation and induces insulin-positive differentiation
GLP-1	Accelerates maturation of beta-cells towards glucose responsive insulin secretion
Exendin-4	Accelerates maturation of beta-cells towards glucose responsive insulin secretion
Pentagastrin	Expands beta-cell mass in combination with other factors

and function of mature beta-cells) [151, 162–164]. How the postnatal maturation occurs in detail is still largely unknown [165].

## 7. Differentiation of MSCs via Chemical Compounds

Most chemical differentiation protocols are based, with slight modifications, on the original protocol from Timper et al., 2006. The general approach of the Timper et al. strategy is a protocol consisting of one or two steps aiming to directly differentiate MSCs to insulin-producing cells (IPCs) without following the developmental steps known from embryonic pancreas development. Culture medium contained high glucose concentrations, activin A, nicotinamide, Exendin-4, HGF, and pentagastrin among other supplements (Table 1). Following the procedure, MSCs expressed nestin, SCF, Thyl (CD90), Pax6, and Isl1. While Isl1, Pdx1 (=Ipfl), and Ngn3 were upregulated, the expression level of Pax6 remained unchanged. Besides insulin, specific for beta-cells, expression of glucagon (alpha-cell) and somatostatin (delta-cell) was reported [49].

Dave et al. adjusted the differentiation process developed by Timper et al. onto a serum-free condition using 20% human albumin instead (Figure 3). The cultured cells were described as positive for Pax6, Isl1, and Pdx1 and they were insulin and C-peptide positive upon glucose stimulation (Table 2). They also proposed that stepwise and long-term culture conditions over several weeks would not be necessary [52]. This would be contradictory to the findings of other groups, as described below.

The second major approach is adapted from protocols for beta-cell differentiation from embryonic stem cells (ESCs), trying to mimic the steps in human pancreas development via a stepwise differentiation. Therefore, the added chemicals are changed every two to three days, accompanied by measuring the expression of typical markers of the expected stage, like definitive endoderm or pancreatic progenitor cells (Figure 3).

Li et al. found an upregulation of Brachyury, Mixl1 (mesendoderm-related genes), FoxA2, Sox17 (DE-related genes), Sox1, and Pax6 (ectoderm-related genes) depending on activin exposure in a dosage dependent manner. They did

not find upregulation of mesoderm related genes (Figure 3). Activation of Wnt-signaling in step 1 reduced the expression of ectodermal and favored endodermal genes. To drive DE cells towards pancreatic progenitor (PP) cells the cells were cultivated with a Wnt-signaling inhibitor, retinoic acid (RA), FGF2, and other cytokines. After 6 days, pancreatic endoderm and progenitor cell markers, like Pdx1, Sox9, Hnf6, Nkx2.2, and Nkx6.1, were upregulated and the expression of FoxA2, Sox17 (DE-related genes), and Mixl1 (mesendoderm-related gene) was downregulated. The combined approach of activating RA/FGF signals and inhibiting Wnt signals was reported to provide similar results to differentiation protocols of ESCs and iPS-cells. Is this more evidence that MSCs are a suitable substitute for ESCs? Li et al. studied the differentiation potential of AD-MSC-derived PP cells to further differentiate into downstream endocrine and exocrine pancreatic lineages. They found cooverexpression of insulin (beta-cell-specific), glucagon (alpha-cell-specific), somatostatin (delta-cell-specific), pancreatic polypeptide (PP) (PP-cell-specific), ghrelin (epsilon-cell-specific), MafA, and Glut2. Not all expressed proteins were specific for beta-cells. Rather a potpourri of hormones expressed from immature endocrine islet cells was detected. Still, those immature cells responded upon glucose stimulation with insulin/C-peptide. Moreover, PP cells were shown to be driven towards an exocrine expression pattern [53].

When BM-MSCs were cultured for several weeks up to months in the presence of high glucose concentrations, a differentiation process was promoted initially, but at a later stage low glucose and low serum conditions were beneficial to raise glucose-sensitive IPCs, characterized by Pdx1, Ngn3, Isl1, NeuroD, Pax4, and insulin. Interestingly, IPCs did not overlap with other endocrine cell types. Reduction of hyperglycemia, but unfortunately also tumor formation, was reported [166]. Mohamad Buang et al. [54] chose a two-step protocol over 21 days for AD-MSCs. They found that round cells after two weeks which started to form clusters could be positively stained with dithizone (DTZ) and contained small secretory granules, all characteristics for beta-cells. They released insulin in a glucose responsive manner. Similar to Tang et al. [166], they utilized high glucose followed by low glucose concentrations in the culture media.

TABLE 2: Resultant expression of key pancreatic transcription factors, hormones, and improvement of diabetes *in vivo* after differentiation of MSCs via chemical compounds.

	Cell source	PDX-1	FoxA2/HNF3β	NGN-3	Pax-4	Pax-6	NeuroD	Isl-1	Glut-2	GCK	Insulin	Glucagon	Somatostatin	C-peptide	DTZ staining	GSIS <i>in vitro</i>	GSIS <i>in vivo</i>	Ameliorates diabetes
Dave et al. 2014 [52]		+	ND	ND	ND	+	ND	+	ND	ND	+	ND	ND	+	ND	+	Tx human	
Li et al. 2013 [53]		+	+	ND	ND	+	ND	ND	+	ND	+	+	Like basal	+	ND	+	ND	ND
Marappagounder et al. 2013 [51]	Adipose	+	ND	+	+	ND	ND	+	ND	ND	+	ND	ND	ND	+	+	ND	ND
Mohamad Buang et al. 2012 [54]	tissue	ND	ND	ND	ND	ND	ND	ND	ND	ND	+	ND	ND	ND	+	+	+	+
Chandra et al. 2011 [50]		+	+	+	+	+	+	+	+	ND	+	+	+	+	ND	+	+	+
Timper et al. 2006 [49]		+	ND	+	ND	Like basal	ND	+	ND	ND	+	+	+	+	ND	ND	ND	ND
Gabr et al. 2015 [56]		+(Tx)	ND	ND	ND	ND	ND	ND	+(Tx)	+(Tx)	+(Tx)	+(Tx)	+(Tx)	+(Tx)	+	ND	+(Tx)	+(Tx)
Czubak et al. 2014 [55]	Bone marrow	ND	ND	ND	ND	ND	ND	ND	ND	ND	ND	ND	ND	+	+	+	+	+
Jafarian et al. 2014 [57]		+	+	+	+	ND	ND	ND	+	ND	+	+	+	+	+	+	+	+
Marappagounder et al. 2013 [51]		+	ND	+	+	+	ND	+	ND	ND	+	ND	ND	ND	+	+	ND	ND

ND = not determined, Tx after transplantation of MSC, and Tx (human) = recent clinical trial [61].



AD-MSCs		<div>Days</div> <div>012345678910111213141516171819202122232425</div>																											
	Normal growth media																												
Dave et al. 2014	$\alpha$ -MEM, 20% human albumin, FGF2, pyruvate	DMEM/F-12 (1:1), B-27, N-2														Activin A, nicotinamide, Exendin-4, HGF, pentagastrin													
Li et al. 2013	$\alpha$ -MEM, 20% human albumin, FGF2, pyruvate, dexamethasone, IL-6, EGF, PDGF BB	DMEM-LG, 0,5% FBS														DMEM-LG, 0,5% FBS, B-27, N2, NEAA													
		Activin A, Wnt3a	Activin A												RA, Dkk1, EGF, FGF2	Exendin-4, activin A, nicotinamide													
Marappagounder et al. 2013	DMEM-LG, 10% FBS	DMEM-HG, 10% FBS				DMEM-LG, serum-free, N-2, B27																							
		RA				Activin A, Nicotinamide, EGF												Activin A, nicotinamide, EGF, Exendin-4											
Mohamad Buang et al. 2012	DMEM, 10% FBS	DMEM-HG, 10% FBS														DMEM-LG, 10% FBS													
		Nicotinamide, activin A, GLP-1														Nicotinamide, activin A, GLP-1													
Chandra et al. 2011	DMEM/ Ham's F12	Serum-free medium (SFM), DMEM/F12 (1:1), HG, BSA, ITS																											
		Activin A, Na-butyrate, FGF2				Taurine				Taurine, GLP-1, nicotinamide																			
Timper et al. 2006	DMEM, 10% FBS, FGF2, pyruvate	DMEM/F-12, HG, B-27, N-2																											
		Activin A, nicotinamide, Exendin-4, HGF, pentagastrin																											
BM-MSCs		<div>Days</div> <div>012345678910111213141516171819202122232425</div>																											
	Normal growth media																												
Gabr et al. 2015	DMEM-LG, 10% FBS	DMEM-LG, serum-free				DMEM-HG/DMEM/F-12 (1:1), 10% FBS																							
		Trichostatin A				GLP-1																							
Czubak et al. 2014	DMEM-LG, 10% FBS	DMEM-HG serum-free				DMEM-HG, serum-free, NEAA, B-27										DMEM-HG, serum-free, B-27													
		$\beta$ - Mercapto- ethanol				FGF2, EGF										$\beta$ -cellulin, activin A, nicotinamide													
Jafarian et al. 2014	DMEM-LG, 10% FBS	DMEM : F-12 (1:1), serum-free, HG, BSA, ITS										DMEM : F-12 (1:1), serum-free , HG, BSA, ITS										DMEM : F-12 (1:1), serum free, HG, BSA, ITS, B-27, N-2, NEAA							
		Activin A, taurine, butyrate, HGF										Exendin-4, taurine										Exendin-4, activin A, nicotinamide							
Marappagounder et al. 2013	DMEM-LG, 10% FBS	DMEM-HG, 10% FBS				DMEM-LG, serum-free, N-2, B-27								DMEM-LG, serum-free, N-2, B-27															
		RA				Activin A, nicotinamide, EGF								Activin A, nicotinamide, EGF, Exendin-4															

FIGURE 3: Differentiation of MSCs via chemical compounds. AD-MSCs [49–54] and BM-MSCs [51, 55–57].

One group examined human BM-MSCs and human AD-MSCs in a three-step protocol in parallel. Both cell types could differentiate into IPCs with BM-MSCs-derived IPCs appearing to generate more islet-like clusters than

those derived from AD-MSCs. The gene expression profile included nestin, Pdx1, Isl-1, Pax4, and Ngn3 and was similar in both cell types, also showing glucose dependent insulin release (Table 2). MSCs from both sources seem

to be useful for beta-cell replacement strategies [51]. The authors concluded that BM-MSCs are more feasible for MSC differentiation towards IPCs than AD-MSCs. However, due to the expression profiles of both experiments being nearly identical to each other, this conclusion seems rather premature and optimistic and is in need of confirmation.

The advantage of a stepwise procedure is the possibility of obtaining progenitor cells first, which can be directed to pancreatic cell types in the last step. For example, recent studies postulate that Wnt- and BMP-signaling are relevant for differentiating MSCs indicating that MSCs are directed towards beta-cell differentiation like iPS cells. Therefore, in early differentiation steps, Wnt should be activated but in later stages inhibited. In stepwise differentiation protocols, the signaling pathways can be better controlled, postulating an advantage of stepwise differentiation protocols over one-step protocols [53].

How to reproduce competent pancreatic progenitors is actually under debate. There are no consensus reagents or standard protocols available to characterize progenitor cell lines. Moreover, it is not clear if differentiation of MSCs should undergo the same stages as embryonic cells/embryonic stem cells. Whether MSCs can fully transdifferentiate into cells of other germ layers is under discussion, because developmental biologists have restricted the definition of transdifferentiation to an irreversible switch of one cell type to another [167]. In several studies, MSCs showed a new expression pattern of formerly not expressed genes specific to the new somatic cell type; on the other hand they still express MSC specific markers, like CD90 and CD73. Given these results, transdifferentiation of MSC may need to be reevaluated.

## 8. Differentiation of MSCs via Genetic Manipulation

Experiments with transgenic mice have identified essential transcription factors that control the formation of islets during embryonic development; among these are FoxA2 (formerly named HNF3beta), PDX1 (IPF1), NGN3 (NeuroG3), NeuroD1, Nkx2.2, Pax4, Nkx6.1, and Pax6. Among these factors, FoxA2 and PDX1 play a central role in initiating the differentiation of the beta-cells.

Several research groups induced differentiation in MSCs through overexpression of genes involved in the beta-cell development and beta-cell function, either by transduction with viral vectors, like lentivirus or adenovirus, or by transfection with plasmids. Some tried PDX1 gene alone and others in combination with NGN3 or NGN3 and MafA. Only few groups tried other genes like FoxA2 or HLXB9 (Table 3).

In the studies, which induced differentiation through the selective overexpression of PDX1, several key transcription factors are increased by exogenous PDX1, like FoxA2, Nkx2.2, and NeuroD (Table 3). However, FoxA2 is not specific for pancreas development; it also plays a role in the hepatic lineage. Lee et al. changed the medium to a high glucose containing one for up to 4 weeks, when over 60% of the cells were PDX1-positive following infection. During this

time period, PDX1-induced cells began to form clusters [63]. Allahverdi et al. also transduced Pdx1 but did not change the medium to high glucose [67]. All groups reported morphological alterations after 3 to 5 days and cluster formation after 7 or 14 days [63, 65, 67]. At the same time, cell proliferation slowed down. Lee et al. and Lin et al. found FoxA2, Nkx2.2, and NeuroD at low basal expression levels in nontransduced control cells and upregulated in PDX1-overexpressing cells under high glucose conditions. Additionally, GLP-1, glucokinase (GK), and GLUT2 were expressed at low level with PDX1 induction. Mouse PDX1 overexpression induces the expression of the human homolog PDX1 (=IPF1). It was concluded that PDX1 was able to upregulate its own expression [63]. In contrast, Karnieli et al. did not find activation of the human Pdx1 gene through rat Pdx1 overexpression [69]. Transplantation of PDX1-overexpressing hAD-MSCs into diabetic rodents reduced blood glucose levels and prevented severe hyperglycemic states but did not achieve euglycemia. The transplanted cells stained positive for insulin [63, 65]. Karnieli et al. did not find Ngn3 expression and only found NeuroD1 expression after transplantation of Pdx1<sup>+</sup> MSCs in STZ-induced diabetic mice. They postulated a maturation process *in vivo*. Allahverdi et al. measured Pdx1 and insulin and detected a higher expression of Pdx1 not earlier than day 7 and insulin not before day 14 with maximum expression of both at day 21 after transplantation. Insulin and C-peptide levels stimulated by glucose were increased in recipients of transplants [67]. As they did not compare insulin and C-peptide secretion to nondiabetic individuals, there is no conclusion whether the quantity of released insulin was biologically significant. Karnieli et al. reported that insulin release after glucose challenge was clearly subnormal [69].

Two studies directly compared insulin release of manipulated MSCs through genetic manipulation, chemical compounds, and conditioned medium with human islets and/or cocultured human islets [68, 168]. Moriscot et al. compared different infection rates of the adenovirus, different transcription genes PDX1, FoxA2, and/or HLXB9. Transduction was combined with conditioned medium from pancreatic islets or chemical compounds. They observed different transcription factor patterns, depending on the virus titer. If the multiplicity of infection (MOI) ratio was high, insulin would be released from the cells. On the other hand, coculture or conditioned medium from pancreatic islets was additionally needed with low MOIs. Some of their protocols resulted in Pax4, Isl1, NGN3, and insulin expression, while in others only Pax4 or Pax4 and low insulin were expressed [168].

Limbert et al. compared chemical differentiation with genetic manipulated differentiation. One very important finding was that chemical differentiation leads to clustered cells with decreasing proliferation till the cells died after two weeks in culture. Cells induced by chemicals expressed Pax4, Isl1, Pdx1, NeuroD, somatostatin, pancreatic polypeptide (PP), insulin, and Glut2 but neither Ngn3 nor glucagon. Pax6 was detected in untreated and treated MSCs as well. In contrast to chemical induction, Pdx1, Ngn3, and Pdx1-Ngn3-cooverexpression did not result in distinct islet-like clusters in the genetically treated cells. Combined overexpression showed induction of Pax4, Isl1, GLUT2, insulin, glucagon, PP,

TABLE 3: Overview of studies addressing ectopic transduction of genes to promote beta-cell differentiation in BM-MSC and AD-MSC. Resultant expression of key pancreatic transcription factors, hormones, and improvement of diabetes *in vivo*.

	Cell source	PDX-1	FoxA2/HNF3β	NGN-3	Pax-4	Pax-6	NeuroD	Isl-1	Glut-2	GCK	Insulin	Glucagon	Somatostatin	C-peptide	DTZ staining	GSIS <i>in vitro</i>	GSIS <i>in vivo</i>	Ameliorates diabetes
<i>Adipose tissue</i>																		
Bahrebar et al. 2015 [62]	LV-Pdx1	+	ND	+	ND	ND	ND	ND	ND	ND	+	ND	ND	ND	+	+	ND	ND
Lee et al. 2013 [63]	pAd-Pdx1-ZsGreen	+	+	ND	ND	ND	+	ND	+	+	+	ND	ND	+	ND	+	+	-
Boroujeni and Aleyasin 2013 [64]	LV-Pdx1	+	ND	+	ND	ND	ND	ND	+	ND	+	+	+	ND	ND	+	+	+
Lin et al. 2009 [65]	LV-Pdx1	+	ND	ND	ND	ND	+	ND	ND	ND	+	+	ND	ND	ND	+	ND	+
<i>Bone marrow</i>																		
Jafarian et al. 2015 [66]	miR-375, anti-miR-9	+	+	+	ND	ND	ND	ND	+	ND	+	+	+	+	+	+	ND	ND
Allahverdi et al. 2015 [67]	LV-Pdx1	+	ND	ND	ND	ND	ND	ND	ND	ND	+	ND	ND	+	ND	+	ND	ND
Limbert et al. 2011 [68]	Pdx1-pDNA6/Ngn3-pcDNA3.1	+	ND	+	+	+	+	+	+	+	+	+	+	+	ND	-	ND	ND
	Pdx1-pDNA6	+	ND	-	+	+	+	+	+	+	+	+	+	+	ND	-	ND	ND
Limbert et al. 2011 [68]	Ngn3-pcDNA3.1	+	ND	+	+	+	+	+	+	+	+	+	+	+	ND	-	ND	ND
Karnieli et al. 2007 [69]	RV-Pdx1	+	ND	-	+	Like basal	-	Like basal	+	+	+	+	Like basal	+	ND	+	ND	+

and somatostatin. Pax6 expression was also upregulated. C-peptide and insulin expression remained below biologically significant levels and as the cells also expressed non-beta-cell hormones, a further maturation of these cells was desired [68].

Boroujeni and Aleyasin combined exogenous Pdx1 lentiviral expression with high glucose medium containing additional compounds, nicotinamide, and bFGF for 21 days. After 7–10 days of culture, Pdx1<sup>+</sup> MSCs changed their morphology and formed clusters. Higher expression of Pdx1, Ngn3, Glut2, and somatostatin was detected. After transplantation of these cells in diabetic mice, hyperglycemia was reverted [64].

Recently Bahrebar et al. combined Pdx1 transfection with cultivation under high glucose condition till islet-like clusters were formed after 10 days of cultivation. Pdx1, Ngn3, Nkx2.2, and insulin gene expressions were measured in the group transduced with Pdx1 [62]. Insulin gene activation was glucose responsive and it was concluded that cultivation of Pdx1<sup>+</sup> MSCs in high glucose was beneficial to the maturation of these cells towards a beta-cell phenotype [54]. Posttransplant maturation of *in vitro* differentiated MSCs was claimed [56, 65, 69]. By contrast, spontaneous *in vivo* maturation without prior specific cultivation protocol was denied [169].

Jafarian et al. utilized microRNAs (miRNAs) to differentiate MSCs towards insulin-producing cells. Several miRNAs have potential roles in pancreas development, islet function, and insulin secretion. miR-375 was involved in pancreas development and control of insulin gene expression. miR-9 downregulated insulin expression and was described as a negative regulator for insulin-producing cells [170–173]. MSCs were transduced with miR-375 and anti-miR-9. The morphology of the MSCs changed within 3 days from spindle-like to round cells and in the next 14 days cell clusters formed. The clusters showed gene upregulation of Sox17, FoxA2, Nkx2.2, Glut2, Pdx1, Ngn3, insulin, PP, and somatostatin (Table 3). Cells cotransduced with miR-375 and anti-miR-9 proved to be insulin glucose dependent and therefore they showed synergistic effects in MSC differentiation to insulin-producing cells [66].

Most groups agree that reduction of hyperglycemia via transplantation of differentiated MSCs should be further investigated to elucidate the underlying mechanisms. MSCs do not strictly possess beta-cell characteristics prior to transplantation as only part of the genes important for beta-cell function are detectable. Other issues are first the number of cells that are required to significantly reduce blood glucose and second how to improve the condition of the cells at the time of transplantation to increase their *in vivo* viability [65].

## 9. Prerequisites for Clinical Use of Insulin-Producing Cells Derived from Differentiated MSCs

In spite of a lot of different approaches to differentiate MSCs towards insulin-producing cells and trials toward the curing potential of IPCs in animal models, there are still some issues which are not yet addressed but are crucial for clinical

application. The outstanding concerns are, for example, as follows: “Are obtained IPCs stable in *in vivo* conditions or is dedifferentiation an issue?” “Which of the protocols are adaptable to xeno-free, GMP-complaint standard procedures?” “Is it enough to transplant insulin-producing cells, which are only part of functional islets?” What can we learn from islet transplantation and what can be adapted from those approaches to MSCs-derived IPCs? Are the IPCs on the long term stable? What about cell viability subsequent to transplantation?

The following list delineates major prerequisites for clinical use of IPCs derived from MSCs:

- (1) High purity and quality of cells in terms of bacterial, viral, and mycoplasma contamination; no animal-derived substances including safety tested compounds of animal origin.
- (2) Culturing, expanding, and biobanking of MSCs under GMP conditions.
- (3) Quality of *in vitro* generated cells: pancreatic islets as control cells, glucose responsiveness of C-peptide, and/or insulin expression close to physiological conditions.
- (4) Long-term *in vitro* and *in vivo* stability of IPCs derived from MSCs.
- (5) Exact dosage of MSC-derived IPCs to reverse diabetic condition and feasibility of producing such dosage *in vitro*.
- (6) Improvement of cell survival after transplantation, engraftment, and homing of IPCs and MSCs.
- (7) Exclusion of tumor risks.

It is of importance to bring the glucose responsiveness and the maturation of the IPCs to a similar level of original beta-cells. At present, glucose dependent insulin release is in most reported studies far below physiological level of beta-cells [68, 69, 168, 174, 175]. If insulin expression and release cannot be significantly raised, transplanted patients will be still dependent on insulin shots. Given transplantation of allogenic, gene-manipulated tissue as such an invasive procedure, the expected outcome does not justify the potential risks. The goal should not only be to ameliorate blood glucose levels and to prevent acute events of diabetic ketoacidosis but to give diabetes patients the chance of normal life [175, 176].

A very important question for the clinical use of MSCs is the risk of tumor formation. There are contradictory reports, some excluding tumors, but others measured changes in karyotype and telomere length, describing the presence of tumor markers, and some groups even reported *in vivo* tumor formation in mice. However, MSC culture conditions potentially leading to tumor formation were not investigated. Unfortunately, in publications observing tumor growth, GMP standards were not reported. Additionally, whether immunosuppressive properties of MSCs cause adverse effects is discussed, such as infections or graft versus host disease. A series of clinical trials using MSCs for treatment purpose is already going on [64, 166, 177–180]. It seems that if MSCs

pose a risk of tumor formation, it can be hypothesized to be a lot weaker and perhaps better controllable as in the case of ESCs and iPS cells.

In spite of immunosuppressive properties of MSCs, there is still evidence of graft rejection and impaired cell survival after transplantation which calls for further investigation and leads to the prerequisite that pretransplantation conditions have to be optimized. There is only little data available in this direction of preconditioning the MSCs before transplantation to increase *in vivo* viability, but further research is certainly required.

## 10. Increase of Survival of MSC for Transplantation and Clinical Application

After transplantation of MSCs, most of them diminish due to apoptosis [181]. To overcome the current limitation and improve transplantation therapy, pretreatment of MSCs with different modulatory factors is an approach to boost their predefined potential for type 1 diabetes and other disorders.

When MSCs were cultivated at hypoxia or when transplanted *in vivo*, MSCs likewise suffered from low oxygen concentration (0.5% to 2.3%) [182–184]. This change in O<sub>2</sub> concentration of MSCs may contribute to DNA damage and early senescence [185–187]. However, hypoxia-inducible factor 1 (HIF-1) plays vital role in regulating different gene expression of stem cells in cellular response to hypoxia and pretreatment of MSCs with hypoxia condition can improve engraftment potential [187]. Liu et al. demonstrated increase in angiogenic factor (HIF-1, ANG, VEGF, and MMP-9) and Bcl-2 expression with hypoxic preconditioned MSC (5% O<sub>2</sub>) [188]. Therefore, hypoxia can provide a protective shelter to transplanted MSCs to some extent. Apelin 13 is an endogenous ligand for G protein coupled APJ receptor [189]. Apelin has been involved in maintaining cardiovascular functions and other biological activities [190]. HIF-1 pathway provides protective effect to hypoxic treated MSCs as discussed above. However, hyperglycemia along with hypoxia preconditioned MSCs could produce reactive oxygen species and affect cell integrity [191, 192]. Apelin 13 provides the protective effect from apoptosis via MAPK/ERK1/2 and PI3K/AKT signaling pathways in bone marrow derived mesenchymal stem cells [193]. Mottaghi et al. hypothesized that pretreatment of hypoxic preconditioned mesenchymal stem cells with apelin 13 could provide protective effect against apoptosis in stem cell transplantation therapy by reducing ROS level via MAPK/ERK1/2 and PI3K/AKT signaling pathways [192]. Therefore, hypoxia-MSCs-apelin 13 combination can be considered as one strategy to rescue transplanted cells in diabetic condition.

Pretreatment with modulatory factors can ameliorate the surviving capacity and engraftment properties and have potential to resolve current limitation of MSCs in transplantation therapy. However future strategies and better understanding of unfavorable microenvironment of post-transplanted MSCs could provide a better approach.

## 11. More Efficient Insulin Release and Immunosuppression

In a healthy person, the pancreas consists of 10<sup>9</sup> cells and a normal insulin release of 1–15 mg per day [81, 194]. As MSC-derived IPCs are far away from clinically relevant insulin concentrations, either the insulin release capacity of each cell has to rise or more IPCs have to be transplanted. Some groups estimate an amount of 10<sup>9</sup> IPCs to be transplanted per patient, which amounts to the total cell mass of the whole pancreas in IPCs alone [175]. However, most studies report that MSCs stop or slow proliferation in the differentiation process. Therefore it is important to work on the yield of IPCs. At present, all studies are conducted in small-scale flask cultures. An upscale towards a bioreactor-volume needs to be established, but only few groups are working on this end.

## 12. GMP

Progressing cell and tissue manipulation techniques from pure research towards clinical application, that is, cellular or gene therapies, demands an additional framework laid down by regulatory bodies like the FDA or EU called good manufacturing practice (GMP). GMP requires that a therapeutic product is of the highest possible quality and poses no risk for the recipient [195]. Working in compliance to GMP encompasses not only the process for production of the therapeutic product but the whole laboratory as well.

Since stem cell therapies are comparatively new, the corresponding regulatory requirements are still developing. Currently cell therapy requirements are classified according to the degree of manipulation involved and the expected process-related risks. While minimal manipulations, such as cryopreservation of tissues or cells, are regulated under good tissue practices (GTPs), which is already present in most clinical labs, more extensive manipulations, for example, transduction, *ex vivo* expansion, activation, and use for other than the tissues function, fall under the more strict GMP. MSCs are classified as advanced therapy medicinal products per European Regulation No. 1394/2007 and are further considered as somatic therapy or tissue-engineered products, depending on source, manufacturing, and indication. Therefore, production and delivery of MSCs must be carried out in accordance with European regulations [196–201].

The major disparity of GMP cell engineering and the established GMP in the biopharmaceutical industry is that most cell therapies are custom-made to the individual patient whereas biopharmaceutical GMP aims towards bulk production. In an ongoing process adjustment of the regulations is required. However, continuous renewal makes the classification and GMP requirements of cell therapeutic products subject to change. For example, first GMP complaint procedures for cell expansions are already established [202, 203]; in contrast GMP procedures for differentiation are still not defined.

Translating research-based protocols into GMP complaint procedures for the production of clinical-grade MSCs requires an in-depth assessment of all critical aspects and involved risks. All phases of production must be subjected to



quality control. This includes, but is not limited to, process controls, which qualify cell production technique, including functional tests, and production controls, for example, bacteriological tests, phenotypic controls, and a visual follow-up. Critical is the analysis that the culture protocol does not lead to cell transformation (karyotype, FISH, quantitative expression of telomerase, c-myc, etc.). Tests of viability and phenotype must be performed at the final stage but must additionally be compatible with a rapid release of the finished product [177].

One of the most crucial aspects for the maintenance of phenotype and genotype of cultured MSCs during multiple passages is the cell culture media. Agreement on the optimal media for MSC cultivation is not reached in present. Most commonly DMEM, MEM, EMEM,  $\alpha$ -MEM, and RPMI with supplementation of FBS, human serum or plasma, and growth factors are used [49, 50, 52, 68, 202]. This leaves much room for improvement; apart from the lack of standardized protocols, the use of FBS is undesirable by GMP standards, which favor a xeno-free approach to eliminate the risk of cross-species disease transmission. Furthermore, utilizing FBS in GMP production requires additional certification of the used FBS, significantly raising the costs. First steps towards wholly synthetic culture media are already undertaken, with the aim of eliminating these concerns. Salzig et al. tested a chemical defined culture medium for expansion of MSC and established this for flask cultures up to bioreactor scale. They specify “chemical defined” as being xeno-free as well as free from components derived from or consisting of lysates, hormones, transferrin, or similar compounds, arguing that their composition or activity is susceptible to deviation. This approach is almost unique for MSCs, efforts by other groups research limiting themselves to xeno-free-only culture media until now, which is not chemical defined in the strictest definition [204].

### 13. Concluding Remarks

As diabetes is a disease which strikes millions of people worldwide, which goes along with lifetime necessity of insulin shots and high risk of side effects because the best glucose control is still not comparable with physiological glucose regulation, a beta-cell replacement treatment is highly desirable. The option of transplanting pancreas or isolated islets is limited because of a lack of suitable organs relative to the large amount of potential recipients, combined with severe side effects caused by lifelong immunosuppression, which has to be weighed against the necessity of insulin shots and is therefore only recommendable for a subgroup of patients with severe medical history. The option of xenotransplantation, which would resolve the lack of donors, for example, with pig islets, poses even bigger risks of other adverse effects. Despite these concerns, important knowledge comes from clinical and experimental islet transplantation and it is still one of several treatment options that are worthwhile to follow in the future.

As there are a multitude of approaches in the field of regenerative medicine, ranging from novel ways to induce

beta-cell proliferation, reprogramming of other pancreatic cells or nonpancreatic cells like liver cells, the differentiation research on iPSC, fetal stem cells, or adult stem cells (among them, MSCs), it is not possible yet to anticipate which technique(s) will come out on top. Therefore, it is very important that each path is worked on among researchers in the diabetic field. In this review, MSCs are highlighted, because they have great potential and do not come with ethical issues as opposed to ESCs due to the fact that for ESCs embryos have to be destroyed. Additionally, MSCs can possibly act as supporting cells along with classical islet transplantation or ameliorate diabetes by using the MSCs in an undifferentiated status. Some clinical studies are already going on, using MSCs, because of their anti-inflammatory potential.

Preliminary results seem to show that the tumor risk is low to absent in MSCs compared to iPS cells and ESCs. In spite of the fact that research is underway for the use of MSCs in diabetes treatment, clinical application is still a long way to go as there is still a lack of standardized protocols to produce and expand MSCs, to better control the risk of malignant formation or *in vivo* differentiation and the release of cytokines, and finally to improve engraftment. These are the crucial issues which have to be addressed in future research to reach clinical utility and viability.

### Common Abbreviations

AD-MSCs:	Adipose tissue derived mesenchymal stem cells
ALCAM:	Activated leukocyte cell adhesion molecule
AM-MSCs:	Amniotic membrane and fluid mesenchymal stem cells
ANG:	Angiogenin
APJ:	Apelin receptor, a G-protein coupled receptor
ASCs:	Adipose tissue derived stem cells
AT-MSCs:	Adipose tissue derived stem cells
Bcl-2:	Founding member of the b-cell lymphoma-2 regulator proteins and correspondent genes that regulate apoptosis
BM-MSCs:	Bone marrow derived mesenchymal stem cells
Brachyury:	Transcription factor within the T-box complex of genes highly expressed in inner cell mass of blastocyst, defining midline of a bilateral organism
CD:	Cluster of differentiation
CITR:	Collaborative Islet Transplant Registry
c-myc:	V-myc avian myelocytomatosis viral oncogene homolog
Cxcr4:	Gene encoding the CXC (cysteine-x-cysteine motif) chemokine receptor type 4
DMEM:	Dulbecco's Modified Eagle Medium, LG = low glucose, and HG = high glucose
DPSCs:	Dental pulp mesenchymal stem cells

DTZ:	Dithizone, sulfur-containing organic compound forming complexes with metal cations, such as Zn, used to assess the purity of islet cell preparations	Ngn3:	Neurogenin gene encoding class A basic helix loop helix transcription factor
EGF:	Epithelial growth factor	Nkx2.2 NK2:	Homeobox 2 transcription factor encoded by correspondent gene also named TTF1
ESCs:	Embryonic stem cells	NO:	Nitric oxide
FBS:	Fetal bovine serum	OCT4:	Octamer binding transcription factor 4
FcR gamma:	Fc receptor gamma	P-MSC:	Pancreas
FGF:	Fibroblast growth factor	PL-MSC:	Placenta
FGF2:	Fibroblast growth factor 2	PAF:	Platelet activating factor
FISH:	Fluorescent DNA <i>in situ</i> hybridization	Pax6:	Gene encoding the transcription factor Paired box protein 6
FoxA2:	Gene encoding Forkhead box protein A2 transcription factor	PDGF:	Platelet derived growth factor
GFR:	Glomerular filtration rate	PDX-1:	Pancreatic and duodenal homeobox 1, synonymous with insulin promoter factor 1
Glut2:	Glucose transporter 2	PP:	Pancreatic progenitor
Glp-1:	Glucagon-like peptide-1	RA:	Retinoic acid
GM-CSF:	Colony stimulating factor 2 (granulocyte-macrophage)	SCF:	Stem cell factor, a cytokine produced by fibroblasts and endothelial cells, in its soluble form binding to c-KIT (CD117)
GK:	Glucokinase	SOX2:	Sex-determining region-related High-Mobility-Group-Box gene 2
GMP:	Good manufacturing practice	STRO-1:	Stromal cell derived factor 1
GPIIB:	Glycoprotein IIB	STRO-3:	Stromal cell derived factor 3
GPIIIa:	Glycoprotein IIIa	STZ:	Streptozotocin, chemical for induction of experimental diabetes in rodents
GPVI:	Glycoprotein VI	STZ mice:	Streptozotocin-induced diabetes in mice
GRI:	Granulocyte marker 1	T1DM:	Type 1 diabetes mellitus
GTPs:	Good tissue practices	TCDAb:	T-cell depleting antibody
HbA <sub>1c</sub> :	Hemoglobin glycosylated	TGF:	Tissue growth factor
HBSS:	Hank's Balanced Salt Solution	TGF beta:	Tissue growth factor beta
HGF:	Hepatocyte growth factor	Thy1:	Thymocyte differentiation antigen 1
HIF-1:	Hypoxia-inducible factor 1	TNF-alpha:	Tumor necrosis factor alpha
HLA-DR:	Human leukocyte antigen receptor D	TNF-alpha-i:	Tumor necrosis factor alpha inhibitor
HNF2:	Hepatocyte nuclear factor 2	TXA:	Thromboxane
IBMIR:	Instant blood mediated immune reaction	UC-MSCs:	Umbilical cord matrix mesenchymal stem cells
ICAM-1:	Intercellular adhesion molecule 1	UCB-MSCs:	Umbilical cord blood mesenchymal stem cells
IFN-gamma:	Interferon gamma	VCAM:	Vascular cell adhesion molecule-1
IPCs:	Insulin-producing cells	VEGF:	Vascular endothelial growth factor
iPSCs:	Induced pluripotent stem cells	VLA-4:	Integrin alpha4beta1
IL:	Interleukin	Wnt:	Wingless Int-1 characterizing a group of proteins passing signals from outside to inside of the cell membrane
ISCT:	International Society for Cellular Therapy	WT-MSCs:	Wharton's jelly mesenchymal stem cells.
Isl1:	Insulin gene enhancer protein 1, a protein encoded by the correspondent gene		
MafA:	V-maf musculoaponeurotic fibrosarcoma oncogene homolog A, a protein encoded by the MafA gene		
MCP-1:	Monocyte chemotactic protein 1		
Mixl1:	Mix paired-like homeobox gene encoding transcription factor		
MMP:	Metalloprotease		
MOI:	Multiplicity of infection		
MSCs:	Mesenchymal stem cells		
MSCA-1:	Mesenchymal stem cell antigen-1		
NANOG:	(Old Irish Tir na nOg = land of youth) gene encoding a transcription factor regulating self-renewal in stem cells		
NCV:	Nerve conduction velocity		
NK cells:	Natural killer cells		
NeuroD1:	Neurogenic Differentiation 1 gene encoding basic helix loop helix transcription factor of the NeuroD family		

## Conflict of Interests

The authors declare that there is no conflict of interests regarding the publication of this paper.

## References

- [1] A. M. J. Shapiro, J. R. T. Lakey, E. A. Ryan et al., "Islet transplantation in seven patients with type 1 diabetes mellitus using a glucocorticoid-free immunosuppressive regimen," *The New England Journal of Medicine*, vol. 343, no. 4, pp. 230–238, 2000.

- [2] R. G. Bretzel, H. Jahr, M. Eckhard, I. Martin, D. Winter, and M. D. Brendel, "Islet cell transplantation today," *Langenbeck's Archives of Surgery*, vol. 392, no. 3, pp. 239–253, 2007.
- [3] M. McCall and A. M. J. Shapiro, "Islet cell transplantation," *Seminars in Pediatric Surgery*, vol. 23, no. 2, pp. 83–90, 2014.
- [4] The Diabetes Control and Complications Trial Research Group, "Hypoglycemia in the diabetes control and complications trial," *Diabetes*, vol. 46, no. 2, pp. 271–286, 1997.
- [5] E. A. Ryan, J. R. T. Lakey, B. W. Paty et al., "Successful islet transplantation: continued insulin reserve provides long-term glycemic control," *Diabetes*, vol. 51, no. 7, pp. 2148–2157, 2002.
- [6] E. A. Ryan, J. R. T. Lakey, R. V. Rajotte et al., "Clinical outcomes and insulin secretion after islet transplantation with the Edmonton protocol," *Diabetes*, vol. 50, no. 4, pp. 710–719, 2001.
- [7] A. M. J. Shapiro, C. Ricordi, B. J. Hering et al., "International trial of the Edmonton protocol for islet transplantation," *The New England Journal of Medicine*, vol. 355, no. 13, pp. 1318–1330, 2006.
- [8] B. Hirshberg, K. I. Rother, B. J. Dignon III et al., "Benefits and risks of solitary islet transplantation for type 1 diabetes using steroid-sparing immunosuppression," *Diabetes Care*, vol. 26, no. 12, pp. 3288–3295, 2003.
- [9] T. Kenmochi, T. Asano, M. Maruyama et al., "Clinical islet transplantation in Japan," *Journal of Hepato-Biliary-Pancreatic Surgery*, vol. 16, no. 2, pp. 124–130, 2009.
- [10] E. A. Ryan, T. Shandro, K. Green et al., "Assessment of the severity of hypoglycemia and glycemic lability in type 1 diabetic subjects undergoing islet transplantation," *Diabetes*, vol. 53, no. 4, pp. 955–962, 2004.
- [11] E. A. Ryan, B. W. Paty, P. A. Senior et al., "Five-year follow-up after clinical islet transplantation," *Diabetes*, vol. 54, no. 7, pp. 2060–2069, 2005.
- [12] B. J. Hering, R. Kandaswamy, J. D. Ansate et al., "Single-donor, marginal-dose islet transplantation in patients with type 1 diabetes," *The Journal of the American Medical Association*, vol. 293, no. 7, pp. 830–835, 2005.
- [13] M. D. Bellin, R. Kandaswamy, J. Parkey et al., "Prolonged insulin independence after islet allotransplants in recipients with type 1 diabetes," *American Journal of Transplantation*, vol. 8, no. 11, pp. 2463–2470, 2008.
- [14] M. D. Bellin, F. B. Barton, A. Heitman et al., "Potent induction immunotherapy promotes long-term insulin independence after islet transplantation in type 1 diabetes," *The American Journal of Transplantation*, vol. 12, no. 6, pp. 1576–1583, 2012.
- [15] T. Froud, C. Ricordi, D. A. Baidal et al., "Islet transplantation in type 1 diabetes mellitus using cultured islets and steroid-free immunosuppression: Miami experience," *American Journal of Transplantation*, vol. 5, no. 8, pp. 2037–2046, 2005.
- [16] P. J. O'Connell, D. J. Holmes-Walker, D. Goodman et al., "Multicenter Australian trial of islet transplantation: improving accessibility and outcomes," *American Journal of Transplantation*, vol. 13, no. 7, pp. 1850–1858, 2013.
- [17] M. Qi, K. Kinzer, K. K. Danielson et al., "Five-year follow-up of patients with type 1 diabetes transplanted with allogeneic islets: the UIC experience," *Acta Diabetologica*, vol. 51, no. 5, pp. 833–843, 2014.
- [18] N. A. Turgeon, J. G. Avila, J. A. Cano et al., "Experience with a novel efalizumab-based immunosuppressive regimen to facilitate single donor islet cell transplantation," *American Journal of Transplantation*, vol. 10, no. 9, pp. 2082–2091, 2010.
- [19] B. Ludwig, A. Reichel, A. Kruppa et al., "Islet transplantation at the Dresden diabetes center: five years' experience," *Hormone and Metabolic Research*, vol. 47, no. 1, pp. 4–8, 2015.
- [20] F. B. Barton, M. R. Rickels, R. Alejandro et al., "Improvement in outcomes of clinical islet transplantation: 1999–2010," *Diabetes Care*, vol. 35, no. 7, pp. 1436–1445, 2012.
- [21] M. R. Rickels, C. Liu, R. D. Shlansky-Goldberg et al., "Improvement in  $\beta$ -cell secretory capacity after human islet transplantation according to the CIT07 protocol," *Diabetes*, vol. 62, no. 8, pp. 2890–2897, 2013.
- [22] M.-C. Vantyghem, V. Raverdy, A.-S. Balavoine et al., "Continuous glucose monitoring after islet transplantation in type 1 diabetes: an excellent graft function ( $\beta$ -score greater than 7) is required to abrogate hyperglycemia, whereas a minimal function is necessary to suppress severe hypoglycemia ( $\beta$ -score greater than 3)," *The Journal of Clinical Endocrinology & Metabolism*, vol. 97, no. 11, pp. E2078–E2083, 2018.
- [23] M. Ang, C. Meyer, M. D. Brendel, R. G. Bretzel, and T. Linn, "Magnitude and mechanisms of glucose counterregulation following islet transplantation in patients with type 1 diabetes suffering from severe hypoglycaemic episodes," *Diabetologia*, vol. 57, no. 3, pp. 623–632, 2014.
- [24] M. R. Rickels, M. H. Schutta, R. Mueller et al., "Glycemic thresholds for activation of counterregulatory hormone and symptom responses in islet transplant recipients," *Journal of Clinical Endocrinology and Metabolism*, vol. 92, no. 3, pp. 873–879, 2007.
- [25] M. R. Rickels, M. H. Schutta, R. Mueller et al., "Islet cell hormonal responses to hypoglycemia after human islet transplantation for type 1 diabetes," *Diabetes*, vol. 54, no. 11, pp. 3205–3211, 2005.
- [26] C. B. Leitão, T. Tharavanij, P. Cure et al., "Restoration of hypoglycemia awareness after islet transplantation," *Diabetes Care*, vol. 31, no. 11, pp. 2113–2115, 2008.
- [27] M. R. Rickels, S. M. Kong, C. Fuller et al., "Improvement in insulin sensitivity after human islet transplantation for type 1 diabetes," *Journal of Clinical Endocrinology and Metabolism*, vol. 98, no. 11, pp. E1780–E1785, 2013.
- [28] C. Toso, A. M. J. Shapiro, S. Bowker et al., "Quality of life after islet transplant: impact of the number of islet infusions and metabolic outcome," *Transplantation*, vol. 84, no. 5, pp. 664–666, 2007.
- [29] B. Fullerton, K. Jeitler, M. Seitz, K. Horvath, A. Berghold, and A. Siebenhofer, "Intensive glucose control versus conventional glucose control for type 1 diabetes mellitus," *The Cochrane Database of Systematic Reviews*, vol. 2, Article ID CD009122, 2014.
- [30] Diabetes Control and Complications Trial Research Group, "The effect of intensive treatment of diabetes on the development and progression of long-term complications in insulin-dependent diabetes mellitus," *The New England Journal of Medicine*, vol. 329, no. 14, pp. 977–986, 1993.
- [31] P. H. Wang, J. Lau, and T. C. Chalmers, "Meta-analysis of effects of intensive blood-glucose control on late complications of type I diabetes," *The Lancet*, vol. 341, no. 8856, pp. 1306–1309, 1993.
- [32] P. Fiorina, F. Folli, G. Zerbini et al., "Islet transplantation is associated with improvement of renal function among uremic patients with type I diabetes mellitus and kidney transplants," *Journal of the American Society of Nephrology*, vol. 14, no. 8, pp. 2150–2158, 2003.
- [33] P. Fiorina, M. Venturini, F. Folli et al., "Natural history of kidney graft survival, hypertrophy, and vascular function in

- end-stage renal disease type 1 diabetic kidney-transplanted patients: beneficial impact of pancreas and successful islet cotransplantation," *Diabetes Care*, vol. 28, no. 6, pp. 1303–1310, 2005.
- [34] A. Andres, C. Toso, P. Morel et al., "Impact of a sirolimus/tacrolimus-based immunosuppressive regimen on kidney function after islet transplantation," *Transplantation Proceedings*, vol. 37, no. 2, pp. 1326–1327, 2005.
- [35] P. Maffi, F. Bertuzzi, F. De Taddeo et al., "Kidney function after islet transplant alone in type 1 diabetes: impact of immunosuppressive therapy on progression of diabetic nephropathy," *Diabetes Care*, vol. 30, no. 5, pp. 1150–1155, 2007.
- [36] P. A. Senior, M. Zeman, B. W. Paty, E. A. Ryan, and A. M. J. Shapiro, "Changes in renal function after clinical islet transplantation: four-year observational study," *American Journal of Transplantation*, vol. 7, no. 1, pp. 91–98, 2007.
- [37] M. A. Fung, G. L. Warnock, Z. Ao et al., "The effect of medical therapy and islet cell transplantation on diabetic nephropathy: an interim report," *Transplantation*, vol. 84, no. 1, pp. 17–22, 2007.
- [38] G. L. Warnock, D. M. Thompson, R. M. Meloche et al., "A multi-year analysis of islet transplantation compared with intensive medical therapy on progression of complications in type 1 diabetes," *Transplantation*, vol. 86, no. 12, pp. 1762–1766, 2008.
- [39] D. M. Thompson, M. Meloche, Z. Ao et al., "Reduced progression of diabetic microvascular complications with islet cell transplantation compared with intensive medical therapy," *Transplantation*, vol. 91, no. 3, pp. 373–378, 2011.
- [40] T. C. Lee, N. R. Barshes, C. A. O'Mahony et al., "The effect of pancreatic islet transplantation on progression of diabetic retinopathy and neuropathy," *Transplantation Proceedings*, vol. 37, no. 5, pp. 2263–2265, 2005.
- [41] M. Venturini, P. Fiorina, P. Maffi et al., "Early increase of retinal arterial and venous blood flow velocities at color doppler imaging in brittle type 1 diabetes after islet transplant alone," *Transplantation*, vol. 81, no. 9, pp. 1274–1277, 2006.
- [42] D. M. Thompson, I. S. Begg, C. Harris et al., "Reduced progression of diabetic retinopathy after islet cell transplantation compared with intensive medical therapy," *Transplantation*, vol. 85, no. 10, pp. 1400–1405, 2008.
- [43] U. Del Carro, P. Fiorina, S. Amadio et al., "Evaluation of polyneuropathy markers in type 1 diabetic kidney transplant patients and effects of islet transplantation: neurophysiological and skin biopsy longitudinal analysis," *Diabetes Care*, vol. 30, no. 12, pp. 3063–3069, 2007.
- [44] M.-C. Vantyghem, D. Quintin, R. Caiazzo et al., "Improvement of electrophysiological neuropathy after islet transplantation for type 1 diabetes: a 5-year prospective study," *Diabetes Care*, vol. 37, no. 6, pp. e141–e142, 2014.
- [45] P. Fiorina, F. Folli, F. Bertuzzi et al., "Long-term beneficial effect of islet transplantation on diabetic macro-/microangiopathy in type 1 diabetic kidney-transplanted patients," *Diabetes Care*, vol. 26, no. 4, pp. 1129–1136, 2003.
- [46] P. Fiorina, F. Folli, P. Maffi et al., "Islet transplantation improves vascular diabetic complications in patients with diabetes who underwent kidney transplantation: a comparison between kidney-pancreas and kidney-alone transplantation," *Transplantation*, vol. 75, no. 8, pp. 1296–1301, 2003.
- [47] P. Fiorina, C. Gremizzi, P. Maffi et al., "Islet transplantation is associated with an improvement of cardiovascular function in type 1 diabetic kidney transplant patients," *Diabetes Care*, vol. 28, no. 6, pp. 1358–1365, 2005.
- [48] F. D'Addio, P. Maffi, P. Vezzulli et al., "Islet transplantation stabilizes hemostatic abnormalities and cerebral metabolism in individuals with type 1 diabetes," *Diabetes Care*, vol. 37, no. 1, pp. 267–276, 2014.
- [49] K. Timper, D. Seboek, M. Eberhardt et al., "Human adipose tissue-derived mesenchymal stem cells differentiate into insulin, somatostatin, and glucagon expressing cells," *Biochemical and Biophysical Research Communications*, vol. 341, no. 4, pp. 1135–1140, 2006.
- [50] V. Chandra, G. Swetha, S. Muthyala et al., "Islet-like cell aggregates generated from human adipose tissue derived stem cells ameliorate experimental diabetes in mice," *PLoS ONE*, vol. 6, no. 6, Article ID e20615, 2011.
- [51] D. Marappagounder, I. Somasundaram, S. Dorairaj, and R. J. Sankaran, "Differentiation of mesenchymal stem cells derived from human bone marrow and subcutaneous adipose tissue into pancreatic islet-like clusters in vitro," *Cellular and Molecular Biology Letters*, vol. 18, no. 1, pp. 75–88, 2013.
- [52] S. D. Dave, A. V. Vanikar, and H. L. Trivedi, "In-vitro generation of human adipose tissue derived insulin secreting cells: up-regulation of Pax-6, Ip1-1 and Isl-1," *Cytotechnology*, vol. 66, no. 2, pp. 299–307, 2014.
- [53] J. Li, L. Zhu, X. Qu et al., "Stepwise differentiation of human adipose-derived mesenchymal stem cells toward definitive endoderm and pancreatic progenitor cells by mimicking pancreatic development in vivo," *Stem Cells and Development*, vol. 22, no. 10, pp. 1576–1587, 2013.
- [54] M. L. Mohamad Buang, H. K. Seng, L. H. Chung, A. B. Saim, and R. B. H. Idrus, "In vitro generation of functional insulin-producing cells from lipoaspirated human adipose tissue-derived stem cells," *Archives of Medical Research*, vol. 43, no. 1, pp. 83–88, 2012.
- [55] P. Czubak, A. Bojarska-Junak, J. Tabarkiewicz, and L. Putowski, "A modified method of insulin producing cells' generation from bone marrow-derived mesenchymal stem cells," *Journal of Diabetes Research*, vol. 2014, Article ID 628591, 7 pages, 2014.
- [56] M. M. Gabr, M. M. Zakaria, A. F. Refaie et al., "Differentiation of human bone marrow-derived mesenchymal stem cells into insulin-producing cells: evidence for further maturation in vivo," *BioMed Research International*, vol. 2015, Article ID 575837, 10 pages, 2015.
- [57] A. Jafarian, M. Taghikhani, S. Abroun, Z. Pourpak, A. Allahverdi, and M. Soleimani, "Generation of high-yield insulin producing cells from human bone marrow mesenchymal stem cells," *Molecular Biology Reports*, vol. 41, no. 7, pp. 4783–4794, 2014.
- [58] W. Bennet, B. Sundberg, C.-G. Groth et al., "Incompatibility between human blood and isolated islets of langerhans: a finding with implications for clinical intraportal islet transplantation?" *Diabetes*, vol. 48, no. 10, pp. 1907–1914, 1999.
- [59] W. Bennet, C.-G. Groth, R. Larsson, B. Nilsson, and O. Korsgren, "Isolated human islets trigger an instant blood mediated inflammatory reaction: implications for intraportal islet transplantation as a treatment for patients with type 1 diabetes," *Uppsala Journal of Medical Sciences*, vol. 105, no. 2, pp. 125–133, 2000.
- [60] Y. Lai, C. Chen, and T. Linn, "Innate immunity and heat shock response in islet transplantation," *Clinical and Experimental Immunology*, vol. 157, no. 1, pp. 1–8, 2009.
- [61] U. G. Thakkar, H. L. Trivedi, A. V. Vanikar, and S. D. Dave, "Insulin-secreting adipose-derived mesenchymal stromal cells with bone marrow-derived hematopoietic stem cells from



- autologous and allogenic sources for type 1 diabetes mellitus," *Cytotherapy*, vol. 17, no. 7, pp. 940–947, 2015.
- [62] M. Bahrebar, M. Soleimani, M. H. Karimi, A. Vahdati, and R. Yaghobi, "Generation of islet-like cell aggregates from human adipose tissue-derived stem cells by lentiviral overexpression of PDX-1," *International Journal of Organ Transplantation Medicine*, vol. 6, no. 2, pp. 61–76, 2015.
- [63] J. Lee, S. C. Kim, S. J. Kim et al., "Differentiation of human adipose tissue-derived stem cells into aggregates of insulin-producing cells through the overexpression of pancreatic and duodenal homeobox gene-1," *Cell Transplantation*, vol. 22, no. 6, pp. 1053–1060, 2013.
- [64] Z. N. Boroujeni and A. Aleyasin, "Insulin producing cells established using non-integrated lentiviral vector harboring PDX1 gene," *World Journal of Stem Cells*, vol. 5, no. 4, pp. 217–228, 2013.
- [65] G. Lin, G. Wang, G. Liu et al., "Treatment of type 1 diabetes with adipose tissue-derived stem cells expressing pancreatic duodenal homeobox 1," *Stem Cells and Development*, vol. 18, no. 10, pp. 1399–1406, 2009.
- [66] A. Jafarian, M. Taghikani, S. Abroun et al., "The generation of insulin producing cells from human mesenchymal stem cells by MiR-375 and anti-MiR-9," *PLoS ONE*, vol. 10, no. 6, Article ID e0128650, 2015.
- [67] A. Allahverdi, S. Abroun, A. Jafarian, M. Soleimani, M. Taghikani, and F. Eskandari, "Differentiation of human mesenchymal stem cells into insulin producing cells by using a lentiviral vector carrying PDX1," *Cell Journal*, vol. 17, no. 2, pp. 231–242, 2015.
- [68] C. Limbert, G. Pth, R. Ebert et al., "PDX1- and NGN3-mediated in vitro reprogramming of human bone marrow-derived mesenchymal stromal cells into pancreatic endocrine lineages," *Cytotherapy*, vol. 13, no. 7, pp. 802–813, 2011.
- [69] O. Karnieli, Y. Izhar-Prato, S. Bulvik, and S. Efrat, "Generation of insulin-producing cells from human bone marrow mesenchymal stem cells by genetic manipulation," *STEM CELLS*, vol. 25, no. 11, pp. 2837–2844, 2007.
- [70] J. P. Maloney, C. C. Silliman, D. R. Ambruso, J. Wang, R. M. Tuder, and N. F. Voelkel, "In vitro release of vascular endothelial growth factor during platelet aggregation," *The American Journal of Physiology—Heart and Circulatory Physiology*, vol. 275, no. 3, part 2, pp. H1054–H1061, 1998.
- [71] B. Nieswandt, W. Bergmeier, A. Eckly et al., "Evidence for cross-talk between glycoprotein VI and Gi-coupled receptors during collagen-induced platelet aggregation," *Blood*, vol. 97, no. 12, pp. 3829–3835, 2001.
- [72] B. Nieswandt, I. Pleines, and M. Bender, "Platelet adhesion and activation mechanisms in arterial thrombosis and ischaemic stroke," *Journal of Thrombosis and Haemostasis*, vol. 9, no. 1, pp. 92–104, 2011.
- [73] B. Nieswandt, C. Brakebusch, W. Bergmeier et al., "Glycoprotein VI but not  $\alpha 2\beta 1$  integrin is essential for platelet interaction with collagen," *The EMBO Journal*, vol. 20, no. 9, pp. 2120–2130, 2001.
- [74] B. Nieswandt, V. Schulte, W. Bergmeier et al., "Long-term antithrombotic protection by in vivo depletion of platelet glycoprotein VI in mice," *The Journal of Experimental Medicine*, vol. 193, no. 4, pp. 459–469, 2001.
- [75] T. Linn, J. Schmitz, I. Hauck-Schmalenberger et al., "Ischaemia is linked to inflammation and induction of angiogenesis in pancreatic islets," *Clinical and Experimental Immunology*, vol. 144, no. 2, pp. 179–187, 2006.
- [76] N. R. Barshes, S. Wyllie, and J. A. Goss, "Inflammation-mediated dysfunction and apoptosis in pancreatic islet transplantation: implications for intrahepatic grafts," *Journal of Leukocyte Biology*, vol. 77, no. 5, pp. 587–597, 2005.
- [77] J. A. Emamaullee and A. M. J. Shapiro, "Factors influencing the loss of  $\beta$ -cell mass in islet transplantation," *Cell Transplantation*, vol. 16, no. 1, pp. 1–8, 2007.
- [78] Y. Yasunami, S. Kojo, H. Kitamura et al., "V $\alpha$ 14 NKT cell-triggered IFN- $\alpha$  production by Gr-1<sup>+</sup>CD11b<sup>+</sup> cells mediates early graft loss of syngeneic transplanted islets," *The Journal of Experimental Medicine*, vol. 202, no. 7, pp. 913–918, 2005.
- [79] H. Brandhorst, D. Brandhorst, B. J. Hering, and R. G. Bretzel, "Significant progress in porcine islet mass isolation utilizing liberase HI for enzymatic low-temperature pancreas digestion," *Transplantation*, vol. 68, no. 3, pp. 355–361, 1999.
- [80] A. M. J. Shapiro, E. Hao, R. V. Rajotte, and N. M. Kneteman, "High yield of rodent islets with intraductal collagenase and stationary digestion—a comparison with standard technique," *Cell Transplantation*, vol. 5, no. 6, pp. 631–638, 1996.
- [81] H. Brandhorst, D. Brandhorst, M. D. Brendel, B. J. Hering, and R. G. Bretzel, "Assessment of intracellular insulin content during all steps of human islet isolation procedure," *Cell Transplantation*, vol. 7, no. 5, pp. 489–495, 1998.
- [82] L. Piemonti and A. Pileggi, "25 Years of the Ricordi automated method for islet isolation," *CellR4*, vol. 1, no. 1, article e128, 2013.
- [83] H. Brandhorst, N. Raemisch-Guenther, C. Raemisch et al., "The ratio between collagenase class I and class II influences the efficient islet release from the rat pancreas," *Transplantation*, vol. 85, no. 3, pp. 456–461, 2008.
- [84] J. D. Carter, S. B. Dula, K. L. Corbin, R. Wu, and C. S. Nunemaker, "A practical guide to rodent islet isolation and assessment," *Biological Procedures Online*, vol. 11, no. 1, pp. 3–31, 2009.
- [85] A. O. Gaber and D. Fraga, "Advances in long-term islet culture: the Memphis experience," *Cell Biochemistry and Biophysics*, vol. 40, no. 3, supplement, pp. 49–54, 2004.
- [86] R. D. Ramnath, E. Maillard, K. Jones et al., "In vitro assessment of human islet vulnerability to instant blood-mediated inflammatory reaction (IBMIR) and its use to demonstrate a beneficial effect of tissue culture," *Cell Transplantation*, vol. 24, no. 12, pp. 2505–2512, 2015.
- [87] P.-O. Carlsson, E. Schwarcz, O. Korsgren, and K. Le Blanc, "Preserved  $\beta$ -cell function in type 1 diabetes by mesenchymal stromal cells," *Diabetes*, vol. 64, no. 2, pp. 587–592, 2015.
- [88] J. Hu, X. Yu, Z. Wang et al., "Long term effects of the implantation of Wharton's jelly-derived mesenchymal stem cells from the umbilical cord for newly-onset type 1 diabetes mellitus," *Endocrine Journal*, vol. 60, no. 3, pp. 347–357, 2013.
- [89] A. J. Friedenstein, K. V. Petrakova, A. I. Kurolesova, and G. P. Frolova, "Heterotopic of bone marrow. Analysis of precursor cells for osteogenic and hematopoietic tissues," *Transplantation*, vol. 6, no. 2, pp. 230–247, 1968.
- [90] M. Owen, "Marrow stromal stem cells," *Journal of Cell Science*, no. 10, pp. 63–76, 1988.
- [91] M. Owen and A. J. Friedenstein, "Stromal stem cells: marrow-derived osteogenic precursors," *Ciba Foundation Symposium*, vol. 136, pp. 42–60, 1988.
- [92] A. I. Caplan, "Mesenchymal stem cells," *Journal of Orthopaedic Research*, vol. 9, no. 5, pp. 641–650, 1991.
- [93] J. T. Williams IV, S. S. Southerland, J. Souza, A. F. Calcutt, and R. G. Cartledge, "Cells isolated from adult human skeletal



- muscle capable of differentiating into multiple mesodermal phenotypes," *American Surgeon*, vol. 65, no. 1, pp. 22–26, 1999.
- [94] G. Bartsch Jr., J. J. Yoo, P. De Coppi et al., "Propagation, expansion, and multilineage differentiation of human somatic stem cells from dermal progenitors," *Stem Cells and Development*, vol. 14, no. 3, pp. 337–348, 2005.
- [95] U. Riekstina, R. Muceniece, I. Cakstina, I. Muiznieks, and J. Ancans, "Characterization of human skin-derived mesenchymal stem cell proliferation rate in different growth conditions," *Cytotechnology*, vol. 58, no. 3, pp. 153–162, 2008.
- [96] P. A. Zuk, M. Zhu, H. Mizuno et al., "Multilineage cells from human adipose tissue: implications for cell-based therapies," *Tissue Engineering*, vol. 7, no. 2, pp. 211–228, 2001.
- [97] K. L. Seeberger, J. M. Dufour, A. M. James Shapiro, J. R. T. Lakey, R. V. Rajotte, and G. S. Korbutt, "Expansion of mesenchymal stem cells from human pancreatic ductal epithelium," *Laboratory Investigation*, vol. 86, no. 2, pp. 141–153, 2006.
- [98] S. Gronthos, M. Mankani, J. Brahimi, P. G. Robey, and S. Shi, "Postnatal human dental pulp stem cells (DPSCs) in vitro and in vivo," *Proceedings of the National Academy of Sciences of the United States of America*, vol. 97, no. 25, pp. 13625–13630, 2000.
- [99] N. Rotter, J. Oder, P. Schlenke et al., "Isolation and characterization of adult stem cells from human salivary glands," *Stem Cells and Development*, vol. 17, no. 3, pp. 509–518, 2008.
- [100] A. N. Schüring, N. Schulte, R. Kelsch, A. Röpke, L. Kiesel, and M. Götte, "Characterization of endometrial mesenchymal stem-like cells obtained by endometrial biopsy during routine diagnostics," *Fertility and Sterility*, vol. 95, no. 1, pp. 423–426, 2011.
- [101] Y. Fukuchi, H. Nakajima, D. Sugiyama, I. Hirose, T. Kitamura, and K. Tsuji, "Human placenta-derived cells have mesenchymal stem/progenitor cell potential," *STEM CELLS*, vol. 22, no. 5, pp. 649–658, 2004.
- [102] A. D. Hoyes, "Structure and function of the amnion," *Obstetrics and Gynecology Annual*, vol. 4, pp. 1–38, 1975.
- [103] M. Macek, J. Hurych, and D. Rezacova, "Collagen synthesis in long-term cultures of amniotic fluid," *Ceskoslovenská Pediatrie*, vol. 28, no. 9, pp. 478–480, 1973.
- [104] M. Macek, J. Hurych, and D. Rezacova, "Letter: collagen synthesis in long term amniotic fluid cell cultures," *Nature*, vol. 243, no. 5405, pp. 289–290, 1973.
- [105] K. I. Pappa and N. P. Anagnou, "Novel sources of fetal stem cells: where do they fit on the developmental continuum?" *Regenerative Medicine*, vol. 4, no. 3, pp. 423–433, 2009.
- [106] A. Erices, P. Conget, and J. J. Minguell, "Mesenchymal progenitor cells in human umbilical cord blood," *British Journal of Haematology*, vol. 109, no. 1, pp. 235–242, 2000.
- [107] Y. A. Romanov, V. A. Svintsitskaya, and V. N. Smirnov, "Searching for alternative sources of postnatal human mesenchymal stem cells: candidate MSC-like cells from umbilical cord," *STEM CELLS*, vol. 21, no. 1, pp. 105–110, 2003.
- [108] K. E. Mitchell, M. L. Weiss, B. M. Mitchell et al., "Matrix cells from Wharton's jelly form neurons and glia," *Stem Cells*, vol. 21, no. 1, pp. 50–60, 2003.
- [109] M. F. Pittenger, A. M. Mackay, S. C. Beck et al., "Multilineage potential of adult human mesenchymal stem cells," *Science*, vol. 284, no. 5411, pp. 143–147, 1999.
- [110] J. Sanchez-Ramos, S. Song, F. Cardozo-Pelaez et al., "Adult bone marrow stromal cells differentiate into neural cells in vitro," *Experimental Neurology*, vol. 164, no. 2, pp. 247–256, 2000.
- [111] W. Wagner, F. Wein, A. Seckinger et al., "Comparative characteristics of mesenchymal stem cells from human bone marrow, adipose tissue, and umbilical cord blood," *Experimental Hematology*, vol. 33, no. 11, pp. 1402–1416, 2005.
- [112] A. Winter, S. Breit, D. Parsch et al., "Cartilage-like gene expression in differentiated human stem cell spheroids: a comparison of bone marrow-derived and adipose tissue-derived stromal cells," *Arthritis and Rheumatism*, vol. 48, no. 2, pp. 418–429, 2003.
- [113] V. Planat-Benard, J.-S. Silvestre, B. Cousin et al., "Plasticity of human adipose lineage cells toward endothelial cells: physiological and therapeutic perspectives," *Circulation*, vol. 109, no. 5, pp. 656–663, 2004.
- [114] K. M. Safford, K. C. Hicok, S. D. Safford et al., "Neurogenic differentiation of murine and human adipose-derived stromal cells," *Biochemical and Biophysical Research Communications*, vol. 294, no. 2, pp. 371–379, 2002.
- [115] P. Stock, S. Brückner, S. Winkler, M. M. Dollinger, and B. Christ, "Human bone marrow mesenchymal stem cell-derived hepatocytes improve the mouse liver after acute acetaminophen intoxication by preventing progress of injury," *International Journal of Molecular Sciences*, vol. 15, no. 4, pp. 7004–7028, 2014.
- [116] A. Wilkins, K. Kemp, M. Ginty, K. Hares, E. Mallam, and N. Scolding, "Human bone marrow-derived mesenchymal stem cells secrete brain-derived neurotrophic factor which promotes neuronal survival in vitro," *Stem Cell Research*, vol. 3, no. 1, pp. 63–70, 2009.
- [117] D. Orlic, J. Kajstura, S. Chimenti et al., "Bone marrow cells regenerate infarcted myocardium," *Nature*, vol. 410, no. 6829, pp. 701–705, 2001.
- [118] E. M. Horwitz, D. J. Prockop, L. A. Fitzpatrick et al., "Transplantability and therapeutic effects of bone marrow-derived mesenchymal cells in children with osteogenesis imperfecta," *Nature Medicine*, vol. 5, no. 3, pp. 309–313, 1999.
- [119] M. Morigi, B. Imberti, C. Zoja et al., "Mesenchymal stem cells are renoprotective, helping to repair the kidney and improve function in acute renal failure," *Journal of the American Society of Nephrology*, vol. 15, no. 7, pp. 1794–1804, 2004.
- [120] R. E. Schwartz, M. Reyes, L. Koodie et al., "Multipotent adult progenitor cells from bone marrow differentiate into functional hepatocyte-like cells," *The Journal of Clinical Investigation*, vol. 109, no. 10, pp. 1291–1302, 2002.
- [121] M. Dominici, K. Le Blanc, I. Mueller et al., "Minimal criteria for defining multipotent mesenchymal stromal cells. The International Society for Cellular Therapy position statement," *Cytotherapy*, vol. 8, no. 4, pp. 315–317, 2006.
- [122] E. M. Horwitz, K. Le Blanc, M. Dominici et al., "Clarification of the nomenclature for MSC: The International Society for Cellular Therapy position statement," *Cytotherapy*, vol. 7, no. 5, pp. 393–395, 2005.
- [123] H. Sauer, F. Sharifpanah, M. Hatry et al., "NOS inhibition synchronizes calcium oscillations in human adipose tissue-derived mesenchymal stem cells by increasing gap-junctional coupling," *Journal of Cellular Physiology*, vol. 226, no. 6, pp. 1642–1650, 2011.
- [124] P. J. Simmons and B. Torok-Storb, "Identification of stromal cell precursors in human bone marrow by a novel monoclonal antibody, STRO-1," *Blood*, vol. 78, no. 1, pp. 55–62, 1991.
- [125] S. Gronthos, S. Fitter, P. Diamond, P. J. Simmons, S. Itescu, and A. C. W. Zannettino, "A novel monoclonal antibody (STRO-3) identifies an isoform of tissue nonspecific alkaline phosphatase

- expressed by multipotent bone marrow stromal stem cells," *Stem Cells and Development*, vol. 16, no. 6, pp. 953–963, 2007.
- [126] V. L. Battula, S. Treml, P. M. Bareiss et al., "Isolation of functionally distinct mesenchymal stem cell subsets using antibodies against CD56, CD271, and mesenchymal stem cell antigen-1," *Haematologica*, vol. 94, no. 2, pp. 173–184, 2009.
- [127] N. Quirici, D. Soligo, P. Bossolasco, F. Servida, C. Lumini, and G. L. Deliliers, "Isolation of bone marrow mesenchymal stem cells by anti-nerve growth factor receptor antibodies," *Experimental Hematology*, vol. 30, no. 7, pp. 783–791, 2002.
- [128] M. T. Aye, S. Hashemi, B. Leclair et al., "Expression of stem cell factor and c-kit mRNA in cultured endothelial cells, monocytes and cloned human bone marrow stromal cells (CFU-RF)," *Experimental Hematology*, vol. 20, no. 4, pp. 523–527, 1992.
- [129] B. M. Strem, K. C. Hicok, M. Zhu et al., "Multipotential differentiation of adipose tissue-derived stem cells," *Keio Journal of Medicine*, vol. 54, no. 3, pp. 132–141, 2005.
- [130] D. A. De Ugarte, Z. Alfonso, P. A. Zuk et al., "Differential expression of stem cell mobilization-associated molecules on multi-lineage cells from adipose tissue and bone marrow," *Immunology Letters*, vol. 89, no. 2–3, pp. 267–270, 2003.
- [131] D. A. De Ugarte, K. Morizono, A. Elbarbary et al., "Comparison of multi-lineage cells from human adipose tissue and bone marrow," *Cells Tissues Organs*, vol. 174, no. 3, pp. 101–109, 2003.
- [132] P. J. Simmons, B. Masinovsky, B. M. Longenecker, R. Berenson, B. Torok-Storb, and W. M. Gallatin, "Vascular cell adhesion molecule-1 expressed by bone marrow stromal cells mediates the binding of hematopoietic progenitor cells," *Blood*, vol. 80, no. 2, pp. 388–395, 1992.
- [133] T. Südhoff and D. Söhlgen, "Circulating endothelial adhesion molecules (sE-selectin, sVCAM-1 and sICAM-1) during rHUG-CSF-stimulated stem cell mobilization," *Journal of Hematotherapy and Stem Cell Research*, vol. 11, no. 1, pp. 147–151, 2002.
- [134] P. Auquier, G. Macquart-Moulin, J. Moatti et al., "Comparison of anxiety, pain and discomfort in two procedures of hematopoietic stem cell collection: leukapheresis and bone marrow harvest," *Bone Marrow Transplantation*, vol. 16, no. 4, pp. 541–547, 1995.
- [135] J.-A. Dahl, S. Duggal, N. Coulston et al., "Genetic and epigenetic instability of human bone marrow mesenchymal stem cells expanded in autologous serum or fetal bovine serum," *International Journal of Developmental Biology*, vol. 52, no. 8, pp. 1033–1042, 2008.
- [136] L. A. Meza-Zepeda, A. Noer, J. A. Dahl, F. Micci, O. Myklebost, and P. Collas, "High-resolution analysis of genetic stability of human adipose tissue stem cells cultured to senescence," *Journal of Cellular and Molecular Medicine*, vol. 12, no. 2, pp. 553–563, 2008.
- [137] D. Hess, L. Li, M. Martin et al., "Bone marrow-derived stem cells initiate pancreatic regeneration," *Nature Biotechnology*, vol. 21, no. 7, pp. 763–770, 2003.
- [138] R. H. Lee, M. J. Seo, R. L. Reger et al., "Multipotent stromal cells from human marrow home to and promote repair of pancreatic islets and renal glomeruli in diabetic NOD/scid mice," *Proceedings of the National Academy of Sciences of the United States of America*, vol. 103, no. 46, pp. 17438–17443, 2006.
- [139] D. J. Borg, M. Weigelt, C. Wilhelm et al., "Mesenchymal stromal cells improve transplanted islet survival and islet function in a syngeneic mouse model," *Diabetologia*, vol. 57, no. 3, pp. 522–531, 2014.
- [140] S. Aggarwal and M. F. Pittenger, "Human mesenchymal stem cells modulate allogeneic immune cell responses," *Blood*, vol. 105, no. 4, pp. 1815–1822, 2005.
- [141] Y. Ding, D. Xu, G. Feng, A. Bushell, R. J. Muschel, and K. J. Wood, "Mesenchymal stem cells prevent the rejection of fully allogeneic islet grafts by the immunosuppressive activity of matrix metalloproteinase-2 and -9," *Diabetes*, vol. 58, no. 8, pp. 1797–1806, 2009.
- [142] T. Ito, S. Itakura, I. Todorov et al., "Mesenchymal stem cell and islet co-transplantation promotes graft revascularization and function," *Transplantation*, vol. 89, no. 12, pp. 1438–1445, 2010.
- [143] V. Sordi, R. Melzi, A. Mercalli et al., "Mesenchymal cells appearing in pancreatic tissue culture are bone marrow-derived stem cells with the capacity to improve transplanted islet function," *Stem Cells*, vol. 28, no. 1, pp. 140–151, 2010.
- [144] D. G. Wilkinson, S. Bhatt, and B. G. Herrmann, "Expression pattern of the mouse T gene and its role in mesoderm formation," *Nature*, vol. 343, no. 6259, pp. 657–659, 1990.
- [145] J. J. H. Pearce and M. J. Evans, "Mml, a mouse Mix-like gene expressed in the primitive streak," *Mechanisms of Development*, vol. 87, no. 1–2, pp. 189–192, 1999.
- [146] S.-L. Ang, A. Wierda, D. Wong et al., "The formation and maintenance of the definitive endoderm lineage in the mouse: involvement of HNF3/forkhead proteins," *Development*, vol. 119, no. 4, pp. 1301–1315, 1993.
- [147] C. Payne, J. King, and D. Hay, "The role of activin/nodal and Wnt signaling in endoderm formation," *Vitamins and Hormones*, vol. 85, pp. 207–216, 2011.
- [148] S. K. Kim and M. Hebrok, "Intercellular signals regulating pancreas development and function," *Genes and Development*, vol. 15, no. 2, pp. 111–127, 2001.
- [149] M. A. Guney and M. Gannon, "Pancreas cell fate," *Birth Defects Research Part C—Embryo Today: Reviews*, vol. 87, no. 3, pp. 232–248, 2009.
- [150] J. Jonsson, L. Carlsson, T. Edlund, and H. Edlund, "Insulin-promoter-factor 1 is required for pancreas development in mice," *Nature*, vol. 371, no. 6498, pp. 606–609, 1994.
- [151] G. K. Gittes, "Developmental biology of the pancreas: a comprehensive review," *Developmental Biology*, vol. 326, no. 1, pp. 4–35, 2009.
- [152] R. L. Pictet, W. R. Clark, R. H. Williams, and W. J. Rutter, "An ultrastructural analysis of the developing embryonic pancreas," *Developmental Biology*, vol. 29, no. 4, pp. 436–467, 1972.
- [153] M. Furukawa, Y. Eto, and I. Kojima, "Expression of immunoreactive activin A in fetal rat pancreas," *Endocrine Journal*, vol. 42, no. 1, pp. 63–68, 1995.
- [154] Å. Apelqvist, H. Li, L. Sommer et al., "Notch signalling controls pancreatic cell differentiation," *Nature*, vol. 400, no. 6747, pp. 877–881, 1999.
- [155] P. L. Herrera, "Adult insulin- and glucagon-producing cells differentiate from two independent cell lineages," *Development*, vol. 127, no. 11, pp. 2317–2322, 2000.
- [156] J. M. Oliver-Krasinski and D. A. Stoffers, "On the origin of the  $\beta$  cell," *Genes and Development*, vol. 22, no. 15, pp. 1998–2021, 2008.
- [157] G. Gradwohl, G. Gradwohl, A. Dierich et al., "Neurogenin3 is required for the development of the four endocrine cell lineages of the pancreas," *Proceedings of the National Academy of Sciences of the United States of America*, vol. 97, no. 4, pp. 1607–1611, 2000.
- [158] V. M. Schwitzgebel, D. W. Scheel, J. R. Connors et al., "Expression of neurogenin3 reveals an islet cell precursor population

- in the pancreas," *Development*, vol. 127, no. 16, pp. 3533–3542, 2000.
- [159] M. E. Wilson, D. Scheel, and M. S. German, "Gene expression cascades in pancreatic development," *Mechanisms of Development*, vol. 120, no. 1, pp. 65–80, 2003.
- [160] T. Kim, M. C. Gondré-Lewis, I. Arnaoutova, and Y. P. Loh, "Dense-core secretory granule biogenesis," *Physiology*, vol. 21, no. 2, pp. 124–133, 2006.
- [161] S. Georgia and A. Bhushan, " $\beta$  cell replication is the primary mechanism for maintaining postnatal  $\beta$  cell mass," *Journal of Clinical Investigation*, vol. 114, no. 7, pp. 963–968, 2004.
- [162] I. Artner, B. Bianchi, J. C. Raum et al., "MafB is required for islet  $\beta$  cell maturation," *Proceedings of the National Academy of Sciences of the United States of America*, vol. 104, no. 10, pp. 3853–3858, 2007.
- [163] C. Aguayo-Mazzucato, A. Koh, I. El Khattabi et al., "Maf expression enhances glucose-responsive insulin secretion in neonatal rat beta cells," *Diabetologia*, vol. 54, no. 3, pp. 583–593, 2011.
- [164] W. R. Goodyer, X. Gu, Y. Liu, R. Bottino, G. R. Crabtree, and S. K. Kim, "Neonatal  $\beta$  cell development in mice and humans is regulated by calcineurin/NFAT," *Developmental Cell*, vol. 23, no. 1, pp. 21–34, 2012.
- [165] A. L. Márquez-Aguirre, A. A. Canales-Aguirre, E. Padilla-Camberos, H. Esquivel-Solis, and N. E. Díaz-Martínez, "Development of the endocrine pancreas and novel strategies for  $\beta$ -cell mass restoration and diabetes therapy," *Brazilian Journal of Medical and Biological Research*, vol. 48, no. 9, pp. 765–776, 2015.
- [166] D. Q. Tang, Q. Wang, B. R. Burkhardt, S. A. Litherland, M. A. Atkinson, and L. J. Yang, "In vitro generation of functional insulin-producing cells from human bone marrow-derived stem cells, but long-term culture running risk of malignant transformation," *American Journal of Stem Cells*, vol. 1, no. 2, pp. 114–127, 2012.
- [167] D. Tosh and J. M. W. Slack, "How cells change their phenotype," *Nature Reviews Molecular Cell Biology*, vol. 3, no. 3, pp. 187–194, 2002.
- [168] C. Moriscot, F. De Fraipont, M.-J. Richard et al., "Human bone marrow mesenchymal stem cells can express insulin and key transcription factors of the endocrine pancreas developmental pathway upon genetic and/or microenvironmental manipulation in vitro," *STEM CELLS*, vol. 23, no. 4, pp. 594–603, 2005.
- [169] Y. Dor, J. Brown, O. I. Martinez, and D. A. Melton, "Adult pancreatic  $\beta$ -cells are formed by self-duplication rather than stem-cell differentiation," *Nature*, vol. 429, no. 6987, pp. 41–46, 2004.
- [170] T. Kato, H. Shimano, T. Yamamoto et al., "Granuphilin is activated by SREBP-1c and involved in impaired insulin secretion in diabetic mice," *Cell Metabolism*, vol. 4, no. 2, pp. 143–154, 2006.
- [171] W. P. Kloosterman, A. K. Lagendijk, R. F. Ketting, J. D. Moulton, and R. H. A. Plasterk, "Targeted inhibition of miRNA maturation with morpholinos reveals a role for miR-375 in pancreatic islet development," *PLoS Biology*, vol. 5, no. 8, article e203, 2007.
- [172] V. Plaisance, A. Abderrahmani, V. Perret-Menoud, P. Jacquemin, F. Lemaigre, and R. Regazzi, "MicroRNA-9 controls the expression of Granuphilin/Slp4 and the secretory response of insulin-producing cells," *The Journal of Biological Chemistry*, vol. 281, no. 37, pp. 26932–26942, 2006.
- [173] M. N. Poy, L. Eliasson, J. Krutzfeldt et al., "A pancreatic islet-specific microRNA regulates insulin secretion," *Nature*, vol. 432, no. 7014, pp. 226–230, 2004.
- [174] Y. Tang, B. Cai, F. Yuan et al., "Melatonin pretreatment improves the survival and function of transplanted mesenchymal stem cells after focal cerebral ischemia," *Cell Transplantation*, vol. 23, no. 10, pp. 1279–1291, 2014.
- [175] R. R. Bhonde, P. Sheshadri, S. Sharma, and A. Kumar, "Making surrogate  $\beta$ -cells from mesenchymal stromal cells: perspectives and future endeavors," *International Journal of Biochemistry and Cell Biology*, vol. 46, no. 1, pp. 90–102, 2014.
- [176] H. J. Paek, "Adipose stem cell-based regenerative medicine for reversal of diabetic hyperglycemia," *World Journal of Diabetes*, vol. 5, no. 3, pp. 235–243, 2014.
- [177] L. Sensebé, P. Bourin, and K. Tarte, "Good manufacturing practices production of mesenchymal stem/stromal cells," *Human Gene Therapy*, vol. 22, no. 1, pp. 19–26, 2011.
- [178] K. Tarte, J. Gaillard, J.-J. Lataillade et al., "Clinical-grade production of human mesenchymal stromal cells: occurrence of aneuploidy without transformation," *Blood*, vol. 115, no. 8, pp. 1549–1553, 2010.
- [179] P. Fiorina, M. Jurewicz, A. Augello et al., "Immunomodulatory function of bone marrow-derived mesenchymal stem cells in experimental autoimmune type 1 diabetes," *The Journal of Immunology*, vol. 183, no. 2, pp. 993–1004, 2009.
- [180] J. Tolar, A. J. Nauta, M. J. Osborn et al., "Sarcoma derived from cultured mesenchymal stem cells," *Stem Cells*, vol. 25, no. 2, pp. 371–379, 2007.
- [181] C. Toma, M. F. Pittenger, K. S. Cahill, B. J. Byrne, and P. D. Kessler, "Human mesenchymal stem cells differentiate to a cardiomyocyte phenotype in the adult murine heart," *Circulation*, vol. 105, no. 1, pp. 93–98, 2002.
- [182] N. Haque, M. T. Rahman, N. H. Abu Kasim, and A. M. Alabsi, "Hypoxic culture conditions as a solution for mesenchymal stem cell based regenerative therapy," *The Scientific World Journal*, vol. 2013, Article ID 632972, 12 pages, 2013.
- [183] D. P. Lennon, J. M. Edmison, and A. I. Caplan, "Cultivation of rat marrow-derived mesenchymal stem cells in reduced oxygen tension: effects on in vitro and in vivo osteochondrogenesis," *Journal of Cellular Physiology*, vol. 187, no. 3, pp. 345–355, 2001.
- [184] D. M. Panchision, "The role of oxygen in regulating neural stem cells in development and disease," *Journal of Cellular Physiology*, vol. 220, no. 3, pp. 562–568, 2009.
- [185] R. A. Busuttill, M. Rubio, M. E. T. Dollé, J. Campisi, and J. Vijg, "Oxygen accelerates the accumulation of mutations during the senescence and immortalization of murine cells in culture," *Aging cell*, vol. 2, no. 6, pp. 287–294, 2003.
- [186] C. Fehrer, R. Brunauer, G. Laschober et al., "Reduced oxygen tension attenuates differentiation capacity of human mesenchymal stem cells and prolongs their lifespan," *Aging Cell*, vol. 6, no. 6, pp. 745–757, 2007.
- [187] K. Stamati, V. Mudera, and U. Cheema, "Evolution of oxygen utilization in multicellular organisms and implications for cell signalling in tissue engineering," *Journal of Tissue Engineering*, vol. 2, no. 1, Article ID 2041731411432365, 2011.
- [188] J. Liu, H. Hao, L. Xia et al., "Hypoxia pretreatment of bone marrow mesenchymal stem cells facilitates angiogenesis by improving the function of endothelial cells in diabetic rats with lower ischemia," *PLoS ONE*, vol. 10, no. 5, Article ID e0126715, 2015.
- [189] I. Szokodi, P. Tavi, G. Földes et al., "Apelin, the novel endogenous ligand of the orphan receptor APJ, regulates cardiac contractility," *Circulation Research*, vol. 91, no. 5, pp. 434–440, 2002.



- [190] M. J. Kleinz and A. P. Davenport, "Emerging roles of apelin in biology and medicine," *Pharmacology and Therapeutics*, vol. 107, no. 2, pp. 198–211, 2005.
- [191] T. Ishizuka, T. Hinata, and Y. Watanabe, "Superoxide induced by a high-glucose concentration attenuates production of angiogenic growth factors in hypoxic mouse mesenchymal stem cells," *Journal of Endocrinology*, vol. 208, no. 2, pp. 147–159, 2011.
- [192] S. Mottaghi, B. Larijani, and A. M. Sharifi, "Apelin 13: a novel approach to enhance efficacy of hypoxic preconditioned mesenchymal stem cells for cell therapy of diabetes," *Medical Hypotheses*, vol. 79, no. 6, pp. 717–718, 2012.
- [193] X. Zeng, S. P. Yu, T. Taylor, M. Ogle, and L. Wei, "Protective effect of apelin on cultured rat bone marrow mesenchymal stem cells against apoptosis," *Stem Cell Research*, vol. 8, no. 3, pp. 357–367, 2012.
- [194] D. L. Eizirik, G. S. Korbitt, and C. Hellerström, "Prolonged exposure of human pancreatic islets to high glucose concentrations in vitro impairs the  $\beta$ -cell function," *The Journal of Clinical Investigation*, vol. 90, no. 4, pp. 1263–1268, 1992.
- [195] S. R. Burger, "Design and operation of a current good manufacturing practices cell-engineering laboratory," *Cytotherapy*, vol. 2, no. 2, pp. 111–122, 2000.
- [196] Directive 2001/83/EC of the European Parliament and of the Council of 6 November 2001 on the Community code relating to medicinal products for human use; (OJ L 311, 28.11.2001, p. 67), [http://ec.europa.eu/health/files/eudralex/vol1/dir\\_2001\\_83\\_consol\\_2012/dir\\_2001\\_83\\_cons\\_2012\\_en.pdf](http://ec.europa.eu/health/files/eudralex/vol1/dir_2001_83_consol_2012/dir_2001_83_cons_2012_en.pdf).
- [197] Regulation (EC) no 1394/2007 of the European Parliament and of the Council: Official Journal of the European Union, 2007, [http://ec.europa.eu/health/files/eudralex/vol-1/reg\\_2007\\_1394/reg\\_2007\\_1394\\_en.pdf](http://ec.europa.eu/health/files/eudralex/vol-1/reg_2007_1394/reg_2007_1394_en.pdf).
- [198] D. G. Halme and D. A. Kessler, "FDA regulation of stem-cell-based therapies," *The New England Journal of Medicine*, vol. 355, no. 16, pp. 1730–1735, 2006.
- [199] L. Harvath, "Food and Drug Administration's proposed approach to regulation of hematopoietic stem/progenitor cell products for therapeutic use," *Transfusion Medicine Reviews*, vol. 14, no. 2, pp. 104–111, 2000.
- [200] Committee for Advanced Therapies, "Reflection paper on classification of advanced therapy medicinal products," 2015, [http://www.ema.europa.eu/docs/en\\_GB/document\\_library/Scientific\\_guideline/2015/06/WC500187744.pdf](http://www.ema.europa.eu/docs/en_GB/document_library/Scientific_guideline/2015/06/WC500187744.pdf).
- [201] Regulation (EC) no 1394/2007 of the European Parliament and of the Council, 2007, [http://ec.europa.eu/health/files/eudralex/vol-1/reg\\_2007\\_1394/reg\\_2007\\_1394\\_en.pdf](http://ec.europa.eu/health/files/eudralex/vol-1/reg_2007_1394/reg_2007_1394_en.pdf).
- [202] C. L. Elseberg, J. Leber, D. Salzig et al., "Microcarrier-based expansion process for hMSCs with high vitality and undifferentiated characteristics," *International Journal of Artificial Organs*, vol. 35, no. 2, pp. 93–107, 2012.
- [203] P. Wuchter, K. Bieback, H. Schrezenmeier et al., "Standardization of Good Manufacturing Practice-compliant production of bone marrow-derived human mesenchymal stromal cells for immunotherapeutic applications," *Cytotherapy*, vol. 17, no. 2, pp. 128–139, 2015.
- [204] D. Salzig, J. Leber, K. Merkewitz, M. C. Lange, N. Köster, and P. Czermak, "Attachment, growth and detachment of human mesenchymal stem cells in a chemically defined medium," *Stem Cells International*, In press.

## Research Article

# Attachment, Growth, and Detachment of Human Mesenchymal Stem Cells in a Chemically Defined Medium

Denise Salzig,<sup>1</sup> Jasmin Leber,<sup>1</sup> Katharina Merkewitz,<sup>1</sup> Michaela C. Lange,<sup>1</sup>  
Natascha Köster,<sup>1</sup> and Peter Czermak<sup>1,2,3,4</sup>

<sup>1</sup>*Institute of Bioprocess Engineering and Pharmaceutical Technology, University of Applied Sciences Mittelhessen, 35390 Giessen, Germany*

<sup>2</sup>*Faculty of Biology and Chemistry, Justus Liebig University, 35390 Giessen, Germany*

<sup>3</sup>*Project Group Bioresources, Fraunhofer Institute for Molecular Biology and Applied Ecology (IME), 35394 Giessen, Germany*

<sup>4</sup>*Department of Chemical Engineering, Kansas State University, Manhattan, KS 66506, USA*

Correspondence should be addressed to Denise Salzig; [denise.salzig@lse.thm.de](mailto:denise.salzig@lse.thm.de)

Received 8 October 2015; Revised 18 January 2016; Accepted 26 January 2016

Academic Editor: Tao-Sheng Li

Copyright © 2016 Denise Salzig et al. This is an open access article distributed under the Creative Commons Attribution License, which permits unrestricted use, distribution, and reproduction in any medium, provided the original work is properly cited.

The manufacture of human mesenchymal stem cells (hMSCs) for clinical applications requires an appropriate growth surface and an optimized, preferably chemically defined medium (CDM) for expansion. We investigated a new protein/peptide-free CDM that supports the adhesion, growth, and detachment of an immortalized hMSC line (hMSC-TERT) as well as primary cells derived from bone marrow (bm-hMSCs) and adipose tissue (ad-hMSCs). We observed the rapid attachment and spreading of hMSC-TERT cells and ad-hMSCs in CDM concomitant with the expression of integrin and actin fibers. Cell spreading was promoted by coating the growth surface with collagen type IV and fibronectin. The growth of hMSC-TERT cells was similar in CDM and serum-containing medium whereas the lag phase of bm-hMSCs was prolonged in CDM. FGF-2 or surface coating with collagen type IV promoted the growth of bm-hMSCs, but laminin had no effect. All three cell types retained their trilineage differentiation capability in CDM and were detached by several enzymes (but not collagenase in the case of hMSC-TERT cells). The medium and coating did not affect detachment efficiency but influenced cell survival after detachment. CDM combined with cell-specific surface coatings and/or FGF-2 supplements is therefore as effective as serum-containing medium for the manufacture of different hMSC types.

## 1. Introduction

Human mesenchymal stem/stromal cells (hMSCs) are often used for cell therapy because they offer many advantageous characteristics [1]. Before therapeutic use, hMSCs must be expanded to produce the number of cells needed per patient and per dose (at least  $1\text{--}2 \times 10^6$  hMSCs per kg) [2]. The growth of hMSCs is anchorage-dependent, and the interactions among the growth surface, cells, and surrounding medium are therefore important for the manufacture of suitable numbers of healthy cells.

Cell adhesion is necessary for hMSC expansion and is driven by both nonspecific and specific interactions. Rounded cells in suspension initially attach to the surface due to complementary electrostatic/ionic forces and the growth

surface then interacts with cell surface integrins, the principal receptors mediating cell-matrix adhesion [3]. Integrin activation results in the formation of heterodimers, which initiate signaling cascades that activate downstream genes and ultimately regulate cell morphology and behavior. The cell flattens and spreads due to the activation of protein kinase C (PKC) and the subsequent accumulation of focal adhesion kinase (FAK) and actin filaments at the leading edges of the cells. The completion of cell spreading and strong adhesion to the surface, which is required for proliferation, is characterized by the inactivation of PKC and the cross-linking of actin to defined intracellular stress fibers along with FAK located at the focal adhesion sites. The actin forms a stable cytoskeleton, which maintains the cell in its adherent spread state [4, 5].



Serum (usually bovine, sometimes human) is often included in hMSC expansion media to promote cell adhesion because it contains many attachment-promoting proteins (e.g., collagens, fibronectin, laminins, and vitronectin) as well as hormones and lipids that stimulate cell proliferation *in vitro* [6]. Serum causes problems when hMSC expansion must be carried out according to good manufacturing practice (GMP) because hMSCs in the clinic are considered advanced therapy medicinal products (ATMPs) by the European Medicines Agency (EMA) and US Food and Drug Administration (FDA). These agencies recommend the avoidance of any raw materials derived from mammals, including serum, to reduce the risk of contamination when using ATMPs [7].

The regulatory pressure to eliminate serum has resulted in several innovations [8]. In addition to serum-containing medium (SCM, 10–20% serum) and reduced serum medium (1–5% serum, fortified with insulin, transferrin, and other nutrients), several categories of serum-free medium have been developed including (a) serum-free medium, with additional mammalian hormones, growth factors, proteins, and polyamines; (b) protein-free medium, containing peptide fragments from the enzymatic or acid hydrolysis of proteins derived from animals or plants; (c) recombinant xeno-free medium, containing recombinant proteins/hormones/compounds and chemically defined lipids; and (d) chemically defined medium (CDM) which is a protein-free basal medium containing only low-molecular-weight additives, synthetic peptides or hormones, and a few recombinant or synthetic versions of proteins. Several in-house serum-free media have been developed for hMSC expansion, and these often contain additional factors such as bovine/human serum albumin, insulin, transferrin, hormones (e.g., progesterone, hydrocortisone, and estradiol), growth factors (e.g., bFGF, TGF- $\beta$ , EGF, or PDGF), or heparin [9–18]. Commercial products are also available for this purpose, and although the full ingredient lists are not disclosed they also tend to include a selection of the components listed above. To our knowledge, however, the only protein/peptide-free CDM for hMSC expansion is the StemCell medium from Cell Culture Technologies, which completely lacks any proteinaceous components and each component is a defined concentration of a low-molecular-weight compound (between 50 and 250 Da, except one >1000 Da) that can be identified by its Chemical Abstracts Service registration number.

The absence of growth and attachment-promoting proteins in CDM may necessitate the use of protein coatings on the surface of tissue culture plasticware to encourage cell adhesion. Many serum proteins can be used as coatings, including native or denatured collagen, fibronectin, laminin, and vitronectin. Each protein is recognized by specific integrin heterodimers: native collagen by  $\alpha_1\beta_1$ ,  $\alpha_2\beta_1$ ,  $\alpha_{11}\beta_1$ , and  $\alpha_{1b}\beta_3$ ; denatured collagen by  $\alpha_5\beta_1$ ,  $\alpha_v\beta_3$ , and  $\alpha_{11b}\beta_3$ ; fibronectin by  $\alpha_2\beta_1$ ,  $\alpha_3\beta_1$ ,  $\alpha_4\beta_1$ ,  $\alpha_4\beta_7$ ,  $\alpha_5\beta_1$ ,  $\alpha_8\beta_1$ ,  $\alpha_v\beta_1$ ,  $\alpha_v\beta_3$ ,  $\alpha_v\beta_5$ ,  $\alpha_v\beta_6$ ,  $\alpha_v\beta_8$ , and  $\alpha_{11b}\beta_3$ ; laminin by  $\alpha_1\beta_1$ ,  $\alpha_2\beta_1$ ,  $\alpha_6\beta_1$ ,  $\alpha_7\beta_1$ ,  $\alpha_6\beta_4$ , and  $\alpha_v\beta_3$ ; and vitronectin by  $\alpha_v\beta_1$ ,  $\alpha_v\beta_3$ ,  $\alpha_v\beta_5$ , and  $\alpha_{11b}\beta_3$  [19]. The hMSCs isolated from bone marrow express the integrin subunits  $\alpha_1$ ,  $\alpha_2$ ,  $\alpha_3$ ,  $\alpha_5$ ,  $\alpha_7$ ,  $\alpha_8$ ,  $\alpha_{11}$ ,  $\alpha_v$ ,  $\beta_1$ ,  $\beta_3$ ,

and  $\beta_5$  [20] and potentially also  $\alpha_4$  and  $\alpha_6$  [21]. Integrin expression in hMSCs differs by source, but hMSCs should bind via integrin receptors to each of the coatings listed above.

We investigated the attachment and spreading behavior of an immortalized hMSC cell line (hMSC-TERT) and two types of primary hMSCs derived from bone marrow (bm-hMSCs) and adipose tissue (ad-hMSCs) in the CDM StemCell1. We tested different protein coatings to determine which were able to promote the adhesion and growth of these three cell types in CDM. We also determined whether cells growing on the different coatings differ in terms of their detachment behavior and response to different detachment enzymes.

## 2. Materials and Methods

**2.1. Cell Lines.** We used primary hMSCs from bone marrow (bm-hMSCs, passages 3–10) kindly provided by M. Rook, Merck Millipore, Bedford, MA, USA, and from adipose tissue (ad-hMSCs, passages 3–10) kindly provided by F. Ehlicke, University of Würzburg, Würzburg, Germany. The immortalized cell line hMSC-TERT [22] (passages 74–80) was kindly provided by M. Kassem, University of Southern Denmark, Odense, Denmark.

**2.2. Media.** We used Eagle's minimal essential medium (EMEM) supplemented with 2 mM L-glutamine and 10% standardized fetal bovine serum (FBS, Article no. S0615) as our standard SCM. We used StemCell1 medium (Cell Culture Technologies, Gravesano, Switzerland) supplemented with 2 mM L-glutamine as our CDM. The media were further supplemented with 8 ng/mL recombinant human basic fibroblast growth factor (bFGF; Article no. W1370950050) when required. Unless otherwise specified, all components were purchased from Biochrom (Berlin, Germany).

**2.3. Routine Cell Expansion and Adaption to CDM.** Cryoconserved hMSC-TERT cells (10% DMSO, 90% FBS) and primary hMSCs were thawed and cultivated in tissue flasks (Sarstedt, Nümbrecht, Germany) containing EMEM with seeding densities between 5000 and 10,000 cells  $\text{cm}^{-2}$  at 37°C, in a 5%  $\text{CO}_2$  humidified atmosphere. Passaging was carried out at 80–90% confluence using 0.25 mg  $\text{mL}^{-1}$  trypsin-EDTA. CDM adaptation after the first passage was carried out using a mixture of 50% SCM and 50% CDM, and subsequently 100% CDM was used in Advanced TC™ tissue flasks (Greiner Bio-One, Kremsmünster, Austria). All subsequent passaging was carried out using 25% conditioned medium from earlier cultures. The medium was replaced with 50% fresh medium every 3–4 days. Cells were passaged at least twice in CDM alone before starting the experiments.

**2.4. Coating the Six-Well Plates.** Collagen IV (human, C7521), fibronectin (bovine, F1141), laminin (murine, L2020), and vitronectin (human, SRP3186) were obtained from Sigma-Aldrich Laborchemikalien GmbH (Seelze, Germany). Each protein was applied to six-well plates overnight at 4°C to achieve a coating density of 5  $\mu\text{mol cm}^{-2}$ . A set of plates was coated with 10% (v/v) FBS as a positive control.

**2.5. Analysis of Cell Attachment and Spreading.** The cells were suspended either in SCM or in CDM and plated with 7000 (hMSC-TERT), 8000 (bm-MSCs), or 3000 (ad-MSCs) cells  $\text{cm}^{-2}$  in coated or noncoated six-well plates. Attachment was analyzed for 5 h by counting the adherent and suspended cells every hour. Spreading was analyzed by counting the spread cells on microscopic images and defined as previously described [24].

**2.6. Immunofluorescence Staining of the Cytoskeleton and Cell Surface Integrin  $\alpha_4$ .** Cells were grown for 24 h either in SCM or in CDM on coated or noncoated six-well plates. We fixed the cells by removing the medium, gently washing with 2 mL PBS, and incubating with acetone (Carl Roth, Karlsruhe, Germany) for 10 min at  $-20^\circ\text{C}$ . After two washes with PBS, the sample was incubated with 2 mL blocking solution ( $10 \text{ mg mL}^{-1}$  BSA in PBS) for 30 min at room temperature. The sample was again washed twice and then incubated with a 1:80 dilution of Alexa Fluor<sup>®</sup> 555 Phalloidin (Life Technologies, Darmstadt, Germany, A340555) or a 1:200 dilution of DyLight 488 integrin  $\alpha_4$  antibody MM0417-2L30 (R&D Systems GmbH, Wiesbaden, Germany, NBP2-11738G) in PBS for 2 h at room temperature in the dark. Finally, the nuclei were counterstained with DAPI (AppliChem, Darmstadt, Germany) and the sample was embedded in Mowiol (Carl Roth) according to the manufacturers' recommendations.

**2.7. Analysis of Cell Growth.** The cells were seeded in six-well plates (coated or noncoated) at a density of 7000-10,000 cells  $\text{cm}^{-2}$  and grown in 2 mL SCM or CDM for up to 8 d at  $37^\circ\text{C}$  in a 5%  $\text{CO}_2$  humidified atmosphere. Cells were counted under the microscope every day. The growth rate  $\mu$  was determined during the exponential growth phase using the following equation:

$$\mu \left[ \frac{1}{h} \right] = \frac{\ln(X_2) - \ln(X_1)}{t_2 - t_1}. \quad (1)$$

**2.8. Differentiation of Expanded Cells.** The cells were differentiated using StemMACS AdipoDiff, ChondroDiff, or OsteoDiff media (Miltenyi Biotec, Bergisch Gladbach, Germany) according to the manufacturer's recommendations. After differentiation, the cells were fixed with 4% paraformaldehyde (Carl Roth) for 30 min at room temperature. Adipogenic differentiation was confirmed by nil red staining of the fat droplets as previously described [25]. Finally, the sample was embedded with Mowiol (Carl Roth) according to the manufacturer's recommendations. Chondrogenic differentiation was confirmed by the immunofluorescence staining of collagen type II as described [26]. Osteogenic differentiation was confirmed using the OsteoImage Mineralization Assay (Lonza, Basel, Switzerland) according to the manufacturer's recommendations.

**2.9. Analysis of Cell Detachment.** The cells were suspended in SCM or CDM, seeded at a density of 50,000 cells  $\text{cm}^{-2}$  in coated or noncoated six-well plates and incubated at  $37^\circ\text{C}$  in a 5%  $\text{CO}_2$  humidified atmosphere until attachment was

TABLE 1: Properties of the enzymes used for cell detachment.

Detachment enzyme	Manufacturer	Incubation time (min)
Accutase	Sigma-Aldrich	10
Collagenase	PAA Laboratories GmbH	60
Prolyl-specific peptidase (PsP)	[23]	40
Trypsin	PAA	10

observed. Each well was washed twice with 1 mL PBS to remove the medium. The cells were incubated with 0.5 mL detachment enzyme solution (supplemented with 0.02% EDTA if necessary) as shown in Table 1. The detachment reaction was stopped by adding 1.5 mL SCM, the solution was centrifuged ( $500 \times g$ , 5 min, room temperature), and the remaining cell pellet was resuspended in 0.5 mL SCM. Cell number and viability were determined by trypan blue staining.

### 3. Results

**3.1. Attachment and Spreading of hMSC-TERT Cells and Primary hMSCs.** Efficient cell attachment and spreading on the growth surface are necessary to expand anchorage-dependent hMSCs. In CDM, the hMSC-TERT cells completely attached within 4 h regardless of the presence/absence or type of surface coating. We observed minor surface-dependent differences in the attachment rate; for example, the cells attached more slowly on the collagen IV coating. Nevertheless, there was little difference in the attachment behavior of hMSC-TERT cells growing in SCM and CDM. In contrast, the spreading of the cells in CDM was positively influenced by the protein coatings. In the absence of coating, only 8% of the attached cells spread after 5 h, whereas cells seeded on collagen type IV and fibronectin spread at similar rates to those seeded on FBS or in SCM (Figure 1). The immunofluorescence staining of the cytoskeleton and cell surface integrins revealed that hMSC-TERT cells growing in CDM on surfaces coated with collagen type IV or fibronectin contained better-organized F-actin fibers than cells growing on other surfaces and also expressed integrin  $\alpha_4$  at a higher level (Figure 2).

The bm-hMSCs attached poorly in CDM (Figure 3(a)) but even in SCM complete attachment took up to 24 h. Only a few bm-hMSCs had attached after 5 h in CDM and no spreading was observed within this time period. The attached bm-hMSCs were thin and elongated on each of the coatings and no lamellipodia were observed. Our results showed that no coating was preferable for the attachment or spreading of these cells in CDM, but without coating the attached cells tended to detach again and become rounded (Figure 3(b)).

In contrast, the ad-hMSCs attached rapidly in CDM and more than 90% of the cells had attached within 2 h, regardless of the presence/absence or type of coating. Within 4 h, 59% of the cells had spread on the collagen type IV surface whereas almost 100% of cells had spread on the fibronectin,

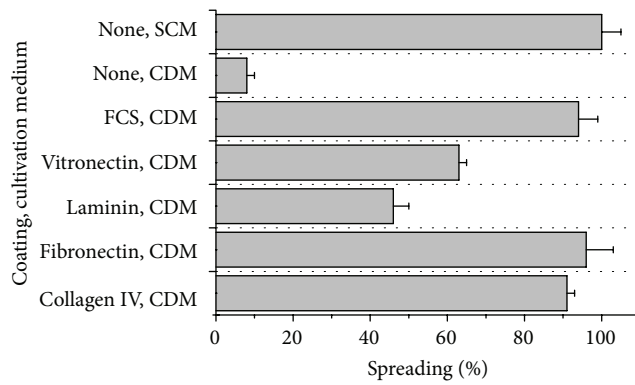


FIGURE 1: Spreading of hMSC-TERT cells on different surface coatings. The hMSC-TERT cells were grown on different coatings either in serum-containing medium (SCM) or in chemically defined medium (CDM). The cells were analyzed by microscopy and those showing at least three lamellipodia were defined as spread. Each measurement was taken in triplicate ( $n = 3$ ).

laminin, and vitronectin surfaces after the same amount of time. The immunofluorescence staining showed that all the expanded ad-hMSCs in CDM expressed integrin  $\alpha_4$ , but the F-actin fibers were not as well organized and distinct as those observed in the cells cultivated in SCM (Figure 2).

**3.2. Growth of hMSC-TERT Cells and Primary hMSCs.** A comprehensive investigation of hMSC-TERT growth behavior in CDM initially showed that the choice of cell culture plastic (CCP) had an enormous influence (Figure 4). In standard CCP, the hMSC-TERT cells had a prolonged lag phase and a slower growth rate ( $\mu_{\text{STD-CCP}} = 0.013 \text{ h}^{-1}$ ) compared to cells growing in SCM ( $\mu_{\text{SCM}} = 0.020 \text{ h}^{-1}$ ). In addition, the maximum density of cells growing on standard CPP was 2.6-fold lower in CDM compared to SCM. On CPP specially designed for compatibility with CDM cultivation (CDM-CPP), the growth rate of the cells was similar in CDM and SCM ( $\mu_{\text{CDM-CPP}} = 0.019 \text{ h}^{-1}$ ). Supplementing the CDM with FGF-2 or coating the CPP with the proteins listed above did not improve the growth rate any further.

The growth of bm-hMSCs in CDM was only tested using CDM-CPP. We found that cell growth was much slower in the absence of coating ( $\mu_{\text{CDM-CCP}} 0.016 \text{ h}^{-1}$ ) when compared to the growth rate in SCM ( $\mu_{\text{SCM}} 0.020 \text{ h}^{-1}$ ), and that the cell number at the end of the cultivation was four times lower in CDM compared to SCM (Figure 5). For both primary hMSCs, supplementing the CDM with FGF-2 significantly improved the cell growth rate ( $\mu_{\text{FGF2}} = 0.019 \text{ h}^{-1}$ ), but the cell number at the end of the cultivation in CDM was only half that achieved using SCM. This probably reflects the duration of the lag phase, which is 48 h longer in CDM compared to SCM. The nature of coating also affected the growth rate of bm-hMSCs in CDM; for example, laminin did not promote cell growth any better than uncoated plates, whereas collagen type IV improved the bm-hMSC growth rate to the same extent as supplementing the medium with FGF-2.

**3.3. Differentiation Potential of hMSC-TERT Cells and Primary hMSCs in CDM.** Trilineage differentiation potential is a minimal criterion for the therapeutic use of hMSCs, so we investigated whether the expansion of cells in CDM had any influence on this property. We found that hMSC-TERTs, bm-hMSCs, and ad-hMSCs each retained their ability to differentiate into adipocytes, chondrocytes, and osteoblasts, as determined by immunofluorescence staining (Figure 6).

**3.4. Detachment of hMSC-TERT Cells and Primary hMSCs.** Detachment is also necessary for hMSC expansion and this process should be efficient without causing cell damage. Compared to hMSC-TERT cells grown in SCM, we found that the same cells growing in CDM were more difficult to detach with trypsin, Accutase, and PsP and that collagenase was completely ineffective even if the surface of the flasks was coated with collagen (Figure 7). For hMSC-TERT cells grown in SCM, the coating had no influence on detachment with trypsin or Accutase because both enzymes achieved almost 100% detachment. For hMSC-TERT cells grown in CDM, trypsin and Accutase detached most cells from laminin-coated surfaces. PsP was unable to detach hMSC-TERT cells from surfaces coated with collagen type IV in either SCM or CDM. This enzyme efficiently removed cells from all other surfaces in both media, but the efficiency of cell detachment from fibronectin was 50% lower in CDM compared to SCM. Although CDM generally had little impact on detachment efficiency, it did affect the viability of the detached cells. For hMSC-TERT cells grown in CDM without a surface coating, the viability fell substantially after detachment with trypsin ( $80.7 \pm 3.3\%$ ), Accutase ( $87.2 \pm 2.0\%$ ), and collagenase ( $83.8 \pm 9.2\%$ ) but remained high after detachment with PsP ( $97.4 \pm 0.1\%$ ). In contrast, the cells grown without a surface coating in SCM only lost viability following detachment with collagenase ( $88.6 \pm 1.9\%$ ). The bm-hMSCs could be detached efficiently from each coating with any of the enzymes, including collagenase. We observed no differences among the four coatings, but detachment was slightly less efficient in the absence of a coating. All detached cells remained highly viable after detachment (Figure 8).

## 4. Discussion

**4.1. Interaction between Cells and the Growth Surface.** The nature of the growth surface can have a profound effect on the behavior of cultured cells, and we found that this was also the case for three different types of hMSCs. Switching from SCM to CDM affected the growth of hMSCs on standard tissue culture plastic, but a specially modified surface designed for compatibility with CDM improved the growth of hMSC-TERT cells to the same extent as SCM, and coating this surface with extracellular matrix (ECM) proteins or adding FGF-2 to the medium did not improve growth any further. The modified plastic surface is prepared by incubating it with plasma, which provides more oxygen groups to increase wettability, protein interactions, and thereby cell proliferation [27]. The impact of further coating with ECM proteins differed according to the cell type. Fibronectin promoted



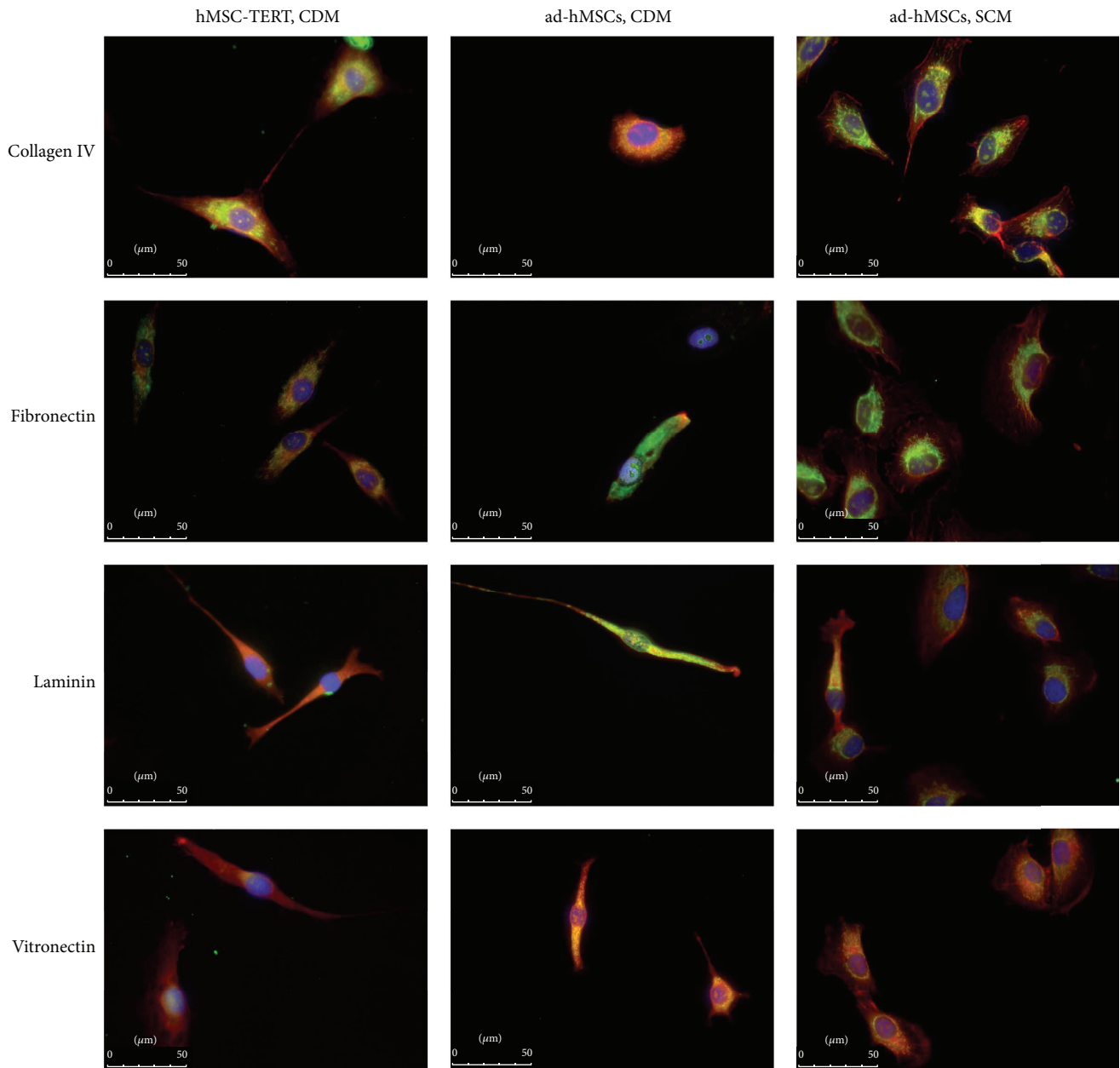


FIGURE 2: Immunofluorescence staining of the cytoskeleton and the cell surface integrin  $\alpha_4$  in hMSC-TERT cells and primary adipose-derived hMSCs (ad-hMSCs). The cells were grown on different coatings either in serum-containing medium (SCM) or in chemically defined medium (CDM). After fixation, immunofluorescence staining was carried out showing F-actin in red, integrin  $\alpha_4$  in green, and nuclei in blue.

the adhesion of hMSC-TERT cells and ad-hMSCs, which is not surprising because hMSCs express more fibronectin receptors than receptors for each of the three other coatings [20, 28]. Integrin  $\alpha_4$  is a major fibronectin receptor [19] and we were able to detect this protein on the surface of these hMSCs grown on fibronectin in SCM and CDM. Interestingly, integrin  $\alpha_4$  was also present on hMSC-TERT cells growing in CDM on collagen type IV although integrins  $\alpha_1$ ,  $\alpha_2$ ,  $\alpha_{10}$ , and  $\alpha_{11}$  combine with integrin  $\beta_1$  to bind collagen IV and integrin  $\alpha_4$  is not involved. Fibronectin and collagen IV are interconnected, and collagen type IV educates other

ECM components and promotes the survival of fibroblasts and tumor cells independent of its integrin and specificity as a way to circumvent apoptosis [29, 30]. We observed this growth-promoting effect for bm-hMSCs growing in CDM on a collagen type IV coating. The coating had the same positive impact as the growth factor FGF-2, which is known to enhance the mitotic potential of hMSCs and increase their growth rate and potential for self-renewal [31, 32].

*4.2. The Behavior of the Three Types of hMSC in CDM.* The attachment and spreading kinetics of the three types of

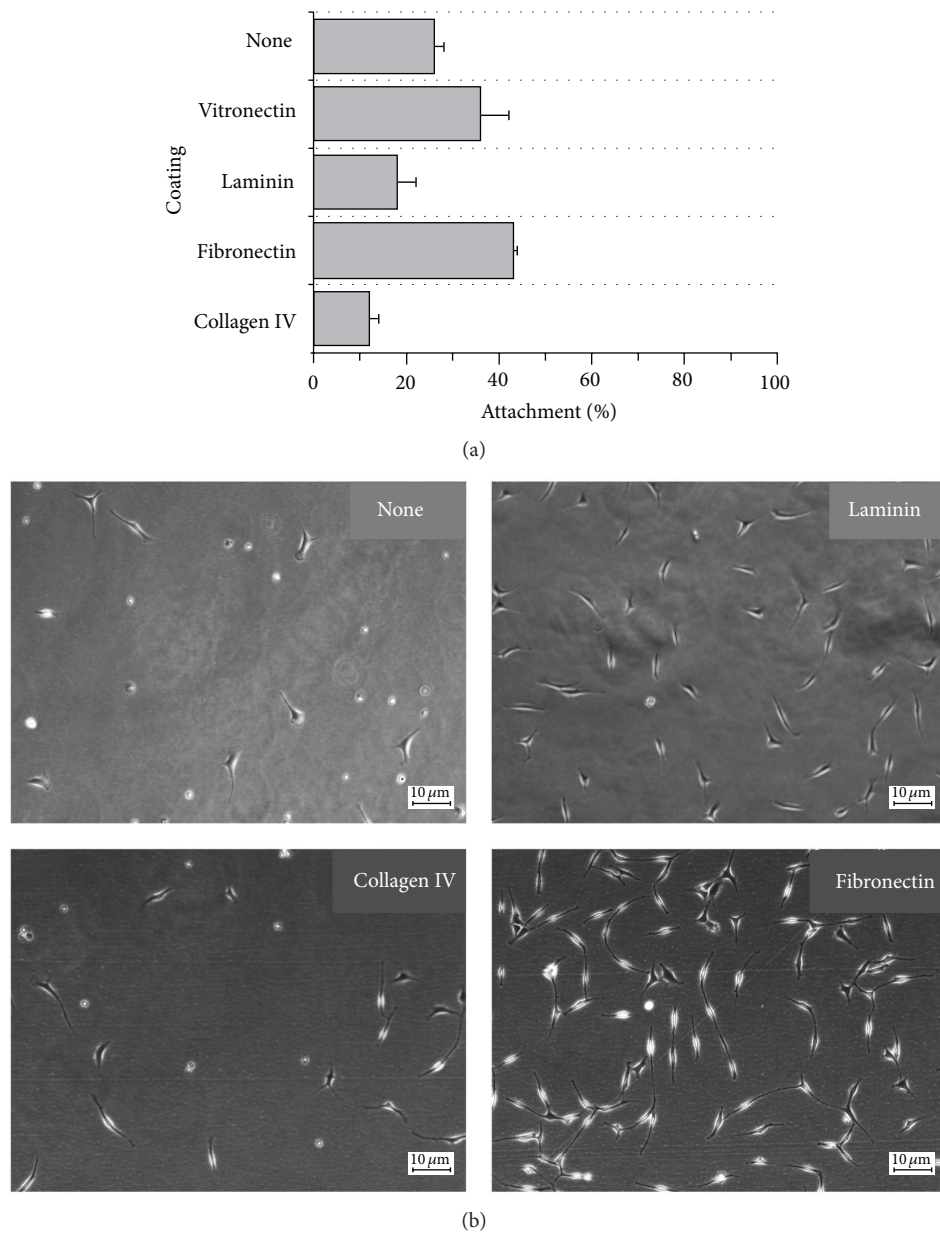


FIGURE 3: Attachment and spreading of primary bone marrow-derived hMSCs (bm-hMSCs) in chemically defined medium (CDM). (a) Attachment was measured by counting the adherent and suspended cells. (b) The cells were analyzed by microscopy and those showing at least three lamellipodia were defined as spread. Each measurement was taken in triplicate ( $n = 3$ ).

hMSC in CDM were strongly dependent on the cell type. Whereas the hMSC-TERT cells and ad-hMSCs attached and spread rapidly, the adhesion of the bm-hMSC was slow and inefficient. The latter were also slow to attach in SCM, which suggests the effect is cell- or donor-dependent rather than indicative of missing attachment-promoting proteins in the CDM. Human MSCs from different sources differ in their integrin profiles [33]; for example, hMSC-TERT cells express integrins  $\alpha_2$ ,  $\alpha_4$ ,  $\alpha_5$ ,  $\alpha_6$ ,  $\alpha_{11}$ ,  $\alpha_v$ ,  $\beta_1$ , and  $\beta_5$  [28], whereas primary hMSCs express integrins  $\alpha_1$ ,  $\alpha_2$ ,  $\alpha_3$ ,  $\alpha_6$ ,  $\alpha_7$ ,  $\alpha_9$ ,  $\alpha_{11}$ , and  $\beta_1$  [34], and this is likely to affect their adhesion behavior. Importantly, cell vigor also depends on the age and health

of the donor. The bm-hMSCs were derived from an older donor than the ad-hMSCs, which could explain their slow attachment and proliferation compared to the ad-hMSCs and the immortalized hMSC-TERT cells. To exclude donor-dependent effects and confirm that the observed behavior in CDM is genuinely cell-dependent, it will be necessary to repeat the experiments using bm-hMSCs and ad-hMSCs from at least five donors.

Strong adhesion is required for cell growth, so the inefficient adhesion of the bm-hMSCs in CDM may explain the long lag phase compared to the same cells grown in SCM. The growth rate was improved by supplementing



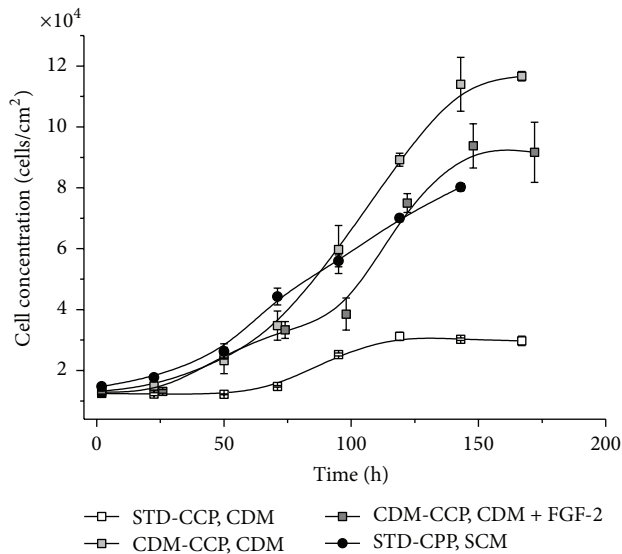


FIGURE 4: Growth of hMSC-TERT cells in chemically defined medium (CDM). The cells were grown on standard cell culture plastic (STD-CCP) or CDM-optimized CCP (CDM-CCP) in either CDM (with or without FGF-2) or serum-containing medium (SCM). Cell growth was analyzed by the counting and the measurement of glucose consumption. Each measurement was taken in triplicate ( $n = 3$ ).

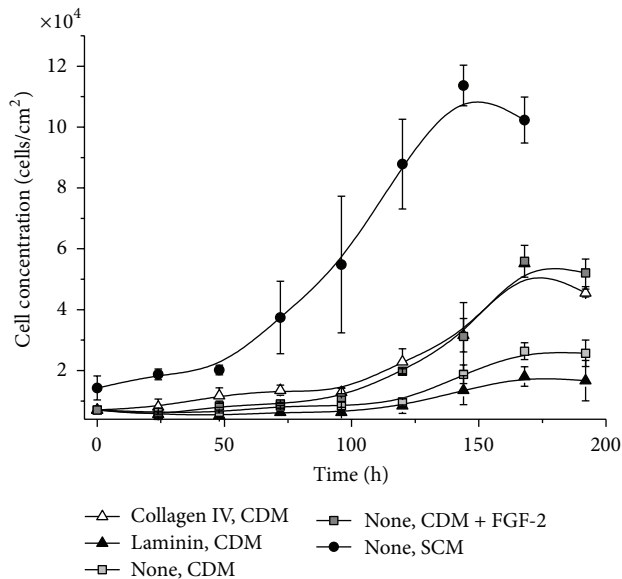


FIGURE 5: Growth of primary bone marrow-derived hMSCs (bm-hMSCs) in chemically defined medium (CDM). The cells were grown on coated or noncoated CDM-optimized cell culture plastic either in CDM (with or without FGF-2) or in serum-containing medium (SCM). Cell growth was analyzed by the counting and the measurement of glucose consumption. Each measurement was taken in triplicate ( $n = 3$ ).

the medium with FGF-2 or coating the surface with collagen type IV, but the lag phase could not be shortened. To confirm this hypothesis, the adhesion strength of the cells should be analyzed in future experiments, for example, by atomic force microscopy [35].

The detachment behavior of the three types of hMSC was also distinct and depended on the medium and the surface coating. For cells grown in CDM, surface coating did not improve the efficiency of detachment, but it did increase cell viability after cell detachment indicating a protective effect. Interestingly, the hMSC-TERT cells could not be detached with collagenase, even if the cells were grown on a collagen-coated surface, despite the fact that collagenase is often used to isolate hMSCs from tissues [36]. In previous studies, we showed that collagenase is not suitable for the detachment of hMSC-TERT cells from glass surfaces because it primarily cleaves cell-cell linkages and not cell surface linkages [37, 38]. In contrast to hMSC-TERT cells, the primary hMSCs could easily be detached with collagenase and the other enzymes.

**4.3. Influence of Surface Coating and the Medium on Stem Cell Potency.** All three hMSC types retained their stem cell phenotype and capacity for multilineage differentiation when expanded in CDM, showing that CDM is suitable for robust hMSC expansion and does not contain soluble factors that promote unwanted differentiation [39].

We did not determine whether the coating influences the potency of hMSCs, but this must be considered because certain ECM components can induce differentiation. For example, fibronectin promotes cell spreading and proliferation while inhibiting adipogenic differentiation, but it plays a pivotal role during osteogenic differentiation. Furthermore, vitronectin and collagen type I can promote osteogenic differentiation in hMSCs, whereas laminin can stimulate the proliferation of hMSCs (although we could not confirm this in our experiments) but suppresses chondrogenesis [40]. This shows that multiple ECM components can provide a suitable attachment and growth surface for hMSCs, but these must be chosen carefully to avoid unwanted differentiation during cell expansion.

## 5. Conclusions

The manufacture of hMSCs for clinical applications requires an appropriate choice of growth surface and expansion medium. We have demonstrated that it is possible to expand different primary hMSCs and an immortalized hMSC line in protein/peptide-free CDM, which means that fewer supplements are required than anticipated and that the cells can survive in a basic medium. The cultivation of cells for a few days or for one or two passages is not enough to declare a robust serum-free medium, because stem cells can proliferate in basal medium [41]. Therefore, it will be necessary to expand the hMSCs for longer periods to determine whether the CDM is suitable for manufacturing. Nevertheless, the behavior of each of the three cell types in CDM was distinct. For example, the fibronectin coating was only advantageous for ad-hMSC and hMSC-TERT attachment but did not affect

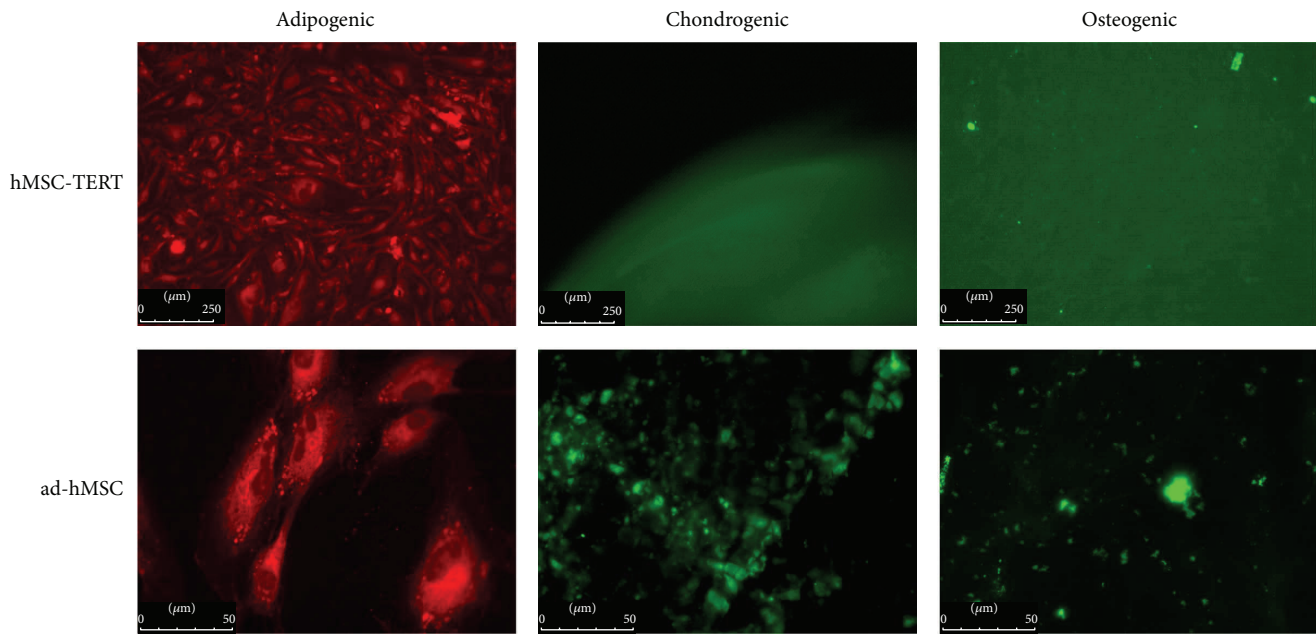


FIGURE 6: Differentiation capacities of hMSC-TERT cells and primary adipose-derived hMSCs (ad-hMSCs). The cells were induced to undergo adipogenic, chondrogenic, or osteogenic differentiation in commercial media after expansion in CDM. Differentiation was confirmed by nil red staining (red, adipogenic), collagen type II immunostaining (green, chondrogenic), or hydroxyapatite staining (green, osteogenic). The primary bone marrow-derived hMSCs (bm-hMSCs) behaved in a similar manner (data not shown).

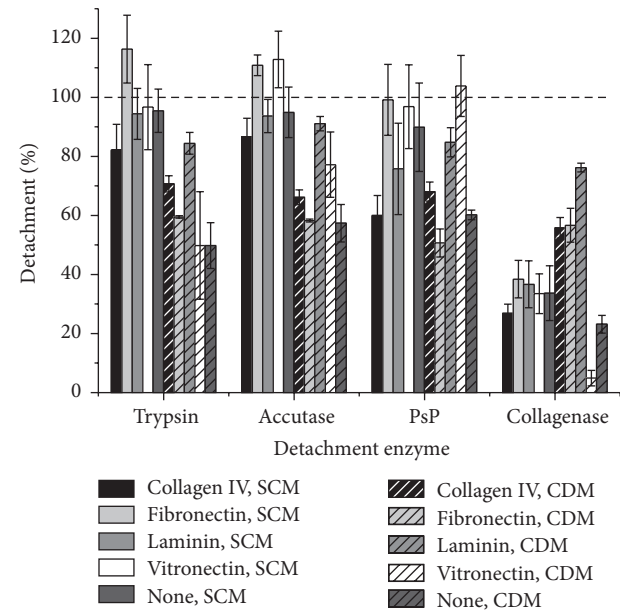


FIGURE 7: Detachment of hMSC-TERT cells using different enzymes. The cells were grown to confluency in coated or noncoated wells and were detached enzymatically. Cell detachment was analyzed by counting cells in suspension. Each experiment was carried out in triplicate ( $n = 3$ ).

bm-hMSCs. Furthermore, FGF-2 and collagen IV promoted the growth of bm-hMSCs but not hMSC-TERT cells. It is not yet possible to recommend a generally advantageous coating or supplement for the expansion of each MSC type in CDM

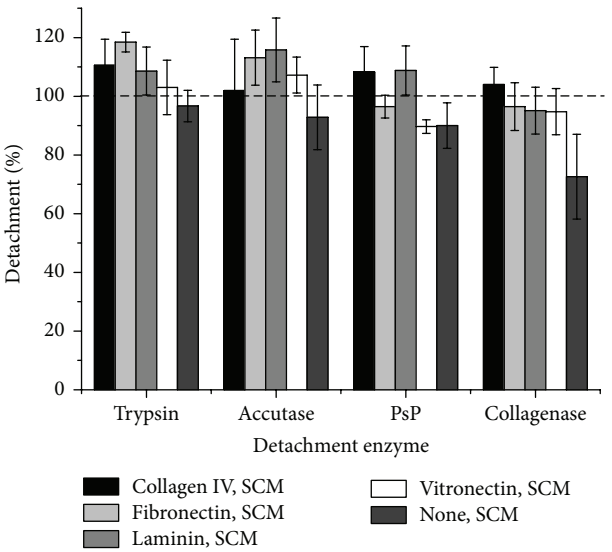


FIGURE 8: Detachment of primary bone marrow-derived hMSCs (bm-hMSCs) using different enzymes. The cells were grown to confluency in coated or noncoated wells and were detached enzymatically. Cell detachment was analyzed by counting cells in suspension. Each experiment was carried out in triplicate ( $n = 3$ ).

because donor-dependent effects could not be excluded. Therefore, more extensive studies with hMSCs from other sources (e.g., umbilical cord) and with more donors per cell type are necessary to determine whether general principles can be drawn from these data. Efficient hMSC manufacturing

requires a detailed understanding of the interactions among the cells, the growth surface, and the cultivation medium.

## Conflict of Interests

The authors declare that there is no conflict of interests regarding the publication of this paper.

## Acknowledgments

This research was financially supported by the Hessen State Ministry of Higher Education, Research and the Arts, within the Hessen initiative for supporting scientific and economic excellence (LOEWE-program). The authors acknowledge Dr. Richard M Twyman for revising the paper.

## References

- [1] T. Opperman, J. Leber, C. Elseberg, D. Salzig, and P. Czermak, "hMSC production in disposable bioreactors in compliance with cGMP guidelines and PAT," *American Pharmaceutical Review*, vol. 17, no. 3, pp. 42–47, 2014.
- [2] K. Cierpka, C. L. Elseberg, K. Niss, M. Kassem, D. Salzig, and P. Czermak, "HMSC production in disposable bioreactors with regards to GMP and PAT," *Chemie-Ingenieur-Technik*, vol. 85, no. 1-2, pp. 67–75, 2013.
- [3] A. L. Berrier and K. M. Yamada, "Cell-matrix adhesion," *Journal of Cellular Physiology*, vol. 213, no. 3, pp. 565–573, 2007.
- [4] M.-H. Disatnik, S. C. Boutet, W. Pacio et al., "The bi-directional translocation of MARCKS between membrane and cytosol regulates integrin-mediated muscle cell spreading," *Journal of Cell Science*, vol. 117, no. 19, pp. 4469–4479, 2004.
- [5] J. E. Murphy-Ullrich, "The de-adhesive activity of matricellular proteins: is intermediate cell adhesion an adaptive state?" *Journal of Clinical Investigation*, vol. 107, no. 7, pp. 785–790, 2001.
- [6] O.-W. Merten and M. C. Flickinger, "Cell detachment," in *Encyclopedia of Industrial Biotechnology: Bioprocess, Bioseparation, and Cell Technology*, pp. 1–22, John Wiley & Sons, New York, NY, USA, 2009.
- [7] FDA, *FDA Proposes Barring Ceratin Cattle Material from Medical Products As BSE Safeguard*, FDA, Silver Spring, Md, USA, 2007.
- [8] D. W. Jayme and S. R. Smith, "Media formulation options and manufacturing process controls to safeguard against introduction of animal origin contaminants in animal cell culture," *Cytotechnology*, vol. 33, no. 1, pp. 27–36, 2000.
- [9] S. Jung, K. M. Panchalingam, L. Rosenberg, and L. A. Behie, "Ex vivo expansion of human mesenchymal stem cells in defined serum-free media," *Stem Cells International*, vol. 2012, Article ID 123030, 21 pages, 2012.
- [10] S. A. Tarle, S. Shi, and D. Kaigler, "Development of a serum-free system to expand dental-derived stem cells: PDLSCs and SHEDs," *Journal of Cellular Physiology*, vol. 226, no. 1, pp. 66–73, 2011.
- [11] D. R. Marshak and J. J. Holecek, "Chemically defined medium for human mesenchymal stem cells," United States Patent 5,908,782, 1999.
- [12] C.-H. Liu, M.-L. Wu, and S.-M. Hwang, "Optimization of serum free medium for cord blood mesenchymal stem cells," *Biochemical Engineering Journal*, vol. 33, no. 1, pp. 1–9, 2007.
- [13] G. Rajaraman, J. White, K. S. Tan et al., "Optimization and scale-up culture of human endometrial multipotent mesenchymal stromal cells: potential for clinical application," *Tissue Engineering Part C: Methods*, vol. 19, no. 1, pp. 80–92, 2013.
- [14] D. P. Lennon, S. E. Haynesworth, R. G. Young, J. E. Dennis, and A. I. Caplan, "A chemically defined medium supports in vitro proliferation and maintains the osteochondral potential of rat marrow-derived mesenchymal stem cells," *Experimental Cell Research*, vol. 219, no. 1, pp. 211–222, 1995.
- [15] A. M. Parker, H. Shang, M. Khurgel, and A. J. Katz, "Low serum and serum-free culture of multipotential human adipose stem cells," *Cytotherapy*, vol. 9, no. 7, pp. 637–646, 2007.
- [16] T. E. Ludwig, V. Bergendahl, M. E. Levenstein, J. Yu, M. D. Probasco, and J. A. Thomson, "Feeder-independent culture of human embryonic stem cells," *Nature Methods*, vol. 3, no. 8, pp. 637–646, 2006.
- [17] J. E. Hudson, R. J. Mills, J. E. Frith et al., "A defined medium and substrate for expansion of human mesenchymal stromal cell progenitors that enriches for osteo- and chondrogenic precursors," *Stem Cells and Development*, vol. 20, no. 1, pp. 77–87, 2011.
- [18] S. Mimura, N. Kimura, M. Hirata et al., "Growth factor-defined culture medium for human mesenchymal stem cells," *International Journal of Developmental Biology*, vol. 55, no. 2, pp. 181–187, 2011.
- [19] E. F. Plow, T. A. Haas, L. Zhang, J. Loftus, and J. W. Smith, "Ligand binding to integrins," *The Journal of Biological Chemistry*, vol. 275, no. 29, pp. 21785–21788, 2000.
- [20] C. Niehage, C. Steenblock, T. Pursche, M. Bornhäuser, D. Corbeil, and B. Hoflack, "The cell surface proteome of human mesenchymal stromal cells," *PLoS ONE*, vol. 6, no. 5, Article ID e20399, 2011.
- [21] D. Docheva, C. Popov, W. Mutschler, and M. Schieker, "Human mesenchymal stem cells in contact with their environment: surface characteristics and the integrin system," *Journal of Cellular and Molecular Medicine*, vol. 11, no. 1, pp. 21–38, 2007.
- [22] J. L. Simonsen, C. Rosada, N. Serakinci et al., "Telomerase expression extends the proliferative life-span and maintains the osteogenic potential of human bone marrow stromal cells," *Nature Biotechnology*, vol. 20, no. 6, pp. 592–596, 2002.
- [23] K. Cierpka, N. Mika, M. C. Lange, H. Zorn, P. Czermak, and D. Salzig, "Cell detachment by prolyl-specific endopeptidase from *Wolfiporia cocos*," *American Journal of Biochemistry and Biotechnology*, vol. 10, no. 1, pp. 14–21, 2014.
- [24] F. Xu, S. Ito, M. Hamaguchi, and T. Senga, "Disruption of cell spreading by the activation of MEK/ERK pathway is dependent on AP-1 activity," *Nagoya Journal of Medical Science*, vol. 72, no. 3-4, pp. 139–144, 2010.
- [25] C. Elseberg, D. Salzig, and P. Czermak, "Bioreactor expansion of human mesenchymal stem cells according to GMP requirements," in *Stem Cells and Good Manufacturing Practices*, K. Turksen, Ed., vol. 1283, pp. 199–218, Springer, New York, NY, USA, 2015.
- [26] F. Ehlicke, D. Freimark, B. Heil, A. Dorresteyn, and P. Czermak, "Intervertebral disc regeneration: influence of growth factors on differentiation of human mesenchymal stem cells (hMSC)," *International Journal of Artificial Organs*, vol. 33, no. 4, pp. 244–252, 2010.
- [27] A. M. P. Pardo, M. Bryhan, H. Krasnow et al., "Corning® CellBIND® surface: an improved surface for enhanced cell attachment," Tech. Rep., 2005.

- [28] L. J. Foster, P. A. Zeemann, C. Li, M. Mann, O. N. Jensen, and M. Kassem, "Differential expression profiling of membrane proteins by quantitative proteomics in a human mesenchymal stem cell line undergoing osteoblast differentiation," *Stem Cells*, vol. 23, no. 9, pp. 1367–1377, 2005.
- [29] K. M. Mak, P. Sehgal, and C. K. Harris, "Type VI collagen: its biology and value as a biomarker of hepatic fibrosis," *Austin Biomarkers & Diagnosis*, vol. 1, pp. 1–9, 2014.
- [30] P. Chen, M. Cescon, and P. Bonaldo, "Collagen VI in cancer and its biological mechanisms," *Trends in Molecular Medicine*, vol. 19, no. 7, pp. 410–417, 2013.
- [31] L. A. Solchaga, K. Penick, J. D. Porter, V. M. Goldberg, A. I. Caplan, and J. F. Welter, "FGF-2 enhances the mitotic and chondrogenic potentials of human adult bone marrow-derived mesenchymal stem cells," *Journal of Cellular Physiology*, vol. 203, no. 2, pp. 398–409, 2005.
- [32] S. Tsutsumi, A. Shimazu, K. Miyazaki et al., "Retention of multilineage differentiation potential of mesenchymal cells during proliferation in response to FGF," *Biochemical and Biophysical Research Communications*, vol. 288, no. 2, pp. 413–419, 2001.
- [33] L. P. Roncoroni, J. K. Maerz, B. Angres et al., "Adhesion to extracellular matrix proteins can differentiate between human bone marrow derived mesenchymal stem cells and fibroblasts," *Journal of Tissue Science & Engineering*, vol. S11, article 008, 2013.
- [34] K. Warstat, D. Meckbach, M. Weis-Klemm et al., "TGF- $\beta$  enhances the integrin  $\alpha 2\beta 1$ -mediated attachment of mesenchymal stem cells to type I collagen," *Stem Cells and Development*, vol. 19, no. 5, pp. 645–656, 2010.
- [35] T. Lanzicher, V. Martinelli, C. S. Long et al., "AFM single-cell force spectroscopy links altered nuclear and cytoskeletal mechanics to defective cell adhesion in cardiac myocytes with a nuclear lamin mutation," *Nucleus*, vol. 6, no. 5, pp. 394–407, 2015.
- [36] N. Rodríguez-Fuentes, O. Reynoso-Ducoing, A. Rodríguez-Hernández et al., "Isolation of human mesenchymal stem cells and their cultivation on the porous bone matrix," *Journal of Visualized Experiments*, vol. 96, pp. 1–7, 2015.
- [37] D. Salzig, A. Schmiermund, P. P. Grace, C. Elseberg, C. Weber, and P. Czermak, "Enzymatic detachment of therapeutic mesenchymal stromal cells grown on glass carriers in a bioreactor," *Open Biomedical Engineering Journal*, vol. 7, no. 1, pp. 147–158, 2013.
- [38] C. Weber, S. Pohl, R. Pörtner et al., "Expansion and harvesting of hMSC-TERT," *The Open Biomedical Engineering Journal*, vol. 1, no. 1, pp. 38–46, 2007.
- [39] R. K. Das and O. F. Zouani, "A review of the effects of the cell environment physicochemical nanoarchitecture on stem cell commitment," *Biomaterials*, vol. 35, no. 20, pp. 5278–5293, 2014.
- [40] Y.-K. Wang and C. S. Chen, "Cell adhesion and mechanical stimulation in the regulation of mesenchymal stem cell differentiation," *Journal of Cellular and Molecular Medicine*, vol. 17, no. 7, pp. 823–832, 2013.
- [41] S. Gottipamula, M. S. Muttigi, U. Kolkundkar, and R. N. Seetharam, "Serum-free media for the production of human mesenchymal stromal cells: a review," *Cell Proliferation*, vol. 46, no. 6, pp. 608–627, 2013.



## Research Article

# Theoretical and Practical Issues That Are Relevant When Scaling Up hMSC Microcarrier Production Processes

Valentin Jossen,<sup>1</sup> Cedric Schirmer,<sup>1</sup> Dolman Mostafa Sindi,<sup>1</sup> Regine Eibl,<sup>1</sup>  
Matthias Kraume,<sup>2</sup> Ralf Pörtner,<sup>3</sup> and Dieter Eibl<sup>1</sup>

<sup>1</sup>Institute of Chemistry and Biotechnology, Zurich University of Applied Sciences, Campus Grüental, 8820 Wädenswil, Switzerland

<sup>2</sup>Department of Process Engineering, Chair of Chemical and Process Engineering, Technical University of Berlin, Strasse des 17.Juni 135, 10623 Berlin, Germany

<sup>3</sup>Department of Bioprocess and Biosystems Engineering, Technical University of Hamburg, Denickestrasse 1, 21073 Hamburg, Germany

Correspondence should be addressed to Valentin Jossen; jose@zhaw.ch

Received 7 October 2015; Revised 22 December 2015; Accepted 5 January 2016

Academic Editor: Robert deans

Copyright © 2016 Valentin Jossen et al. This is an open access article distributed under the Creative Commons Attribution License, which permits unrestricted use, distribution, and reproduction in any medium, provided the original work is properly cited.

The potential of human mesenchymal stem cells (hMSCs) for allogeneic cell therapies has created a large amount of interest. However, this presupposes the availability of efficient scale-up procedures. Promising results have been reported for stirred bioreactors that operate with microcarriers. Recent publications focusing on microcarrier-based stirred bioreactors have demonstrated the successful use of Computational Fluid Dynamics (CFD) and suspension criteria ( $N_{S1u}$ ,  $N_{S1}$ ) for rapidly scaling up hMSC expansions from mL- to pilot scale. Nevertheless, one obstacle may be the formation of large microcarrier-cell-aggregates, which may result in mass transfer limitations and inhomogeneous distributions of stem cells in the culture broth. The dependence of microcarrier-cell-aggregate formation on impeller speed and shear stress levels was investigated for human adipose derived stromal/stem cells (hASCs) at the spinner scale by recording the Sauter mean diameter ( $d_{32}$ ) versus time. Cultivation at the suspension criteria provided  $d_{32}$  values between 0.2 and 0.7 mm, the highest cell densities ( $1.25 \times 10^6$  cells mL<sup>-1</sup> hASCs), and the highest expansion factors ( $117.0 \pm 4.7$  on day 7), while maintaining the expression of specific surface markers. Furthermore, suitability of the suspension criterion  $N_{S1u}$  was investigated for scaling up microcarrier-based processes in wave-mixed bioreactors for the first time.

## 1. Introduction

Cell-based therapies have become increasingly important in the field of regenerative medicine, as global revenues of approximately 1 billion US\$ indicate [1, 2]. There has been an obvious growing interest in hMSCs, particularly in those that have shown great potential for a wide range of allogeneic therapies (e.g., dry eye-related macular degeneration, diabetes, Crohn's disease, graft versus host disease, and acute myocardial infarction [1, 3–8]). By September 2015, 171 Phase 1, 2, and 3 clinical trials with hMSCs had been run (<https://www.clinicaltrials.gov/>), a fact that comes as no surprise. Due to their existence in postnatal tissues (e.g., adipose tissue, bone marrow, umbilical tissue, blood, and peripheral blood) and lower regulatory restrictions than for embryonic stem cells, hMSCs are more easily accessible and

more widely accepted for clinical applications [9–14]. The large amount of hMSCs required for one single therapeutic dose (35–350 million cells per dose) explains the demand for efficient and scalable *in vitro* expansion procedures [1, 15]. Although static stacked plate systems, with up to 40 layers, provide the desired cell numbers of up to  $1 \times 10^9$  cells in semicommercial and commercial production processes, it is difficult to ensure stem cell quantity and quality as the numbers of layers increase [16, 17].

Microcarrier-based bioreactors were identified as an alternative to planar cultivation technology that could meet the requirements in terms of production scale, bioprocess economics, and optimization [18]. The highest hMSC densities ( $1.4 \times 10^5$ – $0.8 \times 10^6$  cells mL<sup>-1</sup>) and maximum expansion factors (EFs) between 40 and 50 were achieved in stirred bioreactors operated with solid or porous microcarriers in



a serum-supplemented (5–10% fetal bovine serum albumin, FBS) culture medium, cultivated for up to 21 days [19–30]. In order to successfully scale up microcarrier-based stirred bioreactor processes with hMSCs, Hewitt et al. [24] and Rafiq et al. [19] applied the suspension criterion  $N_{S1}$ . This criterion that takes the high shear sensitivity [31, 32] of hMSCs into account can be attributed to Zwietering [33] and his studies from the late 1950s.  $N_{S1}$  represents the minimum impeller speed that just fully suspends the microcarriers at minimal shear stresses. However, it does not guarantee a homogenous dispersion of all microcarriers throughout a culture medium. Kaiser et al. [27] and Schirmaier et al. [20] introduced  $N_{S1u}$  criterion and proposed the antecedent prediction of the fluid flow pattern and hydrodynamic forces using Computational Fluid Dynamics (CFD) and Particle Image Velocimetry (PIV).  $N_{S1u}$  criterion represents the lower limit of  $N_{S1}$  criterion and allows for local movement of the microcarriers along the bioreactor bottom, but with none of the microcarriers at rest. By using  $N_{S1u}$  criterion, Schirmaier et al. [20] have achieved the highest number ( $1 \times 10^{10}$ ) of both hASCs and EFs (41.7 within 7 days) in microcarrier-based stirred bioreactors at the pilot scale (35 L working volume) to date. However, as shown by Ferrari et al. [34], with bone marrow-derived hMSCs grown in spinner flasks on dextran microcarriers (Cytodex 1), large microcarrier-cell-aggregates can appear, which may result in mass transfer limitations and, finally, loss of stem cell properties, reduced cell growth, and even cell death. This raises the question of whether there is a dependence between microcarrier-cell-aggregate size, impeller speed, shear stress, cell quantity, and cell quality.

For this reason, one aim of our study was to investigate time-dependent hASC growth in spinners at different impeller speeds (taking the suspension criteria into account) and shear stress levels, while also taking the microcarrier-cell-aggregate size into account. All these investigations are based on the previously published characterization investigations (suspension studies, CFD simulations, and PIV measurements) of our group (Kaiser et al. [27]). The second aim was to examine whether it is possible to use  $N_{S1u}$  criterion for hMSC mass production processes in wave-mixed bioreactors with one-dimensional motion. In this type of bioreactor, mass transfer is accomplished by a propagating wave, whose intensity can be regulated by the bioreactor's rocking angle, rocking rate, and filling level. The wave is induced by rocking a fixed, surface-aerated bag [35–38] containing the medium and microcarriers to which the cells attach. Although this bioreactor type is well established in seed inoculum and microcarrier-based vaccine production processes with continuous animal cell lines, there are only two publications that describe its applicability to the expansion of hMSCs [39, 40]. Timmins et al. [39] cultivated human placental MSCs on CultiSpher-S microcarriers and achieved EFs of up to 16.3 within 7 days under low  $O_2$  (5%) conditions. In normoxic conditions Akerström [40] grew nonspecified hMSCs on Cytodex 3 microcarriers over 18 days and harvested  $20 \times 10^6$  cells, corresponding to an EF of 6. We decided to work with a BIOSTAT CultiBag RM 2L (optical version) and to adopt the shear stress at  $N_{S1u}$  for hASCs in spinner flasks ( $4.9 \times 10^{-3}$  to

$0.18 \text{ N m}^{-2}$ ), which required previous suspension, CFD, and PIV investigations of the cultivation system.

## 2. Materials and Methods

### 2.1. Bioengineering Characterizations of the BIOSTAT CultiBag RM 2L

**2.1.1. Suspension Studies.** The suspension experiments were carried out with a specially developed medium from Lonza containing 5% FBS and two different types of polystyrene-based microcarriers (Pall, USA). Three different working volumes (0.5 L, 1.0 L, and 1.5 L) and microcarrier solid fractions ranging from 0.7 to 2.1% were tested. The polystyrene-based microcarriers consist of particles with densities between 1090 and 1150  $\text{kg m}^{-3}$  (MC-1) and between 1022 and 1030  $\text{kg m}^{-3}$  (MC-2) and diameters between 160 and 200  $\mu\text{m}$  and between 125 and 200  $\mu\text{m}$ , respectively. The resulting nominal growth surfaces per gram were approximately 515  $\text{cm}^2$  and 360  $\text{cm}^2$ . MC-1 was applied to establish an initial multiregression model for the prediction of the suspension criteria ( $N_{S1u}$ ,  $N_{S1}$ ) in the wave-mixed system and has no significance for the further cultivation studies described in Section 2.2.

In order to better assess the bioreactor bottom, a transparent, rigid rocking platform made of acrylic glass was used. In addition, a mirror was placed below the rocking platform to improve optical accessibility of the bioreactor bottom. Suspension characteristics were investigated for different rocking angles between  $4^\circ$  and  $10^\circ$ . The rocking angle was kept constant and the rocking rate was increased stepwise up to a maximum of 35 rpm.  $N_{S1}$  criterion for the wave-mixed bioreactor was defined as the combination of rocking rate and rocking angle, where the microcarriers make contact with the reactor bottom for no longer than 1 s. Likewise, for the stirred bioreactors,  $N_{S1u}$  criterion was the lower limit of  $N_{S1}$ .

**2.1.2. CFD.** The fluid flow inside the BIOSTAT CultiBag RM 2L was modelled using the Fluent 15 finite volume solver (ANSYS, Inc., USA). Due to the motion of the liquid interface, the Volume-of-Fluid (VOF) approach was used for the simulations. For this purpose, a set of single momentum equations, based on the Reynolds-averaged Navier-Stokes (RANS) equations, were solved. The interface between the phases was tracked over time using a balance equation for the fractional volume, which can be described for the  $q$ th phase by the following:

$$\frac{\partial}{\partial t} (\alpha_q \rho_q) + \nabla \cdot (\alpha_q \rho_q \vec{w}_q) = 0. \quad (1)$$

The terms  $\vec{w}_q$ ,  $\alpha_q$ , and  $\rho_q$  in (1) denote the fluid velocity vector, the fluid density, and the volume fraction of the  $q$ th phase. By assuming a shared velocity field among the phases, a single momentum balance equation (see (2)) was solved for the entire fluid domain:

$$\begin{aligned} \frac{\partial}{\partial t} (\rho \vec{w}) + \nabla \cdot (\rho_q \vec{w} \vec{w}) = & -\nabla p + \nabla \cdot [\mu (\nabla \vec{w} + \nabla \vec{w}^T)] \\ & + \rho \vec{g} + \vec{F}, \end{aligned} \quad (2)$$

where  $\vec{F}$  defines all the volumetric forces except gravity. In (2), the viscosity and the density are weighted mean values:

$$\begin{aligned}\rho &= \sum \alpha_q \rho_q, \\ \mu &= \sum \alpha_q \mu_q\end{aligned}\quad (3)$$

whose phase volume fractions are computed based on the following constraint:

$$\sum_{q=1}^n \alpha_q = 1. \quad (4)$$

A good approximation for the rocker-type motion of the bioreactor was described by a harmonic oscillation function, where the deflection angle ( $\varphi$ ) at the time point  $t$  can be predicted by the following equation:

$$\varphi_t = \varphi_{\max} \cdot \sin(\bar{\omega}t). \quad (5)$$

This resulted in (6), which was entered into Fluent as a user-defined function and describes the movement of the bag as a solid body:

$$\bar{\omega}_t = \bar{\omega} \left( \varphi_{\max} \cdot \frac{\pi}{180} \right) \cdot \cos(\bar{\omega} \cdot t). \quad (6)$$

Turbulent flow conditions were modelled using  $k$ - $\omega$  SST model, where a set of transport equations for the turbulent kinetic energy  $k$ , the turbulent dissipation rate  $\varepsilon$ , and the specific turbulent dissipation rate  $\omega$  were solved. Detailed information of the model is provided in [41, 42]. The volume of the pillow-like bag was discretized into  $1.5 \times 10^6$  tetrahedral control volumes, guaranteeing acceptable computational accuracy and a tolerable computational turnaround time. The simulations were performed for three different working volumes (0.5 L, 1.0 L, and 1.5 L) by patching the corresponding liquid phase. Rocking rates (14–35 rpm) and rocking angles ( $4$ – $10^\circ$ ) were selected based on the results of the suspension studies. The velocity-pressure coupling and the prediction of volume fractions were accomplished using the SIMPLE algorithm and geo-reconstruction method provided by Fluent. The time-step size was fixed at 0.005 s. Convergence was assumed when the residuals dropped below  $10^{-5}$ . However, the number of iterations per time-step was restricted to 100 in order to limit the central processing unit turnaround time.

**2.1.3. PIV.** PIV measurements were performed to verify the CFD model. For this purpose, a FlowMaster PIV system (LaVision, Germany) in conjunction with a double-pulsed Nd:YAG laser that generated a 1 mm thick laser sheet was used ( $\lambda = 532$  nm, litron lasers, UK). The fluid flow pattern in the BIOSAT CultiBag RM 2L was captured at two different positions (from the side and from below). For the side recordings, a specially constructed bag with a piece of acrylic glass along the centreline was used. This enabled process images to be recorded at the edges of the bag along the vertical laser plane, which was located in the middle of the half bag. The recordings from below were carried out for the whole bag. For this purpose, again a transparent rocking platform

in combination with a mirror below the platform was used in order to provide optical accessibility to the reactor bottom. The laser sheet was horizontally positioned 1 cm above the bag bottom. An Imager Pro X4 CCD camera (LaVision, Germany) with a resolution of  $2048 \times 2048$  pixels was used to acquire images and was positioned at a  $90^\circ$  angle relative to the laser field for the side measurements and directly on the mirror for the bottom investigations. DaVis® 8.2 software (LaVision, Germany) was used to control the camera, the traverse system, the laser, image acquisition, and flow field prediction. In order to visualise the fluid flow pattern, rhodamine-coated fluorescent particles with a density of  $1.19 \text{ kg/m}^3$  (LaVision) were added to the bag. A set of 800 double frame images per position were recorded in order to obtain statistically significant results, based on an interrogation window of  $8 \times 8$  pixels with an overlap of 50%. The measurements were performed for three working volumes (0.5 L, 1.0 L, and 1.5 L), different rocking angles ( $6^\circ$  and  $10^\circ$ ), and rocking rates (15 rpm, 25 rpm, and 35 rpm). Phase-locked measurements were recorded by means of a photoelectric barrier focused on the edge of the rocking platform. For each experimental set, images were made during the harmonic oscillation at momentary deflection angles of  $4^\circ$  to  $10^\circ$ .

## 2.2. Cultivation Studies

**2.2.1. Cells, Microcarriers, and Medium.** Cryopreserved hASCs (Lonza Cologne GmbH, Germany) obtained from a single informed and consenting donor (hASCs, third passage, population doubling level of 10) were used for all expansions taking place under serum-reduced (5% FBS) conditions in a specially developed medium (Lonza, USA) on polystyrene-based microcarriers (Pall, USA). The microcarriers (MC-2) used had densities ranging from 1090 to  $1150 \text{ kg m}^{-3}$ , particle sizes between 125 and  $212 \mu\text{m}$ , and a mean surface area of approximately  $360 \text{ cm}^2 \text{ g}^{-1}$ .

**2.2.2. Analytics.** Off-line samples were taken daily to determine glucose, lactate, glutamine, and ammonium by biosensors (enzymatic) and ion selective electrodes in the Bio-Profile 100Plus (Nova Biomedical, USA). In addition, 4',6-diamidino-2-phenylindole (DAPI) staining was performed and microcarrier-cell-aggregates were measured. The aggregate measurements were performed based on macroscopic (hand camera) and microscopic pictures, which were analyzed by a user-defined MATLAB (MathWorks, Inc., USA) script and DaVis® 8.2 software. The cell densities were measured in triplicate per sample using a NucleoCounter NC-200 (ChemoMetec, Denmark). All microcarrier-cell-aggregates contained in the spinner flasks and the 2 L bag were washed with TrypLE Select (Gibco by Life Technologies, USA) and incubated for 30 min at  $37^\circ\text{C}$  before the hASC harvest.

Flow cytometric investigations (MACSQuant device from Miltenyi Biotec, Germany) were always performed after cell harvesting with microcarrier-free, purified hASCs samples. The samples were stained with fluorochrome-conjugated anti-human CD14, CD20, CD34, CD45, CD73, CD90, and CD105 antibodies (MSC Phenotyping Kit, Miltenyi Biotec, Germany), which represent minimal surface markers

recommended by the International Society for Cellular Therapy.

**2.2.3. Corning Spinner Flask Cultivations.** In order to investigate the influence of different impeller speeds on cell growth and aggregate formation, six different impeller speeds (25 rpm, 43 rpm,  $N_{S1u} = 49$  rpm,  $N_{S1} = 63$  rpm, 90 rpm, and 120 rpm) were studied under low-serum conditions (5%) in spinner flask (Corning, USA) experiments for MC solid fractions of 0.01%. For each condition, two spinner flasks (100 mL culture volume) with mean microcarrier growth surfaces of  $360\text{ cm}^2$  were inoculated with cryopreserved hASCs ( $3 \times 10^3$  cells  $\text{cm}^{-2}$ ) and cultivated for 8 days at  $37^\circ\text{C}$ , 5%  $\text{CO}_2$ , and 80% humidity (normoxic).

Before inoculation, the microcarrier suspensions were equilibrated for 1 h, as recommended by the vendor. After inoculation, a 4 h attachment phase was realized to support cell attachment before the impeller was switched on. On day 4 after inoculation, 50% of the growth medium was replaced with fresh, preheated medium. For this purpose, the MCs with the attached cells were allowed to settle, before 50% of the medium was replaced with fresh, preheated medium. Cell attachment and harvest procedures were developed and optimized by Schirmaier et al. [20].

**2.2.4. BIOSTAT CultiBag RM 2L Proof-of-Concept Cultivation.** The solid fraction of the polystyrene-based microcarriers was adjusted to 1.43% ( $7722\text{ cm}^2$ ) for the proof-of-concept cultivation in the BIOSTAT CultiBag RM 2L. Equilibration of the microcarriers and inoculation of the cells were performed in two 1 L shake flasks. For this purpose, the microcarrier suspension was incubated overnight at  $37^\circ\text{C}$ , 5%  $\text{CO}_2$ , and 80% humidity. Each of the shake flasks was inoculated with  $6500\text{ cells cm}^{-2}$  of the microcarriers for the cryopreserved hASCs. To promote cell attachment, a 20 h static attachment phase was found to be most suitable after inoculation. Afterwards, a portion of the microcarrier suspension (mean growth surface =  $360\text{ cm}^2$ ) was transferred into a spinner flask as a control. The hASCs in the spinner flasks were cultivated as described for the spinner experiments in Section 2.2.3 (impeller speed = 49 rpm  $N_{S1u}$ ). The remaining microcarrier suspension (mean growth surface =  $7362\text{ cm}^2$ ) was transferred into a BIOSTAT CultiBag RM 2L. Preheated medium was then added to achieve a total working volume of 1.5 L. To achieve similar shear stresses as in the spinner flask, the BIOSTAT CultiBag RM 2L was overfilled with 500 mL medium. The rocking angle and rocking rate were set based on the biochemical engineering investigations ( $N_{S1u} = 4^\circ$  and 31 rpm; Section 3.2.1). The hASCs were cultivated for 9 days at  $37^\circ\text{C}$ , pH 7.3, and 0.05 vvm. On day 5 after inoculation, the rocker platform was switched off and the bag was hung up to allow the MCs with attached cells to settle down. After approximately 15 min, 50% of the culture medium could be replaced with negligible cell and microcarrier lost.

### 3. Results and Discussion

**3.1. Corning Spinner Flask.** Figure 1(a) shows time-dependent profiles of living cell densities measured in the spinner

flask runs. The impeller speed dependent growth parameters are summarized in Table 1. Maximum living cell densities between  $(0.25 \pm 0.02) \times 10^6$  hASCs  $\text{mL}^{-1}$  and  $(1.25 \pm 0.05) \times 10^6$  hASCs  $\text{mL}^{-1}$  were found 7 days after inoculation. The highest living cell densities were achieved at impeller speeds of 49 rpm and 63 rpm for  $N_{S1u}$  and  $N_{S1}$  criteria. Cell densities at the suspension criteria were four to five times higher than the living cell density at 120 rpm. This can be ascribed to the twofold to threefold lower local shear stress levels and the threefold to fivefold lower specific power inputs at  $N_{S1u}$  and  $N_{S1}$  (Table 1).

During the exponential growth phase, the fastest hASC growth (doubling time of  $23.7 \pm 0.1\text{ h}$ ) was calculated for the spinner flask cultivation at 49 rpm ( $N_{S1u}$ ). The slowest hASC growth (doubling time of  $41.3 \pm 0.1\text{ h}$ ) was found at 120 rpm. In spite of lower shear stresses, the hASCs also grew more slowly at impeller speeds below the suspension criteria. This might have been due to insufficient mixing and the resulting sedimentation of the microcarriers, since not all MCs were permanently suspended. Mass transfer limitations that impair cell growth can occur.

It can clearly be seen from Figure 1(b) that statistically significant, higher EFs (one-way ANOVA with pairwise comparison; Holm-Sidak method,  $p < 0.05$ ,  $n = 2$ ) were obtained for  $N_{S1u}$  ( $117 \pm 4.7$ ) and  $N_{S1}$  ( $97.4 \pm 3.7$ ) criteria. The lowest EFs ( $\{28.5 \pm 5.1\}$  and  $\{19.4 \pm 1.3\}$ ) were achieved at the highest impeller speeds, which were up to four times lower than those at the lower impeller speeds of 25 rpm and 43 rpm.

The growth results (cell densities, doubling times, and EFs) support our hypothesis that operating a microcarrier-based stirred bioreactor at the lower suspension criterion  $N_{S1u}$  ensures maximum hMSC growth.

As is obvious from Table 2, the highest lactate production rate was determined at 120 rpm, while the maximum living cell density was the lowest. In contrast, the specific lactate production rate at 49 rpm ( $N_{S1u}$ ) was around 3.6 and 1.7 times lower compared to 120 rpm and 25 rpm. Furthermore,  $Y_{\text{lac/gluc}}$  indicates that the metabolization of glucose into energy is more efficient, when working at  $N_{S1u}$  criterion. After 7 days of cultivation, a decrease in the living cell density was observed, which was independent of the cultivation parameters. Because substrate and metabolite limitations can be excluded (concentrations at the end of the cultivation: glucose/glutamine  $\geq 14.8/4.0\text{ mmol L}^{-1}$ ; lactate/ammonium  $\leq 24.8/1.51\text{ mmol L}^{-1}$ ; [43, 44]), this might be due to the size of the microcarrier-cell-aggregates, which impair cell growth.

Figure 2(a) clearly shows the microcarrier-cell-aggregate development. The time-dependent profiles of the Sauter mean diameters ( $d_{32}$ ) are shown for all tested impeller speeds. As expected, the highest Sauter mean diameter of up to  $3.18 \pm 0.42\text{ mm}$  was measured at the lowest impeller speed (25 rpm) on day 8 and was significantly higher compared to the other conditions. At this impeller speed, accumulation of larger aggregates below the impeller was observed. These findings are in good agreement with our previous CFD investigations published by Kaiser et al. [27]. Due to the circulation loop induced directly below the impeller, lower fluid velocities occur in this region, which promote the sedimentation of

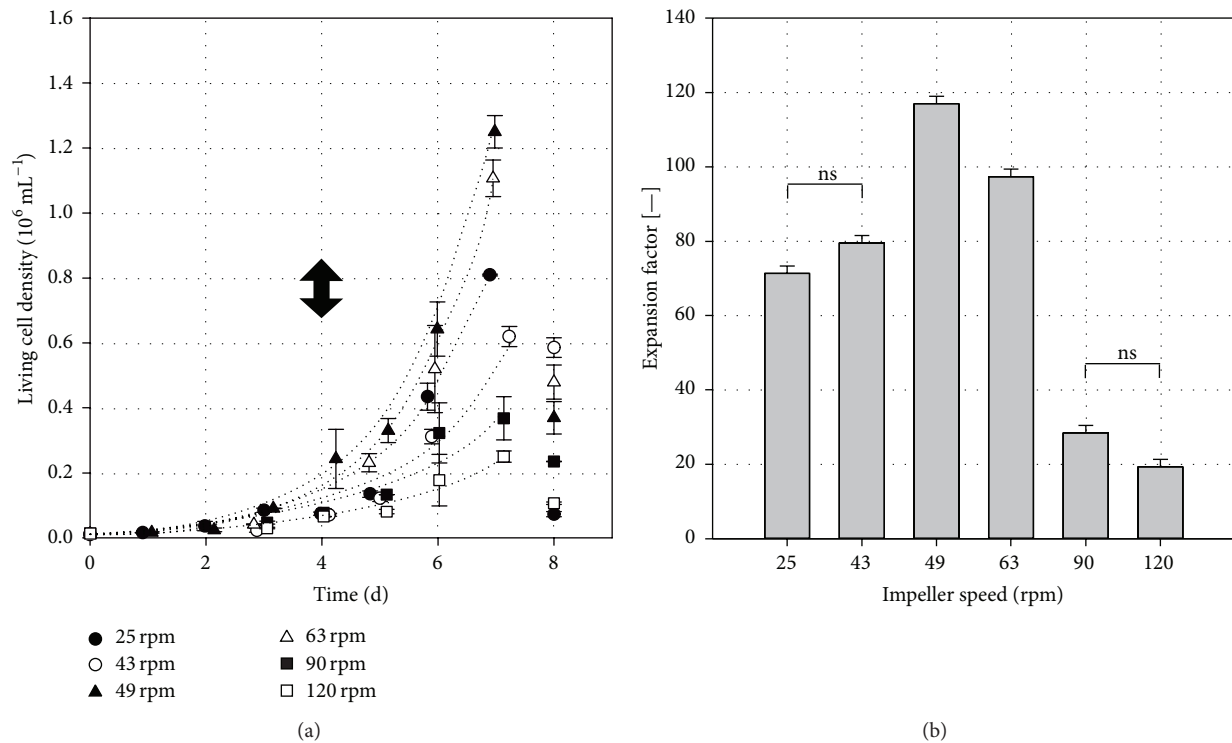


FIGURE 1: Results of hASC cultivations in the Corning spinner flasks. (a) Time-dependent profiles of living cell densities. The dotted lines represent the simulated growth characteristics of the hASCs in the exponential growth phase, based on the calculated specific growth rates. The black arrow indicates the 50% medium exchange on day 4. (b) Comparison of maximum expansion factors calculated for day 7. A one-way ANOVA (Holm-Sidak method,  $n = 2$ ;  $p < 0.05$ ) with pairwise comparison was performed for the maximum EFs. ns = not significant. The error bars represent the standard deviations of the EF given by the two cases of independent spinner cultivation per condition.

larger aggregates. The Sauter mean diameter at the lowest impeller speed was approximately seven times higher than at the suspension criteria. Interestingly, the Sauter mean diameter of  $0.55 \pm 0.06 \text{ mm}$  on day 7 at 120 rpm was not significantly lower than those of the suspension criteria ( $N_{S1u}$ :  $0.58 \pm 0.07 \text{ mm}$ ;  $N_{S1}$ :  $0.47 \pm 0.03 \text{ mm}$ ), demonstrating that the threefold higher specific power input had no significant effect on the overall microcarrier-cell-aggregate size in the spinner flasks. The results indicate that the reduction in the living cell density might be ascribed to two main reasons: (I) too high local shear stresses ( $0.437 \text{ N m}^{-2}$ ) which came along with higher lactate concentrations and (II) mass transfer limitations due to large microcarrier-cell-aggregate sizes ( $d_{32} > 0.6 \text{ mm}$ ) or too low impeller speeds ( $< 49 \text{ rpm}$ ). Figures 2(b) and 2(c) illustrate DAPI staining picture of a microcarrier-cell-aggregate sample taken from a run (day 7) at  $N_{S1u}$  criterion.

At the end of the cultivation (days 7 and 8), the majority of the cells were observed between the microcarriers, especially in the bigger microcarrier-cell-aggregates (Figure 2(c)). A reduction of cell density prevails at Sauter mean diameters of approximately  $0.6 \text{ mm}$ , which was also noted at the end of the cultivation.

Any influence on the expression of specific surface markers (CD14, CD20, CD34, CD45, CD73, CD90, and CD105) was, however, not discovered, either at the maximum impeller speeds and resulting shear stress levels (maximum

specific power inputs of  $3.63 \text{ W m}^{-3}$  and maximum local shear stress level of  $0.437 \text{ N m}^{-2}$ ) or at the maximum Sauter diameters ( $3.2 \text{ mm}$ ) that reflected the maximum microcarrier-cell-aggregation size. Because all flow cytometric results were in good agreement with each other, only those measured in samples from spinner runs at  $N_{S1u}$  are shown in Figure 3. The cells were highly positive ( $> 95\%$ ) for CD73, CD90, and CD105 surface markers. The hematopoietic markers CD34 and CD45 as well as CD14 and CD20 were absent ( $< 2\%$ ) from all samples.

### 3.2. BIOSTAT CultuBag RM 2L

**3.2.1. Suspension Characteristics.** In general, dune-like deposits of microcarriers were seen at rocking rates significantly below  $N_{S1u}$  criterion. This effect was independent of the rocking angle and can be explained by the oscillating fluid flow, in which a type of constructive and destructive interference takes place. As rocking rates increased the dune-like deposits decreased, due to the higher level of mixing. Almost complete suspension of the microcarriers was observed at  $N_{S1u}$  criterion. For all of the investigated conditions,  $N_{S1}$  criterion was fulfilled at 2.5–8.3% higher rocking rates (approximately 1 rpm). The results indicate that the difference between  $N_{S1u}$  and  $N_{S1}$  criteria in wave-mixed systems is much lower than in stirred bioreactors (20–40%) [21, 22, 27, 45, 46]. This phenomenon can be explained by the periodical deceleration



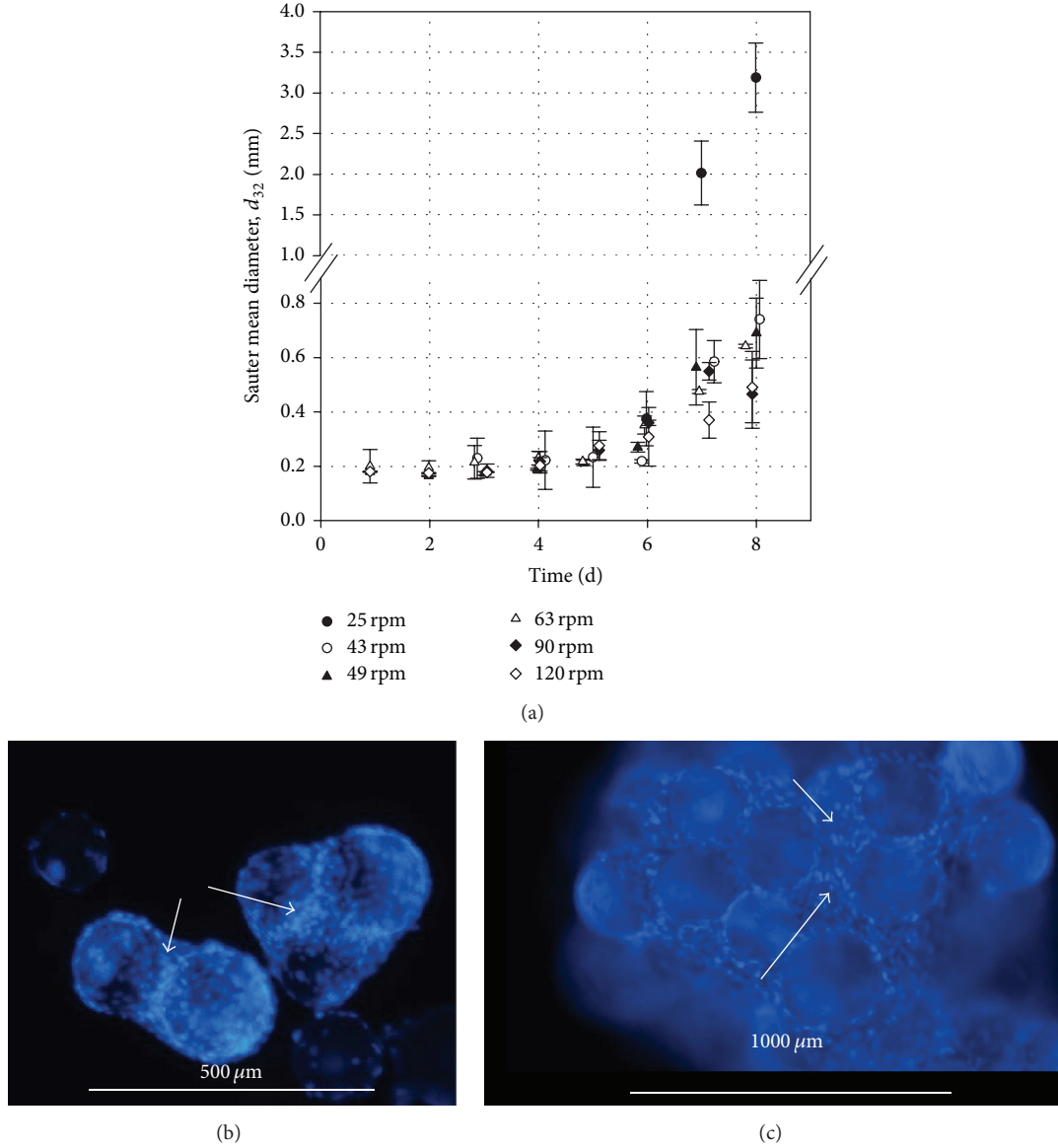


FIGURE 2: Microcarrier-cell-aggregate formation during the cultivation of the hASCs. (a) Time-dependent profiles of the Sauter mean diameters ( $d_{32}$ ) for all tested impeller speeds. (b) and (c) DAPI staining picture of microcarrier-cell-aggregate sample taken from a run at  $N_{Slu}$  suspension criterion (49 rpm, day 7). White arrow indicates that the cell growth takes place over the entire microcarrier surface and between the microcarriers. Focal plane was set in order to see the cell growth between the microcarriers.

and acceleration of the particles in wave-mixed bioreactors. The determined rocking rates that fulfil  $N_{Slu}$  criterion for rocking angles between 4 and 10° ranged between 12 and 26 rpm for a 0.5 L working volume, between 15 and 32 rpm for 1.0 L, and between 17 and 35 rpm for 1.5 L. The corresponding rocking rates for  $N_{Sl}$  criterion were in a comparable range. Surprisingly, linear relationships were found between rocking rates and rocking angles for each specific microcarrier solid fraction. Based on a multiple regression analysis a correlation (see (7)) for  $N_{Slu}$  criterion was found:

$$N_{Slu} = -2.079 \cdot \varphi_{\max} + 7.526 \cdot V_f - 0.119 \cdot m_{MC} + 0.00537 \cdot A_{MC} + 0.0329 \cdot \rho_{MC} - 6.039$$

$$R = 0.977,$$

(7)

where  $\varphi_{\max}$  [°] defines the rocking angle,  $V_f$  [L] the working volume,  $m_{MC}$  [g] the amount of microcarriers,  $A_{MC}$  [ $\text{cm}^2$  100  $\text{mL}^{-1}$ ] the specific growth surface, and  $\rho_{MC}$  [ $\text{kg m}^{-3}$ ] the density of the microcarriers. The maximum deviation between the predicted and the measured values was approximately 3 rpm and, therefore, was acceptable. In Figure 4,  $N_{Slu}$  criterion is shown as a contour plot for the three different working volumes. As can be seen, the dependence of  $N_{Slu}$  criterion on the rocking angle decreases as the working volume rises.

TABLE 1: Summary of growth parameters, CFD-predicted specific power inputs ( $P/V$ ), and local shear stress (LSS) levels.

$N$ [rpm]	$P/V$ [ $\text{W m}^{-3}$ ]	LSS <sup>a</sup> [ $10^{-3} \text{ N m}^{-2}$ ]	Total cell numbers on day 7 [ $10^7$ cells]	Living cell density on day 7 [ $10^6$ cells $\text{mL}^{-1}$ ]	EFs [—]	$\mu_{\max}$ and $t_d$ [ $\text{h}^{-1}$ ] and [h]
25	0.21	3.21/69	$8.1 \pm 0.1$	$0.81 \pm 0.01$	$71.4 \pm 0.2$	$0.026 \pm 0.001$ $26.7 \pm 0.1$
43	0.65	4.43/142	$6.2 \pm 0.6$	$0.62 \pm 0.06$	$79.6 \pm 3.2$	$0.022 \pm 0.001$ $31.5 \pm 0.2$
49	0.80	4.96/187	$12.5 \pm 0.5$	$1.25 \pm 0.05$	$117.0 \pm 4.7$	$0.029 \pm 0.001$ $23.7 \pm 0.1$
63	1.24	6.72/224	$11.1 \pm 0.6$	$1.11 \pm 0.06$	$97.4 \pm 3.7$	$0.028 \pm 0.001$ $24.8 \pm 0.2$
90	2.24	10.22/325	$3.7 \pm 0.7$	$0.37 \pm 0.07$	$28.5 \pm 5.1$	$0.020 \pm 0.002$ $34.4 \pm 0.4$
120	3.63	13.56/437	$2.5 \pm 0.2$	$0.25 \pm 0.02$	$19.4 \pm 1.3$	$0.017 \pm 0.001$ $41.3 \pm 0.1$

<sup>a</sup>LSS; local shear stress given with volume-weighted mean/maximum values. LSS and  $P/V$  were adapted from Kaiser et al. [27].

TABLE 2: Specific metabolic consumption and production rates.

$N$ [rpm]	$-q_{\text{gluc}}$ [ $\text{pmol cell}^{-1} \text{ d}^{-1}$ ]	$q_{\text{lac}}$ [ $\text{pmol cell}^{-1} \text{ d}^{-1}$ ]	$Y_{\text{lac}/\text{gluc}}$ [ $\text{mmol mmol}^{-1}$ ]	$q_{\text{NH}_4^+}$ [ $\text{pmol cell}^{-1} \text{ d}^{-1}$ ]	$Y_{\text{NH}_4^+/\text{gln}}$ [ $\text{mmol mmol}^{-1}$ ]
25	$-1.86 \pm 0.01$	$4.31 \pm 0.03$	$2.87 \pm 0.01$	$0.259 \pm 0.004$	$2.65 \pm 0.41$
43	$-2.30 \pm 0.20$	$4.39 \pm 0.30$	$1.94 \pm 0.30$	$0.252 \pm 0.003$	$2.66 \pm 0.29$
49	$-1.58 \pm 0.11$	$2.43 \pm 0.17$	$1.55 \pm 0.11$	$0.090 \pm 0.001$	$2.46 \pm 0.46$
63	$-1.08 \pm 0.23$	$2.92 \pm 1.04$	$2.51 \pm 0.39$	$0.191 \pm 0.052$	$2.36 \pm 0.49$
90	$-4.09 \pm 0.52$	$7.78 \pm 1.39$	$1.89 \pm 0.10$	$0.596 \pm 0.133$	$2.43 \pm 0.11$
120	$-5.07 \pm 0.19$	$8.82 \pm 0.11$	$1.74 \pm 0.04$	$0.878 \pm 0.085$	$2.57 \pm 0.05$

$-q_{\text{gluc}}$ : specific glucose consumption rate;  $q_{\text{lac}}$ : specific lactate production rate;  $q_{\text{NH}_4^+}$ : specific ammonia production rate;  $Y_{\text{lac}/\text{gluc}}$ : specific lactate yield per unit glucose;  $Y_{\text{NH}_4^+/\text{gln}}$ : specific ammonia yield per unit glutamine. ( $n = 2$ ).

**3.2.2. Fluid Flow.** For a rocking rate of 25 rpm and a rocking angle of  $10^\circ$ , contour plots of the CFD-predicted fluid flow velocities along the mid bioreactor plane are shown in Figure 5(a). Significantly higher fluid flow velocities ( $0.75 \text{ m s}^{-1}$ ) occur at maximum deflection for 0.5 L working volume. This was expected, since the motion of the free surface increases at lower working volumes. A clearly dampened fluid flow with fluid flow velocities of up to  $0.55 \text{ m s}^{-1}$  at maximum deflection was predicted for the higher working volume of 1.5 L. This trend can also be seen for the volume-weighted mean fluid flow velocities in Figure 5(b) and was independent of the rocking rate and the rocking angle. The maximum volume-weighted mean fluid flow velocities at 0.5 L, 25 rpm, and  $10^\circ$  were approximately 1.8 times higher than those at 1.5 L ( $0.14 \text{ m s}^{-1}$ ). Furthermore, the simulation results indicated that a change in the rocking angle has a higher effect on the fluid flow velocities than a change in the rocking rate. The lowest volume-weighted mean fluid flow velocities of up to  $0.05 \text{ m s}^{-1}$  were obtained at 31 rpm and  $4^\circ$  and corresponded to  $N_{\text{S14}}$  criterion in the BIOSTAT CultiBag RM 2L (1.43% microcarrier solid fraction). Kaiser et al. [27] predicted volume-weighted mean fluid flow velocities of up

to  $0.06 \text{ m s}^{-1}$  for  $N_{\text{S1}}$  criterion in the spinner flask. Thus, working at 1.5 L is preferable for the expansion of the hASCs, when comparable flow conditions to those in spinner flasks are desired.

**3.2.3. Shear Stress and Specific Power Input.** An overview of the shear stress distributions and specific power inputs present in the BIOSTAT CultiBag RM 2L (including working volume, rocking angle, and rocking rate) is summarized in Table 3. The shear stresses were calculated according to Wollny [47], where logarithmical normal distributions similar to those of stirred bioreactors were obtained [27, 48]. Unlike stirred bioreactors, the fluid flow behaviour in wave-mixed systems cannot be assumed to be constant. Hence, shear stress distributions were calculated for each deflection angle during a single bag oscillation.

In Figure 6(a), angle-dependent profiles of volume-weighted mean shear stresses are exemplarily presented for three different working volumes at  $10^\circ$  and 25 rpm. The local shear stresses follow a periodic oscillation, where the highest values occur at maximum deflection. This comes as no surprise, since the flowing fluid is decelerated to a lower

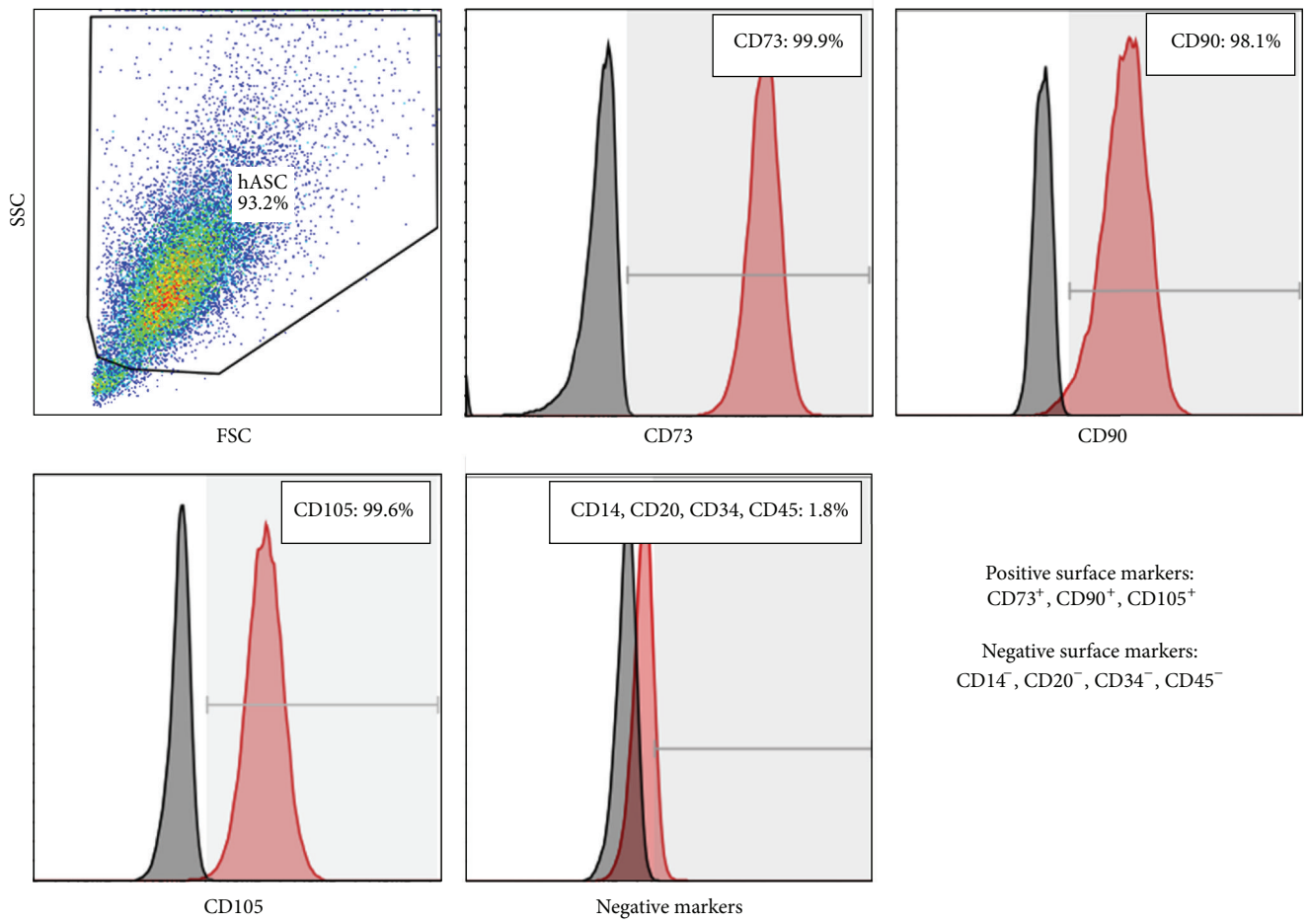


FIGURE 3: Results of flow cytometric analysis (FACS) of hASCs at the end of the cultivation at 49 rpm (day 7). The gates of the flow cytometric analysis were set based on isotype controls.

TABLE 3: Summary of predicted shear stress levels and specific power inputs in the BIOSTAT CultuBag RM 2L.

Working volume [L]	Rocking angle [°]	Rocking rate [rpm]	$P/V^a$ [ $W\ m^{-3}$ ]	MLSS <sup>b</sup> [ $10^{-3}\ N\ m^{-2}$ ]
0.5	4	26	20.61/40.66	5.83/664
0.5	6	22	32.52/53.55	5.44/509
0.5	6	35	156.01/262.60	5.78/597
0.5	8	18	47.71/85.79	29.61/704
0.5	10	14	93.40/149.73	20.61/885
0.5	10	25	144.10/259.76	26.40/3162
1.0	4	29	34.40/65.33	4.91/916
1.0	6	25	53.70/98.16	4.75/1194
1.0	8	20	32.14/53.35	1.09/289
1.0	10	15	81.10/123.77	5.68/1012
1.0	10	25	118.32/203.76	10.80/4042
1.5	4	31	8.92/17.69	0.49/214
1.5	6	27	17.96/32.45	0.60/256
1.5	8	22	26.56/50.04	0.74/279
1.5	10	16	68.85/105.28	3.15/909
1.5	10	25	95.02/155.46	4.86/2959

<sup>a</sup>  $P/V$ : mean and maximum values of specific power input. <sup>b</sup> MLSS: maximum values of local volume-weighted mean and maximum shear stresses over one period.

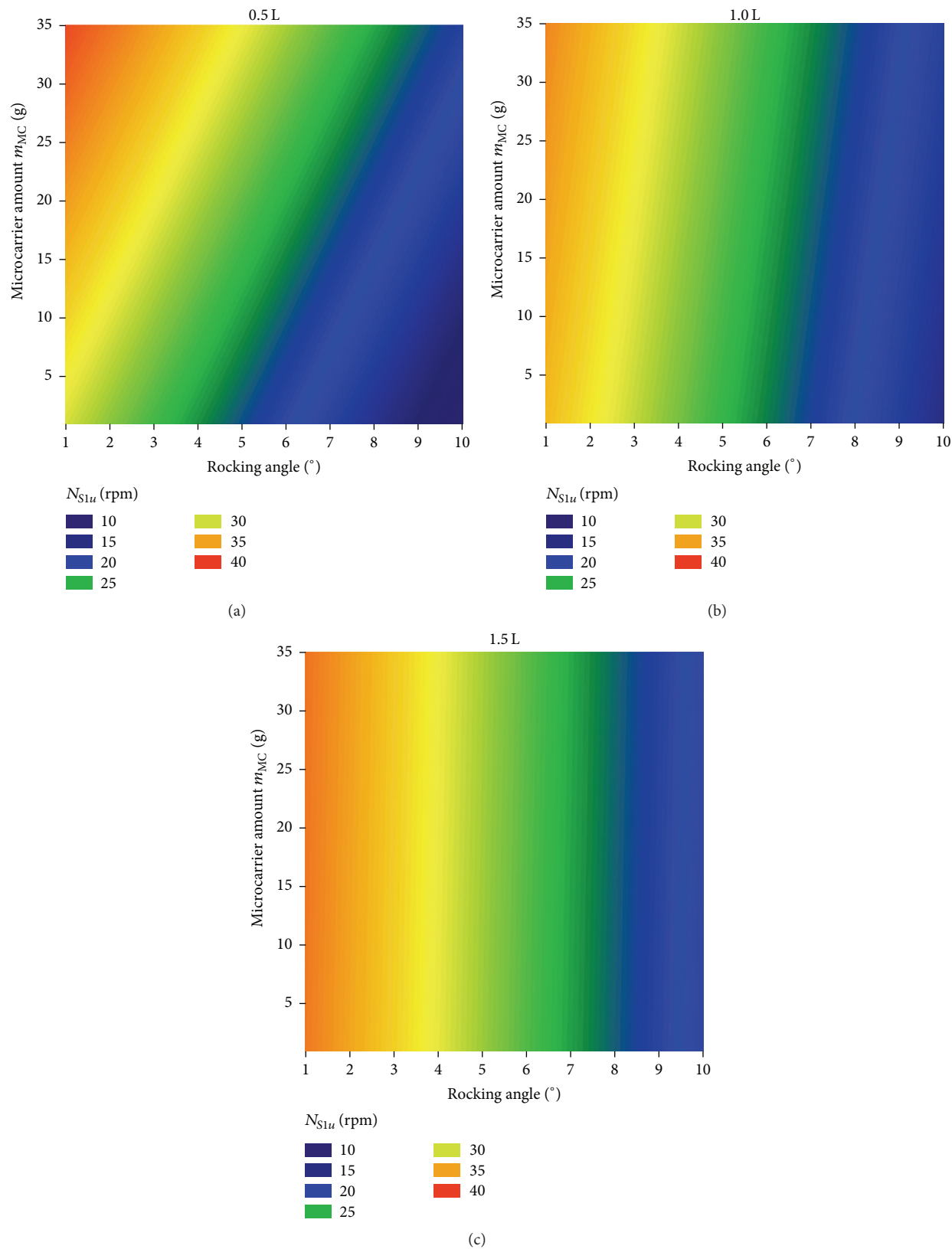


FIGURE 4:  $N_{S1u}$  criterion at the three different working volumes. The contour plots were created on the basis of the measured data and the multiple regression model.



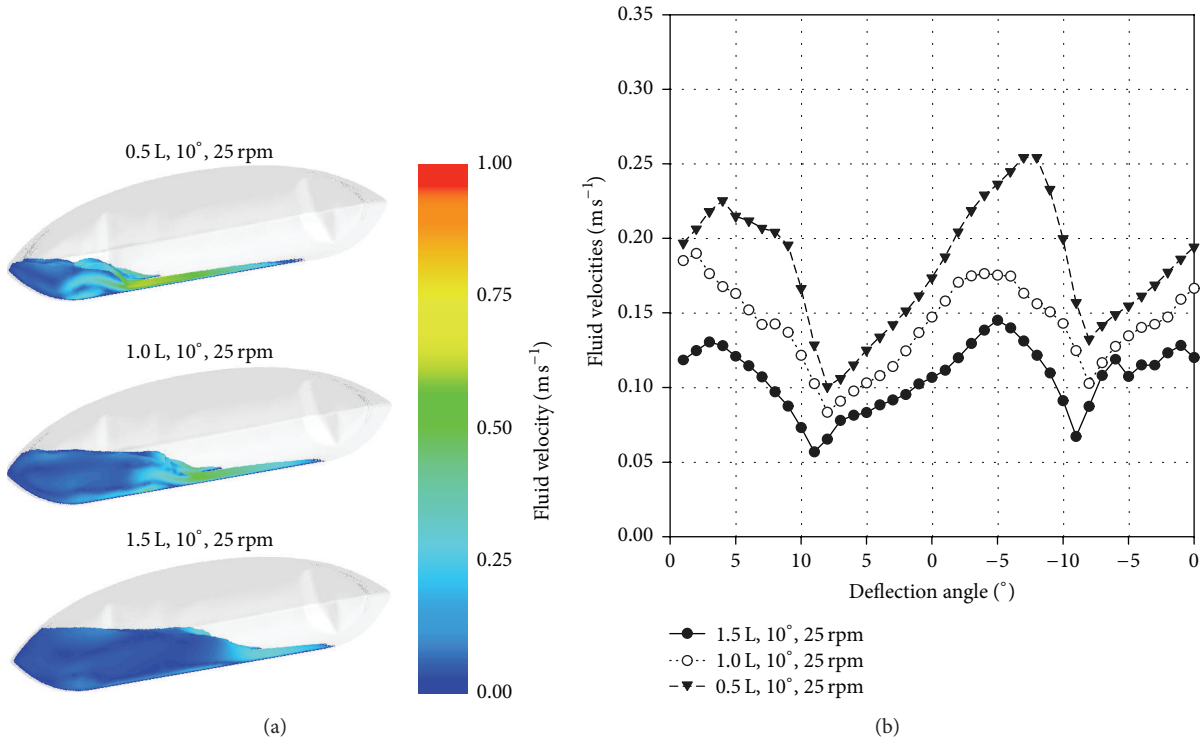


FIGURE 5: Comparison of fluid flow in the BIOSTAT CultiBag RM 2L at three different working volumes (0.5 L, 1.0 L, and 1.5 L). (a) Contour plots of CFD-predicted fluid flow patterns and fluid flow velocities for three different working volumes. The fluid flow patterns and the fluid flow velocities are shown for 25 rpm and 10°. (b) Comparison of volume-weighted mean fluid flow velocities over one period.

velocity and then it accelerates in the other direction. The highest local shear stresses occurred at the lowest working volume of 0.5 L, with values that were up to 6 times higher than the local shear stresses for the 1.0 L and 1.5 L working volumes. The lowest local shear stress values ( $0.214 \text{ N m}^{-2}$ ) were obtained at 1.5 L, 4°, and 31 rpm for  $N_{S1}$  criterion and a microcarrier solid volume fraction of 1.43%. These maximum local shear stresses are similar to those for  $N_{S1}$  criterion in the spinner flask. For 10° and 25 rpm, the angle-dependent specific power inputs based on the moment at the rotational axis are illustrated as an example in Figure 6(b). In general, the profiles of the specific power inputs correspond well to the local shear stresses. The highest specific power inputs appear shortly before the maximum deflection is reached. The highest specific power input of  $262 \text{ W m}^{-3}$  was determined at 0.5 L, whereas the lowest specific power input was  $17.69 \text{ W m}^{-3}$  and was achieved for 1.5 L, 4°, and 31 rpm ( $N_{S1}$  criterion). The power input results coincide with those obtained by Löffelholz et al. [36] and Eibl et al. [35].

**3.2.4. PIV Measurements.** To validate the numerical models, a line was set along the measurement field after analysis of the PIV data (see Figure 7, contour plots of PIV data). For 25 rpm, 10°, and 1.0 L working volume, the CFD-predicted and PIV-measured fluid velocities are depicted as an example for the side (a) and the bottom view recordings (b) in Figure 7. The measurements were performed at a momentary deflection angle of 7° when lowering the bag. Only minor differences in

the mean relative deviation ( $\delta_r$ ), of less than 15%, were found between the predicted CFD and measured PIV data:

$$\delta_r = \frac{\sqrt{(1/X) \sum_{i=1}^X (X_{\text{exp}_i} - X_{\text{sim}_i})^2}}{\sqrt{(1/X) \sum_{i=1}^X X_{\text{exp}_i}^2}}. \quad (8)$$

The discrepancy between the data can be explained by the lowest deviations in the measuring angle and by the shape of the bag, since no fluid structure interactions were considered in the simulations. The largest deviations occur near the edges of the bag (see Figures 7(a) and 7(b);  $l/L_2$  0.23–0.38). The dampening of the fluid flow at higher working volumes was also seen in the PIV measurements. Looking in addition at further results (e.g., spatial characteristics of the wave), it can be postulated that the established VOF model provides reliable fluid flow predictions.

**3.2.5. Proof-of-Concept Cultivation.** The proof-of-concept propagation of the hASCs in the BIOSTAT CultiBag RM 2L was successful, although the EF after 9 days was approximately three times lower ( $6.59 \pm 0.56$ ) than that in the control spinner (Figure 8(a)). The harvest provided  $2.85 \times 10^8$  hASCs. Akerström [40] reported a comparable EF, but over the double cultivation time. However, the cultivation process had not been optimized in terms of the attachment phase performed in shake flasks and the subsequent inoculation of the cells.

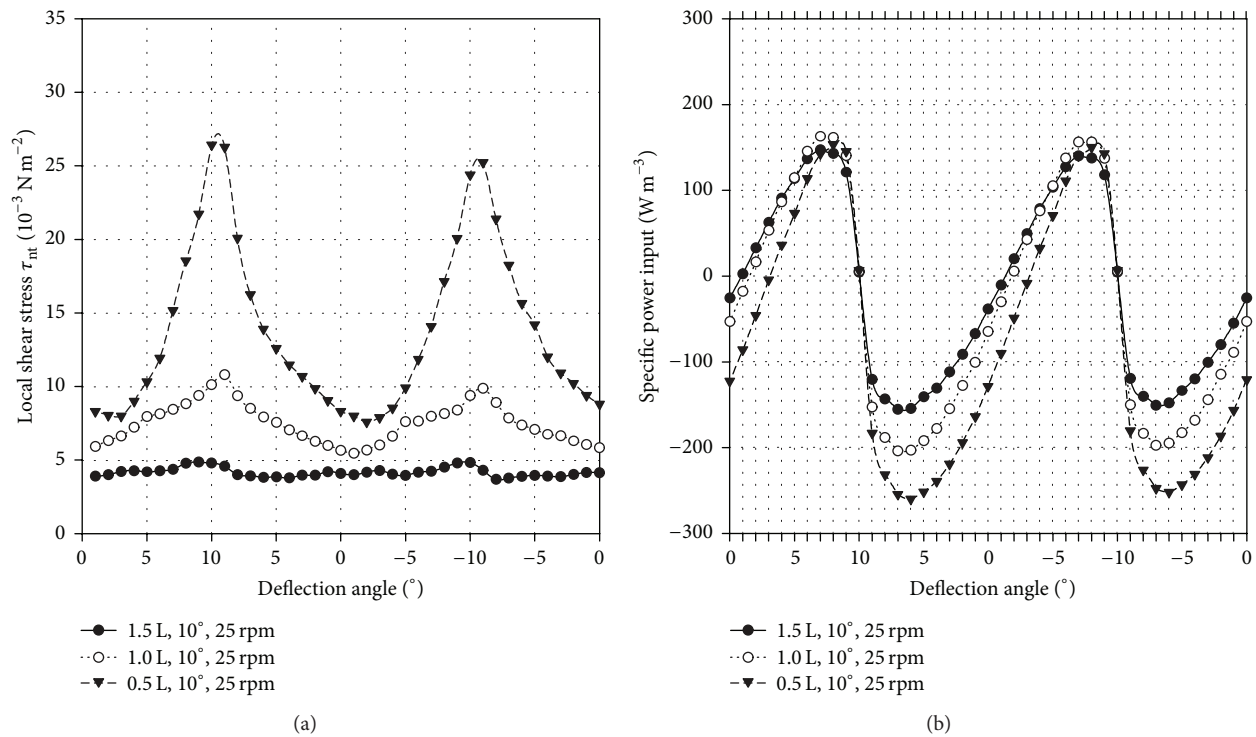


FIGURE 6: Angle-dependent profiles of volume-weighted mean shear stress levels (a) and specific power input (b) at 10° and 25 rpm and different working volumes.

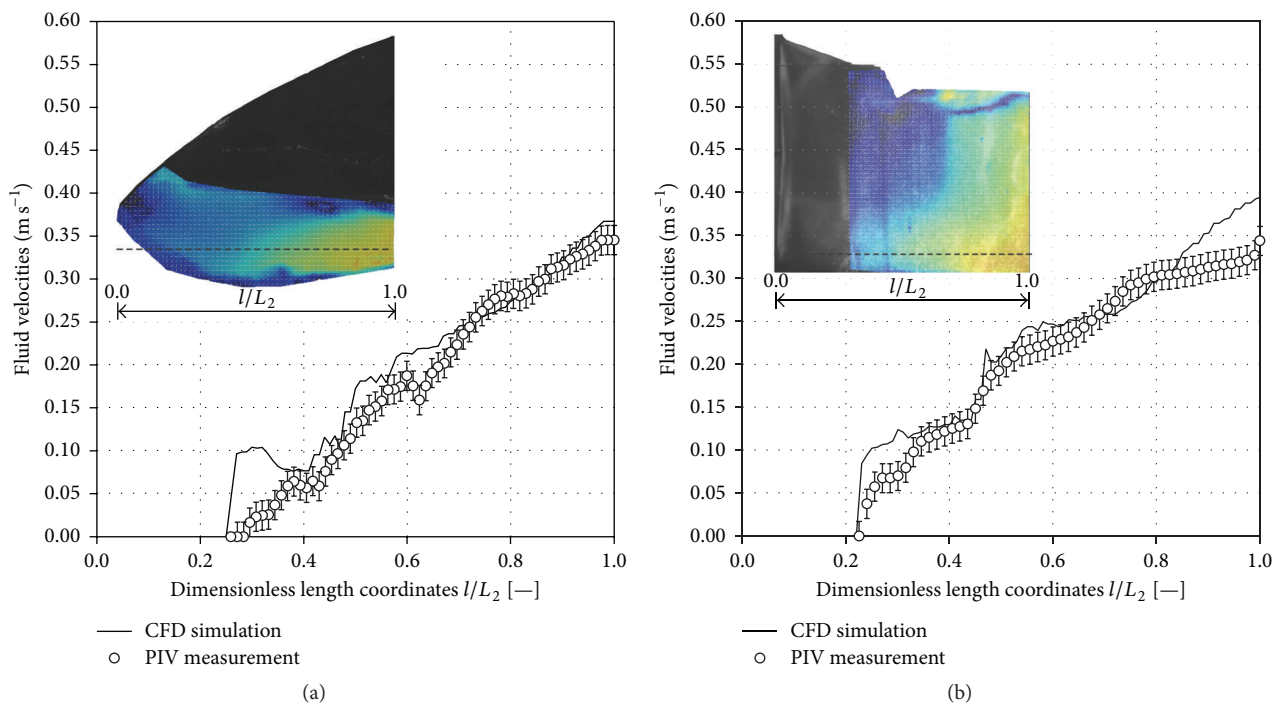


FIGURE 7: Comparison of PIV-measured (symbols) and CFD-predicted fluid flow velocities (solid line) through a horizontal line for side (a) and bottom view recordings (b). The comparison of the fluid flow velocities is given for operational parameters of 1.0 L, 25 rpm, and 10°. The error bars represent the standard deviation calculated over the 800 double frame images. The length coordinates were made dimensionless by the length of the field of view. The contour plots of the PIV data were scaled from 0.0 to 0.45  $\text{m s}^{-1}$ .

The first microcarrier-cell-aggregates were already observed 3 days after inoculation. The diameters of the aggregates increased during the cultivation and reached a maximum size of approximately 6 mm (only a few aggregates) at the end of the cultivation. Figure 8(b) shows representatively a DAPI-stained microcarrier-cell-aggregate sample at the end of the cultivation.

#### 4. Summary and Conclusions

In this study, the superiority of the suspension criterion  $N_{S1u}$  for mass propagating hASCs in microcarrier-based stirred bioreactors was shown. The highest living cell densities and EFs of hASCs were achieved in stirred cultivation systems. These results confirm the observations of Kaiser et al. [27], Schirmaier et al. [20], and Jossen et al. [22].

In spinners, the lowest living cell densities were achieved at the maximum impeller speed (120 rpm). At this impeller speed, the maximum shear stresses were 130% higher than those at  $N_{S1u}$ . Interestingly, the mean Sauter diameter, which was measured to evaluate the time-dependent microcarrier-cell-diameter, was lower than those at 25 rpm but comparable to those at the lower suspension criterion. Independent of the impeller speed, a decrease in the living cell densities was observed for mean Sauter diameters of 0.6 mm, even though shear stress levels were low and substrate limitation was excluded at the spinner scale. The reduction of the cell density might be a result of an undersupply of the cells in the centre of large microcarrier-cell-aggregates, although a change in the expression profile of the specific surface markers was not found. However, as reported for carrier-free cultivations with hASCs, cell aggregate diameters of 0.2 mm may already be critical and reduce the cell proliferation potential [34, 49]. Consequently, subsequent microcarrier-based productions of hASCs in spinners and stirred bioreactors not only should include extended cell quality control (differentiation and apoptosis assays) but also should pay attention to the number of cells in microcarrier-cell-aggregates. The question is whether a critical microcarrier-cell-aggregate size and number of cells in the aggregate can be defined and used as a harvest criterion for achieving maximum cell quantity with desired cell quality in hMSC expansions. These studies require subsequent investigations of diffusion limitations and examination of cell viability on the perimeter of the aggregates versus inside the aggregates.

Such findings represent one more step towards efficient and robust hASC mass production processes, which are also of interest for microcarrier-based, wave-mixed bioreactors, for which the suspension criteria were determined at the first time. An example of such a wave-mixed bioreactor is the BIOSTAT CultiBag RM 2L, which allowed  $2.85 \times 10^8$  hASCs to be harvested after a proof-of-concept cultivation performed at  $N_{S1u}$  conditions. Our established multiregression model makes the rapid definition of the suspension criteria for different working volumes possible and supports the optimization of microcarrier-based, wave-mixed bioreactors used for hASC cultivations. The consideration of further microcarrier types in the regression model would even allow hMSC expansions other than hASCs.

#### Abbreviations

ANOVA:	Analysis of variance
CCD:	Charged-coupled devices
CFD:	Computational Fluid Dynamics
DAPI:	4',6-Diamidino-2-phenylindole
EF:	Expansion factor
FACS:	Fluorescence-activated cell sorting
FBS:	Fetal bovine serum
hASCs:	Human adipose derived stromal/stem cells
hMSCs:	Human mesenchymal stem cells
MSCs:	Mesenchymal stem cells
PIV:	Particle Image Velocimetry
RANS:	Reynolds-averaged Navier-Stokes equations
SIMPLE:	Semi-implicit method for pressure linked equations
VOF:	Volume-of-Fluid
ns:	Not significant.

#### Symbols

##### Latin Symbols

$A_{MC}$ :	Specific growth surface of MCs [ $\text{cm}^2$ 100 mL]
$d_{32}$ :	Sauter mean diameter [mm]
$\vec{F}$ :	Volumetric forces [N]
$\vec{g}$ :	Gravitational acceleration [ $9.81 \text{ m s}^{-2}$ ]
$k$ :	Turbulent kinetic energy [ $\text{m}^2 \text{ s}^{-2}$ ]
$m_{MC}$ :	Amount of MCs [g]
$N_{S1u}/N_{S1}$ :	Suspension criteria [rpm]
$p$ :	Pressure [Pa]
$P/V$ :	Specific power input [ $\text{W m}^{-3}$ ]
$t$ :	Time [s]
$t_d$ :	Doubling time [h]
$V_f$ :	Fluid volume [ $\text{m}^3$ ]
$\vec{w}$ :	Fluid velocity [ $\text{m s}^{-1}$ ].

##### Greek Symbols

$\alpha$ :	Phase volume fraction [—]
$\epsilon$ :	Turbulent energy dissipation rate [ $\text{m}^2 \text{ s}^{-3}$ ]
$\mu$ :	Laminar (molecular) viscosity [Pa s]
$\pi$ :	PI (3.14159) [—]
$\rho$ :	Density [ $\text{kg m}^{-3}$ ]
$\mu_{\max}$ :	Maximum specific growth rate [ $\text{h}^{-1}$ ]
$\varphi_t$ :	Deflection angle at time point $t$ [°]
$\varphi_{\max}$ :	Maximum deflection angle [°]
$\omega$ :	Specific turbulent dissipation rate [ $\text{s}^{-1}$ ]
$\bar{\omega}$ :	Mean angular velocity [ $\text{s}^{-1}$ ].

#### Conflict of Interests

The authors declare that there is no conflict of interests regarding the publication of this paper.

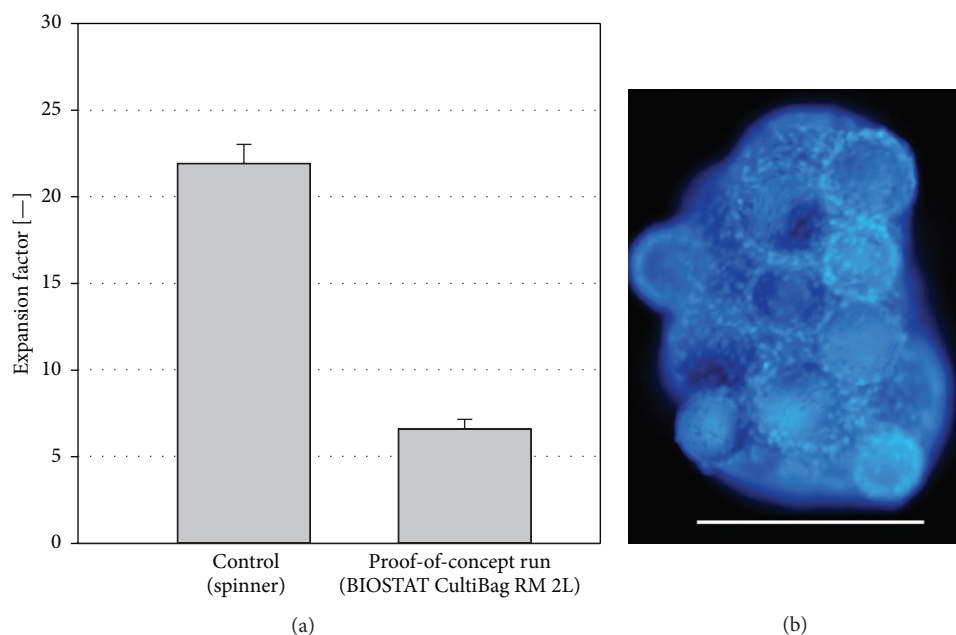


FIGURE 8: Results from the proof-of-concept cultivation in a BIOSTAT CultuBag RM 2L. (a) Comparison of the expansion factors in the BIOSTAT CultuBag RM 2L and the control spinner flask. The error bars represent the standard deviation. (b) DAPI staining picture of an aggregate at the end of the cultivation in the BIOSTAT CultuBag RM 2L. White bare = 500 μm.

## Acknowledgments

The study is based on results of a research project (CTI Project no. 12893.1) technically and financially supported by Lonza and the Commission for Technology and Innovation in Switzerland.

## References

- [1] T. R. Heathman, A. W. Nienow, M. J. McCall, K. Coopman, B. Kara, and C. J. Hewitt, “The translation of cell-based therapies: clinical landscape and manufacturing challenges,” *Regenerative Medicine*, vol. 10, no. 1, pp. 49–64, 2015.
- [2] C. Mason, M. J. McCall, E. J. Culme-Seymour et al., “The global cell therapy industry continues to rise during the second and third quarters of 2012,” *Cell Stem Cell*, vol. 11, no. 6, pp. 735–739, 2012.
- [3] A. Giordano, U. Galderisi, and I. R. Marino, “From the laboratory bench to the patient’s bedside: an update on clinical trials with mesenchymal stem cells,” *Journal of Cellular Physiology*, vol. 211, no. 1, pp. 27–35, 2007.
- [4] A. Trounson, R. G. Thakar, G. Lomax, and D. Gibbons, “Clinical trials for stem cell therapies,” *BMC Medicine*, vol. 9, article 52, 2011.
- [5] N. El-Badri and M. A. Ghoneim, “Mesenchymal stem cell therapy in diabetes mellitus: progress and challenges,” *Journal of Nucleic Acids*, vol. 2013, Article ID 194858, 7 pages, 2013.
- [6] M. Roemeling-van Rhijn, W. Weimar, and M. J. Hoogduijn, “Mesenchymal stem cells: application for solid-organ transplantation,” *Current Opinion in Organ Transplantation*, vol. 17, no. 1, pp. 55–62, 2012.
- [7] J. Voswinkel, S. Francois, N.-C. Gorin, and A. Chapel, “Gastro-intestinal autoimmunity: preclinical experiences and successful therapy of fistulizing bowel diseases and gut Graft versus host disease by mesenchymal stromal cells,” *Immunologic Research*, vol. 56, no. 2–3, pp. 241–248, 2013.
- [8] I. Molendijk, M. Duijvestein, A. E. van der Meulen-de Jong et al., “Immunomodulatory effects of mesenchymal stromal cells in Crohn’s disease,” *Journal of Allergy*, vol. 2012, Article ID 187408, 8 pages, 2012.
- [9] Y. Yao, J. Wang, Y. Cui et al., “Effect of sustained heparin release from PCL/chitosan hybrid small-diameter vascular grafts on anti-thrombogenic property and endothelialization,” *Acta Biomaterialia*, vol. 10, no. 6, pp. 2739–2749, 2014.
- [10] T. Matsuda and Y. Nakayama, “Surface microarchitectural design in biomedical applications: in vitro transmural endothelialization on microporous segmented polyurethane films fabricated using an excimer laser,” *Journal of Biomedical Materials Research*, vol. 31, no. 2, pp. 235–242, 1996.
- [11] L. Bordenave, P. Fernandez, M. Rémy-Zolghadri, S. Villars, R. Daculsi, and D. Midy, “In vitro endothelialized ePTFE prostheses: clinical update 20 years after the first realization,” *Clinical Hemorheology and Microcirculation*, vol. 33, no. 3, pp. 227–234, 2005.
- [12] K. Berger, L. R. Sauvage, A. M. Rao, and S. J. Wood, “Healing of arterial prostheses in man: its incompleteness,” *Annals of Surgery*, vol. 175, no. 1, pp. 118–127, 1972.
- [13] P. Zilla, D. Bezuidenhout, and P. Human, “Prosthetic vascular grafts: wrong models, wrong questions and no healing,” *Biomaterials*, vol. 28, no. 34, pp. 5009–5027, 2007.
- [14] P. Dixit, D. Hern-Anderson, J. Ranieri, and C. E. Schmidt, “Vascular graft endothelialization: comparative analysis of canine and human endothelial cell migration on natural biomaterials,”



- Journal of Biomedical Materials Research*, vol. 56, no. 4, pp. 545–555, 2001.
- [15] C. van den Bos, R. Keefe, C. Schirmaier, and M. McCaman, “Therapeutic human cells: manufacture for cell therapy/regenerative medicine,” *Advances in Biochemical Engineering/Biotechnology*, vol. 138, pp. 61–97, 2014.
  - [16] Q. A. Rafiq, K. Coopman, and C. J. Hewitt, “Scale-up of human mesenchymal stem cell culture: current technologies and future challenges,” *Current Opinion in Chemical Engineering*, vol. 2, no. 1, pp. 8–16, 2013.
  - [17] C. A. V. Rodrigues, T. G. Fernandes, M. M. Diogo, C. L. da Silva, and J. M. S. Cabral, “Stem cell cultivation in bioreactors,” *Biotechnology Advances*, vol. 29, no. 6, pp. 815–829, 2011.
  - [18] A. S. Simaria, S. Hassan, H. Varadaraju et al., “Allogeneic cell therapy bioprocess economics and optimization: single-use cell expansion technologies,” *Biotechnology and Bioengineering*, vol. 111, no. 1, pp. 69–83, 2014.
  - [19] Q. A. Rafiq, K. M. Brosnan, K. Coopman, A. W. Nienow, and C. J. Hewitt, “Culture of human mesenchymal stem cells on microcarriers in a 5 l stirred-tank bioreactor,” *Biotechnology Letters*, vol. 35, no. 8, pp. 1233–1245, 2013.
  - [20] C. Schirmaier, V. Jossen, S. C. Kaiser et al., “Scale-up of adipose tissue-derived mesenchymal stem cell production in stirred single-use bioreactors under low-serum conditions,” *Engineering in Life Sciences*, vol. 14, no. 3, pp. 292–303, 2014.
  - [21] V. Jossen, R. Pörtner, S. C. Kaiser, M. Kraume, D. Eibl, and R. Eibl, “Mass production of mesenchymal stem cells—impact of bioreactor design and flow conditions on proliferation and differentiation,” in *Cells and Biomaterials in Regenerative Medicine*, D. Eberli, Ed., pp. 119–174, InTech, 2014.
  - [22] V. Jossen, S. C. Kaiser, C. Schirmaier et al., “Modification and qualification of a stirred single-use bioreactor for the improved expansion of human mesenchymal stem cells at benchtop scale,” *Pharmaceutical Bioprocessing*, vol. 2, no. 4, pp. 311–322, 2014.
  - [23] K. Cierpka, C. L. Elseberg, K. Niss, M. Kassem, D. Salzig, and P. Czermak, “hMSC production in disposable bioreactors with regards to GMP and PAT,” *Chemie Ingenieur Technik*, vol. 85, no. 1-2, pp. 67–75, 2013.
  - [24] C. J. Hewitt, K. Lee, A. W. Nienow, R. J. Thomas, M. Smith, and C. R. Thomas, “Expansion of human mesenchymal stem cells on microcarriers,” *Biotechnology Letters*, vol. 33, no. 11, pp. 2325–2335, 2011.
  - [25] T. G. Fernandes, M. M. Diogo, and J. M. S. Cabral, “Bioreactors for stem cell culture,” in *Stem Cell Bioprocessing*, chapter 3, pp. 69–114, Elsevier, 2013.
  - [26] T. Oppermann, J. Leber, C. Elseberg, D. Salzig, and P. Czermak, “hMSC production in disposable bioreactors in compliance with cGMP guidelines and PAT,” *American Pharmaceutical Review*, vol. 17, no. 3, pp. 42–47, 2014.
  - [27] S. C. Kaiser, V. Jossen, C. Schirmaier et al., “Fluid flow and cell proliferation of mesenchymal adipose-derived stem cells in small-scale, stirred, single-use bioreactors,” *Chemie Ingenieur Technik*, vol. 85, no. 1-2, pp. 95–102, 2013.
  - [28] K. Siddiquee and M. Sha, “Large-scale production of human mesenchymal stem cells in BioBLU® 5c single-use vessels,” Application Note 334, Eppendorf, 2014.
  - [29] C. Schlottbom, *Controlled Cultivation of Stem Cells—Factors to Consider When Thinking of Scale-Up*, vol. 19 of *White Paper*, Eppendorf, 2014.
  - [30] F. dos Santos, P. Z. Andrade, M. M. Abecasis et al., “Toward a clinical-grade expansion of mesenchymal stem cells from human sources: a microcarrier-based culture system under xeno-free conditions,” *Tissue Engineering—Part C: Methods*, vol. 17, no. 12, pp. 1201–1210, 2011.
  - [31] G. Yourek, S. M. McCormick, J. J. Mao, and G. C. Reilly, “Shear stress induces osteogenic differentiation of human mesenchymal stem cells,” *Regenerative Medicine*, vol. 5, no. 5, pp. 713–724, 2010.
  - [32] S. Stolberg and K. E. McCloskey, “Can shear stress direct stem cell fate?” *Biotechnology Progress*, vol. 25, no. 1, pp. 10–19, 2009.
  - [33] T. N. Zwietering, “Suspending of solid particles in liquid by agitators,” *Chemical Engineering Science*, vol. 8, no. 3-4, pp. 244–253, 1958.
  - [34] C. Ferrari, F. Balandras, E. Guedon, E. Olmos, I. Chevalot, and A. Marc, “Limiting cell aggregation during mesenchymal stem cell expansion on microcarriers,” *Biotechnology Progress*, vol. 28, no. 3, pp. 780–787, 2012.
  - [35] R. Eibl, S. Werner, and D. Eibl, “Bag bioreactor based on wave-induced motion: characteristics and applications,” in *Disposable Bioreactors*, Springer, Berlin, Germany, 2010.
  - [36] C. Löffelholz, S. C. Kaiser, S. Werner, and D. Eibl, “CFD as a tool to characterize single-use bioreactors,” in *Single-Use Technology in Biopharmaceutical Manufacture*, John Wiley & Sons, 2011.
  - [37] A. A. Öncül, A. Kalmbach, Y. Genzel, U. Reichl, and D. Thévenin, “Characterization of flow conditions in 2 L and 20 L wave bioreactors\* using computational fluid dynamics,” *Biotechnology Progress*, vol. 26, no. 1, pp. 101–110, 2010.
  - [38] A. Kalmbach, R. Bordás, A. A. Öncül, D. Thévenin, Y. Genzel, and U. Reichl, “Experimental characterization of flow conditions in 2- and 20-l bioreactors with wave-induced motion,” *Biotechnology Progress*, vol. 27, no. 2, pp. 402–409, 2011.
  - [39] N. E. Timmins, M. Kiel, M. Günther et al., “Closed system isolation and scalable expansion of human placental mesenchymal stem cells,” *Biotechnology and Bioengineering*, vol. 109, no. 7, pp. 1817–1826, 2012.
  - [40] H. Akerström, *Expansion of adherent cells for cell therapy [M.S. thesis]*, Uppsala University Sweden, Uppsala, Sweden, 2009.
  - [41] ANSYS Inc, *Fluent 15.0 Theory Guide*, Canonsburg, Pa, USA, 2013.
  - [42] ANSYS Inc, *Fluent 15.0 User's Guide*, ANSYS Inc, Canonsburg, Pa, USA, 2013.
  - [43] T. Chen, Y. Zhou, and W.-S. Tan, “Influence of lactic acid on the proliferation, metabolism, and differentiation of rabbit mesenchymal stem cells,” *Cell Biology and Toxicology*, vol. 25, no. 6, pp. 573–586, 2009.
  - [44] D. Schop, F. W. Janssen, L. D. S. van Rijn et al., “Growth, metabolism, and growth inhibitors of mesenchymal stem cells,” *Tissue Engineering—Part A*, vol. 15, no. 8, pp. 1877–1886, 2009.
  - [45] M.-L. Collignon, A. Delafosse, M. Crine, and D. Toye, “Axial impeller selection for anchorage dependent animal cell culture in stirred bioreactors: methodology based on the impeller comparison at just-suspended speed of rotation,” *Chemical Engineering Science*, vol. 65, no. 22, pp. 5929–5941, 2010.
  - [46] F. Liepe, R. Sperling, and J. Solomon, *Rührwerke: Theoretische Grundlagen, Auslegung und Bewertung*, Eigenverlag Fachhochschule Köthen, 1998.
  - [47] S. Wollny, *Experimentelle und numerische Untersuchungen zur Partikelbeanspruchung in gerührten (Bio-) Reaktoren [Ph.D. thesis]*, Technische Universität Berlin, Berlin, Germany, 2010.
  - [48] S. Kaiser, C. Löffelholz, S. Werner, and D. Eibl, “CFD for characterizing standard and single-use stirred cell culture bioreactors,”

in *Computational Fluid Dynamics*, I. V. Minin and O. V. Minin, Eds., pp. 97–122, InTech, 2011.

- [49] T. J. Bartosh, J. H. Ylöstalo, A. Mohammadipoor et al., “Aggregation of human mesenchymal stromal cells (MSCs) into 3D spheroids enhances their antiinflammatory properties,” *Proceedings of the National Academy of Sciences of the United States of America*, vol. 107, no. 31, pp. 13724–13729, 2010.

## Research Article

# Standardizing Umbilical Cord Mesenchymal Stromal Cells for Translation to Clinical Use: Selection of GMP-Compliant Medium and a Simplified Isolation Method

**J. Robert Smith,<sup>1</sup> Kyle Pfeifer,<sup>1</sup> Florian Petry,<sup>1,2</sup> Natalie Powell,<sup>1</sup> Jennifer Delzeit,<sup>1</sup> and Mark L. Weiss<sup>1</sup>**

<sup>1</sup>*The Midwest Institute for Comparative Stem Cell Biotechnology, Department of Anatomy and Physiology, Kansas State University, Manhattan, KS 66506, USA*

<sup>2</sup>*Institute of Bioprocess Engineering and Pharmaceutical Technology, University of Applied Sciences Mittelhessen, 35390 Giessen, Germany*

Correspondence should be addressed to Mark L. Weiss; [weiss@vet.k-state.edu](mailto:weiss@vet.k-state.edu)

Received 7 October 2015; Accepted 29 December 2015

Academic Editor: Shimon Slavin

Copyright © 2016 J. Robert Smith et al. This is an open access article distributed under the Creative Commons Attribution License, which permits unrestricted use, distribution, and reproduction in any medium, provided the original work is properly cited.

Umbilical cord derived mesenchymal stromal cells (UC-MSCs) are a focus for clinical translation but standardized methods for isolation and expansion are lacking. Previously we published isolation and expansion methods for UC-MSCs which presented challenges when considering good manufacturing practices (GMP) for clinical translation. Here, a new and more standardized method for isolation and expansion of UC-MSCs is described. The new method eliminates dissection of blood vessels and uses a closed-vessel dissociation following enzymatic digestion which reduces contamination risk and manipulation time. The new method produced >10 times more cells per cm of UC than our previous method. When biographical variables were compared, more UC-MSCs per gram were isolated after vaginal birth compared to Caesarian-section births, an unexpected result. UC-MSCs were expanded in medium enriched with 2%, 5%, or 10% pooled human platelet lysate (HPL) eliminating the xenogeneic serum components. When the HPL concentrations were compared, media supplemented with 10% HPL had the highest growth rate, smallest cells, and the most viable cells at passage. UC-MSCs grown in 10% HPL had surface marker expression typical of MSCs, high colony forming efficiency, and could undergo trilineage differentiation. The new protocol standardizes manufacturing of UC-MSCs and enables clinical translation.

## 1. Introduction

The minimal criteria for defining mesenchymal stromal cells (MSCs) were provided by the International Society of Cellular Therapy (ISCT) MSC working group in 2006 and updated in 2013 with guidelines for characterization of MSC immune properties [1–4]. The physiological properties of MSCs suggest a potential to treat diseases such as graft versus host disease (GVHD) and Crohn's [5–7]. In addition, there are more than 500 clinical trials testing the safety and efficacy of MSCs listed on ClinicalTrials.gov [8].

In 2014, about 53% of the MSC clinical trials worldwide used bone marrow-derived MSCs (BM-MSCs) [9].

BM-MSCs may be used as an autologous cellular product, which is a distinct advantage over allogeneic MSC products. However, the collection of BM is a painful, invasive procedure, when compared to MSCs from umbilical cord stroma (UC-MSCs) which is collected painlessly from tissues that are discarded after birth. Furthermore, adult BM-MSCs have a lower expansion potential, lower immunosuppression capability when cocultured with activated T-cells, and perhaps a more restricted differentiation potential than UC-MSCs [10–15].

UC-MSCs have advantages over BM-MSCs when considered as an allogeneic MSC source. These advantages include a virtually limitless supply of starting material which is

available for producing tissue banks for use as an allogeneic matched product, much like umbilical cord blood banks, the collection of umbilical cords is painless, and the cord donors are of a consistent, young age. *In vitro*, UC-MSCs have high proliferation potential, broad differentiation potential, and improved immune modulation properties [11, 16–18]. For these reasons, the therapeutic potential of UC-MSCs bears testing, and 25 clinical trials worldwide were using UC-MSCs as of 2014 [9].

There are “challenges” to produce MSCs meeting requirements for clinical application [2, 19]. This has led to speculation that MSC manufacturing capacity may not keep pace with the number of MSC clinical studies [19, 20]. These challenges include the lack of a standardized method for isolating, expanding, and validating MSCs. For example, several methods to isolate UC-MSCs from umbilical cord stroma have been described [21] that include the tissue explant method [22, 23], mechanical dissociation of the cord stroma followed by enzymatic digestion [11, 23, 24], isolation of MSCs from the entire umbilical cord including the blood vessels [21, 22], enzymatic digestion of the tissue immediately surrounding the umbilical blood vessels [25], or mincing and enzymatic digestion of the stroma (Wharton’s Jelly) without the blood vessels [24]. Several of these methods require dissection of the umbilical vessels. This dissection step increases processing time and the risk of contamination. For this reason, the goal here was to develop an isolation method which would decrease contamination risk and isolation time and increase the yield of MSCs. In reviewing our MSC expansion protocol, we determined that our medium formulation contained many ingredients and that this created a barrier for clinical manufacturing [24]. Therefore, our second goal was to identify a simplified medium that would provide for robust expansion of MSCs, be xenogen-free, and be suitable for clinical manufacturing.

## 2. Materials and Methods

**2.1. Umbilical Cords.** This research was deemed nonhuman subjects research by the institutional review board of Kansas State University since discarded, anonymous human tissue with all identifying linkages broken was used (IRB #5189). Tissue processing was performed inside a biological safety cabinet (BSC) in a BSL2 laboratory using universal precautions per Occupational Safety and Health Administration (OSHA) recommended blood borne pathogens containment described in 29 CFR. 1910.1030.

In a pilot study whose data is not presented here, 8 umbilical cords were used to identify optimization variables. In the work reported here, 24 umbilical cords (11 females and 13 males) were used; umbilical cords from vaginal births or Caesarean-section births were used. The umbilical cords were stored in sterile tissue sample container in saline solution at 4°C until use. In pilot work not presented here, umbilical cords were stored for up to 5 days prior to processing to extract MSCs; however, no parametric testing was performed to determine whether storage alters the quality of the product. Here, isolations procedures were performed within 4 days after birth. To randomize the treatment effects, we performed

no prescreening and randomly assigned cord samples (biological replicates) to each experimental variable.

**2.2. Isolation Optimization Strategy.** Here our previously described protocol [24] was optimized to decrease contamination risk, increase yield, and improve GMP compatibility. For each umbilical cord (the biological unit), eight randomly selected 1 cm length samples were used to test the effect on the experimental variables identified in the pilot work. Two to four optimization variables were evaluated per cord using technical duplicates and the results were averaged for each experimental variable per biological unit for comparisons. First, we tested mechanical disruption of the tissue using a Miltenyi GentleMACS Dissociator (#130-093-235) using preprogrammed settings A, B, C, D, and E (which corresponds to weakest to strongest dissociation). Next, tissue dissociation conducted before or after enzymatic digestion was tested. Then, the effect of mincing the tissue samples was compared to tissue dissociation using the GentleMACS Dissociator. Next, the effect of filtering using 100  $\mu$ m cell strainers (Fisherbrand #22-363-549) and 60  $\mu$ m Steriflip tubes (Millipore #SCNY00060) was tested. Lastly, the concentration of enzyme was varied to determine the effect on yield. The technical duplicates or triplicates were averaged for each variable per cord sample. Each procedural optimization variable was evaluated using at least three different cord replicates. Decision making strategy was designed-based using process yield (more live cells) or increasing process efficiency (reducing number of processing steps, reducing time, or reducing contamination risk).

**2.3. Final (Optimized) Isolation Method.** A schematic of the revised method is shown in Figure 1. Umbilical cords were rinsed to remove surface blood using 37°C DPBS which had 1% Antibiotic-Antimycotic (Dulbecco’s Phosphate Buffered Saline, Life Technologies #14190-250; Antibiotic-Antimycotic, Life Technologies #15240-062). The cords were then treated with 0.5% Betadine (Dynarex, Providone Iodine Solution, #1416) in DPBS for 5 minutes at room temperature. Inside the biological safety cabinet (BSC), the cord was cut into 1 cm lengths and rinsed repeatedly with 3 volumes of DPBS until no further surface blood could be seen. Each 1 cm length of tissue was cut into four equal size pieces and placed into a Miltenyi Biotech Dissociator C-Tube (Miltenyi #130-096-334). The tissue weight was calculated by subtracting the tare weight of the C-tube and 9 mL of enzyme solution was added. The C-tubes were placed into a Miltenyi Dissociator, processed using program C and incubated for 3–3.5 hours at 37°C with constant 12 rpm rotation. Following the 3–3.5-hour incubation, the tissues were dissociated using program B and filtered through 60  $\mu$ m Steriflip filter (Millipore #SCNY00060) to remove tissue debris. The cells were pelleted by centrifugation at 200  $\times$ g for 5 minutes at room temperature and the supernatant was discarded. The cells were suspended in 0.5 mL of growth media and 0.5 mL RBC lysing solution (Sigma’s RBC lysis solution, #R7757-100ML) was added to remove red blood cell contamination. The cells were mixed gently for one minute followed by addition of 8 mL of DPBS. Cells were centrifuged at 200  $\times$ g



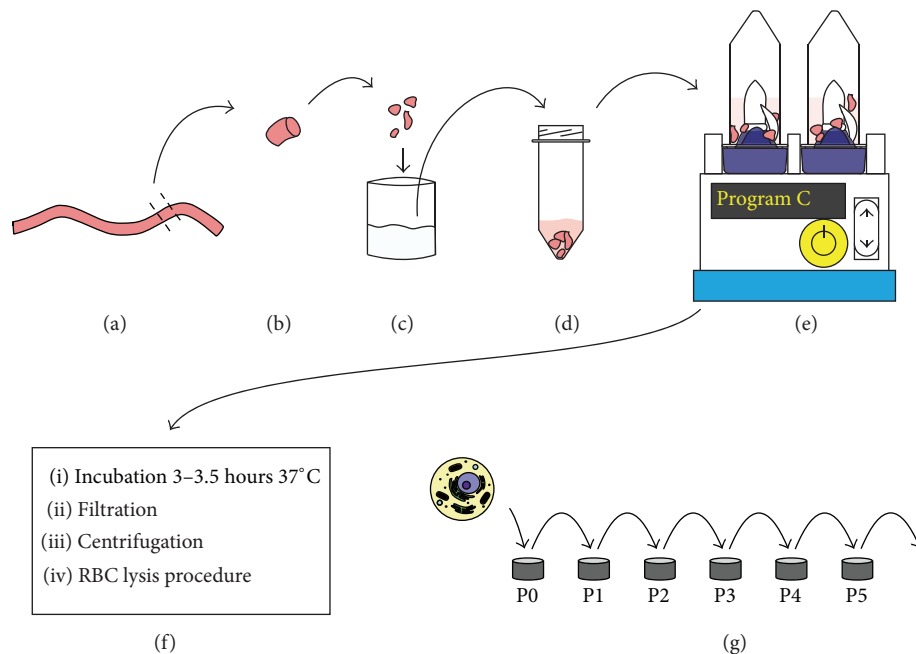


FIGURE 1: A schematic of the optimized isolation method. The major steps: (a) umbilical cord selected. (b) 1 cm section prior to cutting into 4 equal pieces. (c) Cord pieces rinsed in DPBS. (d) The cord pieces inside a C-tube immersed in enzyme solution. (e) Dissociation with C-tubes and Miltenyi Dissociator. (f) Steps following dissociation prior to plating the isolated cells. (g) The isolated cell initial plating at P0 and subsequent expansion over multiple passages.

for 5 minutes at room temperature and the supernatant was discarded. The cells were suspended in 1 mL of media and the number of live cells was determined using a Nexcelom Auto 2000 Cellometer (immune cells program, low RBC) following ViaStain AOPI (acridine orange and propidium iodide) viability staining (Nexcelom cat. #CS2-D106-5ML). Cells were plated at 10,000–15,000 live cells per  $\text{cm}^2$  on tissue culture treated plastic (CytoOne 6-well plates, #CC7682-7506).

**2.4. Optimization of MSC Expansion.** Our previously described method MSC expansion medium was the standard used for comparison. Since that medium contains more than 10 components [24], our goal was to reduce the number of medium components while maintaining the MSC attachment at isolation/startup and maintaining MSC expansion, CFU-F efficiency, trilineage differentiation potential, MSC surface marker expression, and cellular morphology similar to or better than that standard. Here, low glucose Dulbecco's Modified Eagle's Medium (DMEM Life Technologies cat. #14190) supplemented with 1% GlutaMAX (Life Technologies cat. #35050), with 1% Antibiotic-Antimycotic, and, by volume, with 2, 5, or 10% pooled human platelet lysate (HPL, pooled from more than 25 outdated platelet donors, supplied by Kansas University Medical Center diagnostic laboratory, Dr. Lowell Tilzer, director) and 4 units/mL heparin was tested. The cells were plated at 10–15,000 cells per  $\text{cm}^2$  in CytoOne flat bottom tissue culture treated 6-well plates and expanded for 5 passages. Cells were incubated and grown as a monolayer at 37°C, 5%  $\text{CO}_2$ , and 90% humidity (Nuair AutoFlow

4950 or Heracell 150i). Once the cells reached approximately 80–90% confluence they were lifted and plated in fresh medium. To lift the cells, the medium was removed and cells were washed with 37°C DPBS. The DPBS was removed and replaced with 37°C 0.05% trypsin-EDTA (Lifetechn #25200-056). Following a 3–5-minute incubation at 37°C, the plates were tapped to release cells and the enzymatic digestion was terminated with 3 volumes of media. Cells were pelleted at 200  $\times g$  for 5 minutes at room temperature. Supernatant was discarded and 1 mL of media was used to suspend the cells. Cells were counted using the Nexcelom Auto 2000 Cellometer and the ViaStain AOPI staining reagent using the manufacturer's protocol and a built-in settings. At passage, the number of cells, percentage of live cells, cell size, and number of hours in culture were recorded. Cells were initially plated at a density of approximately 10,000 cells/ $\text{cm}^2$ ; using this as the initial cell number and the number of cells at harvest as the final cell number and culture time, population doubling time was calculated using the standard formula. At times, extra cells were frozen for later use. To freeze, cells were cryopreserved using a 1:1 ratio of HPL media and cryopreservative (Globalstem #GSM-4200) and held on ice until transfer to a controlled rate freezing device (Mr. Frosty) and being placed into a  $-80^\circ\text{C}$  freezer overnight. The next day, the vials were moved to the vapor phase of liquid nitrogen for long term storage.

**2.5. CFU-F Assay.** MSCs were plated at 10, 50, or 100 cells per  $\text{cm}^2$  in duplicate in 6-well CytoOne tissue culture plates in 2, 5, and 10% HPL enriched DMEM, as described above.

Four cell lines were expanded 4 days in culture, prior to fixation and methylene blue staining. Subsequent tests used 4–7 days of culture at a density of 5, 10, or 50 cells per  $\text{cm}^2$ . After the required culture period, the medium was removed and the cells were washed with DPBS and then fixed using 4°C 100% methanol for 5 minutes. The cells were washed again with DPBS, stained with 0.5% methylene blue for 15 minutes, rinsed several times with distilled water, and air dried. The stained colonies were counted manually at 40x final magnification. Colonies were defined as isolated groups (clonal groups) of at least 10 cells. Colony number was determined by averaging the number of colonies in the technical replicates at each plating density for a given expansion period. Colony forming efficiency was calculated by dividing the number of plated cells by the number of colonies.

**2.6. Differentiation.** Differentiation of MSCs was induced by replacing the expansion medium with MSC differentiation medium (StemPro, Life Technologies #s A10070-01, A10071-01, and A10072-01 for adipogenic, chondrogenic, and osteogenic differentiation) and following the manufacturer's protocol. After about 21 days of differentiation, the differentiation medium was removed; the MSCs were washed with DPBS, fixed with 4% paraformaldehyde for 10 min, and stained with Oil Red for analysis of adipose cells, Safranin O for chondrogenic cells, or Alizarin Red S for osteogenic cells. Micrographs were taken using an Evos FL Auto microscope (Life Technologies).

**2.7. Flow Cytometry.** The BD human MSCs flow cytometry characterization kit was used for positive and negative surface marker staining (#562245). Using the manufacturer's recommended protocol, MSC samples were stained with four fluorochromes together including positive and negative staining cocktails. The positive marker cocktail stained for CD90, CD105, and CD73 (defined as >97% positive staining). The negative cocktail (all antibodies were stained using a single fluorochrome, PE) stained for CD34, CD45, CD11b, CD19, and HLA-DR (defined as <2% positive staining). A CD44 labeled PE antibody was used as positive control for the negative cocktail to set the compensation and gating of the negative cocktail. For each flow cytometry run, fluorescence minus one controls for each fluorochrome and isotype controls for each antibody were used for compensation and nonspecific fluorescence analysis. Samples were washed with 1% BSA solution before and after staining. A FACScalibur (BD Biosciences) was used for flow cytometry and analysis was conducted using FCS software. Negative staining gate of the isotype control was set at 1% positive staining.

**2.8. Statistics.** After confirmation that ANOVA assumptions of normality and homogeneity of variance were met, ANOVA was used to evaluate significant differences between optimization variables. If the assumptions were violated, the dataset was transformed mathematically and again tested to see if it met ANOVA assumptions. Hypothesis testing was two tailed (e.g., mean 1  $\neq$  mean 2). After running

ANOVA and finding significant main effect(s) or interaction terms, *post hoc* means testing of planned comparisons was conducted using either the Bonferroni correction or Holm-Sidak method. Significance was set at  $p < 0.05$ . Data is presented as average (mean) plus/minus one standard error. In one case, in order to pass the normality test (Shapiro-Wilk) an "outlier" was removed. After the outlier was removed, the dataset passed the normality test and ANOVA determined that there was a significant effect of HPL concentration. SigmaPlot v.12.5 (Systat software) was used for statistics and making of the graphs. The graphs created in SigmaPlot were saved as EPS files and moved into a vector-based graphics package (Adobe InDesign or Adobe Illustrator CS6) for editing and rendering.

### 3. Results

**3.1. Umbilical Cords.** Umbilical cord from Caesarean-section delivery ( $n = 17$ ) and "normal" vaginal delivery ( $n = 7$ ) were used in this research. The biographic data of each cord is shown in Table 1.

**3.2. Isolation Method Comparison.** Note that the MSC expansion comparison was considered for passages 1–5, and passage 0 was considered part of the isolation of MSCs. Results obtained from our previously described method (historical data from 27 umbilical cords [24]) and our optimized method were compared. As shown in Figure 2, the optimized method yielded on average 10 times more MSCs per cm length than the original method and yielded MSCs in 100% of the UC samples. Note that in pilot work where we were identifying variables to optimize, we did fail to isolate MSCs in two cases. But even in these cases, MSCs were isolated from the same UC in different samples (e.g., in no cases did we suspect that the UC did not contain viable MSCs). While we did not test for bacterial, viral, or fungal contamination, no break in sterility was apparent here (e.g., no frank contamination was observed and no cultures were discarded due to contamination). Live cells per cm of length or per gram were compared in Table 1; there was a trend for the coefficient of variation to be less for live cells per gram. The optimized method uses a closed processing system for tissue disruption and takes a total of 4 hours of work time plus a 3-hour enzyme extraction step to isolate the umbilical cord MSCs. MSC attachment was observed within 24 hours of the isolation and proliferation was observed in all three HPL media enrichment conditions. As shown in Figure 2(c), during the isolation phase (P0) UC-MSCs grew more quickly when plated in 5% or 10% HPL enriched DMEM than UC-MSCs plated in 2% HPL enriched DMEM. It is possible that UC-MSCs grown in 5 or 10% HPL enriched DMEM attached more quickly than those grown in 2% HPL enriched DMEM in P0. The growth rate difference for 2% HPL enriched medium was statistically different (slower) at P0 than later passages (see Figures 2(c) and 3(a)) and was significantly different (slower) than 5 and 10% HPL enriched media at isolation and during expansion.

**3.3. MSC Expansion Comparison.** Note that the MSC expansion comparison was considered for passages 1–5, and passage

TABLE 1: Data from 24 umbilical cord MSC isolations.

UC-MSC line	Sex	Birth	Length (cm)	Enzyme	Weight (g)	Gram per cm	Viability	±SE	Live cells per cm	±SE	Live cells per gram	±SE	Theoretical cell yield
241	F	V	46	High	67.9	1.5	76.7%	0.6%	3.7E + 05	2.3E + 05	3.2E + 05	5.6E + 04	2.17E + 07
242	M	V	43	High	60.7	1.4	58.0%	1.9%	2.4E + 05	2.9E + 04	1.7E + 05	2.2E + 04	1.06E + 07
243	F	V	57	High	81.1	1.4	62.8%	2.0%	3.9E + 05	7.4E + 04	2.7E + 05	6.4E + 04	2.17E + 07
244	M	C-S	35	High	66.0	1.9	58.6%	2.6%	2.0E + 05	2.4E + 04	1.2E + 05	1.8E + 04	7.85E + 06
245	M	V	61	High	76.0	1.2	50.6%	6.4%	3.3E + 05	9.9E + 04	2.7E + 05	9.2E + 04	2.06E + 07
246	M	C-S	41	High	60.9	1.5	66.0%	0.9%	1.5E + 05	4.3E + 03	8.5E + 04	8.2E + 03	5.19E + 06
248	F	C-S	47	High	72.6	1.5	68.3%	3.2%	2.9E + 05	4.2E + 04	1.2E + 05	4.3E + 04	8.66E + 06
249	F	C-S	32	High	37.7	1.2	64.2%	10.7%	1.3E + 05	4.9E + 04	1.2E + 05	4.3E + 04	4.50E + 06
250	M	V	26	High	43.3	1.7	84.2%	0.5%	5.3E + 05	4.1E + 04	3.1E + 05	8.8E + 03	1.34E + 07
251	F	V	28	High	30.4	1.1	74.4%	3.8%	9.9E + 04	5.7E + 02	8.8E + 04	1.7E + 04	2.69E + 06
252	M	C-S	54	High	83.6	1.5	79.8%	3.9%	1.9E + 05	3.9E + 04	1.3E + 05	5.0E + 04	1.11E + 07
253	M	V	61	Low	48.8	0.8	58.0%	3.7%	3.4E + 05	9.8E + 04	2.3E + 05	6.5E + 04	1.11E + 07
254	F	C-S	38	Low	59.3	1.6	60.9%	3.9%	1.1E + 05	5.3E + 04	7.9E + 04	4.0E + 04	4.68E + 06
255	F	C-S	47	Low	82.3	1.8	75.1%	8.6%	7.7E + 04	5.2E + 03	4.7E + 04	4.0E + 03	3.85E + 06
256	M	C-S	45	Low	49.0	1.1	70.2%	1.1%	2.4E + 05	5.8E + 04	2.1E + 05	3.3E + 04	1.02E + 07
257	M	C-S	43	Low	105.2	2.4	66.6%	3.0%	3.5E + 05	2.4E + 04	1.5E + 05	1.4E + 04	1.56E + 07
258	M	C-S	37	Low	45.1	1.2	62.5%	4.6%	1.9E + 05	3.8E + 04	1.6E + 05	2.7E + 04	7.01E + 06
259	M	C-S	31	Low	57.8	1.9	62.2%	3.5%	2.7E + 05	2.6E + 04	1.5E + 05	2.2E + 04	8.56E + 06
260	F	C-S	67	Low	100.6	1.5	64.4%	1.8%	1.7E + 05	3.9E + 04	1.1E + 05	2.8E + 04	1.11E + 07
261	M	C-S	51	Low	92.8	1.8	72.3%	2.1%	2.2E + 05	1.9E + 04	1.2E + 05	8.8E + 03	1.10E + 07
262	F	C-S	28.5	Low	25.1	0.9	50.5%	4.1%	1.0E + 05	2.7E + 04	1.5E + 05	5.7E + 04	3.81E + 06
263	F	C-S	28	Low	23.8	0.9	65.3%	3.8%	2.0E + 05	5.4E + 04	2.6E + 05	8.9E + 04	6.27E + 06
264	F	C-S	32	Low	45.7	1.4	59.8%	3.4%	4.5E + 05	4.7E + 04	3.2E + 05	4.3E + 04	1.46E + 07
265	M	C-S	38	Low	38.7	1.0	54.8%	3.2%	1.5E + 05	3.0E + 04	1.5E + 05	3.5E + 04	5.81E + 06
All 24 cords were compared below													
			Length	Weight	g per cm	Viability	Live cells per cm		Live cells per gram		Theo. yield		
Mean			42.4	60.6	1.4	65.25%	2.42E + 05		1.72E + 05		1.01E + 07		
Standard dev.			11.6	22.9	0.4	8.33%	1.16E + 05		7.48E + 04		5.00E + 06		
Coefficient of var.			27.5%	37.7%	26.9%	12.8%	47.9%		43.5%		49.7%		

F = female, M = male, C-S = Caesarean-section, and V = vaginal. The enzyme concentration: low was 300 U/mL and high was 532 U/mL of collagenase. SE = standard error, which was calculated after averaging the technical replicates for each umbilical cord. Live cells per gram were calculated from the live cell number for each tube divided by the weight of the tube. Theoretical yield calculation represents cell numbers achieved assuming the entire umbilical cord was processed and expanded.

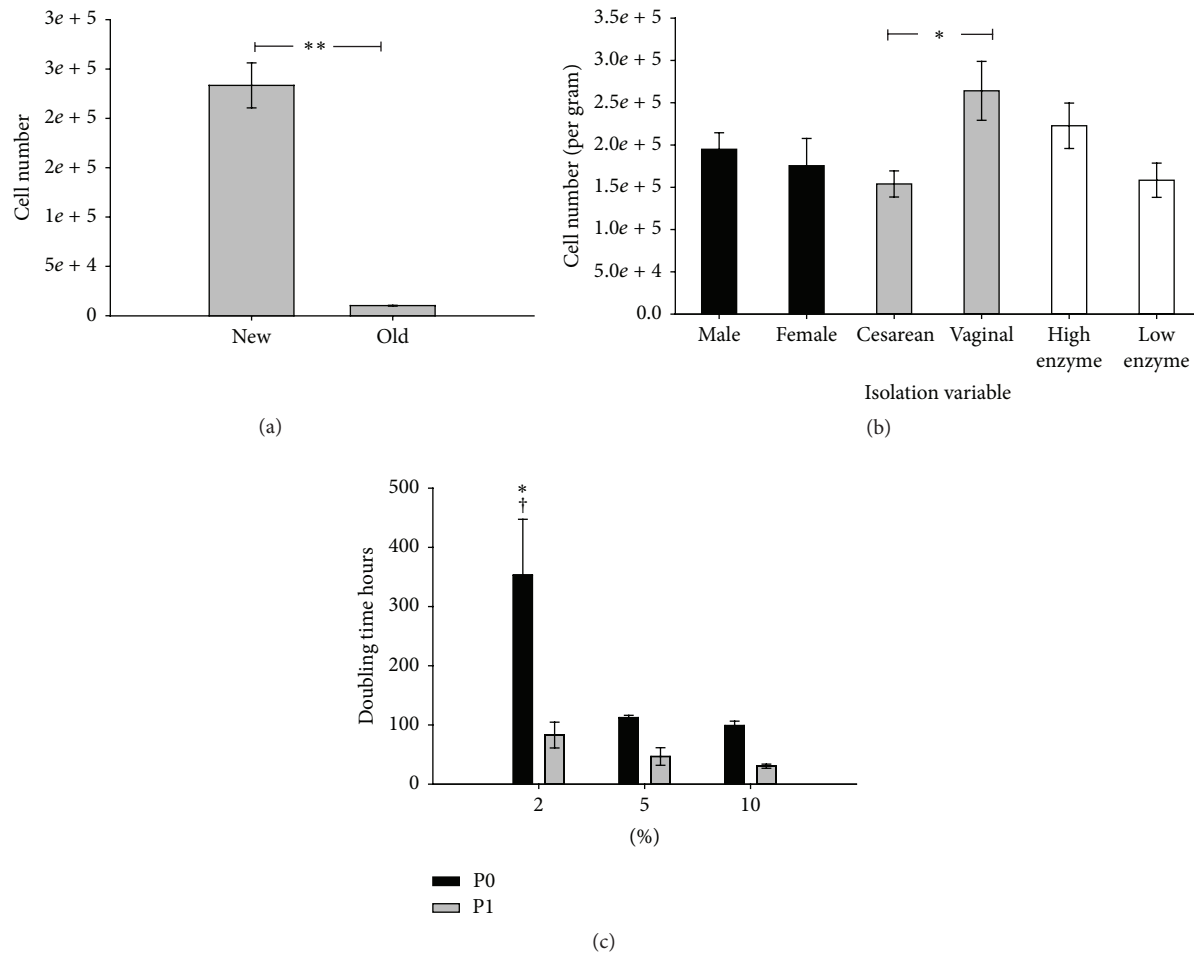


FIGURE 2: Effect of various experimental variables on UC-MSCs isolation. (a) The new methods average cell number per cm of umbilical cord isolated, compared to the old cell number isolated per cm (\*\* means  $p < 0.001$ ). (b) Comparing different experimental variables. Significant difference observed in Caesarean-section delivery versus vaginal delivery (\* means  $p < 0.05$ ). (c) Population doubling time for passage 0 (initial isolation) or passage 1 (first passage of expansion phase). \* represents  $p < 0.05$  for 2% hpl media compared to 5% and 10% media. † represents  $p < 0.05$  for the passages (P0 compared to the P1).

0 was considered part of the isolation of MSCs. UC-MSCs were expanded for passages 1–5 here. UC-MSCs were evaluated in 3 different growth conditions: DMEM supplemented with 2% HPL, 5% HPL, or 10% HPL. A two-way ANOVA (main effects HPL level and expansion over time) found a significant main effect (HPL concentration) on attachment and expansion. In *post hoc* testing, we found significantly more cells—about 30% more were obtained when cells were expanded in 10% HPL enriched DMEM medium compared to 5% HPL enriched medium ( $9.4 \times 10^5 \pm 6.2 \times 10^4$  cells per  $\text{cm}^2$  versus  $6.6 \times 10^5 \pm 3.8 \times 10^4$  for 5% HPL enriched medium (Figure 3(b)). Similarly, *post hoc* testing showed significantly shorter population doubling times when MSCs were expanded in 10% HPL ( $32.4 \pm 2.5$  hours), compared to  $40.7 \pm 4.1$  hours for 5% HPL and  $100.9 \pm 14.8$  hours for 2% HPL enriched medium (shown in Figure 3(c)). As shown in Figure 3(d), MSCs grown in 10% HPL enriched DMEM averaged 17% smaller than those grown in 2% HPL ( $14.7 \pm 0.2 \mu\text{m}$  versus  $17.6 \pm 0.4 \mu\text{m}$ ) and 10% smaller than cell grown in 5% HPL enriched medium (on average over

5 passages,  $16.1 \pm 0.3 \mu\text{m}$ ). The trends in MSC size across HPL medium conditions became noticeable after the second passage (Figure 3(e)). HPL medium enrichment affected the viability of the cells noted at passage (see Figure 3(c)). Subtle but significant differences were found in viability at passage between the three medium conditions: MSCs in expanded in DMEM supplemented with 10% HPL had higher viability than those grown in DMEM supplemented with 2% HPL ( $92.2 \pm 0.9\%$  versus  $84.9 \pm 1.7\%$ ) and 5% HPL supplemented medium had significantly greater viability than 2% HPL medium ( $90.4 \pm 0.9\%$ ; see Figure 3(c)).

The theoretical cell yield was calculated assuming the entire umbilical cord was isolated and expanded in each medium condition to passage 5. As shown in Figure 3(f), it was estimated that the total yield might exceed  $10^{12}$  MSCs (a trillion cells) at passage 5 for UC-MSCs expanded in 10% HPL supplemented medium and exceed  $10^{11}$  MSCs for UC-MSCs expanded in medium supplemented with 5% HPL (Figure 3(f)).



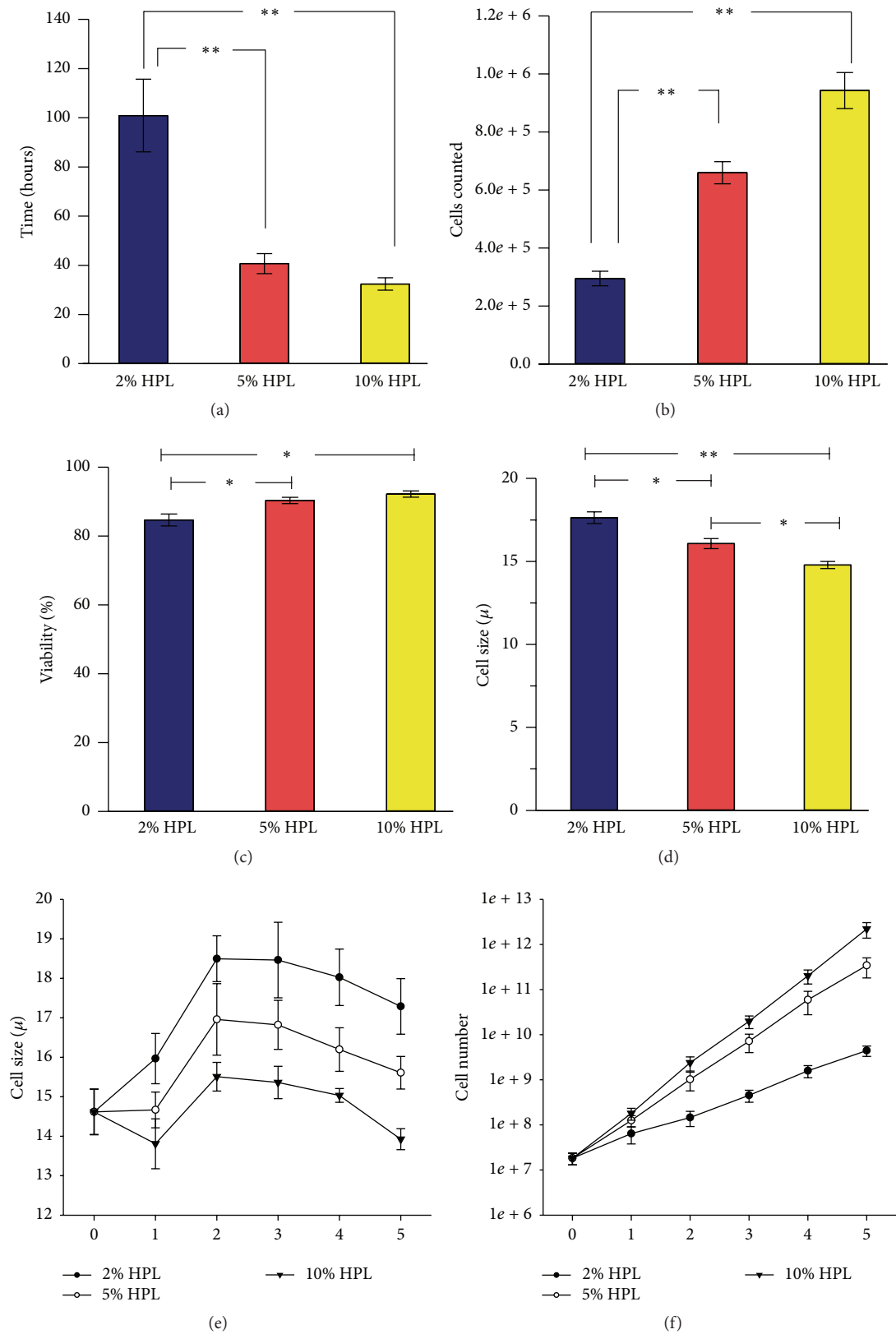


FIGURE 3: Effect of HPL concentration on expansion. (a–d) UC-MS (n = 6) expansion results combined for passages 1–5. (a) Population doubling times for the 3 media conditions. (b) Number of cells counted at passage for each media condition. (c) Cell viability at passage for each media condition. (d) The average size of the cell for each media condition at passage. (e) Cell size over 5 passages for each media condition. (f) The theoretical yield if an entire umbilical cord was isolated and grown to confluence at each passage. \* means  $p < 0.05$  and \*\* means  $p < 0.001$ .

**3.4. Evaluation of UC-MSc Characteristics.** Sex of the donor had no effect on number of MSCs isolated (Figure 2(b)), or the estimated number of MSCs obtained after expansion (data not shown). In contrast, a significant increase in the number of cells isolated was found for UC-MSCs isolated from normal vaginal delivery compared to those collected following Caesarean-section delivery (see Figure 2(b)).

**3.5. Colony Forming Unit-Fibroblast (CFU-F) Data is Presented as a Normalized Unit: Colony Forming Efficiency (CFE;  $CFE = \text{Number of Plated Cells Divided by Number of Colonies}$ ).** As shown in Figure 4(e), the concentration of HPL supplementation had no effect on CFE at 10 cells/cm<sup>2</sup> (100 cells per well of a 6-well plate) after 4 days of culture. In contrast, when plated at a density of 50 cells per cm<sup>2</sup> and 4 days of expansion in culture, 10% HPL supplementation resulted in an increased colony forming efficiency compared to 2 and 5% HPL: 2–4 MSCs were needed to form a colony when plated in medium supplemented with 10% HPL (Figure 4(e)). As seen in Figure 4(e) and as previously reported [26, 27], plating density affects colony forming efficiency and higher efficiency is found at lower plating density. Therefore we determine whether higher efficiency would be found at plating density below 10 cells/cm<sup>2</sup> after plating in HPL. The highest colony forming efficiency was found when MSCs were plated at 5 cells/cm<sup>2</sup> for 6 days (50 cells per well of a six-well plate); in medium supplemented with 10% HPL: on average one out of two MSCs formed a colony (see Supplemental Figure 1 in Supplementary Material available online at <http://dx.doi.org/10.1155/2016/6810980>).

**3.6. Differentiation.** MSCs isolated and expanded using the optimized method undergo differentiation to the three mesenchymal lineages, bone, cartilage, and fat after exposure to differentiation medium conditions for 3 weeks. Figure 4 shows MSCs differentiated to fat and chondrogenic and osteogenic lineages following closed isolation method and expansion to passage 5 in 10% HPL supplemented DMEM. Exposure to adipogenic differentiation medium resulted in formation of lipid droplets in MSCs that stained with Oil Red (Figure 4(a)). Exposure to osteogenic differentiation conditions resulted in calcium deposits formed within MSCs which stained with Alizarin Red S (Figure 4(b)). Cartilage-like tissue formation was observed in clusters of cells after exposure to differentiation medium as indicated by glycosaminoglycan staining by Safranin O for chondrogenic cells (Figure 4(c)).

**3.7. Flow Cytometry.** Flow cytometry was used to analyze the surface marker expression in 5 MSC lines following isolation using the closed processing protocol and expansion using the 10% HPL supplemented DMEM for 5 passages. High expression (>95% positive) for surface markers CD73, CD90, CD105, and CD44 was observed (Figure 5 for representative results, Supplemental Table 1 for all flow cytometry data). Low surface marker expression (<0.5% positive) was observed for CD34, CD45, CD11b, CD19, and HLA-DRT (Supplemental Table 1). To evaluate the effect of freezing and thawing

MSCs on surface marker expression, four MSCs lines were evaluated before and after a freeze/thaw cycle. No significant differences were found in surface marker expression between frozen/thawed and never frozen MSCs in surface marker expression (Supplemental Table 2).

## 4. Discussion

The acceleration of stem cell and regenerative medicine clinical trials, and MSC trials in particular, has produced a renewed effort to standardize production and characterization of MSCs in GMP-compliant SOPs. Umbilical cord MSCs have a number of advantages which suggest that they might be an important source for allogeneic MSCs for cellular therapy, and, as indicated by trends in MSC clinical trials worldwide, this MSC source is a needed one.

In order to develop an SOP for GMP production of UC-MSCs, we identified limitations in our previously described method for UC-MSc isolation and expansion that represented barriers for GMP production. First, our previous isolation method required a lengthy dissection step and the opening of the umbilical cord and manually removing the vessels prior to mincing the Wharton's jelly was time consuming and increased contamination risk. Here, we sought to reduce processing time and reduce contamination risks. We reasoned that a standardized method for liberating MSCs from the Wharton's jelly may produce a more homogenous product. Second, the previously described UC-MSc medium, which was originally described by Catherine Verfaillie's lab for expansion of MAPCs, is complicated with more than 10 components and it contained 2% FBS, a xenogeneic product [28]. We sought to identify a simplified medium that could be free of xenogeneic materials and contain fewer components. We tested human platelet lysate (HPL) enriched medium. Previous work indicated that HPL could be produced in a GMP-compliant format and has been reported to produce good expansion of MSCs [29–31]. Here, we found that 5 or 10% HPL enrichment vastly improved MSC expansion in the P0 (initial isolation). Furthermore, we found robust expansion over passages 1–5. Therefore, use of HPL-enriched medium eliminated two barriers to GMP-compliant manufacturing of UC-MSCs. However, using a pooled human blood product is not without certain risks, they have been somewhat mitigated (discussed below). Due to the sample to sample variability, pooling of platelet lysate is essential to produce a uniform product [32]. For example, human pathogens that escape screening by the providers may contaminate HPL samples. One possible way to address this risk would be to inactivate pathogens in HPL [33]. We did not inactivate pathogens in our pooled HPL, but the repeated freeze-thaw process followed by the filtration through a 0.2  $\mu$ m filter should remove all potential bacteria and parasites. While gamma irradiation is something that may be considered to lower viral risk, the blood products used were obtained from a blood bank for clinical use and thus had met all existing blood screening safety measures.

Here, 1 cm sections of cord were used to optimize the protocol. The one cm length sections of umbilical cord provided enough cells for isolation and expansion, and many

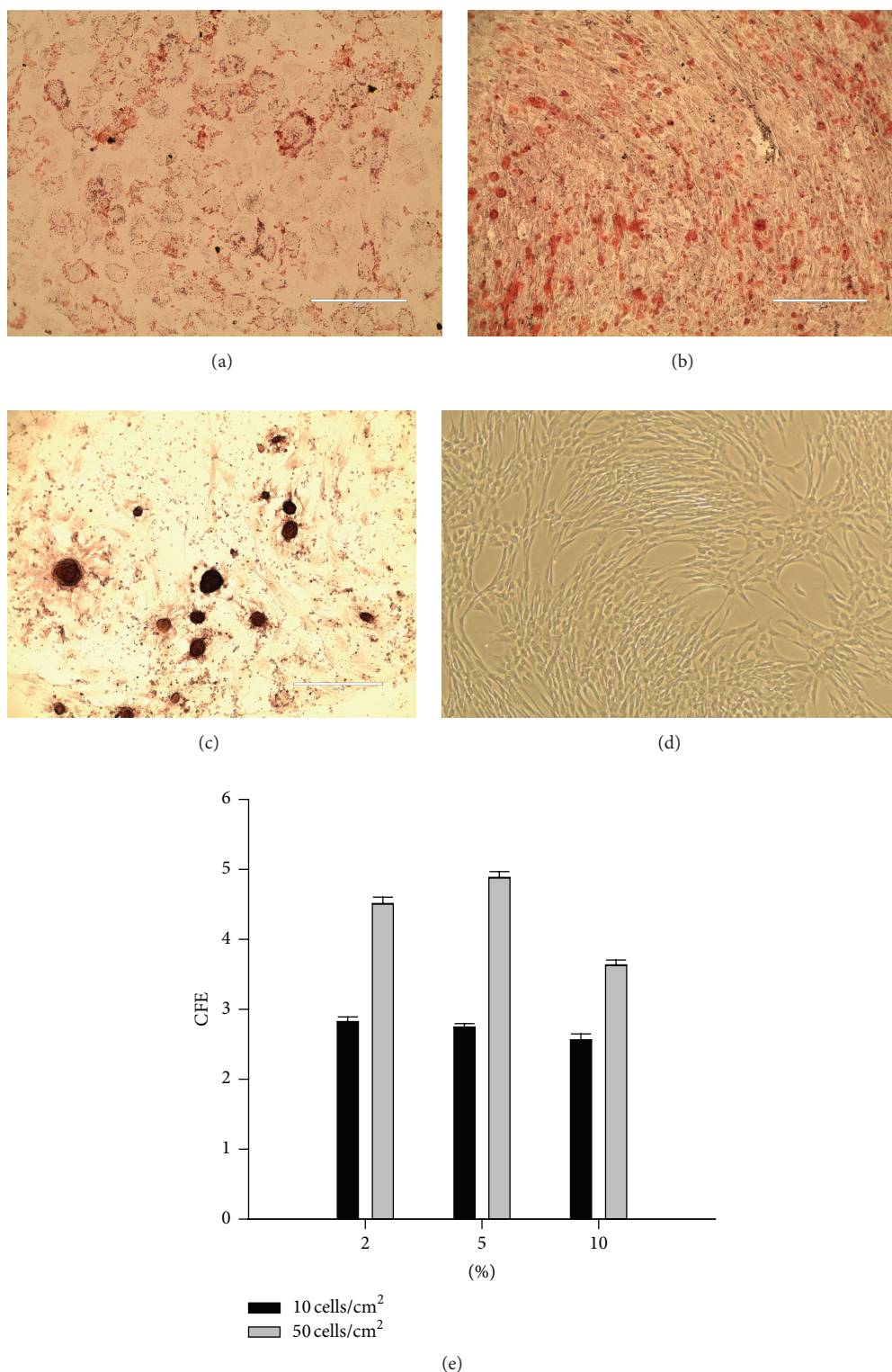


FIGURE 4: Differentiation and colony forming unit fibroblast (CFU-F) results for the characterization of UC-MSCs. (a) After adipogenic differentiation, MSCs were stained with Oil Red which binds to lipid droplets (20x objective magnification; scale bar = 200 micrometers). (b) After osteogenic differentiation, MSCs were stained with Alizarin Red S which binds to calcium deposits. (c) After chondrogenic differentiation, MSCs stained with Safranin O which binds to glycosaminoglycans in cartilage ((b) and (c) at 10x objective magnification; scale bar = 400 micrometers). (d) UC-MSCs in normal growth conditions (control) phase contrast micrograph at 4x objective magnification. (e) CFU-F efficiency was calculated by dividing the number of plated cells by the number of CFU-F colonies observed. Panel (e) shows colony forming efficiency versus human pooled platelet lysate (HPL) concentration in medium (2, 5, or 10% HPL) after plating at 5 (black bars) or 10 (gray bars) cells per cm<sup>2</sup> and 4 days in culture.

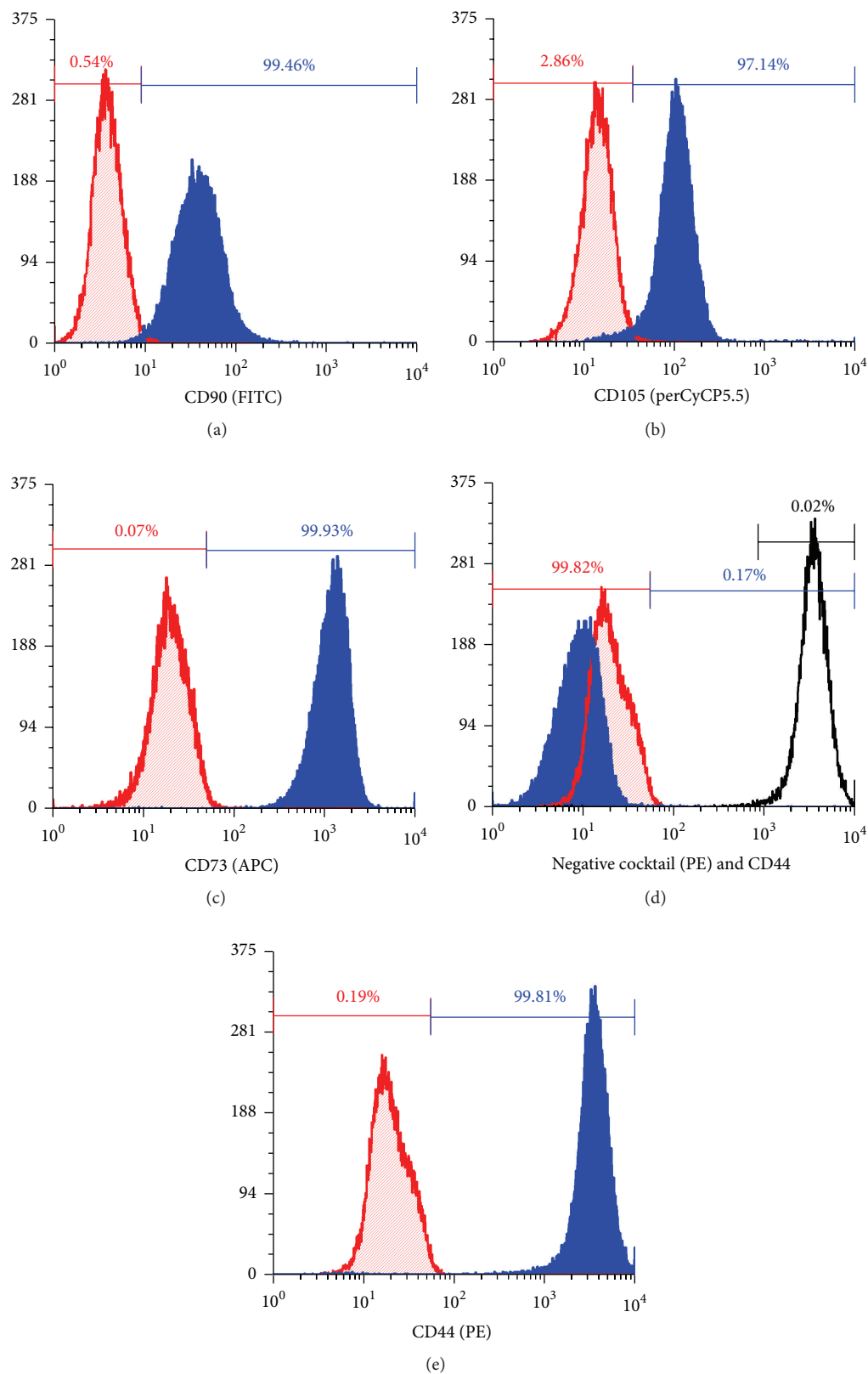


FIGURE 5: Histograms of flow cytometry; blue solid filled overlay represents the test sample; red diagonal line filled overlay represents the isotype control. For each histogram the negative gate (red bar) was set for inclusion of 99% of the isotype. Percentages shown in histograms are for the test samples. (a–c) All are markers in the positive cocktail, CD90, CD105, and CD73. The positive gate percentages shown in blue for each sample. (d) The negative cocktail, with CD44 included as a positive control (unfilled overlay) positive percentage in black. (e) CD44 marker included outside of the positive cocktail.



technical replicates were available from one cord which allows multiple experimental variables to be examined in each cord (the biological variable). We assumed that a randomly selected, one cm length of cord would adequately represent the umbilical cord (e.g., that cellular distribution and umbilical cord extracellular matrix are homogenous). This assumption was not validated by us, nor do we know of any investigation that supports or denies this assumption. Umbilical cords display tremendous biological variation in density (weight per unit length), diameter, and physical mechanical properties perhaps due to the amount of extracellular matrix surrounding the vessels (see Table 1). The gram per cm measurements vary within each technical replicate from a single cord and between different umbilical cords, too. This indicates the importance for multiple biological and technical replicates when performing optimization testing using umbilical cords. The number of cells varied considerably between each umbilical cord as did the density and amount of extracellular matrix. Thus the biological variation limits the ability to manufacture a standard cellular therapy product. For example, does the physiology of MSCs vary between umbilical cords and how can we optimize the clinical effect of MSCs? We have assumed that the cells isolated after an initial passage are similar in physiology, but this assumption will require more assaying to confirm.

Several protocols for isolation of MSCs from different parts of the umbilical cord have been published [26, 34, 35]. These protocols require dissection of different portions of the umbilical cord and a variety of methods to enrich MSCs from the primary isolation population. This contributes to variation in the number of cells in the primary isolation and their ability to undergo expansion in culture. We did not observe frank differences in the population of MSCs isolated following their extraction from Wharton's jelly versus those isolates following disruption of the entire 1 cm cord fragment. We found that extraction of the entire 1 cm length using the methods outlined here gave a >10-fold increase in the number of input cells for the primary culture. We attribute the reduced manipulation of the tissues (elaborate dissection negatively affects the attachment and expansion) and the more efficient removal of red blood cell contamination (blood negatively affects the viability, attachment, and expansion of MSCs) to the improved extraction and expansion efficiency.

Previously we used "cord length" measurement for comparisons of yield between cords. Here, we tracked both length and weight to determine whether either proved to be a better predictor of cell yield in initial isolation. The variation between umbilical cords for both length and weight is represented in Table 1. As seen in Table 1, weight was a more reliable measurement compared to cord length. Additional work is needed to determine differences between the predicted total cell yield from an umbilical cord and the estimated value. We have not processed cells from an entire umbilical cord and therefore cannot confirm the accuracy of these estimates. Our current method is readily scaled up, and so this information is forthcoming.

The increase in cell numbers from the optimized protocol may be attributed to the faster processing and reduced dissection when isolating the MSCs. By not removing the blood

vessels, the optimized method is a significant departure from our previously described method. Therefore, this casts into doubt whether the same cell population has been isolated, and whether the MSCs obtained using the optimized methods are similar or different from those obtained using the previous methods. As mentioned in Section 1, several different methods for obtaining MSCs from the umbilical cord have been described, and it is unclear whether each isolates the same cells. Our data does not directly address this question, but we demonstrate here that following evaluation of 5 umbilical cord MSC isolates; the cells isolated from the optimized methods conform to ISCT criteria for MSCs [4].

As far as we know this paper is the first to demonstrate a difference between MSC isolation efficiency from umbilical cords derived from vaginal births versus Cesarean-section births. Vaginal birth umbilical cords had more cells per after isolation by approximately 41% (Figure 2(b)). Prior to observation, we preferred to use Cesarean-section umbilical cords for MSC isolation because we assumed that surgical collection would have a reduced contamination risk compared to cord collected following the passage through the birth canal. During this study we found no differences in contamination from either vaginal birth or Cesarean-section umbilical cords. Similar to our observations about MSCs from vaginal versus Cesarean-section cords, the volume of umbilical cord blood collected is decreased by vaginal birth over Cesarean-section birth [36, 37]. We did not see a sex difference between the number of cells isolated or MSC expansion rate or number. Enzymatic digestion using a high concentration of digestive enzymes tended to have higher yield at isolation (Figure 2(b)). Visually, higher concentration of enzyme samples appeared to have less debris when compared at initial plating compared to lower enzyme concentration.

After the initial plating of cells during the isolation protocol, there is a delay in cell attachment. Attachment to the substrate is a defining characteristic of MSCs and appears to be necessary for MSCs expansion. We noted that after the isolation of MSCs, in passages 1–5, MSCs attach and begin to expand within 24 hours of plating. In contrast, the time to reach the confluence for the isolation and initial passage is significantly impacted by delays in attachment. Here, we included the P0 data with the isolation of MSCs and considered passages 1 through 5 for the expansion phase of MSC characterization. We noticed a trend that when there was a higher viability at the initial isolation, the cells attached better and expanded more rapidly. In our prior work, cell viability was not recorded at the initial isolation. Here, the use of the Nexcelom and ViaStain AOPI viability assay provided a quantitative method and gave more consistent results than trypan blue and manual counting using the haemocytometer (which is how we counted cells, previously). Automated cell counting lends itself to optimization and producing SOPs.

When considering the production of a public bank of cord samples, freezing the primary isolates at P0 → P1 is likely to be a necessity. Others have reported this affects cells surface marker expression or viability [38]. For that reason, we evaluated surface marker expression in never frozen cells and in cells subjected to a freeze/thaw cycle. The flow

cytometry analysis did not show a difference in surface marker expression between fresh cells (e.g., those never frozen) and cells frozen and thawed cells for four umbilical cord MSCs lines. Future testing is needed to confirm that these results stand up with a larger sample size. Clinical trials will require the freezing of cells for use, the use of fresh cells in clinical trials is not feasible when considering the rigorous quality control and release testing that must be done to determine if these cells meet the standards for clinical use.

Here, human platelet lysate enriched media at three different concentrations (2%, 5%, and 10%) was used to analyze the effect on the initial isolation (P0) and growth of the MSCs for passages 1–5. We evaluated MSCs through passage 5 to characterize expansion potential. We observed that P0 to P1 expansion exhibited the highest amount of variation in growth rate (see Figures 2(c) and 3(a)). Results from six umbilical cords did not show a difference between passages 1–5 for population doubling time, number of cells at passage, and viability at passage (data not shown). However, the three media conditions did affect these variables. Enrichment with 2% HPL enriched medium was significantly different than 5% and 10% HPL enriched media for population doubling, cell size, cell numbers, and viability. Enrichment with 2% HPL had slower population doubling, fewer cells at passage, larger cells, and a lower percentage of viable cells at passage. We observed a trend associated with better results for these measurements as HPL enrichment in the medium increased. For this reason we chose 10% as the new standard media condition to be used to grow the UC-MSCs. Cell size for the UC-MSCs was a variable we did not expect to vary significantly between the different media conditions, but we observed a significant difference in cell size with higher HPL concentration. We noticed a trend for cell size to initially increase after the first passage and then decrease over subsequent passages in all media conditions (Figures 3(d)–3(e)). We cannot explain this observation. Further work is needed to assess whether cell size is affected by passage, since we have previously observed that senescent cells are larger, and because we would expect an increase in cellular senescence with passage. If the contrary is true, for example, the fact that more rapidly dividing cells are smaller, then the cell size data could support our conclusion that 10% HPL is the optimal growth condition for the UC-MSCs. Previous work had indicated that smaller MSCs with a rapidly dividing phenotype could be identified by plating at a density of 3 cells per  $\text{cm}^2$  [39]. Here, we did not evaluate the effect of plating density on proliferation. Future work should evaluate the interaction between plating density and 10% HPL media to optimize manufacturing efficiency.

MSC characterization was done by assessing cell surface markers with flow cytometry, CFU-F, and differentiation capacity. All five cell lines we analyzed with flow cytometry had high levels of the surface markers known to be associated with MSCs. The high percentage of positive cells (>95%) is comparable to the previously published method [24]. These results suggest a homogenous cell population was isolated even though the blood vessels were not removed for the isolation step. Differentiation ability was assessed in the same five cell lines and all display trilineage differentiation capacity.

The capacity for adipogenic differentiation was analyzed by Oil Red O staining for lipid droplet accumulation within the differentiated cells cytoplasm. Analysis showed multiple lipid droplets forming within a large number of the cells (Figure 4(a)). Cell death did occur during the time to differentiate, leading to space between the adipogenic cells in the figure. Osteogenic differentiation was stained with Alizarin Red S to analyze calcium deposit formation. Staining was observed in calcium deposits on the cells and within the cells as seen in Figure 4(b). Chondrogenic differentiated cells were stained with Safranin O to assess if cartilaginous associated with glycosaminoglycan. This differentiation yielded circular colonies, often remaining adhered to the plate and they robustly stained for Safranin O. Typically histological sections of microcolonies are used to assess chondrogenic lineage differentiation. Our results indicate this is not necessary when small colonies of cell remain adherent (Figure 4(c)). Although the results are not quantified, the quality of the staining and duplication between multiple lines provides good evidence that MSCs isolated and expanded by the new method have robust trilineage differentiation potential.

Colony forming unit fibroblast (CFU-F) efficiency analyzed self-renewal potential of UC-MSCs. Compared to previous research for UC-MSCs expanded in 21% oxygen, fewer cells were needed to form a colony using the method described here, suggesting a higher colony forming efficiency [27]. We considered the 10 cells per  $\text{cm}^2$  a more reliable measure for the effect of HPL concentration due to difficulty counting cells at 50 cells per  $\text{cm}^2$ . The fast growth rate for the 10% HPL enriched medium made our previous CFU-F protocols unreliable because the plates grew too fast. We tested growth conditions for measuring colony forming efficiency by analyzing days from plating versus colony counts. We found the number of cells to form colonies decreased with each day of growth; the exception was 50 cells per  $\text{cm}^2$  which increased. The highest CFU-F efficiency was for 5 cells per  $\text{cm}^2$  cells grown for 6 days. We determined using both 10 and 50 cells per  $\text{cm}^2$  yield consistent data for CFU-F. The self-renewal data (colony forming efficiency) is important when estimating the expansion potential of a MSC line. Higher CFU-F efficiencies are associated with MSC lines displaying a more robust growth potential. Determining the method for analyzing CFU-Fs in these fast growing cells allows for analysis of growth potential for future research using UC-MSCs.

Here we provide a new, optimized method to isolate and expand UC-MSCs. When compared to our previous method, an increase in total MSC yield at the initial isolation of more than 10 times was obtained, and less time is needed to isolate MSCs from the umbilical cord. Additionally, this method reduces the overall expansion by reducing the amount of population doubling needed to meet our production target of 2–10 billion cells per batch. The method uses closed system for initial isolation with minimal dissection of the cord and, thus, reduces contamination risk, while simultaneously reducing processing time. The method uses a simplified (5 component), xenogen-free medium that can be upgraded to GMP-compliant components for scale-up.

Characterization of MSCs produced using this optimized processing protocol and simplified medium included *in vitro* expansion, colony forming efficiency, and trilineage differentiation to osteogenic, chondrogenic, and adipogenic lineages, and surface marker expression by flow cytometry indicates that MSCs were produced by this method. Further work is needed to confirm that MSCs isolated and expanded using this method will perform *in vivo* as a cellular therapy. We are developing an *in vivo* model to test the potency of MSCs which may serve as suitable assay to compare the potency of various manipulations such as “priming” or licensing of MSCs. Taken together, this work will speed clinical translation of UC-MSCs by providing the basis of chemistry and manufacturing controls (CMC) portion of an investigation of new drug application (IND).

## 5. Conclusion

The methods we developed for isolation and expansion of UC-MSCs address some challenges to translation to clinical use. We report an increased MSC yield for vaginal births compared to Caesarean-section births. The new isolation method provides the necessary cell yield for banking and uses a closed system that can be easily scaled up and expansion media supplemented with 10% HPL had the best growth rate. These results provide improvements which may support GMP manufacturing of UC-MSCs. To complete the validation of this new method, functional testing for immune modulation or regenerative potential testing is needed.

## Conflict of Interests

The authors declare that there is no conflict of interests regarding the publication of this paper.

## Acknowledgments

The authors would like to thank Dr. Suzanne M. Bennett, MD, of the Women's Health group and the nurses and staff at Via Christie Hospital OB ward for assistance with the collection of umbilical cords. Lab personnel Dr. Hong He, Michael Zuniga, Jake Jimenez, Jenna Klug, Shoshanna Levshin, “Daniel” Thun Quach, and Phuoc Van Bui are thanked for their assistance.

## References

- [1] L. Sensebé, M. Gadelorge, and S. Fleury-Cappellesso, “Production of mesenchymal stromal/stem cells according to good manufacturing practices: a review,” *Stem Cell Research and Therapy*, vol. 4, no. 3, article 66, 2013.
- [2] M. Mendicino, A. M. Bailey, K. Wonnacott, R. K. Puri, and S. R. Bauer, “MSC-based product characterization for clinical trials: an FDA perspective,” *Cell Stem Cell*, vol. 14, no. 2, pp. 141–145, 2014.
- [3] M. Krampera, J. Galipeau, Y. Shi, K. Tarte, and L. Sensebe, “Immunological characterization of multipotent mesenchymal stromal cells—the International Society for Cellular Therapy (ISCT) working proposal,” *Cytotherapy*, vol. 15, no. 9, pp. 1054–1061, 2013.
- [4] M. Dominici, K. Le Blanc, I. Mueller et al., “Minimal criteria for defining multipotent mesenchymal stromal cells. The International Society for Cellular Therapy position statement,” *Cytotherapy*, vol. 8, no. 4, pp. 315–317, 2006.
- [5] O. Ringdén, T. Erkers, S. Nava et al., “Fetal membrane cells for treatment of steroid-refractory acute graft-versus-host disease,” *STEM CELLS*, vol. 31, no. 3, pp. 592–601, 2013.
- [6] M. Duijvestein, A. C. W. Vos, H. Roelofs et al., “Autologous bone marrow-derived mesenchymal stromal cell treatment for refractory luminal Crohn's disease: results of a phase I study,” *Gut*, vol. 59, no. 12, pp. 1662–1669, 2010.
- [7] J. P. McGuirk, J. R. Smith, C. L. Divine, M. Zuniga, and M. L. Weiss, “Wharton's Jelly-derived mesenchymal stromal cells as a promising cellular therapeutic strategy for the management of Graft-versus-host disease,” *Pharmaceuticals*, vol. 8, no. 2, pp. 196–220, 2015.
- [8] ClinicalTrials.gov, “Search of: mesenchymal stem cells,” ClinicalTrials.gov, 2015, <https://clinicaltrials.gov/ct2/results?term=mesenchymal+stem+cells>.
- [9] A. Bersenev, “Cell therapy clinical trials—2014 report,” Cell Trials Blog, 2015, <http://celltrials.info/2015/01/22/2014-report/>.
- [10] D. Baksh, R. Yao, and R. S. Tuan, “Comparison of proliferative and multilineage differentiation potential of human mesenchymal stem cells derived from umbilical cord and bone marrow,” *STEM CELLS*, vol. 25, no. 6, pp. 1384–1392, 2007.
- [11] R. N. Barcia, J. M. Santos, M. Filipe et al., “What makes umbilical cord tissue-derived mesenchymal stromal cells superior immunomodulators when compared to bone marrow derived mesenchymal stromal cells?” *Stem Cells International*, vol. 2015, Article ID 583984, 14 pages, 2015.
- [12] L. Wang, I. Tran, K. Seshareddy, M. L. Weiss, and M. S. Detamore, “A comparison of human bone marrow-derived mesenchymal stem cells and human umbilical cord-derived mesenchymal stromal cells for cartilage tissue engineering,” *Tissue Engineering—Part A*, vol. 15, no. 8, pp. 2259–2266, 2009.
- [13] K. H. Yoo, I. K. Jang, M. W. Lee et al., “Comparison of immunomodulatory properties of mesenchymal stem cells derived from adult human tissues,” *Cellular Immunology*, vol. 259, no. 2, pp. 150–156, 2009.
- [14] H. Zhang, S. Fazel, H. Tian et al., “Increasing donor age adversely impacts beneficial effects of bone marrow but not smooth muscle myocardial cell therapy,” *American Journal of Physiology—Heart and Circulatory Physiology*, vol. 289, no. 5, pp. H2089–H2096, 2005.
- [15] Z.-Y. Zhang, S.-H. Teoh, M. S. K. Chong et al., “Superior osteogenic capacity for bone tissue engineering of fetal compared with perinatal and adult mesenchymal stem cells,” *STEM CELLS*, vol. 27, no. 1, pp. 126–137, 2009.
- [16] T. Deuse, M. Stubbendorff, K. Tang-Quan et al., “Immunogenicity and immunomodulatory properties of umbilical cord lining mesenchymal stem cells,” *Cell Transplantation*, vol. 20, no. 5, pp. 655–667, 2011.
- [17] M. L. Weiss, C. Anderson, S. Medicetty et al., “Immune properties of human umbilical cord Wharton's jelly-derived cells,” *Stem Cells*, vol. 26, no. 11, pp. 2865–2874, 2008.
- [18] M. Zeddou, A. Briquet, B. Relic et al., “The umbilical cord matrix is a better source of mesenchymal stem cells (MSC) than the umbilical cord blood,” *Cell Biology International*, vol. 34, no. 7, pp. 693–701, 2010.



- [19] Y. Wang, Z.-B. Han, Y.-P. Song, and Z. C. Han, "Safety of mesenchymal stem cells for clinical application," *Stem Cells International*, vol. 2012, Article ID 652034, 4 pages, 2012.
- [20] R. R. Sharma, K. Pollock, A. Hubel, and D. McKenna, "Mesenchymal stem or stromal cells: a review of clinical applications and manufacturing practices," *Transfusion*, vol. 54, no. 5, pp. 1418–1437, 2014.
- [21] A. Bongso and C.-Y. Fong, "The therapeutic potential, challenges and future clinical directions of stem cells from the Wharton's jelly of the human umbilical cord," *Stem Cell Reviews and Reports*, vol. 9, no. 2, pp. 226–240, 2013.
- [22] A. Marmotti, S. Mattia, M. Bruzzone et al., "Minced umbilical cord fragments as a source of cells for orthopaedic tissue engineering: an in vitro study," *Stem Cells International*, vol. 2012, Article ID 326813, 13 pages, 2012.
- [23] Y.-F. Han, R. Tao, T.-J. Sun, J.-K. Chai, G. Xu, and J. Liu, "Optimization of human umbilical cord mesenchymal stem cell isolation and culture methods," *Cytotechnology*, vol. 65, no. 5, pp. 819–827, 2013.
- [24] K. Seshareddy, D. Troyer, and M. L. Weiss, "Method to isolate mesenchymal-like cells from Wharton's Jelly of umbilical cord," *Methods in Cell Biology*, vol. 86, pp. 101–119, 2008.
- [25] Y. A. Romanov, V. A. Svintsitskaya, and V. N. Smirnov, "Searching for alternative sources of postnatal human mesenchymal stem cells: candidate MSC-like cells from umbilical cord," *STEM CELLS*, vol. 21, no. 1, pp. 105–110, 2003.
- [26] R. Sarugaser, D. Lickorish, D. Baksh, M. M. Hosseini, and J. E. Davies, "Human umbilical cord perivascular (HUCPV) cells: a source of mesenchymal progenitors," *STEM CELLS*, vol. 23, no. 2, pp. 220–229, 2005.
- [27] Y. López, K. Seshareddy, E. Trevino, J. Cox, and M. L. Weiss, "Evaluating the impact of oxygen concentration and plating density on human wharton's jelly-derived mesenchymal stromal cells," *Open Tissue Engineering and Regenerative Medicine Journal*, vol. 4, no. 1, pp. 82–94, 2011.
- [28] M. Reyes, A. Dudek, B. Jahagirdar, L. Koodie, P. H. Marker, and C. M. Verfaillie, "Origin of endothelial progenitors in human postnatal bone marrow," *Journal of Clinical Investigation*, vol. 109, no. 3, pp. 337–346, 2002.
- [29] S. Castiglia, K. Mareschi, L. Labanca et al., "Inactivated human platelet lysate with psoralen: a new perspective for mesenchymal stromal cell production in good manufacturing practice conditions," *Cytotherapy*, vol. 16, no. 6, pp. 750–763, 2014.
- [30] H. Hemeda, B. Giebel, and W. Wagner, "Evaluation of human platelet lysate versus fetal bovine serum for culture of mesenchymal stromal cells," *Cytotherapy*, vol. 16, no. 2, pp. 170–180, 2014.
- [31] T. Burnouf, D. Strunk, M. B. Koh, and K. Schallmoser, "Human platelet lysate: replacing fetal bovine serum as a gold standard for human cell propagation?" *Biomaterials*, vol. 76, pp. 371–387, 2016.
- [32] K. Schallmoser, E. Rohde, C. Bartmann, A. C. Obenauf, A. Reinisch, and D. Strunk, "Platelet-derived growth factors for GMP-compliant propagation of mesenchymal stromal cells," *Bio-Medical Materials and Engineering*, vol. 19, no. 4-5, pp. 271–276, 2009.
- [33] R. Fazzina, P. Iudicone, A. Mariotti et al., "Culture of human cell lines by a pathogen-inactivated human platelet lysate," *Cytotechnology*, 2015.
- [34] K. E. Mitchell, M. L. Weiss, B. M. Mitchell et al., "Matrix cells from Wharton's jelly form neurons and glia," *STEM CELLS*, vol. 21, no. 1, pp. 50–60, 2003.
- [35] D. L. Troyer and M. L. Weiss, "Concise review: Wharton's Jelly-derived cells are a primitive stromal cell population," *STEM CELLS*, vol. 26, no. 3, pp. 591–599, 2008.
- [36] P. Solves, R. Moraga, E. Saucedo et al., "Comparison between two strategies for umbilical cord blood collection," *Bone Marrow Transplantation*, vol. 31, no. 4, pp. 269–273, 2003.
- [37] E. J. Noh, Y. H. Kim, M. K. Cho, J. W. Kim, Y. J. Byun, and T.-B. Song, "Comparison of oxidative stress markers in umbilical cord blood after vaginal and cesarean delivery," *Obstetrics & Gynecology Science*, vol. 57, no. 2, pp. 109–114, 2014.
- [38] M. François, I. B. Copland, S. Yuan, R. Romieu-Mourez, E. K. Waller, and J. Galipeau, "Cryopreserved mesenchymal stromal cells display impaired immunosuppressive properties as a result of heat-shock response and impaired interferon- $\gamma$  licensing," *Cytotherapy*, vol. 14, no. 2, pp. 147–152, 2012.
- [39] D. J. Prockop, I. Sekiya, and D. C. Colter, "Isolation and characterization of rapidly self-renewing stem cells from cultures of human marrow stromal cells," *Cytotherapy*, vol. 3, no. 5, pp. 393–396, 2001.



## Research Article

# Evaluation of Tissue Homogenization to Support the Generation of GMP-Compliant Mesenchymal Stromal Cells from the Umbilical Cord

Ryan J. Emmett,<sup>1</sup> Aparna Kaul,<sup>1</sup> Aleksandar Babic,<sup>1,2</sup> Vicki Geiler,<sup>1</sup> Donna Regan,<sup>1</sup> Gilad Gross,<sup>3,4</sup> and Salem Akel<sup>1,2</sup>

<sup>1</sup>St. Louis Cord Blood Bank/Cellular Therapy Laboratory, SSM Health Cardinal Glennon Children's Hospital, St. Louis, MO 63110, USA

<sup>2</sup>Department of Pediatrics, Saint Louis University School of Medicine, St. Louis, MO 63104, USA

<sup>3</sup>SSM Health St. Mary's Hospital, St. Louis, MO 63117, USA

<sup>4</sup>Department of Obstetrics, Gynecology and Women's Health, Saint Louis University School of Medicine, St. Louis, MO 63104, USA

Correspondence should be addressed to Salem Akel; [sakel@slcbb.org](mailto:sakel@slcbb.org)

Received 23 September 2015; Revised 2 December 2015; Accepted 14 December 2015

Academic Editor: Peter Czermak

Copyright © 2016 Ryan J. Emmett et al. This is an open access article distributed under the Creative Commons Attribution License, which permits unrestricted use, distribution, and reproduction in any medium, provided the original work is properly cited.

Recent studies have demonstrated that the umbilical cord (UC) is an excellent source of mesenchymal stromal cells (MSCs). However, current protocols for extracting and culturing UC-MSCs do not meet current good manufacturing practice (cGMP) standards, in part due to the use of xenogeneic reagents. To support the development of a cGMP-compliant method, we have examined an enzyme-free isolation method utilizing tissue homogenization (t-H) followed by culture in human platelet lysate (PL) supplemented media. The yield and viability of cells after t-H were comparable to those obtained after collagenase digestion (Col-D). Importantly, kinetic analysis of cultured cells showed logarithmic growth over 10 tested passages, although the rate of cell division was lower for t-H as compared to Col-D. This slower growth of t-H-derived cells was also reflected in their longer population doubling time. Interestingly, there was no difference in the expression of mesenchymal markers and trilineage differentiation potential of cells generated using either method. Finally, t-H-derived cells had greater clonogenic potential compared to Col-D/FBS but not Col-D/PL and were able to maintain CFU-F capacity through P7. This bench scale study demonstrates the possibility of generating therapeutic doses of good quality UC-MSCs within a reasonable length of time using t-H and PL.

## 1. Introduction

A number of studies have highlighted the potential of mesenchymal stromal cells (MSCs) in tissue regeneration, immune regulation, and potentiation of ex vivo expansion of hematopoietic stem cells (HSCs) [1–4]. Clinical applications of MSCs are mainly attributed to their low immunogenicity and ability to home to sites of pathology, differentiate into various cell types, and secrete multiple bioactive molecules capable of modulating growth of other cells like HSCs and immune cells. Traditionally, MSCs have been harvested from adult sources including bone marrow (BM) and adipose tissue. Because of the invasive cell harvest procedure and the inverse relationship between adult age and MSC growth

potential [5, 6], there is a pressing need for developing alternative sources for these cells. In this regard, perinatal tissues, especially placenta and umbilical cord (UC), have become attractive sources of MSCs.

MSCs can be successfully isolated from all UC samples. In vitro expanded UC-MSCs exhibit cell surface markers, differentiation capability, and immune regulatory properties comparable to those of BM-MSCs [7–9], with the added advantage of having a higher proliferation/expansion potential (greater numbers of passages to senescence) [8–10]. Such features reflect the relatively primitive nature of the UC-MSCs compared to their adult counterpart. Additionally, UC-derived cells have not been exposed to viruses and toxins

and may contain less genetic abnormalities than adult tissue-derived MSCs.

UC-MSCs have been identified and isolated from various anatomic compartments especially from UC perivascular regions and Wharton's jelly (WJ) matrix [8, 11, 12]. In the absence of a discernible demarcation between MSC regions within the UC, it is difficult to establish the region-specificity of isolated cells. Although few relevant studies have demonstrated variation in the differentiation potential between MSCs isolated from different UC regions, no significant differences were reported in growth kinetics and phenotype amongst different isolates [11]. Due to the absence of any clear cut regional delineation, many investigators have chosen to obtain cells from the entire length of the UC, which would offer better cell yield for further manipulation.

Basic methods for the generation of UC-MSCs include tissue explants or collagenase-based enzymatic tissue digestion (Col-D) followed by cell culture in the presence of fetal bovine serum (FBS) to support adhesion and expansion of MSCs. Explant cultures allow migration of cells out of tissue and growth of adherent cells which reliably produce MSCs; however, initial culture takes much longer to reach confluence as compared to Col-D, and explant growth may not represent cells from all regions of the cord.

To generate UC-MSCs for potential clinical purposes, a current good manufacturing practices- (cGMP-) compliant production method needs to be developed which can be reliably performed in the absence of enzymes and FBS. The use of enzymes and FBS may complicate the cGMP process development depending on the source of the enzyme and batch-to-batch variations associated with both bioproducts [13]. While some alternatives to FBS have now been developed (e.g., human serum, platelet lysate (PL), and chemically defined media supplements), [14] there is a lack of nonenzymatic methods for cellular extraction. In this study, an enzyme-free, simple cell isolation method consisting of rapid UC tissue homogenization (t-H) using a GentleMACS Dissociator (Miltenyi Biotec) was evaluated. Additionally, growth of isolated cells and generation of MSCs were assessed in the presence of PL with the aim to support the development of a cGMP-compliant protocol for cell isolation and expansion.

## 2. Materials and Methods

### 2.1. Samples

**2.1.1. Umbilical Cord Tissue.** This study was reviewed and approved by the SSM Health Institutional Review Board (IRB). Umbilical cords ( $n = 10$ ) were obtained after vaginal or cesarean deliveries, drained of blood, and clamped at either end. All cords were transported in sterile phosphate buffered saline (PBS) and processed within 24 hours of collection.

**2.1.2. Bone Marrow.** BM-mononuclear cell (BM-MNC) samples ( $n = 3$ ) were purchased from Stem Cell Technologies Inc. and thawed as per the manufacturer's guidelines.

**2.2. Isolation of MSCs from the Umbilical Cord.** Each cord (between 12 and 30 cm long) was divided into 2 cm segments and processed to extract cells using tissue homogenization or collagenase digestion.

**2.2.1. Tissue Homogenization (t-H).** A representative 2 cm segment was further minced, rinsed with PBS, and placed into a MACS C-tube (Miltenyi Biotec). Prewarmed basal media (low dextrose alpha MEM, Life Technologies) was added to a final volume of 10 mL and the tissue was homogenized with the GentleMACS Dissociator (Miltenyi Biotec). Contents of the C-tube were transferred to a new 50 mL falcon tube, diluted with 3 volumes of basal media, and then filtered through a 100  $\mu$ m strainer.

**2.2.2. Collagenase Digestion (Col-D).** For enzymatic digestion, the 2 cm minced tissue was rinsed with PBS, placed into a tube containing 20 mL collagenase I (2.5 mg/mL, Life Technologies), and incubated for 2 hours at 37°C with gentle mixing every 10 min. At this enzyme concentration, a 2-hour incubation time yielded the highest recovery of viable cells (data not shown). At the end of the digestion period, the sample was diluted with basal media to a volume of 50 mL, and the supernatant transferred to a new tube through a 100  $\mu$ m strainer.

t-H and Col-D samples were centrifuged, and cell pellets were washed twice and resuspended in basal culture media. Isolated cells from each method were assessed microscopically (using a hemocytometer) for count and viability using trypan blue (Life Technologies).

**2.3. Culture and Expansion of Isolated UC-MSCs.** Initially isolated cells representing passage zero (P0) were plated in multiple T25 flasks at a density of  $1 \times 10^7$  viable cells/flask in complete media (alpha MEM with 1% penicillin/streptomycin/neomycin and 1% amphotericin B) supplemented with heat inactivated 20% FBS (HyClone) or 10% human pooled cGMP-grade PL (Compass Biomedical). After 3 days, media containing nonadherent cells was removed and adherent cells were allowed to grow in fresh media with half media changes performed every 3-4 days. Once cells reached 80–90% confluence, adherent cells were trypsinized using TrypLE (Life Technologies), counted, and replated as passage 1 (P1) at a density of 2,000 viable cells/cm<sup>2</sup> in culture media supplemented with either FBS or PL. Cultures were continued for 10 passages unless cells showed consistent slow growth or signs of senescence. At the end of each passage, harvested cells were evaluated for count, viability, population doublings (PD) [9], population doubling time (PDT) [2], and cumulative count per cm of UC tissue. Different aliquots of cells from various passages were cryopreserved or prepared for cell characterization as described below.

**2.4. Generation of MSCs from the Bone Marrow.** BM-MNCs were plated at an average of  $2.5 \times 10^6$  cells per well (6-well dish) and cultured in complete alpha MEM supplemented with either 20% FBS or 10% PL. Growth kinetics, MSC

phenotype, and differentiation potential were compared to UC-MSCs.

**2.5. Cryopreservation.** Cells were cryopreserved in a Xeno-free freezing solution containing 50% alpha MEM, 30% human AB serum (Corning), and 20% Cryosure-Dex40 (WAK-Chemie). Following trypsinization of adherent cells,  $2 \times 10^6$  cells were aliquoted, pelleted, and resuspended in 1 mL of cryopreservation media. Cells were transferred into cryovials and passively frozen using Mr. Frosty freezing container (ThermoFisher) overnight at  $-80^\circ\text{C}$  before being relocated to vapor liquid nitrogen storage.

**2.6. Colony Forming Units-Fibroblasts (CFU-F) Assay.** At selected passages (1, 3, 5, and 7), 100 cells were plated in triplicate wells of a 6-well plate in corresponding media (containing FBS or PL) with half media changes performed every 3–4 days. After 10–12 days, the plates were stained with 0.5% crystal violet and the number of individual colonies (>50 cells) were counted [15].

**2.7. Immunophenotyping of Cultured MSCs.** At selected passages (2, 3, 5, 7, and 10), immunophenotyping was performed by flow cytometry using the MSC phenotyping kit (Miltenyi Biotec). The kit consists of two cocktails of antibodies: a phenotyping (FITC-CD90, PE-CD105, APC-CD73, and PerCP-CD34/CD45/CD14/CD20) and an isotype control cocktail. In separate tubes,  $0.5\text{--}1.0 \times 10^6$  cells were suspended in staining buffer containing 1% FBS in PBS and incubated for 10 min at  $4^\circ\text{C}$  with either phenotyping or isotype control antibodies. Cells were then washed and resuspended in the staining buffer. Cells were also stained with PerCP-CD31 (R&D Systems) and APC-CD146 (Miltenyi Biotec) antibodies, along with their isotype controls (R&D Systems and BD Biosciences, resp.), in a similar manner. Data was acquired on the Accuri C6 cytometer (Becton Dickinson) and at least 150,000 events were collected for each marker. Analysis was performed using the BD C6 Accuri software (BD Biosciences) to determine percentage of cells expressing specific markers.

**2.8. Assessment of Trilineage Differentiation Potential.** UC-MSCs and BM-MSCs were assessed for their ability to differentiate into osteogenic, adipogenic, and chondrogenic cells using commercially available differentiation kits (Life Technologies). Briefly, for osteogenic and adipogenic differentiation, cells from passage 3 were plated at a density of  $1.5 \times 10^4$  cells per well (24-well plate), in their respective proliferation media. After 24 hours, differentiation was induced while control wells were continued in culture without induction. Cultures were monitored for differentiation and assayed after 21 days by Alizarin Red staining for osteogenesis or 14 days by Oil Red O staining for adipogenesis.

For chondrogenic differentiation, a micromass culture assay was performed following the manufacturer's instructions. After 18–21 days, chondrogenic pellets were fixed, paraffin-embedded, sectioned, and stained with Alcian Blue to assess chondrogenic differentiation. All photomicrographs

were taken using the 10x objective of a Zeiss Axio Observer A1 inverted microscope and images were captured using the AxioVision (version 4.8.2) software (Zeiss).

**2.9. Statistics.** All data in this study is expressed as mean  $\pm$  SD. Analysis was performed using GraphPad Prism (version 5.0) software using a two-tailed Student's *t*-test. Statistical significance was set at  $p < 0.05$ .

### 3. Results

**3.1. Isolation of UC-MSCs: t-H versus Col-D.** In order to disrupt the UC matrix and release the stromal cells, simple t-H using the GentleMACS Dissociator was performed on 10 different UC samples. When compared to the standard method of Col-D, the t-H-based isolation method had a shorter processing time (approximately 3 hours versus 1 hour). Neither the cell number per cm of tissue nor cell viability was significantly different using both isolation methods. Viable cell count/cm was  $2.04 \pm 1.57 \times 10^7$  versus  $2.69 \pm 2.51 \times 10^7$  and cell viability was  $95.44 \pm 5.17\%$  versus  $96.98 \pm 5.86\%$  for t-H versus Col-D, respectively.

Freshly isolated cells, for three samples, were screened for expression of MSC surface markers. As reported in other tissue sources [16], a very small fraction of isolated cells (<2%), regardless of the isolation method, were positive for CD90, CD105, and CD73 markers (data not shown).

Cells released by both methods were compared for their ability to form MSCs in media supplemented with FBS and PL. Both methods generated an adherent monolayer with fibroblast-like morphology (Figure 1), characteristic of MSCs grown on a plastic culture surface. However, the time to reach 80–90% confluent growth varied among different culture conditions. Cultures of Col-D/FBS or PL reached 80–90% confluent growth within a relatively short time ( $8.88 \pm 3.44$  days) when compared to cultures of t-H/PL ( $18.13 \pm 6.83$  days). Additionally, adherent cells at different passages were verified for MSC identity by flow cytometry using a panel of surface markers suggested for defining MSCs [17] (see results in Section 3.4).

Under t-H/FBS culture conditions, majority of cases showed very slow growth and failure of expansion beyond P5 (data not shown); therefore, this condition (t-H/FBS) was less than adequate for UC-MSC production and it was excluded from our analysis.

**3.2. Growth Characteristics and Expansion Potential of Isolated Cells.** In order to generate clinically relevant numbers of MSCs for therapeutic applications, it is imperative that cells have the potential of logarithmic growth and the ability to significantly expand in culture. Adherent cells generated from the above experiments were trypsinized (P1), seeded at the same density, and evaluated for growth kinetics, PD, and PDT over another 9 passages (P2–P10). For a more informative evaluation, growth of UC-MSCs was compared to the growth of BM-MSCs. In line with previous reports [2, 18, 19], successful logarithmic growth of MSCs was observed over tested 10 passages in all cultures of Col-D samples in FBS and

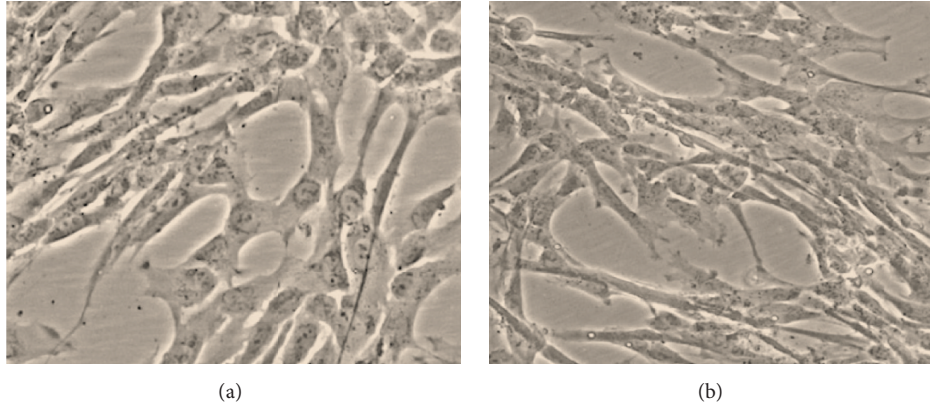


FIGURE 1: Umbilical cord MSCs are plastic-adherent with fibroblast-like morphology. Representative phase-contrast images of cultured cells generated using (a) collagenase digestion or (b) homogenization of umbilical cord tissue.

TABLE 1: Population doubling time for early and late passages.

Culture condition	Doubling time (hours) P1-P3	Doubling time (hours) P7-P9
Homogenization (PL)	41.43 ± 14.68	71.91 ± 31.70
Collagenase (PL)	30.38 ± 2.70	43.64 ± 10.14
Collagenase (FBS)	38.97 ± 6.35	44.48 ± 6.14

PL. However, 8 out of 10 t-H/PL cultures showed successful logarithmic growth through P10 while a very slow growth was observed beyond P7 in cultures of the other 2 samples. As shown in Figure 2(a), the respective kinetic data of all successful cultures demonstrated logarithmic cell growth of UC-MSCs and high expansion potential. Indeed, UC-MSCs could expand through P10 without loss of proliferative activity unlike BM-MSCs where cells showed diminished replicative capacity beyond passage 5 (Figure 2(b)). This agrees with previous studies [2, 7, 20] suggesting superior proliferative potential of UC-MSCs versus BM-MSCs.

At the end of each passage, we calculated cumulative cell number that could theoretically be generated starting with one cm of UC. By the end of P10, calculated cell numbers exceeded  $1 \times 10^{15}$  MSCs/cm under all culture conditions (Col-D/FBS, Col-D/PL, and t-H/PL). However, the cell number attained at P10 in Col-D/PL cultures ( $6.9 \times 10^{20}$ ) was significantly higher than t-H/PL cultures ( $5.34 \times 10^{19}$ ) corresponding to cumulative PD of 45.60 and 29.25, respectively (Figure 3). This relatively slower growth of cells from t-H was also reflected by longer mean PDT estimated for early (P1-P3) and late (P7-P9) passages (Table 1). As expected, under all culture conditions, the PDT increased for late passages indicating a reduction in the proliferative potential of cultured MSCs.

Given the above growth kinetics data, we also analyzed the number of passages and time needed to generate one billion cells from one centimeter of cord tissue. In this regard,

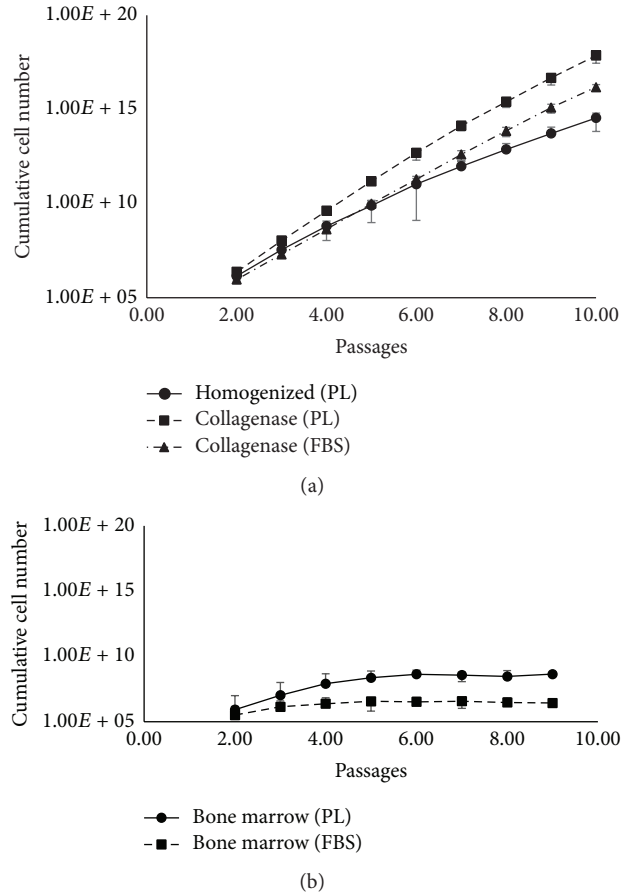


FIGURE 2: Cultured MSCs demonstrate logarithmic growth potential. Each graph depicts logarithmic growth potential and the theoretical number of cells that can be obtained using different isolation methods and culture conditions over several passages for (a) umbilical cord ( $n = 8$ ), and (b) bone marrow ( $n = 3$ ). Equal numbers of cells were plated for each condition and fold changes were determined after each passage (P2-P10) to determine the theoretical cell number that could be obtained starting with 50,000 cells from P1. Error bars denote mean  $\pm$  SD.



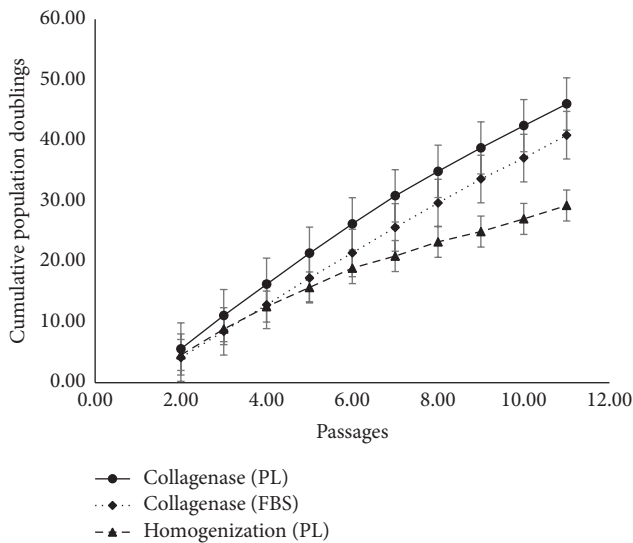


FIGURE 3: UC-MSCs continue to expand robustly in culture at the end of 10 passages. Cumulative population doublings achieved over the duration of culture demonstrate the replicative capacity of UC-MSCs generated using Col-D or t-H. Error bars denote mean  $\pm$  SD.

using either t-H or Col-D and culture in PL, over a billion cells could be generated over 3 passages; however, the time to achieve this expansion varied between isolation methods ( $33.27 \pm 7.00$  days for t-H versus  $22.27 \pm 4.00$  days for Col-D). This data is in agreement with the observation that Col-D cultures reach their first passage faster and once in culture have a shorter PDT. Collectively, this data suggests that although Col-D generates UC-MSCs faster, it is feasible to generate therapeutic doses of such cells using a cGMP-compliant protocol of t-H/PL within a reasonable length of time. Based on data obtained from the 8 cord samples using t-H/PL, a theoretical yield of  $3.0 \times 10^{10}$  UC-MSCs can be generated within approximately 1 month from a single cord of thirty cm length. This yield would allow treatment of forty patients (based on average patient weight of 70 kg and infusion of double doses each dose of 5 million cells/kg) in a phase-I clinical trial.

**3.3. CFU-F Contents of MSC Preparations.** The ability of MSCs to form colonies is considered an important parameter for judging the quality of cultured cells [21]. As the passage number increases, clonogenic potential of cells is expected to decrease [22]. Hence, we evaluated the clonogenic potential of MSCs generated using t-H and Col-D. In agreement with established biological characteristics of MSCs, the number of CFU-F colonies for all conditions decreased with increasing passages (Figures 4(a) and 4(b)). The CFU-F content was higher in cultures supplemented with PL compared to FBS, and UC-MSCs had superior colony forming contents as compared to BM-derived MSCs (Figure 4(b)). Importantly, t-H/PL cultures had a greater colony forming capacity compared to the conventional culture conditions of Col-D/FBS. This indicates that cells generated under cGMP-compliant

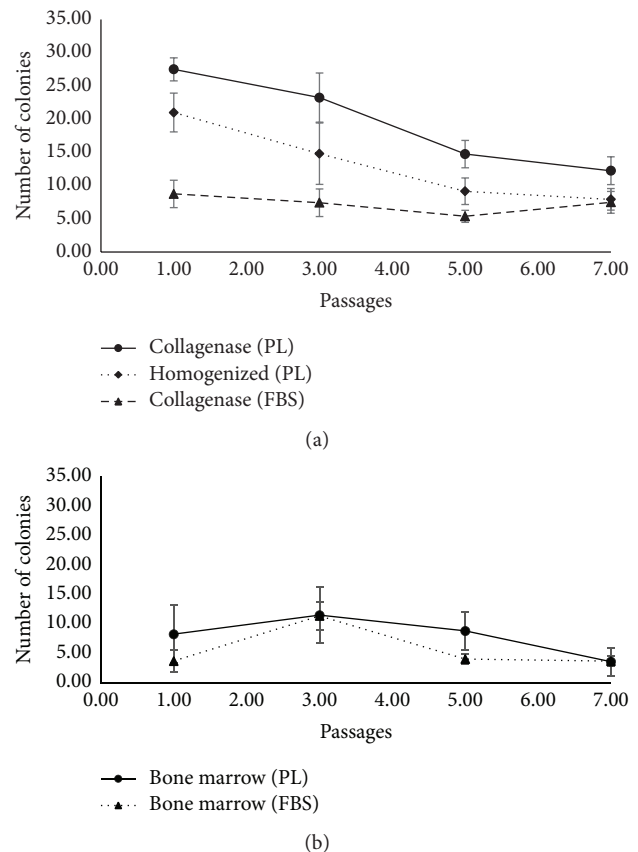


FIGURE 4: Umbilical cord MSCs possess robust self-renewal capability. Graphical representation of mean CFU-F content of MSCs, at different passages, generated by plating 100 cells per well from (a) umbilical cord and (b) bone marrow. Error bars denote mean  $\pm$  SD.

conditions have a good self-renewal capacity when compared with currently used conventional protocols.

**3.4. Phenotypic Characterization and Multilineage Differentiation Potential of UC-MSCs.** To demonstrate that cultures established from UC cells isolated by both methods are MSCs, cells were evaluated by flow cytometry in reference to criteria set forth by the ISCT [17]. In general, more than 80% of cells were found to express mesenchymal markers (CD73, CD90, and CD105) (Figure 5) and were negative (<1%) for hematopoietic (CD45, CD34), monocyte (CD14), B cell (CD20), and endothelial (CD34, CD31) markers. Moreover, UC-MSCs were evaluated for a recently identified phenotype of pericyte-like MSCs ( $CD146^+CD31^-CD34^-CD45^-$ ) [23]. This population represented >75% of UC-MSCs. For both isolation methods, all mesenchymal markers were maintained over long-term culture and did not show any significant change over 10 passages. Additionally, these cells exhibited trilineage mesodermal differentiation (adipogenic, chondrogenic, and osteogenic) potential, a characteristic feature of MSCs (Figure 6). In our analysis, the differentiation potential of UC-MSCs evaluated at P3 appeared comparable in all tested samples irrespective of the isolation method and culture conditions. BM-MSCs were used as a positive

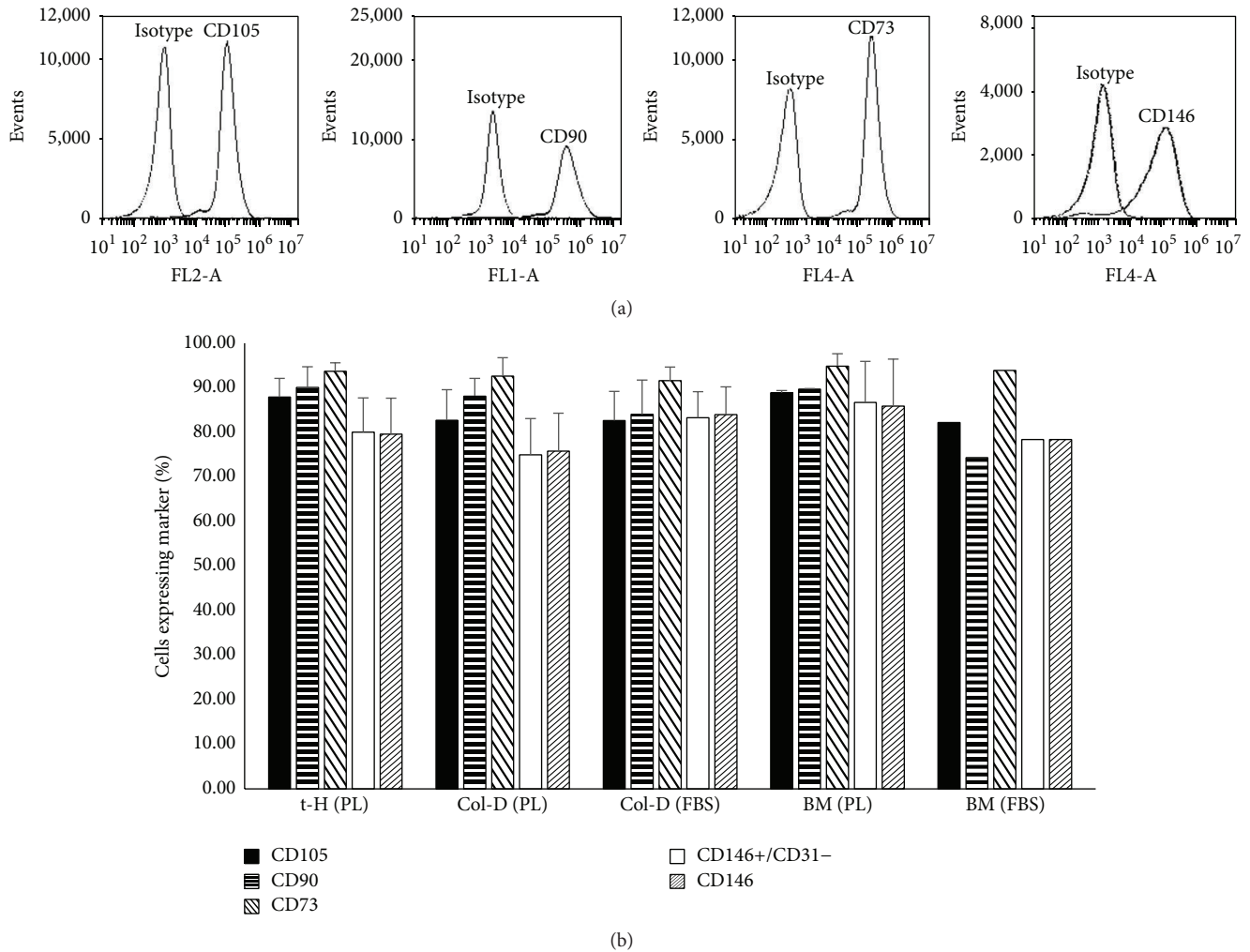


FIGURE 5: Umbilical cord MSCs express characteristic mesenchymal cell surface markers by flow cytometry. (a) Representative histograms from passage 3 demonstrate expression of mesenchymal markers (CD90, CD105, CD73, and CD146) in cultured UC-MSCs. Histograms show antibodies with their respective isotype controls. (b) Bar graph demonstrates the mean expression of different mesenchymal markers by cultured MSCs derived from umbilical cord ( $n = 8$ ). CD45, CD34, CD14, CD20, and CD31 are not shown since expression levels were less than 2%. Bone marrow MSCs were used as controls for cell marker expression. Each bar represents mean  $\pm$  SD.

control for all differentiation experiments. In agreement with previous reports, the ability of UC-MSCs to differentiate into adipocytes was extremely low when compared to BM-MSCs [20, 24].

#### 4. Discussion

Traditionally, isolation of UC stromal cells has been achieved using explant cultures or through collagenase digestion of intracellular fibers. Several methodological variations have been reported (reviewed in [25]) ranging from removal of blood vessels to keeping them intact, using a combination of enzymatic digestion and explant cultures, employing collagenase alone or a combination of collagenase, hyaluronidase, and trypsin. While enzymatic digestion results in a more uniform release of cells, it has the drawbacks of longer initial processing time (anywhere from 3 to 18 hours), lack of

a standard method, and being non-cGMP-compliant since the reagents are obtained from nonhuman sources making it difficult to obtain clinical-grade material. Alternatively, the explant cultures have shorter processing times but they suffer from the nonuniformity of cell migration and improper adherence of tissue fragments to the culture dish resulting in variability in the quantity and quality of cells obtained in culture [26]. Given the compartmental heterogeneity of stem cell distribution within the UC tissue [19], differential cell release may impact the “stemness” or differentiation capability of the generated MSCs [9]. Therefore, we sought to evaluate, at bench scale, a method that would result in the fast and uniform release of cells with the added advantage of using Xeno-free reagents to support the development of a cGMP-compliant protocol.

Previous reports have indicated that collagen is amenable to simple mechanical disruption [27, 28]. Based on this observation, we hypothesized that viable cells could be

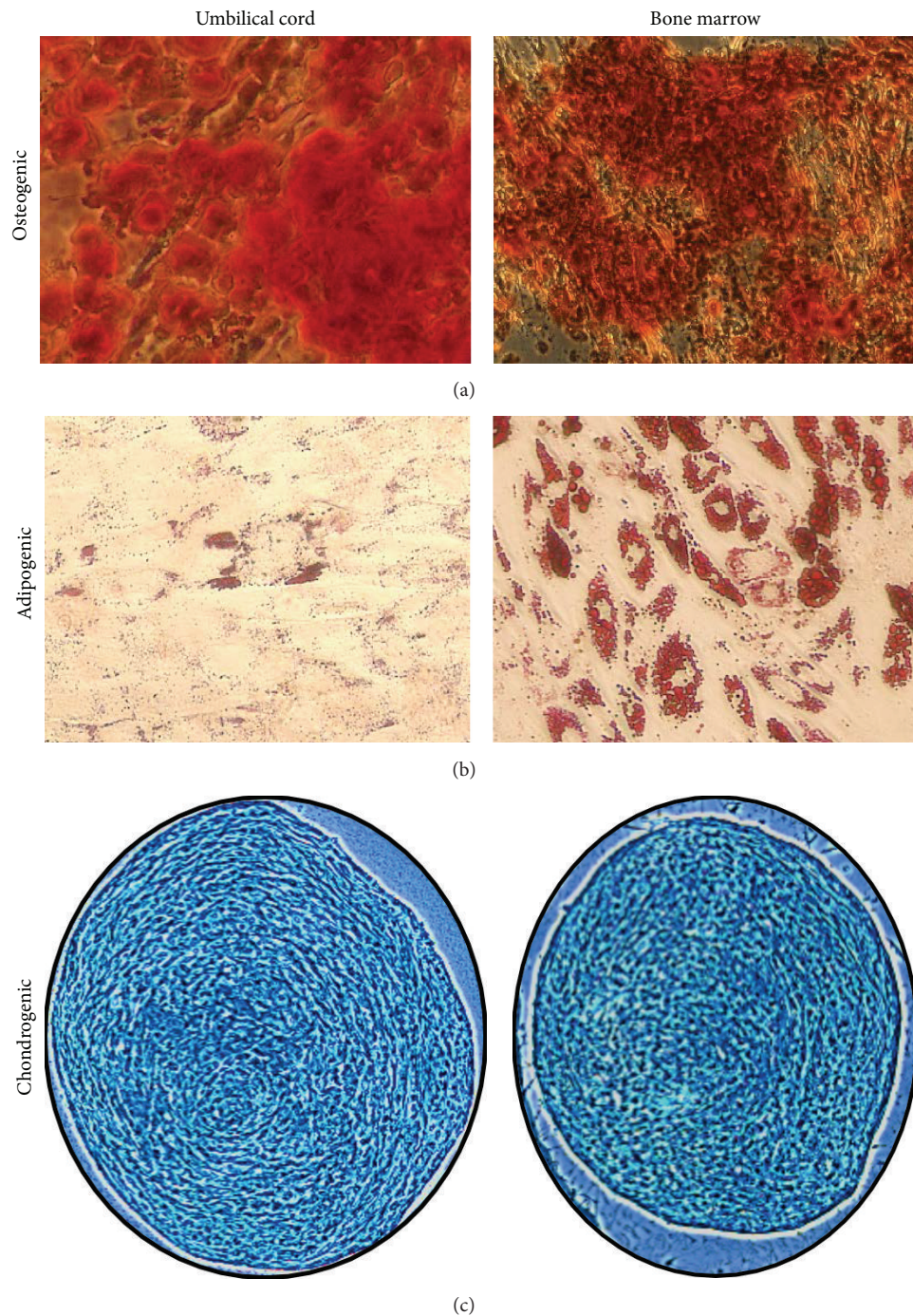


FIGURE 6: Umbilical cord MSCs exhibit trilineage differentiation potential. Representative images from passage 3 demonstrate (a) osteogenic differentiation using Alizarin Red staining, (b) adipogenic differentiation using Oil Red O, and (c) chondrogenic differentiation using Alcian Blue staining of chondrogenic pellets generated via micromass cultures. Bone marrow MSCs were used as positive control for demonstrating trilineage differentiation.

potentially released from the UC tissue using simple t-H in a prewarmed buffer. Therefore, we used the GentleMACS Dissociator to achieve rapid, uniform, and mild disruption of the UC matrix to release the stromal cells. To simplify the protocol and achieve better isolation yield from various tissue compartments, we chose not to strip blood vessels

and amnion prior to cord homogenization. This minimal processing did not impact the purity of MSCs generated, as evidenced by the extremely low percentage of endothelial (CD31) and hematopoietic (CD45) cells in our cultures. Our protocol is based on simply cutting and mincing the entire cord into small pieces, washing to remove blood clots,



and homogenizing the tissue for uniform release of cells. Furthermore, to develop and characterize a cGMP-compliant method for generation of MSCs, cell growth and expansion were tested in human PL, an accepted cGMP-compliant alternative to FBS [9, 29, 30]. In this study, we have demonstrated the possibility of producing large numbers of viable UC-MSCs using simple t-H and expansion in PL-supplemented media. Herein, we have furthered the observations on not only the feasibility but the superiority of pooled PL as a cGMP growth supplement for culturing MSCs [14, 29, 30]. In all cultures, irrespective of cell source and isolation method, PL promoted better growth of MSC when compared to FBS.

The method described here has several advantages including uniform release of cells, shorter processing time, and the absence of any enzyme of bacterial origin. The MSCs generated using t-H demonstrated exponential growth potential, excellent clonogenic capacity, and characteristic mesenchymal phenotype. Although the t-H-derived cells were slower growing when compared to Col-D, they maintained good CFU-F potential even at later passages (through P7). This is in contrast to reports demonstrating diminished or absent clonogenic capacity (beyond passage 5) of cells generated using explant cultures [9]. Furthermore, for clinical purposes, the proposed optimal time for harvesting cells is before passage 5 or 30 population doublings [31]. Using t-H, we can theoretically achieve clinically relevant number of cells in three passages and less than 10 population doublings from one cord, making this method feasible for clinical development. While the collagenase-based method generated more MSCs per cm of the cord in a shorter duration of time, there was no significant difference in terms of cellular phenotype and differentiation potential of the cells derived using t-H. Given the regulatory hurdles associated with the use of reagents of animal origin, tissue homogenization followed by growth in PL represents a simple and practical alternative to the currently used protocols. Our isolation/expansion technique utilizes GMP compatible reagents and could be further adapted into a fully GMP compliant method where other requirements shall be fulfilled such as selection of clinically eligible donors screened for infectious diseases and the assurance of product safety indicated by the absence of bacterial/fungal and mycoplasma contamination, acceptable endotoxin levels, and evidence of the lack of tumorigenicity.

Finally, we have cryopreserved cells from different isolation and culture conditions (t-H/PL, Col-D/PL, and Col-D/FBS) at various passages to generate a master bank of research cells for future studies. As mentioned in the Methods, Xeno-free reagents were used for cryopreservation so as to make this protocol cGMP-compatible at every step of the process. Initial findings after direct thaw of cells frozen for more than six months showed cell recovery and viability above 80%. In parallel, no apparent change in growth kinetic and colony formation potential was observed after thaw (data not shown). Future studies might aim toward extensive characterization of cryostored cells for stability, differentiation potential to nonmesodermal cell types, and assessment for clinically relevant indications like immunosuppression and hematopoietic support capability.

## 5. Conclusions

This study describes a bench-scale, nonenzymatic, cGMP-compatible method using whole cord tissue homogenization followed by growth in platelet lysate as an alternative to the currently used methods for generating UC-MSCs. Using this approach, clinically relevant numbers of cells, which are clonogenic, fulfil the standard criteria of MSC marker expression and mesodermal trilineage differential potential can be efficiently obtained for therapeutic applications.

## Conflict of Interests

The authors declare that there is no conflict of interests regarding the publication of this paper.

## Acknowledgments

This project was funded by the St. Louis Cord Blood Bank and SSM Cardinal Glennon Children's Hospital. The authors would like to thank the staff of the St. Louis Cord Blood Bank for their support during these studies.

## References

- [1] A. Sorrentino, M. Ferracin, G. Castelli et al., "Isolation and characterization of CD146<sup>+</sup> multipotent mesenchymal stromal cells," *Experimental Hematology*, vol. 36, no. 8, pp. 1035–1046, 2008.
- [2] L.-L. Lu, Y.-J. Liu, S.-G. Yang et al., "Isolation and characterization of human umbilical cord mesenchymal stem cells with hematopoiesis-supportive function and other potentials," *Haematologica*, vol. 91, no. 8, pp. 1017–1026, 2006.
- [3] K. Johnson, S. Zhu, M. S. Tremblay et al., "A stem cell-based approach to cartilage repair," *Science*, vol. 336, no. 6082, pp. 717–721, 2012.
- [4] R. Sarugaser, L. Hanoun, A. Keating, W. L. Stanford, and J. E. Davies, "Human mesenchymal stem cells self-renew and differentiate according to a deterministic hierarchy," *PLoS ONE*, vol. 4, no. 8, Article ID e6498, 2009.
- [5] K. Stenderup, J. Justesen, C. Clausen, and M. Kassem, "Aging is associated with decreased maximal life span and accelerated senescence of bone marrow stromal cells," *Bone*, vol. 33, no. 6, pp. 919–926, 2003.
- [6] S. M. Mueller and J. Glowacki, "Age-related decline in the osteogenic potential of human bone marrow cells cultured in three-dimensional collagen sponges," *Journal of Cellular Biochemistry*, vol. 82, no. 4, pp. 583–590, 2001.
- [7] D. Baksh, R. Yao, and R. S. Tuan, "Comparison of proliferative and multilineage differentiation potential of human mesenchymal stem cells derived from umbilical cord and bone marrow," *STEM CELLS*, vol. 25, no. 6, pp. 1384–1392, 2007.
- [8] R. Hass, C. Kasper, S. Böhm, and R. Jacobs, "Different populations and sources of human mesenchymal stem cells (MSC): a comparison of adult and neonatal tissue-derived MSC," *Cell Communication and Signaling*, vol. 9, article 12, 2011.
- [9] C. Capelli, E. Gotti, M. Morigi et al., "Minimally manipulated whole human umbilical cord is a rich source of clinical-grade human mesenchymal stromal cells expanded in human platelet lysate," *Cytotherapy*, vol. 13, no. 7, pp. 786–801, 2011.



- [10] I. Majore, P. Moretti, F. Stahl, R. Hass, and C. Kasper, "Growth and differentiation properties of mesenchymal stromal cell populations derived from whole human umbilical cord," *Stem Cell Reviews and Reports*, vol. 7, no. 1, pp. 17–31, 2011.
- [11] C. Mennan, K. Wright, A. Bhattacharjee, B. Balain, J. Richardson, and S. Roberts, "Isolation and characterisation of mesenchymal stem cells from different regions of the human umbilical cord," *BioMed Research International*, vol. 2013, Article ID 916136, 8 pages, 2013.
- [12] M. T. Conconi, R. D. Liddo, M. Tommasini, C. Calore, and P. P. Parnigotto, "Phenotype and differentiation potential of stromal populations obtained from various zones of human umbilical cord: an overview," *The Open Tissue Engineering and Regenerative Medicine Journal*, vol. 4, no. 1, pp. 6–20, 2011.
- [13] A. Schäffler and C. Büchler, "Concise review: adipose tissue-derived stromal cells—basic and clinical implications for novel cell-based therapies," *Stem Cells*, vol. 25, no. 4, pp. 818–827, 2007.
- [14] N. Ben Azouna, F. Jenhani, Z. Regaya et al., "Phenotypical and functional characteristics of mesenchymal stem cells from bone marrow: comparison of culture using different media supplemented with human platelet lysate or fetal bovine serum," *Stem Cell Research & Therapy*, vol. 3, no. 1, article 6, 2012.
- [15] H. Castro-Malaspina, R. E. Gay, G. Resnick et al., "Characterization of human bone marrow fibroblast colony-forming cells (CFU-F) and their progeny," *Blood*, vol. 56, no. 2, pp. 289–301, 1980.
- [16] R. Peters, M. J. Wolf, M. van den Broek et al., "Efficient generation of multipotent mesenchymal stem cells from umbilical cord blood in stroma-free liquid culture," *PLoS ONE*, vol. 5, no. 12, Article ID e15689, 2010.
- [17] M. Dominici, K. Le Blanc, I. Mueller et al., "Minimal criteria for defining multipotent mesenchymal stromal cells. The International Society for Cellular Therapy position statement," *Cytotherapy*, vol. 8, no. 4, pp. 315–317, 2006.
- [18] V. Sabapathy, B. Sundaram, S. Vm, P. Mankuzhy, and S. Kumar, "Human Wharton's Jelly Mesenchymal Stem Cells plasticity augments scar-free skin wound healing with hair growth," *PLoS ONE*, vol. 9, no. 4, Article ID e93726, 2014.
- [19] R. C. Schugar, S. M. Chirieleison, K. E. Wescoe et al., "High harvest yield, high expansion, and phenotype stability of CD146 mesenchymal stromal cells from whole primitive human umbilical cord tissue," *Journal of Biomedicine and Biotechnology*, vol. 2009, Article ID 789526, 11 pages, 2009.
- [20] J. Hua, J. Gong, H. Meng et al., "Comparison of different methods for the isolation of mesenchymal stem cells from umbilical cord matrix: proliferation and multilineage differentiation as compared to mesenchymal stem cells from umbilical cord blood and bone marrow," *Cell Biology International*, vol. 38, no. 2, pp. 198–210, 2014.
- [21] P. Penfornis and R. Pochampally, "Isolation and expansion of mesenchymal stem cells/multipotent stromal cells from human bone marrow," *Methods in Molecular Biology*, vol. 698, pp. 11–21, 2011.
- [22] M. C. Vemuri, L. G. Chase, and M. S. Rao, "Mesenchymal stem cell assays and applications," *Methods in Molecular Biology*, vol. 698, pp. 3–8, 2011.
- [23] M. Crisan, S. Yap, L. Casteilla et al., "A perivascular origin for mesenchymal stem cells in multiple human organs," *Cell Stem Cell*, vol. 3, no. 3, pp. 301–313, 2008.
- [24] P. Shetty, K. Cooper, and C. Viswanathan, "Comparison of proliferative and multilineage differentiation potentials of cord matrix, cord blood, and bone marrow mesenchymal stem cells," *Asian Journal of Transfusion Science*, vol. 4, no. 1, pp. 14–24, 2010.
- [25] A. Bongso and C.-Y. Fong, "The therapeutic potential, challenges and future clinical directions of stem cells from the Wharton's jelly of the human umbilical cord," *Stem Cell Reviews and Reports*, vol. 9, no. 2, pp. 226–240, 2013.
- [26] Y. Mori, J. Ohshimo, T. Shimazu et al., "Improved explant method to isolate umbilical cord-derived mesenchymal stem cells and their immunosuppressive properties," *Tissue Engineering Part C: Methods*, vol. 21, no. 4, pp. 367–372, 2015.
- [27] S. P. Veres, J. M. Harrison, and J. M. Lee, "Mechanically overloading collagen fibrils uncoils collagen molecules, placing them in a stable, denatured state," *Matrix Biology*, vol. 33, pp. 54–59, 2014.
- [28] E. Bańkowski, K. Sobolewski, L. Romanowicz, L. Chyczewski, and S. Jaworski, "Collagen and glycosaminoglycans of Wharton's jelly and their alterations in EPH-gestosis," *European Journal of Obstetrics Gynecology and Reproductive Biology*, vol. 66, no. 2, pp. 109–117, 1996.
- [29] N. Fekete, M. T. Rojewski, R. Lotfi, and H. Schrezenmeier, "Essential components for *Ex vivo* proliferation of mesenchymal stromal cells," *Tissue Engineering Part C: Methods*, vol. 20, no. 2, pp. 129–139, 2014.
- [30] N. H. Riordan, M. Madrigal, J. Reneau et al., "Scalable efficient expansion of mesenchymal stem cells in xeno free media using commercially available reagents," *Journal of Translational Medicine*, vol. 13, article 232, 2015.
- [31] P. J. Hanley, Z. Mei, M. Da Graca Cabreira-Hansen et al., "Manufacturing mesenchymal stromal cells for phase I clinical trials," *Cytotherapy*, vol. 15, no. 4, pp. 416–422, 2013.

## Review Article

# Stem Cell Therapy for Treatment of Stress Urinary Incontinence: The Current Status and Challenges

**Shukui Zhou,<sup>1</sup> Kaile Zhang,<sup>1</sup> Anthony Atala,<sup>2</sup> Oula Khouury,<sup>2</sup> Sean V. Murphy,<sup>2</sup> Weixin Zhao,<sup>2</sup> and Qiang Fu<sup>1</sup>**

<sup>1</sup>*Department of Urology, Affiliated Sixth People's Hospital, Shanghai Jiao Tong University, Shanghai, China*

<sup>2</sup>*Wake Forest Institute for Regenerative Medicine, Winston Salem, NC, USA*

Correspondence should be addressed to Weixin Zhao; [wezhao@wakehealth.edu](mailto:wezhao@wakehealth.edu) and Qiang Fu; [jamesqfu@aliyun.com](mailto:jamesqfu@aliyun.com)

Received 20 September 2015; Accepted 20 December 2015

Academic Editor: Franca Fagioli

Copyright © 2016 Shukui Zhou et al. This is an open access article distributed under the Creative Commons Attribution License, which permits unrestricted use, distribution, and reproduction in any medium, provided the original work is properly cited.

Stress urinary incontinence (SUI) is a common urinary system disease that mostly affects women. Current treatments still do not solve the critical problem of urethral sphincter dysfunction. In recent years, there have been major developments in techniques to obtain, culture, and characterize autologous stem cells as well as many studies describing their applications for the treatment of SUI. In this paper, we review recent publications and clinical trials investigating the applications of several stem cell types as potential treatments for SUI and the underlying challenges of such therapy.

## 1. Introduction

Stress urinary incontinence (SUI) is a common urogenital disease, defined as the involuntary leakage of urine in the absence of a detrusor contraction, generally due to the weakness of the urethral sphincter and pelvic floor [1]. More than 200 million people worldwide suffered from SUI, which seriously affects the quality of life of patients [2]. As a disease whose prevalence is related to advancing age, it affects more women than men with an approximate ratio of 3:1 [3]. For women, both pregnancy and vaginal birth are associated with an increased risk of the levator ani muscle defects. Pregnancy and delivery decrease the expression of hypoxia inducible factor-1 and vascular endothelial growth factor [4], which may inhibit the angiogenic response and tissue repair of pelvic floor after childbirth. Likewise, SUI can also affect men and is primarily caused by urethral sphincteric deficiency after radical prostatectomy [5]. At present, several treatments for SUI are available, of which bulking agent injection and Tension-Free Vaginal Tape are the most common and effective therapeutic methods. The various injectable bulking agents applied for the treatment of SUI patients include bovine collagen, carbon beads, silicone, and polyacrylamide hydrogel. However, an ideal

periurethral injectable agent for treating SUI has not been found so far. Adverse effects have been reported with all these bulking agents, for example, immunological rejection, sterile abscess formation, foreign-body granuloma, bladder outlet obstruction, and even pulmonary embolism [6, 7]. In addition, due to degradation of bulking agents, their efficacy gradually declines over a period of months or years. Surgery, including sling procedures and bladder neck suspensions, is more efficacious to control the voiding. It is previously reported that the procedures have a 5-year cure rate of more than 80% [8]; however, this procedure has a series of side effects including urinary retention, bladder perforation and hematoma formation. Meanwhile, some patients are not suitable to surgical treatment for contraindication. Most important of all, although the sling procedure and bulking agent injection can enhance the pelvic floor muscles, the urethral sphincter deficiency still remains. Therefore, the key to treating SUI is to improve the mechanism of urethral sphincter insufficiency.

One approach would be the use of stem cells. Stem cells can be easily isolated in high quality and large quantities *in vitro* and have the potential to develop into any cell type especially during phases of early life and growth. In some organs, stem cells constitute a repair mechanism that is able

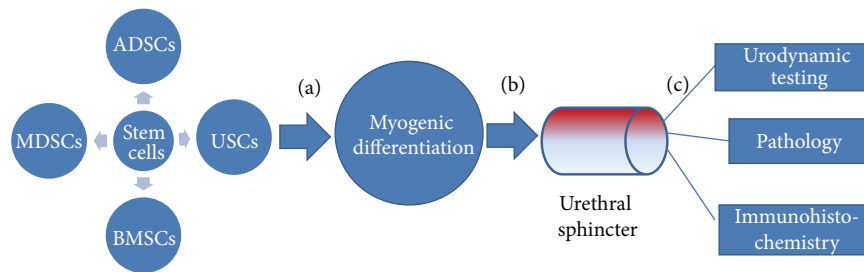


FIGURE 1: The protocol of stem cell therapy for SUI animal models. In most studies that investigate stem cells as potential treatment for SUI, the following criteria need to be established. (a) The polyphyletic stem cells have plasticity to differentiate into functional cells and proliferate in vitro. Myogenic differentiation is demonstrated with the expression of desmin and  $\alpha$ -skeletal muscle actin by immunostaining. (b) They migrate to the damaged external urethral sphincter through periurethral injection. (c) Treatment effects of stem cell transplantation were evaluated through urodynamic testing and morphologic changes of the urethra and frozen urethra sections were submitted to pathology and immunohistochemistry assessment before and after transplantation.

to replenish cells whenever damage or injury occurs. They are unspecialized cells characterized by a self-renewal property where each daughter cell can either remain undifferentiated or become specialized with a defined function. In addition, provided the appropriate environment and conditions, stem cells can be induced to differentiate into a specific cell-like or tissue-like phenotype with a specifically determined function. Additionally, stem cells are known to have antiapoptotic, antiscarring, and neovascularization effects. Moreover, autologous stem cell transplantation eliminates the risk of immunological rejection. Thus, with their multidifferentiation potential, the stem cells can be induced to differentiate into myoblast to solve the problem of urethral sphincter dysfunction. Here, we summarize relevant progress of stem cell therapy research for SUI and discuss the potential challenges in this paper.

## 2. Stem Cell Transplantation for the Treatment of SUI

Based on the rapid progress in stem cell biology, stem cells derived from skeletal muscle, adipose tissue, bone marrow, and urine have been used in animal model and preclinical researches for the treatment of SUI in recent years. Most of current papers about stem cell therapy for SUI are focused on animal experiments and follow similar protocols (Figure 1). Furthermore, relevant clinical research was also reported and has showed certain efficacy for the treatment of SUI.

**2.1. Muscle-Derived Stem Cells (MDSCs) Implantation.** Considering that the etiology of SUI is the weakness or dysfunction of urethral sphincter, improving sphincter function may benefit SUI patients. As the name implies, MDSCs are considered to be the predecessor of satellite cells and are not restricted to mesenchymal or myogenic lineages. They have been shown to differentiate into muscle and bone and aid in cartilage healing [9]. Because the source is rich in muscle tissue, MDSCs are easy to obtain in large quantities under local anesthesia. MDSCs are initially isolated from autologous skeletal muscle biopsies and then expanded in vitro and injected into the urethral sphincter. In previous

studies, autologous muscle-derived cells have successfully integrated in urethra tissue and partly restored sphincter function in short term [10–13]. However, the potential of muscle-derived cell proliferation is relatively poor, it was often required repeated cell injections to provide enough cells. Furthermore, treatment effect is significantly decreased with time. For the past few years, more studies about MDSCs implantation for treatment of SUI have been reported. Lee et al. [14] reported injection of MDSC into the denervated rats can improve sphincter function, leading to a long term (12 weeks) increase in leak point pressure (LPP) and closing pressure (CP) compared to bovine collagen-injected (LPP:  $40.2 \pm 7.0$  versus  $27.8 \pm 3.2$  cmH<sub>2</sub>O and CP:  $30.0 \pm 7.6$  versus  $21.8 \pm 1.9$  cmH<sub>2</sub>O). Carr et al. [15] reported 1-year follow-up on eight cases of female SUI patients (42–65 years of age) who were treated with MDSCs injections under local anesthesia. Five out of the 8 women (62.5%) showed improvement of SUI symptoms, and one achieved total continence. Besides, Wang et al. [16] showed that inhibiting the fibroblast differentiation of MDSCs induced by TGF- $\beta$ 1 could improve the MDSCs-mediated repairing of urethral sphincter function. Xu et al. [17] confirmed the MDSCs-based injection therapies in urethral sphincter restoration can be promoted when combined with biodegradable fibrin glue in a pudendal nerve-transected rat. Compared with MDSCs injection alone, MDSCs plus fibrin glue improved LPP and increased the numbers of surviving MDSCs ( $109 \pm 19$  versus  $82 \pm 11$ /hpf,  $P = 0.026$ ) and muscle/collagen ratio ( $0.40 \pm 0.02$  versus  $0.34 \pm 0.02$ ,  $P = 0.044$ ) at the injection sites.

However, MDSCs often differentiate quickly without stimulation before they can be implanted and expanded in vivo [18]. For another, the biopsy procedure is painful and requires large muscle biopsies to obtain sufficient MDSCs. Cell Harvesting procedures, if not performed properly, may increase the risk of infection in patients.

**2.2. Adipose-Derived Stem Cells (ADSCs) Implantation.** Currently, ADSCs are the most common stem cell type used in autoplasmic transplantation. ADSCs possess more advantages in the clinical application, including sufficient adipose tissue, which can be easily and abundantly obtained by a common

surgical procedure and patients have a very high tolerance for repeated sampling. Adipose tissue contains high content of ADSCs, with approximately 15 million ADSCs that can be obtained per gram of adipose tissue and have the ability to proliferate rapidly even in low serum medium. Our group successfully isolated ADSCs from inguinal adipose tissue of rats and induced differentiation of ADSCs into myoblasts with 5-Aza in vitro. Subsequently, the induced ADSCs were injected into the posterior urethral muscularis of rat models with SUI and follow-up analysis showed that ADSCs can be used to treat SUI [19]. Recently, there has been a significant increase in experimental studies about autologous ADSCs transplantation for treatment of SUI. Shi et al. [20] combined ADSCs with silk fibroin microspheres to treat SUI caused by severe intrinsic sphincter deficiency with encouraging results. Injection of silk fibroin microspheres alone only escalated leak point pressures and lumen area in short term (<4 weeks), while the treatment which included ADSCs restored urethral sphincter structure and function in long term (12 weeks after injection). Lin et al. [21] found that implantation of ADSCs through urethral/intravenous injection significantly decreased abnormal voiding rate of SUI rat model compared to control group (33.3% versus 80%). This was accompanied by increased elastin content and smooth muscle content. There was no significant difference in treatment efficacy between the two methods. Kuismanen et al. [22] first described the treatments of autologous ASCs in combination with collagen gel for five female patients with SUI in a pilot study. The mixture of ADSCs and collagen gel was injected transurethrally into the urethral sphincters through a cystoscope. Three out of five patients displayed a negative cough test with full bladder filled with 500 mL of saline and 2 out of 5 patients experienced improvement of symptoms in 12-month follow-up. Zhao et al. [23] used a combination of autologous ADSCs and controlled-release nerve growth factor for treatment of SUI rat by periurethral injection. This treatment enhanced urethral muscle layer distributions, increased the neuronal density of urethra, improved abdominal leak point pressure, and reduced urethral perfusion pressure in SUI rats. Most recently, Silwal Gautam et al. [24] reported that autologous ADSCs injected into cryoinjured rabbit urethras could reconstruct skeletal and smooth muscle areas in the cell-implanted regions. Compared to the cell-free control group, leak point pressure of the cell-implanted group was significantly higher at 14 days after implantation.

ADSCs therapy may have a role not only in the treatment of female SUI, but also in restoring continence in men after radical prostatectomy. Yamamoto et al. [25] provide evidence suggesting that periurethral injection of the autologous ADSCs is a safe and feasible treatment modality for three men (age from 69 to 77 years) with moderate SUI after radical prostatectomy and holmium laser enucleation of the prostate. The bulking effect and increased blood flow were detected at the site of ADSCs injection and persisted during the entire follow-up period (three months), which indicated that the patients experienced excellent short-term outcomes undergoing this cell therapy. However, there are only minimal published studies using stem cell therapy for the treatment of male SUI, and further studies are needed

with longer follow-up periods and larger numbers of patients [26]. In brief, the results above indicate the regenerative potential of ADSCs for the treatment of SUI.

**2.3. Bone Marrow-Derived Mesenchymal Stem Cell (BMSCs) Implantation.** BMSCs develop in the bone marrow stromal fraction and are capable of self-renewing and differentiating into several cellular types. They were first described in 1966 as bone forming progenitor cells and have been exploited for 50 years, most recently in tissue engineering. BMSCs are relatively easy to obtain at enough density for therapy. Additionally, they are adherent by nature which makes them easy to grow and expand in culture [27, 28]. As the first stem cells to be described, BMSCs have the capacity to induce urethral sphincter regeneration under special conditions. Data from animal models of SUI showed that injected BMSCs can differentiate into muscle cells and restore resistance of urination. Corcos et al. [29] found that periurethral injection of BMSCs in an animal model of SUI restored the damaged external urethral sphincter and significantly improved valsalva leak point pressure. Gunetti et al. [30] also showed that BMSCs can survive for more than 4 months in absence of immunosuppression and migrated into the muscle among fibers and towards neuromuscular endplates. Kinebuchi et al. [31] transplanted autologous BMSCs into injured rat urethral sphincters to evaluate the functional and histological recovery. Although the leak point pressure outcome showed no significant difference between the BMSCs and cell-free medium groups during the following 13 weeks, transplanted cells survived and successfully differentiated into skeletal muscle cells, smooth muscle cells and peripheral nerve cells as these were detected by immunohistochemical staining. Kim et al. [32] reported his findings of an animal study which utilized autologous BMSCs to treat female SUI. The cells were cultured to differentiate into muscle lineage cells in vitro and then injected into the denervated external urethral sphincter in female rats. Both, the leak point pressure and the closing pressure recovered at four weeks after the injection of BMSCs, and the injected BMSCs expressed a strong immunoreactivity for muscle-specific markers. Moreover, a recent study confirmed that BMSCs act via their secretome which is collected from cell culture and was shown facilitate recovery of elastic fiber density and pudendal nerve fascicles in this dual muscle and nerve injury SUI model [33]. Nevertheless, similar to MDSCs, the process of autologous bone marrow extraction is painful. Invasive procedures require the collection of many bone marrow samples under anesthesia to obtain enough BMSCs, so it is with an attendant risk of complications.

**2.4. Urine Derived Stem Cells (USCs) Implantation.** USCs can be easily harvested from human voiding urine and expanded in vitro as they do not require enzyme digestion to maintain cell growth. USCs can be repeatedly obtained from urine samples at any patient age, which could easily meet the requirements of cells number and patients are well-tolerated. In addition, it is reported that urine has acute cytotoxicity to damage the survival of the transplanted bone marrow-derived mesenchymal stem cells in vivo [35], while USCs derived from urine have greater ability to resist the toxicity



of urine than other stem cell types. Statistics show that up to 75% of fresh USCs can be safely maintained in urine for 24 hours while retaining their original stem cell properties [36]. Thus, USCs may be the most promising cell sources for stem cell-based therapies. Currently, to the best of our knowledge, the experimental study of USCs to treat urinary incontinence is rare. Wu et al. [37] isolated urine derived stem cells from 31 urine samples from 6 healthy individuals with ages ranging from 3 to 27 years. The urine derived stem cells were transfected with an adenoviral vector containing the mouse VEGF gene and injected subcutaneously into athymic mice with a collagen-I gel. The results indicated that more nerve fibers and vascular endothelial growth factor were present in transfected urine derived stem cells and vascular endothelial growth factor overexpression enhanced myogenic differentiation of urine derived stem cells. Liu et al. [38] synthesized microbeads of alginate containing growth factors VEGF, IGF-1, FGF-1, PDGF, HGF, and NGF, which were embedded with USCs in the collagen gel type 1 (2 mg/mL) and injected subcutaneously into nude mice. The growth factors can be released from the microbeads to prolong grafted stem cell survival, promote angiogenesis and nerve regeneration, and stimulate myogenic lineage cell growth in vivo. VEGF-expressing USCs and collagen-I gel injection might indicate the potential to restore continence by muscle regeneration and restoration in the clinic application.

### 3. Tissue-Engineered Suburethral Sling

Another way to treat SUI is tissue engineered suburethral sling. It is used to support the hyperactive urethra and bladder neck and narrow proximal urethra. It is shown to be an effective therapy for SUI. However, the material of existing suburethral sling lacks ideal compliance and contractility (including excessively lax or stiff). It simply relies on mechanical action to improve urethral resistance. In addition, there may be postimplantation weakening due to scaffold degradation in vivo [39]. Thus, it is difficult to obtain satisfactory curative effect in the long term. The ideal sling material would be safe and durable, would lack antigenicity, and most importantly would be a functional replacement to an impaired continence mechanism. A better effect and fewer complications could be achieved by tissue-engineered suburethral sling made of a degradable material loaded with therapeutic stem cells. Incorporating stem cells into the suburethral sling has obvious advantages, not only to enhance mechanical strength of the sling after implantation but also to promote regeneration of ligament/sphincter surrounding the urethra. Cannon et al. [34] showed that incorporating MDSCs into small intestinal submucosa (SIS) slings does not adversely alter the advantageous mechanical properties of the SIS sling in a rat model of SUI. Implanted MDSCs could migrate into and distribute throughout the SIS and form differentiated myotube structures. Meanwhile, spontaneous contractile activity is observed in MDSCs/SIS constructs by 4 and 8 weeks in culture. MDSCs transplantation reduces the SIS biological resorption in the body and provides the basis for future functional studies of tissue engineered sling materials with long duration (Figure 2). Zou et al. [40] seeded BMSCs

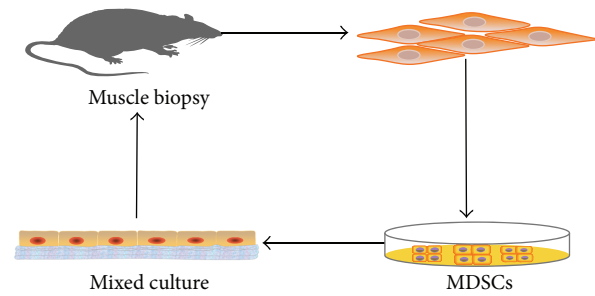


FIGURE 2: The model of MDSC/SIS Sling therapy for SUI (from [34]). MDSCs were firstly obtained from gastrocnemius muscle and subsequently seeded on a SIS scaffold. The MDSC/SIS Sling was cocultured for 2 weeks in vitro. Finally, the tissue-engineered suburethral sling was placed to repair a damaged urethral sphincter of SUI rat model via a midline transabdominal approach.

into degradable silk scaffolds and implanted them in a SUI rat model. The result showed that both scaffolds with and without BMSCs improved leak point pressure, but only scaffolds with BMSCs led to ligament-like tissue formation over time, which suggested potential long-term function. Most recently, Roman et al. [18] combined ADSCs with thermo-annealed poly-L-lactic acid scaffolds to develop a tissue engineered repairing material. The biodegradable scaffolds with ADSCs produced more key extracellular matrix proteins than oral fibroblasts under the same conditions, which improved the ultimate tensile strength and strain of the scaffolds, thus possessing good application prospect for SUI. Subsequently, Roman Regueros et al. [41] further reported the short-term observation about the acute host response after 7 days of implantation. The result showed good integration into host tissues with extensive host cell penetration (ADSCs), new blood vessel formation, and new collagen deposition throughout the full thickness of the samples. There was obvious difference between cell-containing and cell-free scaffolds. Consequently, surgical replantation of suburethral slings combined with patient's stem cells has great promise to provide better long-term efficiency for SUI patients. However, the "ideal" biomechanical properties require further testing in vivo.

### 4. The Challenges of Stem Cells in the Treatment of Stress Urinary Incontinence

Although stem cell therapy has been reported with encouraging results in the preclinical experiments and had great potential for therapeutic applications of SUI, there are still many challenges in clinical treatment of SUI (Figure 3). The life span of implanted stem cells is relatively short and cell death can be observed within the first week, most probably due to ischemia, inflammation, or apoptosis due to detachment from the extracellular matrix [42]. Meanwhile, the size and function of bioengineered muscle also decline with age [43]. In addition, results of EdU-staining also showed that only a small fraction of the transplanted ADSCs might have differentiated into smooth muscle cells and the majority of the transplanted ADSCs remain undifferentiated [21]. Evidence

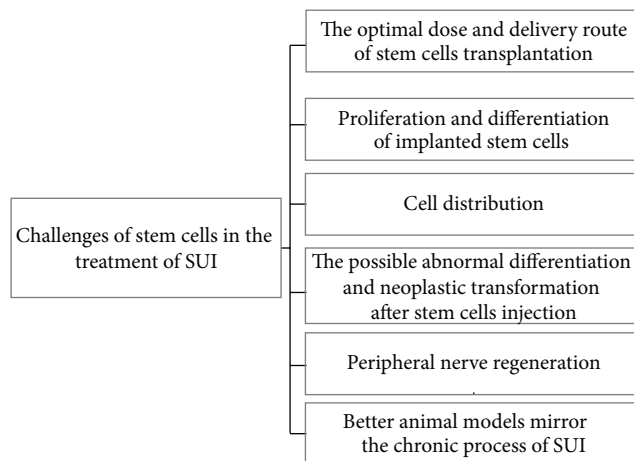


FIGURE 3: The challenges of stem cells in the treatment of stress urinary incontinence. There are many challenges for stem cells in clinical treatment of SUI, the following facts were shown: (a) an important step to determine the optimal dose and delivery route of stem cells transplantation; (b) how to maintain or promote the ability of proliferation and differentiation of implanted stem cells; (c) the injected stem cells' tendency to gather around the injection site and how to form a uniform cell distribution after stem cell injection; (d) stem cells implantation having the risk of neoplastic transformation and how to avoid the possible abnormal differentiation, even neoplastic transformation, after stem cells injection; (e) peripheral nerve regeneration after stem cell transplantation; (f) better animal models that mirror the chronic process of SUI which should be used in preclinical experiments.

shows that the inclusion of cytokines and growth factors are able to enhance the ability of stem cell proliferation and differentiation, such as transforming growth factor beta1 [44], vascular endothelial growth factor [45], and basic fibroblast growth factor [46]. Hence, it would be efficient to deliver growth factors to the transplantation site or directly along with stem cells to enhance their differentiation. However, such studies have not been extensively conducted in vivo. Additional studies are needed to further examine the conditions required to better maintain and promote proliferation and differentiation of stem cells after transplantation. One challenge for stem cell therapies is the need for large amount of cells to be transplanted with numbers ranging from  $0.5 \times 10^6$  to  $128 \times 10^6$  cells and the appropriate dose of cells is yet to be determined. Current results of stem cell therapy for SUI may not be as reproducible as hoped, the overall success rates (complete continence) ranging from 12 to 79% and improvement rates (quality of life and/or pad test) from 13 to 66% in short-term follow-up [12, 15, 47]. In 3 to 12 months' follow-up, almost all injected cells gathered around the injection site; only a small number of cells were regularly distributed along the normal muscle fiber tissue. Therefore, more studies are needed to achieve a more uniform cell distribution. In the past, experimental results have shown that stem cells transplantation had increased the risk of neoplastic transformation in vivo [48–50]. Moreover, stem cells may promote cancer metastasis through regulating epithelial-mesenchymal transition, including breast cancer

[51] and pancreatic cancer [52]. Although the great majority of stem cells have been induced into myogenic cells before urethral injection, how to avoid the possible abnormal differentiation and even malignant transformation in vivo remains unresolved. Additional studies should be carried out for assurance of the long-term safety before stem cells can be used as therapy tools for SUI. Nerve density of urethral tissue declines with age, with a sevenfold age-related loss of nerve density in these same striated urogenital sphincters directly correlated with the loss in striated muscle density in the same tissues [53]. Furthermore, reduced nerve density throughout the striated urogenital sphincter correlates with fewer muscle cells [53]. However, at present, most studies of stem cells therapy for SUI focused on the reconstruction of urethral sphincter and vessel, neglecting peripheral nerve regeneration. More studies are needed to investigate the possible applications of tissue-engineered urethra along with applications to improve distribution of nerve tissue and implanted muscles. Undoubtedly, an ideal animal model for SUI could provide further insight. The formation of SUI is a chronic process that is experienced over years or decades with the urethral sphincter degeneration, while almost all of animal models of SUI mentioned above in the review were established by completely transection of the bilateral pudendal nerve or the vaginal balloon dilatation, which cannot truly simulate the pathophysiology of most of SUI patients. Pauwels et al. [54] established a chronic rat model of SUI with surgical transposition of the urethra to a vertical position. All of the rats leaked urine continuously during the entire study period in the urethral transposition group, while spontaneous recovery of continence (within 1–2 weeks) was seen mostly in the vaginal dilatation group and repetition of the dilatation is needed. Therefore, in order to further comply with clinical practice, more chronic animal models of SUI should be used in preclinical experiments in the future.

## 5. Conclusions

The ultimate goal has always been clinical application of this technology. The published data show that stem cell transplantation as a therapy for SUI has great promise, with some currently used in clinical trials. However, there is still lack of efficient SUI treatments. Additional information is needed from preclinical studies to determine optimal timing and route of stem cell administration. Moreover, many fundamental questions related to the optimal type of stem cells, animal model, implanted stem cells location, stem cells dose, and the long-term safety and efficacy require further examination.

## Disclosure

Weixin Zhao and Qiang Fu are co-senior authors.

## Conflict of Interests

None of the authors has a financial disclosure or a conflict of interests.

## Authors' Contribution

Shukui Zhou and Kaile Zhang contributed equally to this paper.

## Acknowledgment

This study was supported by the National Natural Science Foundation of China, 2014, no. 81470917.

## References

- [1] C.-S. Lin and T. F. Lue, "Stem cell therapy for stress urinary incontinence: a critical review," *Stem Cells and Development*, vol. 21, no. 6, pp. 834–843, 2012.
- [2] P. Norton and L. Brubaker, "Urinary incontinence in women," *The Lancet*, vol. 367, no. 9504, pp. 57–67, 2006.
- [3] C. F. Gibbs, T. M. Johnson II, and J. G. Ouslander, "Office management of geriatric urinary incontinence," *The American Journal of Medicine*, vol. 120, no. 3, pp. 211–220, 2007.
- [4] A. T. Lenis, M. Kuang, L. L. Woo et al., "Impact of parturition on chemokine homing factor expression in the vaginal distention model of stress urinary incontinence," *The Journal of Urology*, vol. 189, no. 4, pp. 1588–1594, 2013.
- [5] J. C. Kim and K. J. Cho, "Current trends in the management of post-prostatectomy incontinence," *Korean Journal of Urology*, vol. 53, no. 8, pp. 511–518, 2012.
- [6] A. Gafni-Kane and P. K. Sand, "Foreign-body granuloma after injection of calcium hydroxylapatite for type III stress urinary incontinence," *Obstetrics & Gynecology*, vol. 118, no. 2, pp. 418–421, 2011.
- [7] D. Nikolavasky, K. Stangel-Wójcikiewicz, M. Stec, and M. B. Chancellor, "Stem cell therapy: a future treatment of stress urinary incontinence," *Seminars in Reproductive Medicine*, vol. 29, no. 1, pp. 61–69, 2011.
- [8] K. L. Ward and P. Hilton, "Tension-free vaginal tape versus colposuspension for primary urodynamic stress incontinence: 5-year follow up," *BJOG: An International Journal of Obstetrics and Gynaecology*, vol. 115, no. 2, pp. 226–233, 2008.
- [9] R. J. Jankowski, B. M. Deasy, and J. Huard, "Muscle-derived stem cells," *Gene Therapy*, vol. 9, no. 10, pp. 642–647, 2002.
- [10] C. Praud, P. Sebe, A.-S. Biérinx, and A. Seville, "Improvement of urethral sphincter deficiency in female rats following autologous skeletal muscle myoblasts grafting," *Cell Transplantation*, vol. 16, no. 7, pp. 741–749, 2007.
- [11] Y. T. Kim, D. K. Kim, R. J. Jankowski et al., "Human muscle-derived cell injection in a rat model of stress urinary incontinence," *Muscle & Nerve*, vol. 36, no. 3, pp. 391–393, 2007.
- [12] K. Stangel-Wójcikiewicz, D. Jarocha, M. Piowar et al., "Autologous muscle-derived cells for the treatment of female stress urinary incontinence: a 2-year follow-up of a polish investigation," *Neurourology and Urodynamics*, vol. 33, no. 3, pp. 324–330, 2014.
- [13] K. M. Peters, R. R. Dmochowski, L. K. Carr et al., "Autologous muscle derived cells for treatment of stress urinary incontinence in women," *Journal of Urology*, vol. 192, no. 2, pp. 469–476, 2014.
- [14] J. Y. Lee, S. Y. Paik, S. H. Yuk, J. H. Lee, S. H. Ghil, and S. S. Lee, "Long term effects of muscle-derived stem cells on leak point pressure and closing pressure in rats with transected pudendal nerves," *Molecules and Cells*, vol. 18, no. 3, pp. 309–313, 2004.
- [15] L. K. Carr, D. Steele, S. Steele et al., "1-year follow-up of autologous muscle-derived stem cell injection pilot study to treat stress urinary incontinence," *International Urogynecology Journal and Pelvic Floor Dysfunction*, vol. 19, no. 6, pp. 881–883, 2008.
- [16] Y. Wang, H. Xu, X. Liu, L. Liu, and Z. Liang, "Inhibition of fibroblast differentiation of muscle-derived stem cells in cell implantation treatment of stress urinary incontinence," *Cellular Reprogramming*, vol. 13, no. 5, pp. 459–464, 2011.
- [17] Y. Xu, Y. F. Song, and Z. X. Lin, "Transplantation of muscle-derived stem cells plus biodegradable fibrin glue restores the urethral sphincter in a pudendal nerve-transected rat model," *Brazilian Journal of Medical and Biological Research*, vol. 43, no. 11, pp. 1076–1083, 2010.
- [18] S. Roman, A. Mangera, N. I. Osman, A. J. Bullock, C. R. Chapple, and S. Macneil, "Developing a tissue engineered repair material for treatment of stress urinary incontinence and pelvic organ prolapse-which cell source?" *Neurourology and Urodynamics*, vol. 33, no. 5, pp. 531–537, 2014.
- [19] Q. Fu, X.-F. Song, G.-L. Liao, C.-L. Deng, and L. Cui, "Myoblasts differentiated from adipose-derived stem cells to treat stress urinary incontinence," *Urology*, vol. 75, no. 3, pp. 718–723, 2010.
- [20] L. B. Shi, H. X. Cai, L. K. Chen et al., "Tissue engineered bulking agent with adipose-derived stem cells and silk fibroin microspheres for the treatment of intrinsic urethral sphincter deficiency," *Biomaterials*, vol. 35, no. 5, pp. 1519–1530, 2014.
- [21] G. Lin, G. Wang, L. Banie et al., "Treatment of stress urinary incontinence with adipose tissue-derived stem cells," *Cytherapy*, vol. 12, no. 1, pp. 88–95, 2010.
- [22] K. Kuismanen, R. Sartoneva, S. Haimi et al., "Autologous adipose stem cells in treatment of female stress urinary incontinence: results of a pilot study," *Stem Cells Translational Medicine*, vol. 3, no. 8, pp. 936–941, 2014.
- [23] W. Zhao, C. Zhang, C. Jin et al., "Periurethral injection of autologous adipose-derived stem cells with controlled-release nerve growth factor for the treatment of stress urinary incontinence in a rat model," *European Urology*, vol. 59, no. 1, pp. 155–163, 2011.
- [24] S. Silwal Gautam, T. Imamura, O. Ishizuka et al., "Implantation of autologous adipose-derived cells reconstructs functional urethral sphincters in rabbit cryoinjured urethra," *Tissue Engineering Part: A*, vol. 20, no. 13–14, pp. 1971–1979, 2014.
- [25] T. Yamamoto, M. Gotoh, M. Kato et al., "Periurethral injection of autologous adipose-derived regenerative cells for the treatment of male stress urinary incontinence: report of three initial cases," *International Journal of Urology*, vol. 19, no. 7, pp. 652–659, 2012.
- [26] C. Giberti, F. Gallo, M. Schenone, P. Cortese, and G. Ninotta, "Stem cell therapy for male urinary incontinence," *Urologia Internationalis*, vol. 90, no. 3, pp. 249–252, 2013.
- [27] M. F. Pittenger, A. M. Mackay, S. C. Beck et al., "Multilineage potential of adult human mesenchymal stem cells," *Science*, vol. 284, no. 5411, pp. 143–147, 1999.
- [28] L. Jackson, D. Jones, P. Scotting, and V. Sottile, "Adult mesenchymal stem cells: differentiation potential and therapeutic applications," *Journal of Postgraduate Medicine*, vol. 53, no. 2, pp. 121–127, 2007.
- [29] J. Corcos, O. Loutochin, L. Campeau et al., "Bone marrow mesenchymal stromal cell therapy for external urethral sphincter restoration in a rat model of stress urinary incontinence," *Neurourology and Urodynamics*, vol. 30, no. 3, pp. 447–455, 2011.
- [30] M. Gunetti, S. Tomasi, A. Giammò et al., "Myogenic potential of whole bone marrow mesenchymal stem cells in vitro and in vivo for usage in urinary incontinence," *PLoS ONE*, vol. 7, no. 9, Article ID e45538, 2012.



- [31] Y. Kinebuchi, N. Aizawa, T. Imamura, O. Ishizuka, Y. Igawa, and O. Nishizawa, "Autologous bone-marrow-derived mesenchymal stem cell transplantation into injured rat urethral sphincter," *International Journal of Urology*, vol. 17, no. 4, pp. 359–368, 2010.
- [32] S.-O. Kim, H. S. Na, D. Kwon, S. Y. Joo, H. S. Kim, and Y. Ahn, "Bone-marrow-derived mesenchymal stem cell transplantation enhances closing pressure and leak point pressure in a female urinary incontinence rat model," *Urologia Internationalis*, vol. 86, no. 1, pp. 110–116, 2011.
- [33] K. Deng, D. L. Lin, B. Hanzlicek et al., "Mesenchymal stem cells and their secretome partially restore nerve and urethral function in a dual muscle and nerve injury stress urinary incontinence model," *American Journal of Physiology—Renal Physiology*, vol. 308, no. 2, pp. F92–F100, 2015.
- [34] T. W. Cannon, D. D. Sweeney, D. A. Conway et al., "A tissue-engineered suburethral sling in an animal model of stress urinary incontinence," *BJU International*, vol. 96, no. 4, pp. 664–669, 2005.
- [35] J. Adamowicz, T. Kloskowski, J. Tworokiewicz, M. Pokrywczynska, and T. Drewna, "Urine is a highly cytotoxic agent: does it influence stem cell therapies in urology?" *Transplantation Proceedings*, vol. 44, no. 5, pp. 1439–1441, 2012.
- [36] R. Lang, G. Liu, Y. Shi et al., "Self-renewal and differentiation capacity of urine-derived stem cells after urine preservation for 24 hours," *PLoS ONE*, vol. 8, no. 1, Article ID e53980, 2013.
- [37] S. Wu, Z. Wang, S. Bharadwaj, S. J. Hodges, A. Atala, and Y. Zhang, "Implantation of autologous urine derived stem cells expressing vascular endothelial growth factor for potential use in genitourinary reconstruction," *Journal of Urology*, vol. 186, no. 2, pp. 640–647, 2011.
- [38] G. Liu, R. A. Pareta, R. Wu et al., "Skeletal myogenic differentiation of urine-derived stem cells and angiogenesis using microbeads loaded with growth factors," *Biomaterials*, vol. 34, no. 4, pp. 1311–1326, 2013.
- [39] W. S. Hilger, A. Walter, M. E. Zobitz, K. O. Leslie, P. Magtibay, and J. Cornella, "Histological and biomechanical evaluation of implanted graft materials in a rabbit vaginal and abdominal model," *American Journal of Obstetrics and Gynecology*, vol. 195, no. 6, pp. 1826–1831, 2006.
- [40] X. H. Zou, Y. L. Zhi, X. Chen et al., "Mesenchymal stem cell seeded knitted silk sling for the treatment of stress urinary incontinence," *Biomaterials*, vol. 31, no. 18, pp. 4872–4879, 2010.
- [41] S. Roman Regueros, M. Albersen, S. Manodoro et al., "Acute in vivo response to an alternative implant for urogynecology," *BioMed Research International*, vol. 2014, Article ID 853610, 10 pages, 2014.
- [42] D. Qin, T. Long, J. Deng, and Y. Zhang, "Urine-derived stem cells for potential use in bladder repair," *Stem Cell Research and Therapy*, vol. 5, no. 3, article 69, 2014.
- [43] D. M. Delo, D. Eberli, J. K. Williams, K.-E. Andersson, A. Atala, and S. Soker, "Angiogenic gene modification of skeletal muscle cells to compensate for ageing-induced decline in bioengineered functional muscle tissue," *BJU International*, vol. 102, no. 7, pp. 878–884, 2008.
- [44] Y. I. Kim, J.-S. Ryu, J. E. Yeo et al., "Overexpression of TGF- $\beta$ 1 enhances chondrogenic differentiation and proliferation of human synovium-derived stem cells," *Biochemical and Biophysical Research Communications*, vol. 450, no. 4, pp. 1593–1599, 2014.
- [45] F. Colazzo, F. Alrashed, P. Saratchandra et al., "Shear stress and VEGF enhance endothelial differentiation of human adipose-derived stem cells," *Growth Factors*, vol. 32, no. 5, pp. 139–149, 2014.
- [46] L. C. Rose, R. Fitzsimmons, P. Lee, R. Krawetz, D. E. Rancourt, and H. Uludağ, "Effect of basic fibroblast growth factor in mouse embryonic stem cell culture and osteogenic differentiation," *Journal of Tissue Engineering and Regenerative Medicine*, vol. 7, no. 5, pp. 371–382, 2013.
- [47] R. Boissier and G. Karsenty, "Cellular therapy and urinary incontinence," *Progres en Urologie*, vol. 22, no. 8, pp. 454–461, 2012.
- [48] W. Zhu, W. Xu, R. Jiang et al., "Mesenchymal stem cells derived from bone marrow favor tumor cell growth in vivo," *Experimental and Molecular Pathology*, vol. 80, no. 3, pp. 267–274, 2006.
- [49] J. M. Yu, E. S. Jun, Y. C. Bae, and J. S. Jung, "Mesenchymal stem cells derived from human adipose tissues favor tumor cell growth in vivo," *Stem Cells and Development*, vol. 17, no. 3, pp. 463–473, 2008.
- [50] G. V. Røslund, A. Svendsen, A. Torsvik et al., "Long-term cultures of bone marrow-derived human mesenchymal stem cells frequently undergo spontaneous malignant transformation," *Cancer Research*, vol. 69, no. 13, pp. 5331–5339, 2009.
- [51] F. T. Martin, R. M. Dwyer, J. Kelly et al., "Potential role of mesenchymal stem cells (MSCs) in the breast tumour microenvironment: stimulation of epithelial to mesenchymal transition (EMT)," *Breast Cancer Research and Treatment*, vol. 124, no. 2, pp. 317–326, 2010.
- [52] A. Kabashima-Niibe, H. Higuchi, H. Takaishi et al., "Mesenchymal stem cells regulate epithelial-mesenchymal transition and tumor progression of pancreatic cancer cells," *Cancer Science*, vol. 104, no. 2, pp. 157–164, 2013.
- [53] M. Pandit, J. O. L. DeLancey, J. A. Ashton-Miller, J. Iyengar, M. U. A. Blaivas, and D. Perucchini, "Quantification of intramuscular nerves within the female striated urogenital sphincter muscle," *Obstetrics and Gynecology*, vol. 95, no. 6, pp. 797–800, 2000.
- [54] E. Pauwels, S. De Wachter, and J.-J. Wyndaele, "Evaluation of different techniques to create chronic urinary incontinence in the rat," *BJU International*, vol. 103, no. 6, pp. 782–786, 2009.



## Clinical Study

# Stem Cell Mobilization with G-CSF versus Cyclophosphamide plus G-CSF in Mexican Children

José Eugenio Vázquez Meraz,<sup>1</sup> José Arellano-Galindo,<sup>2</sup> Armando Martínez Avalos,<sup>3</sup>  
Emma Mendoza-García,<sup>4</sup> and Elva Jiménez-Hernández<sup>5</sup>

<sup>1</sup>Banco de Sangre, Hospital General de Ecatepec las Américas, Simón Bolívar esq. Libertadores de América Fracc. las Américas, 55076 Ecatepec de Morelos, MEX, Mexico

<sup>2</sup>Area de Virología, Laboratorio de Microbiología y Enfermedades Infecciosas, Hospital Infantil de México Federico Gómez, Mexico

<sup>3</sup>Departamento de Oncología, Instituto Nacional de Pediatría, Mexico

<sup>4</sup>Laboratorio de Hematología e Investigación, Hospital General de México, OD and Laboratorio Clínico, Central Hospital Infantil de México Federico Gómez, Ciudad de México, DF, Mexico

<sup>5</sup>Departamento de Hematología Pediátrica, UMAE CMN la Raza IMSS, Mexico

Correspondence should be addressed to José Eugenio Vázquez Meraz; euvame59@hotmail.com

Received 2 October 2015; Accepted 16 November 2015

Academic Editor: Mahendra S. Rao

Copyright © 2016 José Eugenio Vázquez Meraz et al. This is an open access article distributed under the Creative Commons Attribution License, which permits unrestricted use, distribution, and reproduction in any medium, provided the original work is properly cited.

Fifty-six aphaereses were performed in 23 pediatric patients with malignant hematological and solid tumors, following three different protocols for PBPC mobilization and distributed as follows: A: seventeen mobilized with 4 g/m<sup>2</sup> of cyclophosphamide (CFA) and 10 µg/kg/day of granulocyte colony stimulating factor (G-CSF), B: nineteen with CFA + G-CSF, and C: twenty only with G-CSF when the WBC count exceeded  $10 \times 10^3$ /L. The average number of MNC/kg body weight (BW)/aphaeresis was  $0.4 \times 10^8$  (0.1–1.4),  $2.25 \times 10^8$  (0.56–6.28), and  $1.02 \times 10^8$  (0.34–2.5) whereas the average number of CD34+ cells/kg BW/aphaeresis was  $0.18 \times 10^6$ /kg (0.09–0.34),  $1.04 \times 10^6$  (0.19–9.3), and  $0.59 \times 10^6$  (0.17–0.87) and the count of CFU/kg BW/aphaeresis was  $1.11 \times 10^5$  (0.31–2.12),  $1.16 \times 10^5$  (0.64–2.97), and  $1.12 \times 10^5$  (0.3–6.63) in groups A, B, and C, respectively. The collection was better in group B versus group A ( $p = 0.007$  and  $p = 0.05$ , resp.) and in group C versus group A ( $p = 0.08$  and  $p = 0.05$ , resp.). The collection of PBPCs was more effective in the group mobilized with CFM + G-CSF when the WBC exceeded  $10 \times 10^3$ /µL in terms of MNC and CD34+ cells and there was no toxicity of the chemotherapy.

## 1. Introduction

With the discovery that peripheral blood progenitor cells (PBPC) could be obtained by aphaeresis, several reports have shown that these stem cells can be used to reconstitute hematopoiesis, after myeloablative therapy in cancer patients [1–3]. Chemotherapy increases the amount of PBPC 20–50 times [4, 5]. Therefore high dose of cyclophosphamide (CFA) has been frequently used to mobilize PBPC [6–10]. Hematopoietic growth factors such as G-CSF and GM-CSF used after chemotherapy increase the efficacy of stem cells mobilization even more. However, G-CSF in combination with chemotherapy must be administrated during 8–12 days compared with only 4 to 6 days when it is applied without chemotherapy [11–16].

There is not enough experience in children to establish the optimal method for PBPC mobilization, as it could be done with hematopoietic growth factors either alone or in combination with chemotherapy. We determined the number of mononuclear cells (MNC), CD34+ cells, and colony forming units (CFU) in the leukapheresis products of pediatric patients with malignant hematological diseases and solid tumors, following three different protocols for stem cells mobilization.

## 2. Patients and Methods

The study included twenty-three pediatric patients with malignant hematological diseases and solid tumors. The main

TABLE 1: Clinical characteristics of the patients.

Number	Age (years)	Sex	Weight (Kg.)	Diagnosis
1	3	M	15	WT S-IV 1°CR
2	10	F	39	LMA-M2 2°CR
3	16	M	38	HD S-IVB 2°CR
4	7	F	22	LMA-M1 1°CR
5	3	F	15	LAL-L1 t(9;22) 1°CR
6	3	M	17	LAL-L1 t(4;11) 1°CR
7	9	F	32	LAL-L1 t(9;22) 1°CR
8	12	M	32	HD S-IVB 2°CR
9	16	M	55	LAL-L2 t(9;22) 1°CR
10	11	M	56	LMA-M4 1°CR
11	16	M	43	LAL-L1 t(9;22) 2°CR
12	2	M	13	NBL S-IV 3°CR
13	8	F	29	LAL-L2 t(9;22) 1°CR
14	8	M	26	LMA-M4 1°CR
15	9	F	22	WT S-IV 3°CR
16	4	M	21	LAL-L1 t(9;22) 1°CR
17	6	M	25	LMA-M2 2°CR
18	5	F	22	WT S-IV 2°CR
19	7	F	21	LMA-M1 2°CR
20	10	M	38	LAL-L1 t(9;22) 1°CR
21	8	M	25	LAL-L1 t(9;22) 1°CR
22	13	M	31	HD S-IVB 2°CR
23	6	F	26	LAL-L1 t(9;22) 1°CR

HD: Hodgkin disease, WT: Wilms' tumor, LMA: myeloblastic acute leukemia, LAL: lymphoblastic acute leukemia, NBL: neuroblastoma, CR: complete remission, and S: stage.

characteristics of the patients are shown in Table 1. Parent's consent of the study was obtained in all cases.

**2.1. PBPC Mobilization.** The patients were divided into three groups: group A was assigned to high dose ( $4 \text{ g/m}^2$ ) of cyclophosphamide (CFA) and ( $10 \mu\text{g/kg/day}$ ) of G-CSF applied subcutaneously, and the aphaeresis procedures were started when the white blood cell count (WBC) exceeded  $1.0 \times 10^9/\text{L}$ . Group B was subjected to the same regimen (CFM + G-CSF), but the WBC was  $>10 \times 10^9/\text{L}$  at the time of starting the cell collection, and group C was treated subcutaneously with G-CSF alone for 4 days and the aphaeresis was started at day 5.

**2.2. PBPC Collection.** Collections were performed by placement of a double lumen dialysis catheter with a Baxter Fenwal CS 3000 plus machine using large volume leukapheresis (LVL) ( $200 \text{ mL/kg}$ ). The inlet flow was  $30\text{--}50 \text{ mL/min}$ . The target number of MNC and CD34+ cells was  $4 \times 10^8/\text{kg}$  and  $2 \times 10^8/\text{kg}$ , respectively. A minimum of  $1 \times 10^6/\text{kg}$  CD34+ cells and  $2 \times 10^8/\text{kg}$  of MNC were considered sufficient though. When the yield of a single aphaeresis was considered insufficient, the process was continued daily until the CD34+

cells and MNC target dose were achieved. The final products were frozen and stored in liquid nitrogen at  $-196^\circ\text{C}$ .

**2.3. Aphaeresis Products.** The obtained product of MNC was processed by Coulter Max M, and the number of CD34+ cells was determined by flow cytometry in a FACSCalibur by using the ProCount software (Becton Dickinson).

**2.4. Cell Cultures.** The cell cultures were prepared in Methocult GF H4434 (Stem Cell Technology Inc, Vancouver, BC), contained  $1 \times 10^5$  MNCs per mL, and were incubated at  $37^\circ\text{C}$ , in presence of  $\text{CO}_2$ , and the colony forming units (CFUs) were determined on day 14 by using an inverted microscope as described previously [3].

**2.5. Statistical Analysis.** Not normally distributed data are presented as median and range. Differences were compared using the nonparametrical Kruskal-Wallis test. The Stata software program (Stata Corporation, College Station, TX, USA) was used for statistical analysis.

### 3. Results

**3.1. Patient's Characteristics.** Twenty-three children were included in the study. Seven patients were assigned to group A, eight to group B, and eight to group C. Seventeen, nineteen, and twenty leukaphereses were performed in each group, respectively. Patients characteristics are shown in Table 1.

The average number of days of G-CSF administration was 6.1 (4–8) in group A, 11.8 (10–15) in group B, and 5.7 (5–7) in group C. The average of MNC in the aphaeresis products was  $0.4 \times 10^8/\text{kg}$  (0.1–1.4) in group A,  $2.25 \times 10^8$  (0.56–6.28) in group B, and  $1.02 \times 10^8$  (0.34–2.5) in group C. The mean number of CD34+ cells was  $0.18 \times 10^6/\text{kg BW}$  (0.09–0.34) in group A,  $1.04 \times 10^6$  (0.19–9.3) in group B, and  $0.59 \times 10^6$  (0.17–0.87) in group C. The mean count of CFU/kg BW was  $1.11 \times 10^5$  (0.31–2.12) in group A,  $1.16 \times 10^5$  (0.64–2.97) in group B, and  $1.12 \times 10^5$  (0.3–6.63) in group C (Table 2).

The differences between the three groups were statistically significant for the number of MNC/kg BW ( $p = 0.007$ ) and CD34+ cells/kg ( $p = 0.05$ ) in group B versus group A and for CD34+ cells in the group C versus group A ( $p = 0.05$ ). The UFC  $\times 10^5/\text{kg BW}$  was similar in the different groups (Table 3).

In the group treated with chemotherapy, patients were hospitalized due to severe neutropenia ( $<0.5 \times 10^9/\text{L}$ ), but no one required antibiotic or platelet transfusion.

### 4. Discussion

Mobilized peripheral blood is now the main hematopoietic progenitor cell source for cellular support following myeloablative chemotherapy. PBPC transplantation results in a more rapid hematopoietic recovery than bone marrow cell transplantation, mainly due to the larger number of hematopoietic progenitor cells infused. G-CSF alone or combined with chemotherapy is commonly used in mobilization

TABLE 2: PBPC results by group.

	Group A CFA + G-CSF WBC > $1.0 \times 10^9/L$ Mean and range	Group B CFA + G-CSF WBC > $10 \times 10^9/L$ Mean and range	Group C G-CSF alone Mean and range
Days of G-CSF	6.1 (4–8)	11.8 (10–15)	5.7 (5–7)
MNC $\times 10^8/kg$	0.4 (0.1–1.4)	2.25 (0.56–6.28)	1.02 (0.34–2.5)
CD34+ $\times 10^6/kg$	0.18 (0.09–0.34)	1.04 (0.19–9.3)	0.59 (0.17–0.87)
CFU $\times 10^5/kg$	1.11 (0.31–2.12)	1.16 (0.64–2.97)	1.12 (0.3–6.63)

WBC: white blood cells; MNC: mononuclear cells; CFU: colony forming units.

TABLE 3: Statistical analysis using the nonparametrical Kruskal-Wallis test.

	MNC $\times 10^8/kg$	CD34+ cells $\times 10^6/kg$	UFC $\times 10^5/kg$
A versus B	0.007	0.055	0.297
A versus C	0.082	0.055	0.526
B versus C	0.248	0.172	0.833

protocols and it appears to be able to achieve adequate progenitor cell yields for single transplants in most patients and [17] observed that the combination of myelosuppressive chemotherapy and G-CSF can mobilize better PBPC than chemotherapy alone and the administration of these cytokines in combination with chemotherapy may reduce the blood volume processed by leukapheresis. Additionally the optimal procedure for PBPC mobilization in children has not yet been determined because data on the engraftment are not enough [17–19]. Clinical collection of PBPC by leukapheresis has been more difficult to perform in a child than in an adult, especially after receiving an extensive therapy for their malignancies [20–22]. It has been shown that heavy and prolonged cytotoxic treatments seem to exhaust the mobilizable stem cell pool; therefore PBPC should be collected as early as possible after diagnosis [17, 23].

In order to optimize mobilization and to obtain a larger number of CD34+ cells, we simultaneously administered CFA + G-CSF or only G-CSF. Our results demonstrated that the number of CD34+ cells collected was similar for all groups (Table 2). The difference in obtained results was statistically significant when we compared group B (CFA + G-CSF WBC >  $10 \times 10^3/\mu L$ ) and group A (CFA + G-CSF WBC >  $1.0 \times 10^3/\mu L$ ) ( $p = 0.05$ ) and also for group C (G-CSF) and group A ( $p = 0.05$ ), but it was not statistically significant for group B versus group C. This suggests that the efficacy of G-CSF is similar in the presence or absence of CFA, when the leucocytes count exceeded  $10 \times 10^9/L$ ; findings similar to ours were reported by Costa et al. [17]. The difference in the amount of UFC was not statistically significant between the studied groups.

The main limitations of chemotherapy mobilizations are neutropenia, sepsis, and bleeding diathesis and the unpredictability of starting time for collection procedure [24–27]. In our group of patients with CFA, there have been no serious complications, but patients did require more days of G-CSF application.

From the present data, we conclude that PBPC mobilization with CFM + G-CSF when the WBC is  $>10 \times 10^9/L$  has a similar efficacy in comparison with mobilization using only G-CSF, and the last one has less adverse effects.

## Conflict of Interests

The authors declare that there is no conflict of interests regarding the publication of this paper.

## References

- [1] A. C. Zovein and E. C. Forsberg, “Hematopoietic development at high altitude: blood stem cells put to the test,” *Development*, vol. 142, no. 10, pp. 1728–1732, 2015.
- [2] O. Blau, “Bone marrow stromal cells in the pathogenesis of acute myeloid leukemia,” *Frontiers in Bioscience*, vol. 19, no. 1, pp. 171–180, 2014.
- [3] K. B. McCredie, E. M. Hersh, and E. J. Freireich, “Cells capable of colony formation in the peripheral blood of man,” *Science*, vol. 171, no. 3968, pp. 293–294, 1971.
- [4] G. Tridente, “Pluripotent growth factors,” in *Adverse Events with Biomedicines: Prevention Through Understanding*, pp. 583–585, Springer, Milan, Italy, 2014.
- [5] L. B. To, K. M. Shepperd, D. N. Haylock et al., “Single high doses of cyclophosphamide enable the collection of high numbers of hemopoietic stem cells from the peripheral blood,” *Experimental Hematology*, vol. 18, no. 5, pp. 442–447, 1990.
- [6] M. K. Angelopoulou, P. Tsirkinidis, G. Boutsikas, T. P. Vassilakopoulos, and P. Tsirigotis, “New insights in the mobilization of hematopoietic stem cells in lymphoma and multiple myeloma patients,” *BioMed Research International*, vol. 2014, Article ID 835138, 11 pages, 2014.
- [7] A. M. Carella, F. Frassoni, N. Pollicardo et al., “Philadelphia-chromosome-negative peripheral blood stem cells can be mobilized in the early phase of recovery after a myelosuppressive chemotherapy in Philadelphia-chromosome-positive acute lymphoblastic leukaemia,” *British Journal of Haematology*, vol. 89, no. 3, pp. 535–538, 1995.
- [8] M. Reiser, A. Josting, A. Draube et al., “Successful peripheral blood stem cell mobilization with etoposide (VP-16) in patients with relapsed or resistant lymphoma who failed cyclophosphamide mobilization,” *Bone Marrow Transplantation*, vol. 23, no. 12, pp. 1223–1228, 1999.

- [9] R. Sorasio, M. Bonferroni, M. Grasso et al., "Peripheral blood CD34+ percentage at hematological recovery after chemotherapy is a good early predictor of harvest: a single-center experience," *Biology of Blood and Marrow Transplantation*, vol. 20, no. 5, pp. 717–723, 2014.
- [10] D. D. Kotasek, K. M. Shepherd, R. E. Sage et al., "Factors affecting blood stem cell collections following high dose cyclophosphamide mobilization in lymphoma, myeloma and solid tumors," *Bone Marrow Transplantation*, vol. 9, no. 1, pp. 11–17, 1992.
- [11] G. Milone, M. Martino, A. Spadaro et al., "Plerixafor on-demand combined with chemotherapy and granulocyte colony-stimulating factor: significant improvement in peripheral blood stem cells mobilization and harvest with no increase in costs," *British Journal of Haematology*, vol. 164, no. 1, pp. 113–123, 2014.
- [12] J. M. Vantelon, S. Koscielny, P. Brault et al., "Scoring system for the prediction of successful peripheral blood stem cell (PBSC) collection in non-Hodgkin's lymphoma (NHL): application in clinical practice," *Bone Marrow Transplantation*, vol. 25, no. 5, pp. 495–499, 2000.
- [13] J. Gómez-Espuch, J. M. Moraleda Jiménez, F. Ortuño et al., "Mobilization of hematopoietic progenitor cells with paclitaxel (taxol) as a single chemotherapeutic agent, associated with rhG-CSF," *Bone Marrow Transplantation*, vol. 25, no. 3, pp. 231–236, 2000.
- [14] A. Gianni, M. Bregni, A. Stern et al., "Granulocyte-macrophage colony-stimulating factor to harvest circulating hematopoietic stem cell for auto transplantations," *The Lancet*, vol. 334, no. 8663, pp. 580–585, 1989.
- [15] M. Socinski, A. Elias, L. Schnipper, S. Cannistra, K. Antman, and J. Griffin, "Granulocyte-macrophage colony stimulating factor expands the circulating haemopoietic progenitor cell compartment in man," *The Lancet*, vol. 331, no. 8596, pp. 1194–1198, 1988.
- [16] M. Fukuda, S. Kojima, K. Matsumoto, and T. Matsuyama, "Auto transplantation of peripheral blood stem cells mobilized by chemotherapy and recombinant human granulocyte colony-stimulating factor in childhood neuroblastoma and non-Hodgkin's lymphoma," *British Journal of Haematology*, vol. 80, no. 3, pp. 327–331, 1992.
- [17] L. J. Costa, G. L. Uy, P. N. Hari et al., "Contribution of chemotherapy mobilization to disease control in multiple myeloma treated with autologous transplantation," *Blood*, vol. 124, no. 21, p. 2447, 2014.
- [18] S. Emir, H. A. Demir, T. Aksu, A. Kara, M. Özgüner, and B. Tunç, "Use of plerixafor for peripheral blood stem cell mobilization failure in children," *Transfusion and Apheresis Science*, vol. 50, no. 2, pp. 214–218, 2014.
- [19] Y. Takaue, T. Watanabe, Y. Kawano et al., "Isolation and storage of peripheral blood hematopoietic stem cells for autotransplantation into children with cancer," *Blood*, vol. 74, no. 4, pp. 1245–1251, 1989.
- [20] K. A. de Brito Eid, E. C. M. Miranda, and S. dos Santos Aguiar, "Mobilization and collection of CD34<sup>+</sup> cells for autologous transplantation of peripheral blood hematopoietic progenitor cells in children: analysis of two different granulocyte-colony stimulating factor doses," *Revista Brasileira de Hematologia e Hemoterapia*, vol. 37, no. 3, pp. 160–166, 2015.
- [21] L. C. Lasky, B. Bostrom, J. Smith, T. J. Moss, and N. K. C. Ramsay, "Clinical collection and use of peripheral blood stem cells in pediatric patients," *Transplantation*, vol. 47, no. 4, pp. 613–616, 1989.
- [22] M. Körbling and H. Martin, "Transplantation of hemapheresis-derived hemopoietic stem cells: a new concept in the treatment of patients with malignant lymphohemopoietic disorders," *Plasma Therapy and Transfusion Technology*, vol. 9, no. 1, pp. 119–132, 1988.
- [23] P. A. Rowlings, C. A. Rowling, L. B. To et al., "a comparison of peripheral blood stem cell mobilization after chemotherapy with cyclophosphamide as a single agent in doses of 4gr/m2 in patients with advanced cancer," *Australian & New Zealand Journal of Medicine*, vol. 22, article 600, 1992.
- [24] J. W. Sweetenham and M. L. Turner, "Haemopoietic progenitor homing and mobilization," *British Journal of Haematology*, vol. 94, no. 4, pp. 592–596, 1996.
- [25] W. P. Sheridan, R. M. Fox, C. G. Begley et al., "Effect of peripheral-blood progenitor cells mobilised by filgrastim (G-CSF) on platelet recovery after high-dose chemotherapy," *The Lancet*, vol. 339, no. 8794, pp. 640–644, 1992.
- [26] N. J. Chao, J. R. Schriber, K. Grimes et al., "Granulocyte colony-stimulating factor 'mobilized' peripheral blood progenitor cells accelerate granulocyte and platelet recovery after high dose chemotherapy," *Blood*, vol. 81, no. 8, pp. 2031–2035, 1993.
- [27] D. C. Link, "Mechanisms of granulocyte colony-stimulating factor induced hematopoietic progenitor-cell mobilization," *Seminars in Hematology*, vol. 37, supplement 2, pp. 25–32, 2000.